The role of PQM-1 in proteostasis and transcellular chaperone signalling

Daniel Thomas O'Brien

Submitted in accordance with the requirements for the degree of Doctor of Philosophy

The University of Leeds

School of Molecular and Cellular Biology

September 2019

The candidate confirms that the work submitted is his own, except where work which has formed part of jointly-authored publications has been included. The contribution of the candidate and the other authors to this work has been explicitly indicated below. The candidate confirms that appropriate credit has been given within the thesis where reference has been made to the work of others. Further details of the jointly-authored publications and the contributions of the candidate and the other authors to the work should be included below this statement.

Chapters 2 and 4 of this thesis contain work which contributed to the following publication:

O'Brien et al., 2018 Cell Reports 23, 3905–3919.

Fig 1F, 3 A, B, C, D, E, F, generation of strains for 4B, imaging for 4C, S4A-G data are attributable to me.

Other figures, referenced in this thesis were contributed by other authors:

Figure 1E: Figure provided by Sarah Good

Figure 2: Figure provided by Patricija van Oosten-Hawle

Figure 4C: Nuclear scoring was done by Laura Jones

Acknowledgements

I would like to express my gratitude to my supervisor Dr Patricija van Oosten-Hawle for her help, patience, and encouragement as I have worked towards my PhD. I would also like to thank Prof. David Westhead for his supervision, and in particular his guidance of my bioinformatics studies.

I would like to thank all the members of the van Oosten-Hawle lab, in particular Sarah, Jay and Laura who have been fantastic colleagues, and helped to keep me sane.

I would also like thank to my family for their support during the writing up of my thesis and providing me with free food and board at this time.

And thanks to Becky for being great.

Abstract

C. elegans are free living nematodes which are well placed as a model organism for the heat shock response. I have investigated the zinc finger transcription factor PQM-1 to discern its function in both acute heat stresses and long term suppression of aggregation prone proteins. I found that PQM-1 is required for *C. elegans* heat stress survival and that its presence helps suppress the aggregation of polyglutamine rich proteins. I followed this result up with an appraisal of the transcriptome of *C. elegans* during heat stress, in the presence and absence of *pqm-1* to ascertain which genes were regulated by PQM-1 during heat stress. I also investigated the localisation and regulation of PQM-1 in heat stress conditions and found that the abundance of the protein and its subcellular localisation is influenced by both the ubiquitin ligase *uba-1*, and the kinase *sgk-1*.

As a result of my studies I have discovered a novel role for PQM-1 in the heat shock response, and that it is required for proteostasis maintenance as the organism ages. Furthermore, I have also determined that a specific transcriptional programme is regulated by PQM-1 post-heat stress and identified several proteins that PQM-1 interacts with under these conditions.

Table of Contents

List of Tables

List of Figures

List of Abbreviations

BiP	**Binding immunoglobulin Protein**
ChIP	**Chromatin Immunoprecipitation**
CTD	**C-Terminal Domain**
DR	**Dietary Restriction**
ER	**Endoplasmic Reticulum**
ESI-TOF	**Electrospray Ionisation Time of Flight**
GSC	**Germline Stem Cell**
HS	**Heat Shock**
HSE	**Heat Shock Element**
HSP	**Heat Shock Protein**
ILS	**Insulin-like Signalling**
MD	**Middle Domain**
NTD	**N-Terminal Domain**
PN	**Proteostasis Network**
ROS	**Reactive Oxygen Species**
SBD	**Substrate-binding Domain**
SERSS	**Secreted ER Stress Signal**
ts	**Temperature sensitive**
UPR	**Unfolded Protein Response**
UPS	**Ubiquitin-Proteasome System**

Chapter 1 Introduction

The free-living nematode *Caenorhabditis elegans* has been widely used as a model organism owing to its relative simplicity for a metazoan, its short lifecycle and its fully mapped genome. *C. elegans* has been extensively used as a model system to investigate how organisms respond to a variety of stresses including hypoxia; oxidative stress; osmotic stress; and heat shock (Rodriguez et al., 2013).

Proteostasis is the process by which cells maintain a healthy proteome through ensuring proper folding of proteins and refolding or removal of misfolded or damaged entities. The maintenance of effective proteostasis is important for cells to avoid the devastating consequences of a compromised proteome, leading to cell damage and death (Balch et al., 2008; Hipp et al., 2014; Labbadia and Morimoto, 2015). The proteostasis network (PN) is composed of stress responsive transcription factors such as HSF-1; molecular chaperones including Hsp70s and Hsp90s; and the ubiquitin-proteasome system (UPS) consisting of ubiquitin conjugating enzymes and the proteasome (Kim et al., 2013), which will be explored in the following sections.

1.1 Cell-autonomous and cell-nonautonomous stress response pathways

1.1.1 The Heat Shock Response

1.1.1.1 Cell autonomous regulation of the HSR

All living organisms need to be able to respond efficiently to stresses that challenge the integrity of the cellular proteome to ward against malfunction and death. To accomplish this all cells within an organism have developed mechanisms to refold misfolded proteins back into their native state and degrade those that cannot be restored. A major group of proteins responsible for the folding and refolding of proteins are the chaperone proteins such as HSP70 (Heat Shock Protein 70) and HSP90 (Heat Shock Protein 90) which bind to proteins and help them to adopt their native configurations (Kim et al., 2013). An ancient stress response mechanism that upregulates the expression of these chaperones in the event of stress is the heat shock response (HSR) (Lindquist and Craig, 1988; Morimoto, 1993; Vihervaara and Sistonen, 2014). Heat shock proteins that are upregulated by the HSR in *C. elegans* include the small heat shock protein *hsp-16.2*, and *C12C8.1* and *F44E5.4,* which are both cytosolic and heat inducible members of the *hsp-70* family. The master regulator of the HSR is Heat Shock Factor 1 (HSF1), a highly conserved transcription factor that is essential for all organisms to survive exposures to acute stress (Akerfelt et al., 2010). Upon organismal exposure to extreme stress such as heat or oxidative stress HSF-1 rapidly trimerises and translocates to the nucleus to drive the HSR (Westwood et al., 1991), HSF1 is further described in section 1.2.1.

1.1.1.2 Cell-non-autonomous regulation of the HSR

In eukaryotes the proteostasis of cells is surveilled by stress signalling pathways which detect and respond to stressful conditions encountered by an organism. In multicellular organisms, these signalling pathways have been shown to act both cell-autonomously – i.e. the response is orchestrated in the stressed cell; as well as cell-non-autonomously, whereby the stress is also responded to in distal tissues that do not immediately experience the stress condition (Anckar and Sistonen, 2007; Gardner et al., 2013; Taylor et al., 2014; Seah et al., 2016; Miles et al., 2019). These discoveries are still relatively new and as such there are a number of unanswered questions surrounding how these responses are regulated (O'Brien and van Oosten-Hawle, 2016). Stress signalling responses need to be coordinated during development and aging to avoid the potentially deleterious consequences to the organism of unregulated activity.

In *C. elegans* the cell-non-autonomous HSR is regulated by two thermosensory AFD neurons which are responsible for directing thermotactic behaviour, and navigating the nematode to the optimal temperature (Mori and Ohshima, 1995). The AFD neuron, in partnership with the AIY neuron, is known to be responsible for sensing ambient temperature and regulating the response of the organism to external temperature cues (Inglis, 2007). These neurons were also found to be responsible for the HSF-1 mediated HSR in *C. elegans* – which means the same neurons which detect heat and elicit a behavioural response also relay signals to the rest of the organism to enact the HSR when confronted with thermal distress (Prahlad et al., 2008). This cell-non-autonomous HSR is dependent on the activity of *gcy-8* (which encodes a receptor type guanylyl cyclase which regulates thermotaxis) and serotonin signalling in the neurons to relay the

signal to the periphery of the organism (Prahlad et al., 2008; Tatum et al., 2015). In this way the detection of heat stress by the neurons promotes activation of HSF-1 and the subsequent expression of heat shock proteins in distal tissues such as muscle and the reproductive organs. Indeed the role of the AFD neurons in the activation of HSF-1 across the organism was confirmed by optogenetic means – excitation of the AFD neurons induces HSF-1 activation in the absence of heat stress (Tatum et al., 2015).

1.1.2 The Unfolded Protein Response of the Endoplasmic Reticulum

1.1.2.1 Cell autonomous regulation of the UPR-ER

The unfolded protein response of the endoplasmic reticulum (UPR^{ER}) is induced by the accumulation of unfolded proteins in the ER of eukaryotic cells. There are generally considered to be three branches of signalling response pathways: PERK; ATF-6; and IRE-1 (Walter and Ron, 2011). Of these, IRE-1 is the most studied as it is conserved from yeast to mammals. IRE-1 recognises unfolded protein in the ER which causes it to oligomerise and trans-auto-phosphorylate. The resulting IRE-1 oligomers have endoribonucleic activity which cleaves the *XBP-1 (X-box binding protein 1)* mRNA to form *XBP-1s* (Calfon et al., 2002). The protein resulting from the translation of this edited mRNA, XBP-1s enters the nucleus and directs the activation of UPR^{ER} genes including the HSP-70 GRP78/BiP (Binding immunoglobulin protein) (Figure 1.1; Walter and Ron, 2011; Gardner et al., 2013). XBP-1 is essential for host protection against immune activation in *C. elegans*, the increased stress placed on the folding capacity of the ER during activation of innate immunity to counter pathogens is detrimental to organismal health, and requires the protective activation of the UPR^{ER} (Richardson et al., 2010).

1.1.2.2 Cell-non-autonomous regulation of the UPR-ER

The UPR^{ER} is also regulated in a cell-non-autonomous fashion, with the nervous system once again acting as the sensory tissue directing the activation of the UPR^{ER} across the organism. Expression of XBP-1s in the neurons activates XBP-1 in the intestine and induces the expression of BiP in these distal tissues, which increases resistance to ER stress and lifespan of the organism (Taylor and Dillin, 2013). This neuronal signalling pathway depends on neuronal vesicles: lack of *unc-13,* which leads to reduction in small clear vesicle release (Richmond et al., 1999; Taylor and Dillin, 2013), interferes with the process, blocked UPR^{ER} upregulation in distal tissues by cell-non-autonomous signalling from the neurons. This result points towards a secreted ER stress signal (SERSS) which allows signalling between neurons and other tissue types to promote ER stress resistance and longevity (Taylor and Dillin, 2013). Recently, it was uncovered that expression of *xbp-1s* in the neurons or intestine increases *C. elegans* lifespan through upregulation of lysosomal genes such as *asp-3* and *lipl-1* and activation of lysosomes in the intestine (Imanikia et al., 2019). This activation of intestinal lysosomes is crucial for the enhanced proteostasis and increased longevity mediated by neuronal *xbp-1s*.

In *C. elegans* XBP-1 is regulated by OCTR-1, a G protein-coupled octopamine receptor which is expressed in sensory neurons (Sun et al., 2011; Sun et al., 2012). During nematode development, XBP-1 is always active to meet the higher demand for protein synthesis and folding, and at the onset of adulthood OCTR-1 is switched on to prevent ongoing activation of the UPR^{ER} post-development (Sun et al., 2012). OCTR-1 also supresses innate immunity by downregulating the non-canonical UPR pathway, and as such blocks XBP-1 mediated resistance to pathogens (Sun et al., 2012).

To exemplify the importance of these cell-non-autonomous stress response mechanisms from nematodes to vertebrates, it was found that the expression of XBP-1s in the pro-opiomelanocortin (POMC) neurons of mice leads to XBP-1s activation in the liver (Williams et al., 2014). Furthermore, this cell-non-autonomous activation of the UPR^{ER} was able to protect the mice from diet induced obesity.

1.1.3 The Unfolded Protein Response of the mitochondria

1.1.3.1 Cell autonomous regulation of the mitochondrial UPR

The UPR of the mitochondria relies on molecular chaperones such as the mitochondria specific mtHSP70 to promote protein folding in the organelle (Shpilka and Haynes, 2018). Mitochondrial proteostasis can perturbed by the reactive oxygen species (ROS) produced by the electron transport chain (ETC) during respiration (Runkel et al., 2013). ROS can damage the structures of proteins that they encounter, causing them to misfold, which adds a burden to the local proteostasis machinery. Furthermore, mutations to the components of the ETC can induce stress in the mitochondrial protein folding environment by impairing the assembly of individual ETC complexes (Yoneda et al., 2004; Runkel et al., 2013). In *C. elegans* the excess unfolded protein in the mitochondrial matrix is thought to be cleaved into short peptide fragments by the ATP-dependent protease ClpP. These peptides are then likely to be pumped across the inner mitochondrial membrane (IMM) by HAF-1 (Haynes et al., 2010). It is thought that the peptides are of a small enough size that they can freely cross the outer membrane. The UPR^{mito} is activated by the subsequent action of ATFS-1 (activating transcription factor associated with stress 1) (Haynes et al., 2010). The accumulation of cleaved peptides in

the cytosol leads to the accumulation of the ubiquitin-like protein UBL-5, which forms a transcriptionally active complex when paired with DVE-1 (Figure 1.1). Both ATFS-1 and UBL-5/DVE-1 contribute to the induction of mitochondrial chaperones (Pellegrino et al., 2013). The function of ATFS-1 is conserved – in *C. elegans* which lack ATFS-1, the mammalian protein ATF5 is able to regulated the UPR^{mito} (Fiorese et al., 2016). This result indicates that regulation of the UPR^{mito} is conserved from nematodes to mammalian systems.

1.1.3.2 Cell-non-autonomous regulation of the mitochondrial UPR

Reduced expression of components of the ETC or mutations which induce ETC dysfunction have been shown to significantly extend the lifespan of organisms ranging from *C. elegans* through *Drosophila* to murine models, via the activation of the UPR^{mito} at an organismal level (Schulz and Haynes, 2015). Reduced neuronal expression of an ETC subunit component, *cco-1*, activates the expression of mtHSP70 in the intestine and is sufficient to extend the lifespan of the organism. The unfolded protein response of the mitochondria (UPR^{mito}) that is induced by mitochondrial stress has been found to signal in a cell-non-autonomous fashion in *C. elegans*. The knockdown of the mitochondrial respiratory chain complex protein *cco-1* required only in a single tissue, either intestine or neurons, was sufficient to extend *C. elegans* lifespan (Dillin et al., 2002; Durieux et al., 2011).

UPR^{mito} can also be induced in distal tissues when activated in the muscle – mitochondrial damage in the flight muscles of *D. melanogaster* induces the expression

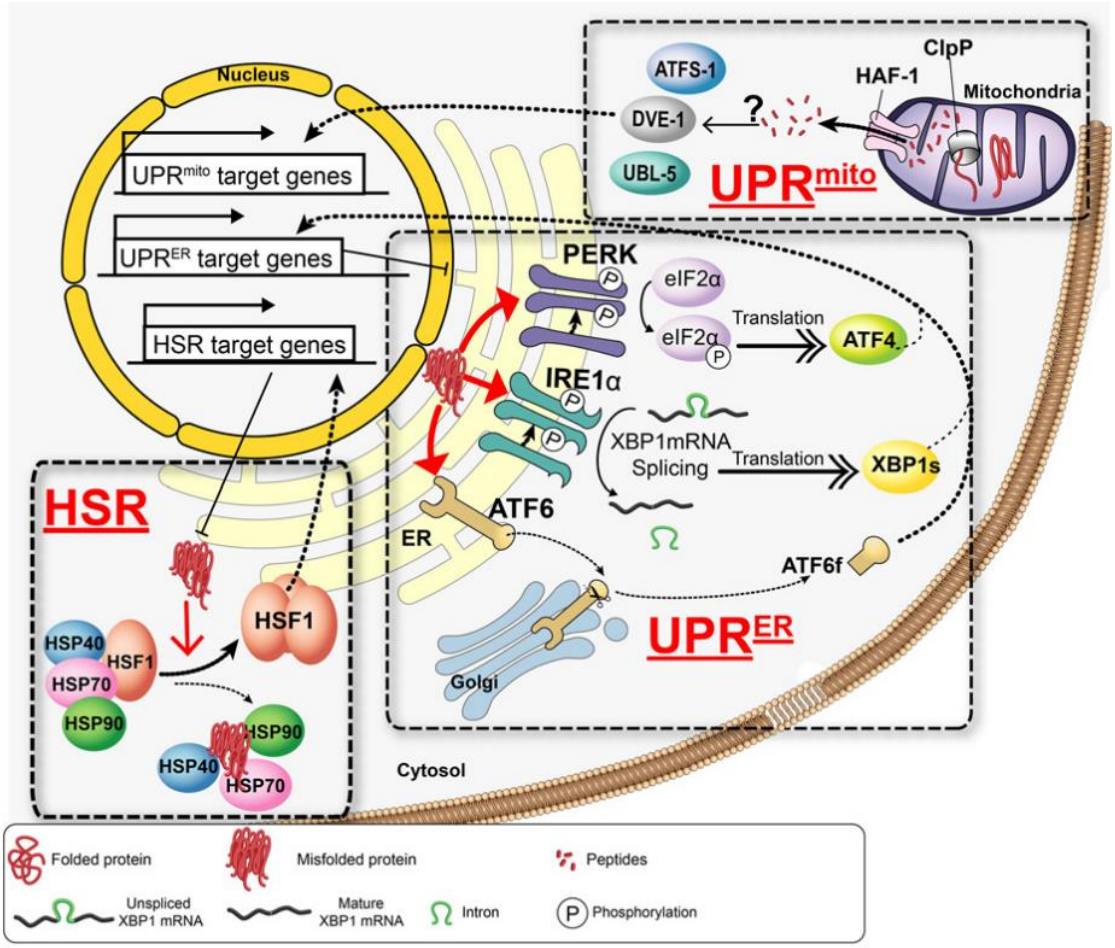

Figure 1.1. Stress signalling pathways regulating cellular proteostasis, including the HSR, the UPR^{ER} and the UPR^{mito}.

These stress response pathways can be triggered by environmental challenges, which lead to protein folding stress and the accumulation of misfolded proteins. The HSR is regulated by HSF-1. Proteotoxic stress results in the appearance of misfolded proteins in the cytosol, which releases HSF-1 from its inhibitory interactions with HSP-90, HSP-70 and HSP-40. This induces trimerization of HSF-1 and translocation into the nucleus where it regulates expression of heat-shock genes. The UPR^{ER} is triggered by protein folding stress in the ER lumen, which activates transmembrane protein IRE-1, PERK or ATF6, comprising the three branches of the UPRER. Activation of IRE-1 leads to splicing of XBP-1 mRNA in the cytosol and translation of XBP-1s, the active form of the transcription factor, which regulates expression of UPR-specific proteostasis components. The UPR^{mito} is activated upon protein misfolding in the mitochondrial matrix, which leads to cleavage of misfolded peptides by ClpP and subsequent transport into the cytosol by HAF-1. This results in formation of a transcriptionally active complex consisting of ATFS-1, DVE-1 and UBL-5 which induces transcription of mitochondria-specific chaperones. From (O'Brien and van Oosten-Hawle, 2016).

of ImpL2, an insulin antagonist, which reduces insulin signalling in both muscle and distal tissues (Owusu-ansah et al., 2013).

In addition to the cell-non-autonomous coordination of major stress responsive transcription factors HSF-1; XBP-1; ATFS-1, which are summarised in Figure 1.1, the metazoan proteostasis network is also supported by specific forkhead family transcription factors such as FOXO3A/DAF-16 and FOXA/PHA-4, which are described in the following sections.

1.1.4 Transcellular Chaperone Signalling

Another cell-non-autonomous signalling pathway that regulates proteostasis across different tissues in an organism is transcellular chaperone signalling (TCS) (van Oosten-Hawle et al., 2013). TCS is induced upon perturbation to basal expression levels of molecular chaperones such as *hsp-90* in a tissue-specific manner which results in the upregulation of chaperones in distinct, distal tissues in *C. elegans* (van Oosten-Hawle et al., 2013). This observation led to the idea that tissues can act as both sensors, and sentinels, of stress - communicating stressful conditions to neighbouring tissues. The communication of the chaperone expression levels in the organism between tissues is known as transcellular chaperone signalling. For example, increased expression of HSP-90 in the neurons leads to induced expression of *hsp-90* in the muscle, which can have cytoprotective effects on the protein folding environment in the muscle (van Oosten-Hawle et al. 2013). In the model proposed, tissue specific introduction of a metastable protein induced *hsp-90* locally in a PHA-4 dependent manner, which was beneficial for the PN to increase local folding capacity but repressed the activity of HSF-1. The localised

increase in HSP-90 represses HSF-1 and thereby overrides the neuronal HSF-1 signalling from the AFD that regulates the HSR (Prahlad et al., 2008), which uncoupled HSP-90 from neural regulation of HSF-1 so that it is regulated by PHA-4.

Interestingly, the increased folding capability does not translate to increased heat stress resistance, each of the strains that overexpress HSP-90 (HSP-90::RFP) in the intestine, the neurons and the body wall muscle are more sensitive to thermal stress than wildtype (van Oosten-Hawle et al., 2013). An explanation for this observation is that HSP-90 sequesters HSF-1 – the master regulator of the HSR, and thereby prevents it from driving heat shock protein expression (Zou et al., 1998; van Oosten-Hawle et al., 2013). Work done by other members of the van Oosten-Hawle group revealed that TCS induced by tissue specific HSP-90 overexpression is mediated by the zinc-finger transcription factor PQM-1, in addition to PHA-4 (O'Brien et al., 2018). PQM-1 is required in the "sensor" tissue, i.e. the tissue which overexpresses HSP-90, to relay the transcellular signal to a receiver tissue (Figure 1.2). Overexpression of HSP-90 in the neurons requires PQM-1 to be present in the neurons, in order to initiate TCS. In this case, PQM-1 in the neurons regulates CLEC-41 for the signal to be sent to the responding tissues. CLEC-41 is an innate immune peptide which is predicted to be plasma membrane-associated. It contains two beta-barrel forming domains known as CUB domains which are found almost exclusively in extracellular and plasma membrane-associated proteins (Bork and Beckmann, 1993). CLEC-41 is enriched in the neurons and intestine (Reece-Hoyes et al., 2007; Spencer et al., 2011).

Likewise, if HSP-90 is overexpressed in the intestine, PQM-1 and its downstream intestinal effector ASP-12 are required in the intestine for signal transduction to the

responding tissues. ASP-12 (ASpartyl Protease) is predicted to have aspartic-type endopeptidase activity and is involved in the immune response (Shaye and Greenwald, 2011).

1.2 Stress-responsive transcription factors

1.2.1 HSF-1

Heat shock factor 1 (HSF-1) is the major regulator of the HSR in metazoans and upregulates HSPs during heat stress through binding to the heat shock element (HSE) and promoting transcription (Akerfelt et al., 2010). In the canonical heat shock response HSF1 is converted from its inactive monomeric form, in which it is sequestered by Hsp90 and Hsp70 away from the nucleus, to an activated trimeric form with multiple post-translational modifications. Trimeric HSF1 enters the nucleus and binds to the HSE in the promoter region of heat shock protein genes leading to their upregulation and the canonical cellular heat shock response (Figure 1.1; Morimoto, 1998; Williams and Morimoto, 1990; Xiao etal., 1991; Prahlad et al., 2008).

One of the major molecular chaperones upregulated by the HSF-1 mediated HSR is heat shock protein (Hsp)70 (Mayer, 2013). Hsp70 has chaperone functions that involve allosteric control between the 40 kDa N-terminal nucleotide binding domain (NBD), which binds and hydrolyses ATP to enact conformational change in the molecule, and the 25-kDa C-terminal substrate-binding domain (SBD) which binds to the exposed hydrophobic regions of client polypeptides (Zuiderweg et al., 2017). Hsp70s are highly conserved and are both central to the protein surveillance network and key for many

client proteins-folding processes (Mayer and Bukau, 2005; Meimaridou et al., 2009). Hsp70 binds to unfolded, misfolded and aggregate proteins, but not to proteins in their correctly folded conformations. In addition to this, Hsp70s are also able to recognise a limited set of proteins in their natively folded state as a regulatory mechanism, including HSF-1 (Abravaya et al., 1992). Hsp70s interact with client polypeptides in multiple scenarios. Hsp70s bind to nascent polypeptides produced by the ribosome to aid with de novo folding; following translocation through cellular compartments; intermediate folding states; and misfolded protein aggregates. Hsp70 is able to bind to such a wide variety of clients as it recognises a short motif which consists of a core of 5 hydrophobic residues flanked by positively charged amino acids (Rüdiger et al., 1997).

Another major molecular chaperone is Hsp90. Hsp90 is a highly conserved molecular chaperone which is found in prokaryotic species (as the homologous HtpG (Bardwell and Craig, 1987)) to mammals (Pearl and Prodromou, 2006). It is essential for correct protein folding and the maintenance of proteome integrity. Hsp90 is comprised of a highly conserved N-terminal domain (NTD) which is responsible for nucleotide binding; a middle domain (MD) which is important for client recognition and ATP hydrolysis and the C-terminal domain (CTD) through which it is able to dimerise with another Hsp90 molecule (Pearl and Prodromou, 2006; Taipale et al., 2010). HSP90 contains a conserved MEEVD motif at the C-terminus (Young et al., 1998) and is a highly abundant cellular protein, comprising 1-2% of cellular protein under ambient conditions, which can increase during times of stress (Taipale et al., 2010; Finka and Goloubinoff, 2013).

The interplay of the branches of the proteostasis network are clear if we examine the overlap of the chaperone activity of the Hsp70-Hsp90 complex and the UPS. CHIP (C

terminal Hsp70 binding protein), a Hsp70-Hsp90 cochaperone, is an E3 ubiquitin ligase which promotes degradation of its substrate proteins through the proteasomal machinery (Ballinger et al., 1999; McDonough and Patterson, 2003). For example, CHIP can bind to tau protein and promote its ubiquitination, targeting it for degradation (Petrucelli et al., 2004).

1.2.2 DAF-16

In the early 1990s it was discovered that the mutation of the *daf-2* gene led to a lifespan extension in *C. elegans* that more than doubles the wildtype lifespan (Kenyon et al., 1993; Lin et al., 1997). *Daf-2* encodes the insulin/insulin-like growth factor (IGF)-1 receptor which relays insulin-like signalling (ILS) through the cell via the PI3K/AKT pathway (Lin et al., 2001). The lifespan extension afforded by the *daf-2* mutant was found to be reliant on the presence of the forkhead transcription factor family member DAF-16 (Kenyon et al., 1993; Lin et al., 1997). DAF-16 was initially isolated as a gene which caused a dauer-defective genotype when mutated (Albert et al., 1981).

Insulin-like molecules bind to receptor encoded by *daf-2*, an ortholog of the insulin and insulin-like growth factor-1 (IGF-1). The DAF-2 receptor activates the PIP3 pathway composed of AGE-1, PDK-1, SGK-1 and AKT-1/-2. The pathway negatively regulates the nuclear localisation of DAF-16 by phosphorylation which sequesters the transcription factor in the cytosol (Figure 1.3). The loss of function mutants of *daf-16* and *daf-2* led to a complete loss of the lifespan extension which the *daf-2* mutant demonstrated (Kenyon et al., 1993; Lin et al., 1997).

DAF-16 was found to be expressed in all cell types tested by single-cell transcriptional profiling (Cao et al., 2017). DAF-16 binds to the core consensus DNA sequence, TTGTTTAC, the DAF-16 binding element (DBE) *in vitro* (Furuyama et al., 2000). The DBE is overrepresented in the promoters of genes that are upregulated in *daf-2* mutants in a DAF-16 dependent manner (Class I genes) (Murphy et al., 2003); and it has been suggested that DAF-16 directly binds these target genes (Schuster et al., 2010). In contrast, a group of genes were found to be downregulated in *daf-2* mutants in a DAF-16 dependent manner (Class II genes), these promoters contain a reverse GATA sequence named the DAE (DAF-16 Associated Element); ChIPseq data identified PQM-1, a zinc finger transcription factor, as the DAE-binding factor (Tepper et al., 2013).

DAF-16 is regulated by the E3 ubiquitin ligase RLE-1, which polyubiquitinates DAF-16 to target the protein for degradation (W. Li et al., 2007). Furthermore, the NAD^+ - dependent deacetylase gene, *sir-2.1* regulates DAF-16. In the event of heat stress but not low levels of insulin signalling, SIR-2.1 and DAF-16 physically interact, with the requirement of 14-3-3 proteins (Berdichevsky et al., 2006). This lends itself to the possibility that *C. elegans DAF-16/FOXO* is repressed by acetylation in an analogous manner to mammalian FoxO by SIRT1 (Brunet et al., 2004; Motta et al., 2004). The *C. elegans* ortholog of mammalian host cell factor, HCF-1, is a nuclear protein that binds to and inhibits DAF-16 by preventing its association with target gene promoters (Li et al., 2008). Indeed, gene expression profiling revealed an 80% overlap between DAF-16 target genes responsive to *hcf-1* mutation and *sir-2.1* overexpression and that SIR-2.1 and HCF-1 proteins associate (Rizki et al., 2011). This implies that SIR-2.1 could regulate DAF-16 activity via HCF-1.

DAF-16 interacts with the 14-3-3 proteins PAR-5 and FTT-2 during development which act to sequester it in the cytoplasm (Berdichevsky et al., 2006; J. Li et al., 2007). In adults FTT-2 inhibits DAF-16 target gene expression, but promotes lifespan extension in a SIR-2.1 and DAF-16 dependent manner (Berdichevsky et al., 2006; J. Li et al., 2007).

As well as its role in insulin-like signalling-dependent lifespan extension, DAF-16 is a stress responsive transcription factor which regulates the chaperones *hsp-16s, hsp-12.6* (Murphy et al., 2003; Halaschek-Wiener et al., 2005) and the antioxidative superoxide dismutase (*sod-3*) (Honda and Honda, 1999; Honda and Honda, 2002), promoting stress survival. DAF-16 also regulates innate immunity in *C. elegans* (Singh and Aballay, 2009) as its overactivation leads to increased *C. elegans* susceptibility to bacterial infections.

1.2.3 SKN-1

SKN-1 is an important oxidative stress responsive transcription factor in *C. elegans.* SKN-1 initiates the development of the mesoendodermal tissues including the intestine in early *C. elegans* embryogenesis (Bowerman et al., 1992). SKN-1 is widely expressed in *C. elegans* (Cao et al., 2017) and accumulates in intestinal nuclei in response to oxidative stress and is required for oxidative stress resistance (An and Blackwell, 2003). Furthermore, *skn-1* mutants have shortened lifespans. SKN-1 is an ortholog of the mammalian Nrf/CNC proteins Nrf1 and Nrf2, with which it shares the DIDLID transactivation motif (Walker et al., 2000) and these orthologs function similarly to regulate Phase II detoxification genes. SKN-1 is negatively regulated by phosphorylation by the kinases AKT-1, -2, and SGK-1 (Tullet et al., 2008; Figure 1.3) as well as glycogen synthase kinase-3 (GSK-3) (An et al., 2005). SKN-1 is regulated by the notch ligand OSM-

11 which antagonises SKN-1 during embryonic development, preventing nuclear accumulation (Dresen et al., 2015). The inactivation of OSM-11 in adult *C. elegans* increases lifespan and enhances resistance to environmental stress. SKN-1 is required for longevity, heat and oxidative stress resistance, but not osmotic stress survival (Dresen et al., 2015). SKN-1 is regulated on the protein level by constant turnover by the proteasome owing to the WD-40 repeat protein WDR-23 which interacts with CUL-4/DDB-1 ubiquitin ligase to target SKN-1 for degradation by the proteasome (Choe et al., 2009), the proteasome is also known to regulate SKN-1 nuclear accumulation (Kahn et al., 2008), possibly through regulation of overall SKN-1 cellular levels. SKN-1 has also been implicated in *C. elegans* pathogenic response to both gram negative *Pseudomonas aeruginosa* and gram positive *Enterococcus faecalis* bacteria (Papp et al., 2012).

1.2.4 The Zinc-finger transcription factor PQM-1 – a novel stress transcription factor

PQM-1 (ParaQuat-Methylviologen responsive-1) was first discovered because it was noted to be a highly upregulated transcript when *C. elegans* are exposed to oxidative stress, as induced by the oxidative agent paraquat (Tawe et al., 1998).

PQM-1 promotes *C. elegans* development in larval stages, and as such, it is present in intestinal nuclei during development (Tepper et al., 2013; O'Brien et al., 2018). PQM-1 expression has been detected in the intestine and the head ganglia and ciliated sensory neurons (Reece-Hoyes et al., 2007; Cao et al., 2017). PQM-1 has therefore been considered as a developmental transcription factor. It has, however, also been implicated in *C. elegans* response to pathogenic bacteria. For example, PQM-1 plays a key role in the innate immune response: when *pqm-1* is depleted by RNAi, survival of *C. elegans* exposed to the pathogenic *P. aeruginosa* is significantly reduced (Shapira et al., 2006).

In addition to these roles, PQM-1 also negatively regulates fat transport from the intestine to the germline during adulthood (Dowen et al., 2016). This negative regulation of reproduction is mediated by the *lin-4* and *let-7* miRNAs via mTORC2 signalling in the intestine. PQM-1 represses the expression of the vitellogenin genes in the intestine which transport fats to the germline for yolk formation (Dowen et al., 2016). This pathway functions in parallel to the ILS pathway to modulate the activity of the kinase SGK-1 which in turn regulates PQM-1 (Dowen et al., 2016; Figure 1.3).

To promote reproduction, PQM-1 associates with CEH-60 at the DAF-16-associated element (DAE) at the promoter of stress-responsive genes to control gene expression (Dowen, 2019). PQM-1 has previously been shown to bind to the DAE and regulate the expression of genes associated with DAF-16 (Tepper et al., 2013). Furthermore, the mutation of a TST motif in PQM-1 to AAA attenuated CEH-60 activity, indicating that these residues are important for PQM-1's function as a corepressor of CEH-60 (Dowen, 2019). The TST motif lies within a RERSTI sequence, which is an SGK-1 consensus site (Kobayashi et al., 1999). Taken together, these results suggest that PQM-1 is negatively regulated by SGK-1 via phosphorylation.

In addition to our own observation that PQM-1 plays an important role for proteostasis maintenance, as discussed in Chapter 2, this key role for PQM-1 was also identified in an independent study investigating chronic and acute stress, by Shpigel et al. The importance of PQM-1 in cytoprotective proteostasis was confirmed as the dietary restriction (DR) dependent rescue of proteostasis collapse in adults requires PQM-1 (Shpigel et al., 2018). In germline stem cell (GSC)-arrested *C. elegans* the improved HS survival rates were dependent on *daf-16,* but not *pqm-1.* Furthermore, it was demonstrated that DR vastly improved *C. elegans* response to chronic misfolding stress and folding maintenance, coupled with a moderate improvement to HS survival rates, dependent on *pqm-1*. In contrast, the *daf-16* reliant GSC-arrest rescued the HS response activation in adults, but only mildly improved the folding maintenance (Shpigel et al., 2018). Interestingly, PQM-1 is predicted to regulate 21 chaperone genes, including the heat inducible Hsp-70s, *hsp-4* and *F44E5.4*, and the small HSPs *hsp-17, hsp-12.1* and *hsp-43* (Shpigel et al., 2018). Another important indication that PQM-1 is involved in proteostasis is its role in *daf-2* mediated lifespan extension (Tepper et al., 2013). PQM-

1 and DAF-16 exhibit an anticorrelation of localisation – when DAF-16 is nuclear PQM-1 is excluded from the nucleus, which allows the pathways regulating DAF-16 to influence PQM-1 transcriptional activity (Tepper et al., 2013). These results build a model whereby the "partners" DAF-16 and PQM-1 complement each other by remodelling the PN in different ways in response to different signalling pathways (see Figure 1.3).

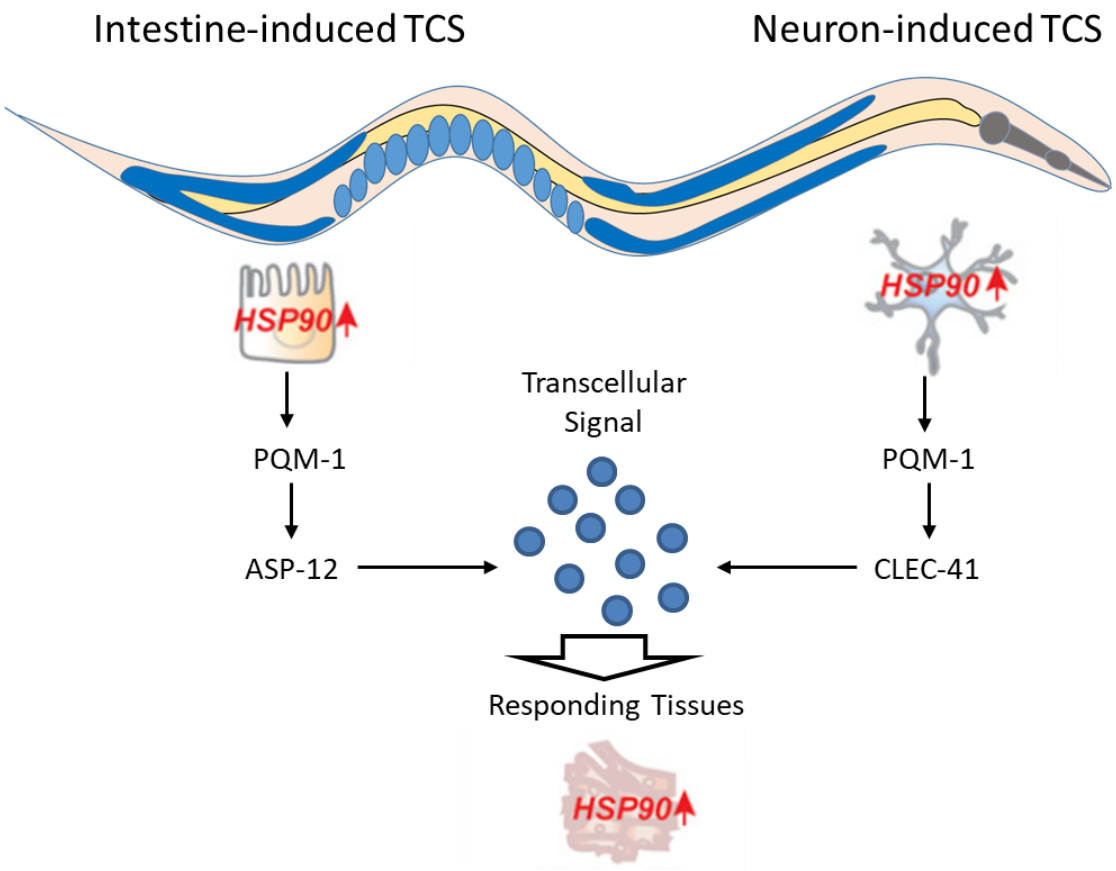

Figure 1.2. Transcellular Chaperone Signalling is mediated by PQM-1.

Overexpression of HSP-90 in the intestine or neurons leads to an upregulation of HSP-90 in distal tissues. The TCS pathway is mediated by PQM-1 with signalling via the aspartic protease ASP-12 or the C-type lectin CLEC-41 in the intestine and neurons respectively.

1.3 *C. elegans* models of human protein folding diseases

1.3.1 Huntington's Disease

Huntington's disease (HD) is a neurodegenerative disease, characterised by its heritability and relatively early onset in the prime of adult life (Bates et al., 2015; McColgan and Tabrizi, 2018). HD is caused by polyglutamine (CAG) trinucleotide repeat expansion in the huntingtin (*HTT)* gene on chromosome 4 (MacDonald et al., 1993). The resultant mutant huntingtin (mHTT) protein contains extended polyglutamine repeats and the accumulation of the resulting unstable protein in the cell leads to the disease emergence (DiFiglia et al., 1995).

In the *C. elegans* HD model, the expression of proteins containing polyglutamine expansions perturbs global proteostasis which leads to loss of function of multiple metastable temperature-sensitive (ts) mutant proteins (Gidalevitz et al., 2006; Brignull et al., 2007). Conversly, these metastable proteins which are not damaging under normal protein quality control environments, enhance the aggregation of glutamine-rich PolyQ proteins (Gidalevitz et al., 2006). A stretch of 35 glutamines has been seen to be a threshold length in *C. elegans*, above which aggregation of the exogenous protein occurs before day 3 of life (Morley et al., 2002). Therefore, Q35 is well placed as a proteostasis sensor: under normal conditions it does not aggregate during development; only once adulthood is reached do aggregates begin to tell. Therefore the aggregation is especially sensitive to perturbations in the efficacy of the PN.

1.3.2 Alzheimer's Disease

Alzheimer's Disease (AD) is the single greatest cause of dementia, responsible for between 50% and 75% of cases (Prince et al., 2014). The major features of Alzheimer pathology are amyloid plaques and neurofibrillary tangles. Amyloid plaques consist of mostly abnormally folded beta-amyloid (Aβ) with lengths of 40 or 42 peptides, which are by-products of amyloid precursor protein (APP) metabolism (Serrano-Pozo et al., 2011). Neurofibrillary tangles composed of hyper-phosphorylated tau protein are also hallmarks of Alzheimer's disease (Takahashi et al., 2017). A *C. elegans* model expressing $A\beta_{(3\text{-}42)}$ in the muscle has been characterised, which causes progressive paralysis of the nematodes during aging as the aggregation prone protein overwhelms the PN (Link, 1995; Wu and Luo, 2005).

An RNAi screen revealed that there are 16 members of the proteostasis network that lead to enhanced Aβ and polyglutamine toxicity in *C .elegans* when knocked down (Brehme et al., 2014). Among these were the molecular chaperones Hsp70 and Hsp90, which have been shown to be important in cellular defence against misfolded proteins (Lackie et al., 2017). Furthermore, Aβ toxicity can be suppressed by HSP-16.2 overexpression propping up the PN (Fonte et al., 2008). Therefore, we hypothesised that TCS, which upregulates major molecular chaperones in distal tissues, could be protective against disease protein aggregation. We reasoned that it is important to further study the PN to discern whether there are factors that can be utilised to upregulate components of the PN and combat proteostasis collapse.

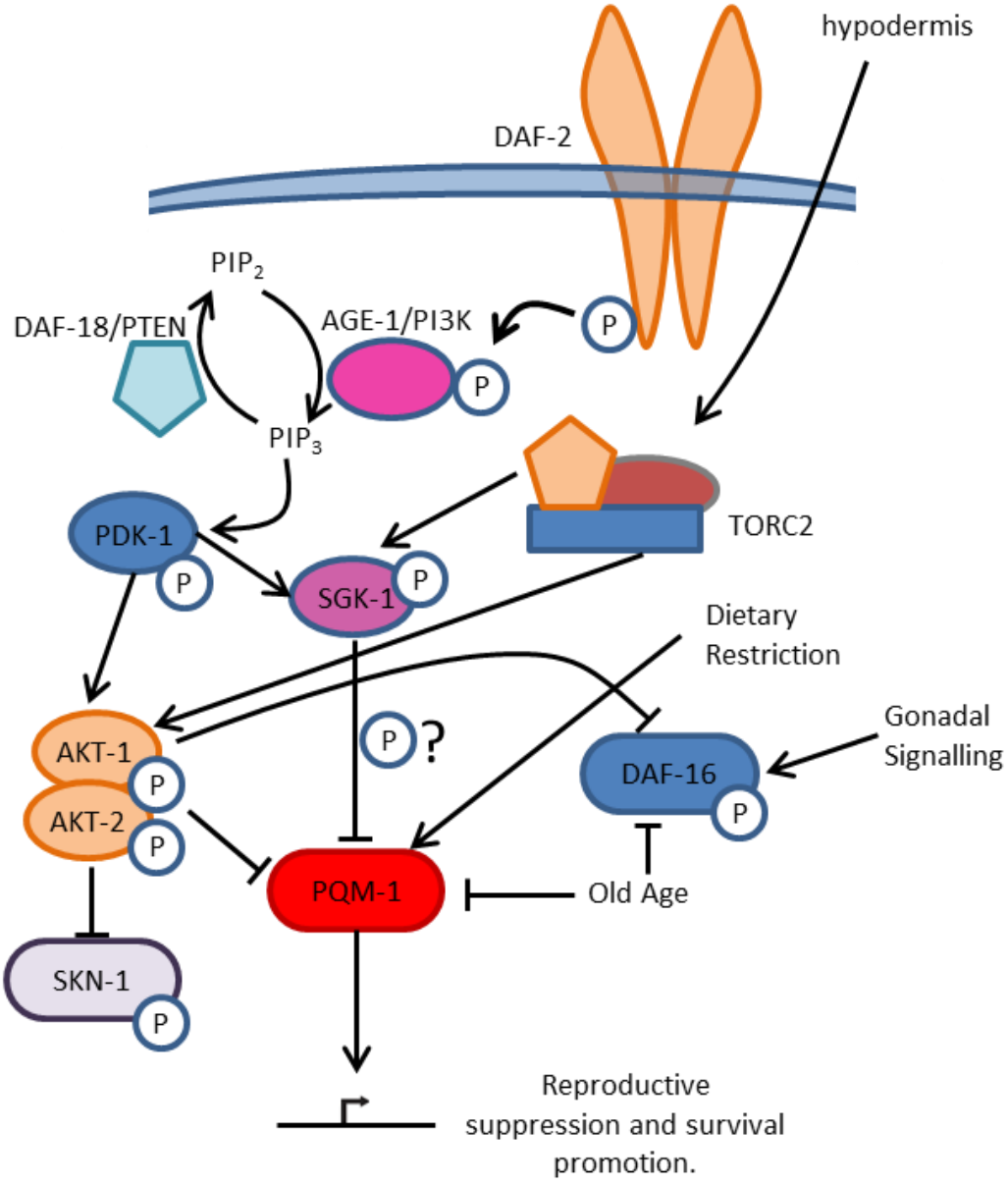

Figure 1.3. Model of PQM-1 regulation.

Our working model for the regulation of PQM-1 in the intestine, where PQM-1 is regulated by signalling from the ILS pathway; mTORC signalling; dietary restriction and the transition to adulthood. These pathways are likely to regulated PQM-1 activity through inhibitory phosphorylation to prevent its nuclear entry and subsequent effect on transcription.

1.4 Aims

This study was designed to investigate whether PQM-1 might be an important, but to this point relatively understudied, stress-responsive transcription factor. My working hypothesis was that PQM-1 has a role in proteostasis, specifically in response to heat stress and chronic stress caused by the expression of aggregation prone proteins.

My work was focussed on the zinc-finger transcription factor PQM-1 and its role, localisation and interacting partners during stress conditions. In order to interrogate the role that PQM-1 plays in stress response, I investigated its role for survival during heat stress conditions as well as for proteostasis maintenance (Chapter 2); *pqm-1* dependent gene expression profiles in response to heat stress in *C. elegans* (Chapter 3); and investigated its subcellular localisation pattern and interactors during heat stress (Chapter 4).

PQM-1 does not have a direct homolog in mammals, the closest human ortholog is SALL2 (*spalt-like transcription factor 2)* which is a transcription factor implicated in eye-formation, neurogenesis and tumorigenesis (Li et al., 2004; Sung and Yim, 2017). Sall2 and the tumour suppressor p53 share growth arrest and pro-apoptotic functions by independently inducing p21Cip1/Waf1 and BAX. Indeed, the loss of both p53 and Sall2 in mice causes significantly higher mortality and metastasis rates compared with p53 single mutant mice (Sung and Yim, 2017). Although PQM-1 and Sall2 share 32.5% protein identity it may be that they share a conserved fold/biological role (Friedberg and Margalit, 2002).

Chapter 2 PQM-1 in Proteostasis

Throughout its lifespan an organism is likely to encounter diverse sources of stress that can perturb protein folding and function, and these can arise intracellularly or externally. These misfolded proteins are non-functional and therefore deleterious to the survival of the affected organism. Therefore, adaptation to and survival of proteotoxic stress is essential for cells to mitigate damage to thrive in an ever-changing environment. The proteostasis network acts to maintain the integrity of the proteome of the nematodes in the face of stresses such as heat, oxidative stress or the chronic expression of disease-inducing proteins (Labbadia and Morimoto, 2015).

Stresses can occur extracellularly which lead to a cellular response e.g. heat stress leads to upregulation of heat shock protein expression. Some stresses, however, occur intracellularly, such as the misfolding of aggregation-prone or metastable proteins. Stress occurring in a specific tissue is responded to cell-autonomously, but can be communicated between tissues and organs thus acting in a cell-nonautonomous manner in a multicellular organism such as *C. elegans* (Miles et al., 2019).

In this chapter we have examined the role of PQM-1 in *C. elegans* in response to acute stresses (heat shock) and chronic stress conditions, such as caused by the expression of aggregation prone disease proteins.

2.1 Transcellular chaperone signalling is mediated by PQM-1

The discovery that cells can communicate to and influence the state of proteostasis across different tissues within an organism, is one of the major recent findings in the chaperone field (Prahlad et al., 2008; van Oosten-Hawle et al., 2013; Taylor and Dillin, 2013; Zhang et al., 2018).

When there is a tissue specific proteostasis imbalance, this can be communicated to, and cause an upregulation of molecular chaperones in, distal tissues. This effect is known as transcellular chaperone signalling (TCS). For example, when HSP-90 is overexpressed in a tissue-specific manner, in the neurons or intestine of *C. elegans,* there is a compensatory upregulation of *hsp-90* in distal tissues including the body wall muscle (van Oosten-Hawle et al., 2013; O'Brien et al., 2018). This phenomenon was discovered using a reporter strain that expresses *GFP* under the control of the *hsp-90* promoter.

Our group has sought to further elucidate the underlying mechanisms that guide TCS in *C. elegans* and to that end, an RNAseq analysis was performed using *C. elegans* that exhibits TCS driven by the tissue specific overexpression of HSP-90 in the neurons and intestine. This analysis identified a number of genes that are upregulated under these conditions, and analysis of the promoter regions of these genes using Hypergeometric Optimization of Motif EnRichment (HOMER) (Heinz et al., 2010) identified an overrepresentation of a consensus binding sequence that matched the binding motif of the zinc-finger transcription factor *pqm-1*. There is a significant reduction in the expression of *hsp-90* in distal tissues in a *pqm-1* (ko) deletion mutant relative to the wildtype, and this phenotype also presented when RNAi-mediated *pqm-1* knock-down

was used (O'Brien et al., 2018). These results confirmed the *pqm-1* was indeed a mediator of transcellular chaperone signalling (Figure 2.1, O'Brien et al., 2018). Figure 2.1 shows that *hsp-90p::GFP* expression is low in a control strain at 20C (Figure 2.1A i-iii). If, however, *HSP-90::RFP* is over-expressed tissue specifically in either the neurons, intestine, or muscle there is an upregulation of *hsp-90* expression, as measured by the GFP reporter (Figure 2.1; van Oosten-Hawle et al., 2013; O'Brien et al., 2018). The overexpression of HSP-90 in the neurons causes compensatory upregulation of *hsp-90* in distal tissues, particularly in the body wall muscle (Figure 2.1B i-iii). Similarly, the overexpression of HSP-90 in the intestine causes upregulation of *hsp-90* distally, again most noticeably in the body wall muscle (Figure 2.1C i-iii). When HSP-90 is upregulated in the body wall muscle, distal activation of *hsp-90* can be observed by increased *GFP* expression in the pharynx (Figure 2.1D i-iii). When these strains are crossed into a *pqm-1* (ko) background, the intensity of the GFP is reduced compared to the control strain, indicating the requirement of *pqm-1* for TCS when HSP-90 is tissue specifically overexpressed (Figure 2.1B iv-vi; C iv-vi; D iv-vi).

PQM-1 is required in the 'stressed' sender tissue, i.e. the tissue overexpressing *hsp-90.* Our group identified that PQM-1 in the sender tissue acts to upregulate tissue dependent downstream effectors: For example, in the neurons PQM-1 upregulates *clec-41* to activate TCS and *hsp-90* upregulation in the muscle; in the intestine PQM-1 upregulates *asp-12* to enact TCS (O'Brien et al., 2018).

2.2 PQM-1 and longevity

Previously, PQM-1 has been shown to play a role in *C. elegans* aging - it was found that nematodes which lack *pqm-1* develop more slowly than wildtype, but lifespan is unaffected (Tepper et al., 2013). Depletion of *pqm-1* in a *daf-2* mutant background however reduces the lifespan extension afforded by the *daf-2* mutant (Tepper et al., 2013). Therefore, although *pqm-1* alone does not influence lifespan, it is important for *daf-2* mediated lifespan extension.

This result led us to explore the possibility that PQM-1 played a role in the regulation of proteostasis, during extraneous stress as well as conditions that activate TCS.

Heat stress acts rapidly to perturb the proteostasis network – many proteins are stable only in favourable conditions including pH (Tanford and Roxby, 1972), salt content (Takeda et al., 1989), and in a narrow temperature range (Gidalevitz et al., 2011). The abrupt increase in temperature from 20°C to 35°C is a stress that can be fatal after a matter of hours to wildtype *C. elegans*, and extended exposure to 30°C for more than a few hours can cause sterility (Lithgow et al., 1994).

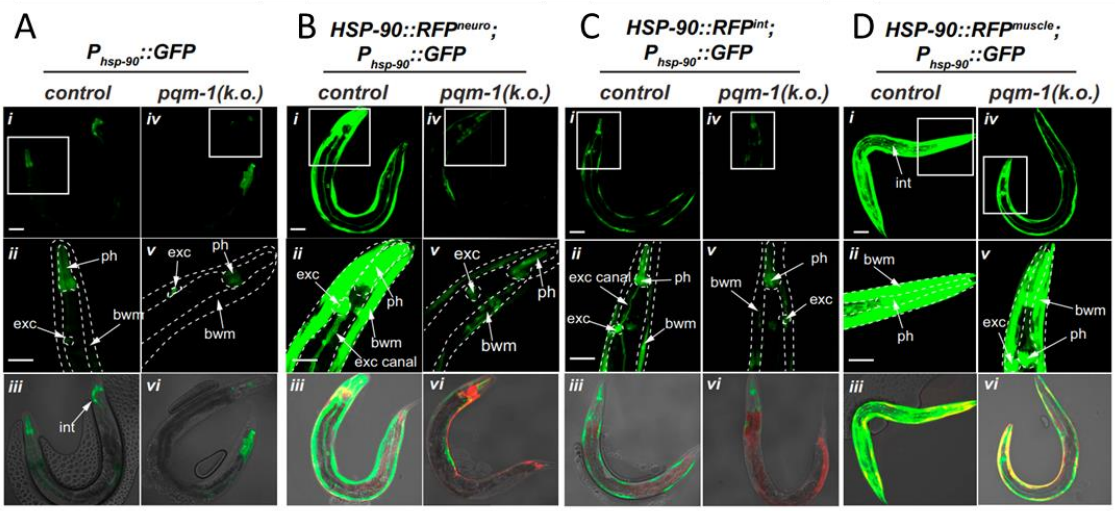

Figure 2.1. PQM-1 Mediates TCS in *C. elegans*.
Collapsed z-stack images of young adult *C. elegans* expressing the P_{hsp-90}::GFP reporter in control background (Ai), *HSP-90::RFP*^{neuro} (Bi), *HSP-90::RFP*^{int} (Ci), and *HSP-90::RFP*^{muscle} (Di) compared with expression of the P_{hsp-90}::GFP reporter in a *pqm-1*(ko) mutant background. Expression of *Phsp-90::GFP* in a *pqm-1*(ko) mutant background (Aiv), *HSP-90::RFP*^{neuro}*;pqm-1* (ko) (Biv), *HSP-90::RFP*^{int}*;pqm-1*(ko) (Civ), or *HSP-90::RFP*^{muscle}*;pqm-1* (Div). 20x magnification of the anterior (head) region (Aii, Av, Bii, Bv, Cii, Cv, Dii, and Dv). Differential interference contrast (DIC) Nomarski, GFP, RFP overlay images. Tissues showing P_{hsp-90}::GFP expression are indicated with a white arrow. (bwm) bodywall muscle; (exc) excretory cell; (exc canal) excretory canal; (ph) pharynx; and (int) intestine. Figure provided by Patricija van Oosten-Hawle (O'Brien et al., 2018).

2.2.1 PQM-1 and DAF-16

The expression of PQM-1 is thought to be largely confined to the intestine, with some expression also thought to occur in neurons (Reece-Hoyes et al., 2007; Tepper et al., 2013; O'Brien et al., 2018). It has been reported that PQM-1 has a complementary role to the FOXO transcription factor DAF-16. It was found that DAF-16 did not directly bind to a subset of the genes that it appeared to regulate, and that these genes held a common motif (TGATAAG), termed the DAF-16 - associated element (DAE) (Tepper et al., 2013). The authors found that the motif matched the binding site for PQM-1, as determined by a previous ChIPseq experiment as part of the modENCODE project (Niu et al., 2011). Tepper and colleagues also demonstrated that PQM-1 and DAF-16 had a mutually antagonistic relationship, whereby the presence of one of the transcription factors in the intestinal nuclei prevented the entry of the other (Tepper et al., 2013).

2.2.2 *C. elegans* models of protein misfolding diseases

As previously mentioned, there are several useful protein misfolding disease model strains in *C. elegans*. The expression of aggregation prone proteins adds extra burden to the PN, and leads to paralysis in the nematodes (Morley et al., 2002). Perturbations to the PN can influence the rate of paralysis in these nematodes e.g. in an *age-1* mutant background, the toxicity of the aggregation prone protein is delayed (Morley et al., 2002). Likewise, RNAi mediated knockdown of *age-1* leading to activation of HSF-1 and DAF-16 supresses the slow movement of ts mutations of paramyosin and myosin heavy chain B at the restrictive temperatures (Ben-Zvi et al., 2009). Furthermore, the knockdown of either *hsf*-1 or *daf-16* by RNAi exacerbated the ts phenotype (Ben-Zvi et

al., 2009). Therefore, we used the aggregation-prone Q35 model to assess whether the loss of *pqm-1* influenced the efficacy of the PN.

The expression of $A\beta_{(3-42)}$ in the muscle causes paralysis at a faster rate than in the wildtype and to generate amyloid aggregates in the affected cells (Link, 1995). We hypothesised that *C. elegans* with active TCS, due to overexpression of *hsp-90* in the neurons or intestine could be beneficial to the protein folding environment in the muscle of Aβ expressing nematodes.

2.3 Overview

At the outset of the project we had identified that PQM-1 is required for transcellular chaperone signalling caused by a tissue-specific imbalance of proteostasis through HSP-90 overexpression. Second, *pqm-1* has been shown to be strongly upregulated at the transcript level when populations of *C. elegans* are exposed to the oxidative stress-inducing agent paraquat (Tawe et al., 1998). Building on this we sought to find out whether PQM-1 was required for *C. elegans* response to acute heat stress, or the chronic stress placed on the PN by the accumulation of misfolded toxic protein aggregates.

2.4 Materials and Methods

2.4.1 Nematode Maintenance and strains

Nematodes were grown at 20°C, fed on the *E. coli* strain OP50-1, and maintained as previously described (Brenner, 1974). The following strains were used: N2 Bristol (wildtype strain); PS3551 (*hsf-1 (sy441) I);* RB711 (*pqm-1 (ok485) II);* CL2006 (*dvIs2 [pcL12(unc-54/human Abeta peptide minigene)+pRF4*] which were obtained from the *Caenorhabditis* Genetics Center. The Q35 Huntington's Disease model was a gift from Dr. Richard I. Morimoto (AM167 (*rmIs156[unc-54p::Q35::YFP]*)). The *pqm-1(ok435)* mutant was crossed into AM167 to result in PVH45 *(rmIs156[unc-54p::Q35::YFP; pqm-1(ok435)]* and into PS351 to generate PVH46 ((*hsf-1 (sy441) I); (pqm-1 (ok485) II)).* The $A\beta_{(3\text{-}42)}$ expressing strain (CL2006) was crossed into the genetic background of strains overexpressing HSP-90::RFP in the neurons (HSP-90::GFP^{neuro} (AM778 (*rmIs314 [F25B3.3p::DAF-21::GFP]; pCFJ90[myo-2p::RFP*])) or, intestine (HSP-90::$RFP^{intestine}$ (AM986 *rmIs346[vha-6p::DAF-21::RFP*])), or body wall muscle (HSP-90::RFP^{bwm} (AM988 (*rmIs347(unc-54p::DAF-21::RFP*]), resulting in strains PVH85 (*rmIs345[F25B3.3p::DAF-21::RFP]; dvIs2*), PVH127 (*rmIs346[vha-6p::DAF-21::RFP]; dvIs2*), and PVH50 (AM988 (*rmIs347(unc-54p::DAF-21::RFP]; dvIs2*), respectively.

2.4.2 RNAi mediated knockdown

In order to knockdown the indicated genes by RNAi, L4 nematodes were placed onto NGM plates supplemented with Ampicilin and IPTG seeded with *E. coli* strain HT115(DE3) transformed with RNAi vectors (J. Ahringer, University of Cambridge, Cambridge, UK) and allowed to lay eggs, adult nematodes were removed and the progeny was grown until L4. Nematodes were then collected into ice cold M9 and flash frozen in liquid nitrogen. When it was not possible to grow nematodes in this way, starved L1s from bleached populations were deposited onto plates to generate synchronous populations.

2.4.3 Thermotolerance Assays

Nematodes were picked at L4 stage and placed onto 6 cm NGM plates. Plates were sealed with waterproof tape and then placed in a water bath which held a temperature of 35°C for the times indicated. The survival of the nematodes was scored after 16 hours recovery at 20°C by a touch nose response assay (Kaplan and Horvitz, 1993).

2.4.4 RT-qPCR

RNA was extracted from *C. elegans* following addition of TriZOL reagent and disruption of the nematodes in a microcentrifuge tube using a battery powered grinder. RNA was subsequently purified using the Zymo-prep RNA Mini Isolation kit (Zymo Research, Cambridge Biosciences). RNA concentrations were measured using a nanodrop device. mRNA was reverse transcribed using the iScript cDNA Synthesis Kit (Bio-Rad) and the q-PCR was performed using iQ SYBR Green Supermix (Bio-Rad). qPCR was performed using

the iCycler system (Bio-Rad). *cdc-42* was used as a control in each case as a reference gene (Hoogewijs et al., 2008).

2.4.5 Western blot

For Western Blot analysis, cell extracts were prepared of 10.000 age-synchronised animals grown on 10 cm NGM plates at a population density of 1000 nematodes per plate. Young adult animals were harvested into a nematode pellet of 200 ul and flash frozen in liquid nitrogen. The frozen pellet was supplemented with an equal volume of Nematode Lysis Buffer (10 mM Tris pH 7.5; 150 mM NaCl; 0.5 mM EDTA; 0.5% NP-40), supplemented with EDTA-free protease inhibitor cocktail tablet (Complete Mini, EDTA-free, Roche) and ground with a pestle. The cell extract was prepared by centrifugation at 10 000 x g for 5 minutes at 4°C and protein concentration was determined using the Bio Rad protein assay kit (Bradford assay). Cell extracts were mixed with 5x SDS sample buffer and boiled for 5 min. 25 µg total protein was loaded onto a 10 % SDS-PAGE and western blot analysis was performed as described previously (van Oosten-Hawle et al., 2013). To detect *C. elegans* endogenous HSP-90 or a poly clonal anti-C.e. HSP-90 antibody raised in rabbit was used (van Oosten-Hawle et al., 2013). A monoclonal mouse anti-tubulin antibody (Sigma) was used to detect tubulin to act as a loading control. HRP-conjugated anti-mouse or anti-rabbit antibodies were used as secondary antibodies and ECL reagent (Thermo Fisher Scientific) was used for detection.

2.4.6 Western Blotting of Aβ species

The Aβ species of *C. elegans* which express $A\beta_{(3-42)}$ in the body wall muscle (CL2006) or in strains overexpressing HSP-90::RFP in the muscle (PVH50), intestine (PVH127) or

neurons (PVH85) was identified by immunoblotting. Briefly, samples were loaded on a 16% Tris-Tricine gel containing 6M urea, and the standard Western blotting protocol was followed, except that the 0.2 µm nitrocellulose membranes were boiled in 50ml PBS buffer for 5 min post transfer. 200 age synchronised nematodes per strain were collected at day 3 of adulthood into M9 buffer on ice, washed in cold M9 and flash frozen in liquid nitrogen. Lysis buffer consisting of 62 mM Tris-HCl pH 6.8, 5% β-mercaptoethanol, 10% glycerol, 2% SDS, and 1x protease inhibitor cocktail tablet (Roche) was added to the frozen pellets which were then ground using a pestle to release the protein. Samples were then spun for 5 minutes at 10, 000 x *g*. 50 µg of total protein for each sample was loaded onto the 16% Tris-Tricine gel. Amyloid monomeric and oligomeric species were detected with 6E10 monoclonal antibody (1:500, Absolute Antibody). Tubulin (anti-tubulin antibody; Sigma) was used as a loading control.

2.4.7 Confocal microscopy

Nematodes were imaged using a Zeiss LSM880 confocal microscope through a 10x 1.0 or a 20x 1.0 numerical aperture objective with a 488 nm line for excitation of GFP, 561nm line for excitation of mCherry (RFP) and 405 nm line for excitation of X-34. For imaging, age-synchronised animals were immobilised using 5 mM Levamisole solution in M9 buffer and mounted on 2% agarose pads.

2.4.8 Paralysis

Paralysis assays were performed on 100 age synchronised nematodes which expressed *Q35::YFP* in the body wall muscle of the animal in a *pqm-1(ok485)* or wildtype. Nematodes were scored for mobility and transferred each day to a fresh plate.

Nematodes were recorded as being paralysed if they failed to complete a full body movement (Mccoll et al., 2012).

2.4.9 Aggregate counting

Age synchronised nematodes expressing *unc-54p::Q35::YFP (mQ35)* were imaged using a Leica MZ10F fluorescent stereoscope combined with a YFP filter. The number of aggregates were counted for each animal and recorded.

2.4.10 X-34 staining

Nematodes were transferred into 500µL M9 in a microcentrifuge tube. The supernatant was removed, and the animals were resuspended in 1mM X-34 (10mM Tris pH 8.0, from 62mM X-34 stock in DMSO stored at 4°C). Samples were then incubated for 2 hours at 20°C on a rotating platform. Supernatant was once again removed once the nematodes had settled to the bottom. The pellet was resuspended in M9 and plated onto fresh NGM plates. Plates were then incubated for 12-16 hours at 20°C before imaging using the confocal microscope as detailed in section 2.4.7.

2.5 Results

The aim of this chapter is to address the role of the zinc finger transcription factor PQM-1 in the heat stress response and proteostasis. I therefore performed thermotolerance assays on *C. elegans* lacking PQM-1 by using *pqm-1* (ko) deletion mutants or RNAi mediated knockdown of *pqm-1*. Investigation of the expression of certain key chaperones in *C. elegans* revealed a role for HSP-90. Further assays using aggregation prone exogenous proteins reinforced the importance of PQM-1 in overcoming proteotoxic stress. I also investigated the underlying molecular basis for the disruption of Aβ paralysis rescue by TCS in a *pqm-1* knockout background. The loss of *pqm-1* alters the profile of the Aβ oligomeric species as well as the accumulation of amyloid in the body wall muscle.

2.5.1 PQM-1 is required for heat stress survival in *C. elegans*

At the outset of the project, there was no evidence in the literature that PQM-1 was required for heat stress survival, yet the identification of PQM-1 as a mediator of transcellular chaperone signalling suggested that PQM-1 could be involved in stress response signalling and proteostasis. To investigate whether PQM-1 plays a role for heat stress survival, we took advantage of a *pqm-1* knockout (ko) strain, RB711 *[pqm-1(ok485)]*. Our studies revealed that when *pqm-1* is genetically ablated, heat stress survival is significantly worse when nematodes are exposed to 35°C conditions for 4, 5 or 6 hours (Figure 2.2A). After 4 hours of heat stress on control RNAi (*EV*), survival of the *pqm-1* (ko) was less than 60% with more than 80% of wildtype nematodes surviving in the equivalent conditions (Figure 2.2A).

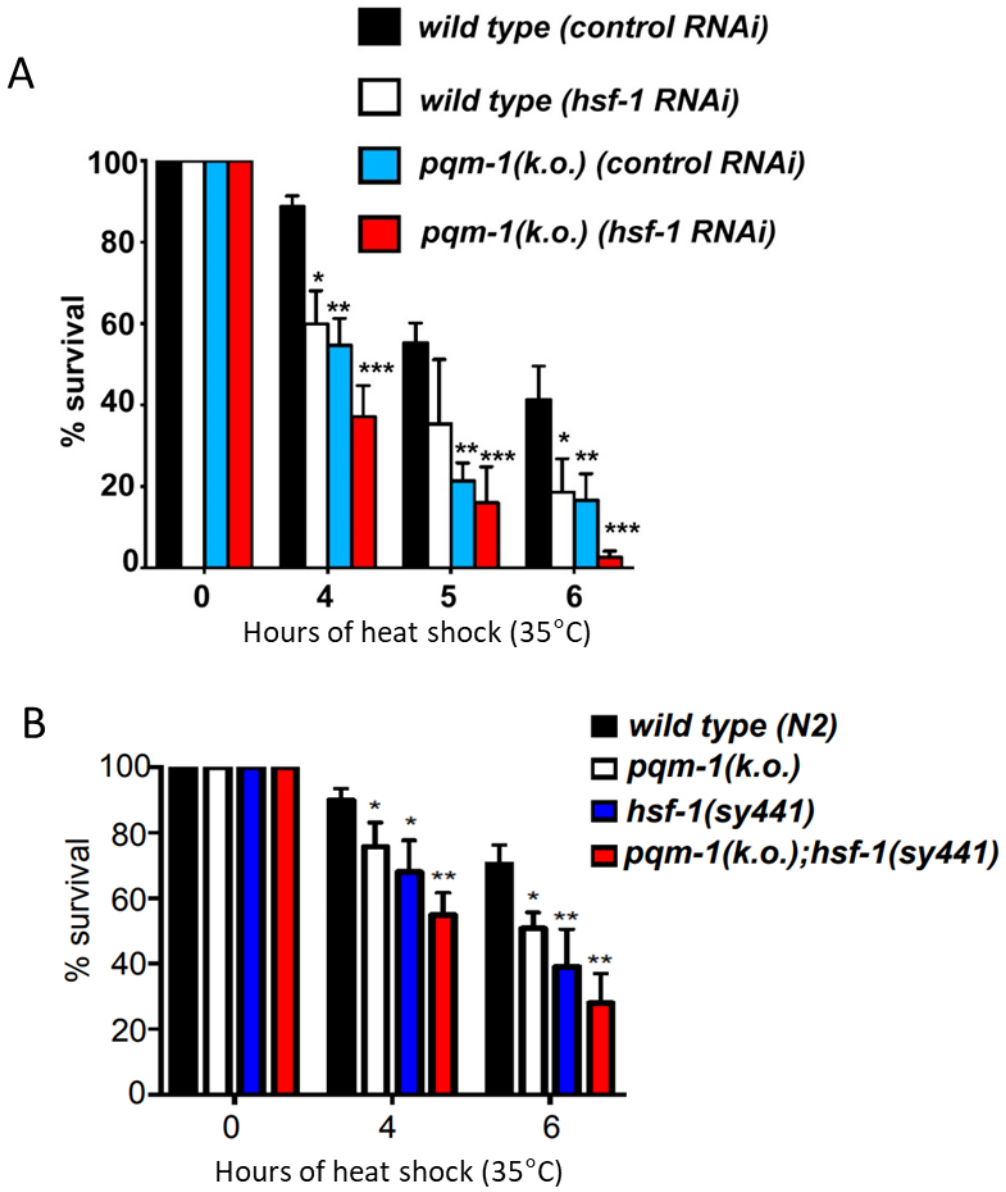

Figure 2.2. PQM-1 is required for heat stress survival in *C. elegans.*

(A)Thermotolerance of L4 animals (n = 20; five biological replicates) with indicated genotypes: wildtype (N2); *pqm-1 (ok485),* during control or *hsf-1* RNAi after exposure to a 35°C heat shock for 4, 5, or 6 hours. Survival was measured after a recovery period of 16 hours at 20°C. * P < 0.05 ** P < 0.01 ***P < 0.001 Error bars represent ± SEM. (B) Thermotolerance of L4 animals (n ≥ 20) with indicated genotypes: wildtype; *pqm-1 (ok485); hsf-1 (sy441); (pqm-1 (ok485);hsf-1 (sy441)),* after exposure to 35°C heat shock for 4 or 6 hours. Survival was measured after a recovery period of 16 hours at 20°C. * P < 0.05 ** P < 0.01. Error bars represent ± SEM.

At 5 hours heat exposure only 25% of *pqm-1* (ko) animals survived, compared to 50% survival measured in control animals (Figure 2.2A). After 6 hours of heat stress conditions only 20% of *pqm-1* (ko) nematodes survived compared to more than 40% of wildtype nematodes. In each case the survival of the *pqm-1* (ko) strain is very similar to the *hsf-1 (sy441)* mutant or *C. elegans* fed with *hsf-1* RNAi – indicating that there is a detrimental effect to removal of PQM-1 under these conditions (Figure 2.2A). Furthermore, when *pqm-1* (ko) nematodes are grown on *hsf-1* RNAi there was an exacerbated heat sensitivity at all conditions measured (Figure 2.2A). After 4 hours of heat exposure only 40% of *pqm-1* (ko) animals treated with *hsf-1* RNAi survived. At 5 hours less than 20% survived the heat stress, and at 6 hours only 5% of the nematodes survived the stress conditions.

To confirm the result, *pqm-1* (ko) nematodes were fed OP50-1 *E. coli* and assayed for their resistance to thermal stress (Figure 2.2B). Once again at the 4 hour and 6 hour time points, the *pqm-1* (ko) animals had significantly worse survival than the wildtype control. Once again *hsf-1 (sy441)* nematodes were used as a control for the heat shock experiments - the *hsf-1 (sy441)* strain produces an HSF-1 product that does not properly enact the heat shock response (Hajdu-Cronin et al., 2004). The *hsf-1 (sy441)* mutation truncates the terminal 86 amino acids of the HSF-1 protein, eliminating the hydrophobic heptad repeat (HR-C) and the transcriptional activation domain (TAD) which are required for transcription at the heat-shock promoter. A full *hsf-1* knockout has an embryonic lethal phenotype. In each case the *hsf-1 (sy441)* mutant strain was more thermosensitive than the wildtype – acting as a positive control for the conditions that the animals were exposed to. Interestingly, when the *pqm-1* (ko) mutant was genetically crossed into the *hsf-1* mutant background, these nematodes were more susceptible to

heat stress than when either transcription factor was individually compromised (Figure 2.2B). This demonstrates that the two transcription factors independently confer heat stress resistance to the organism.

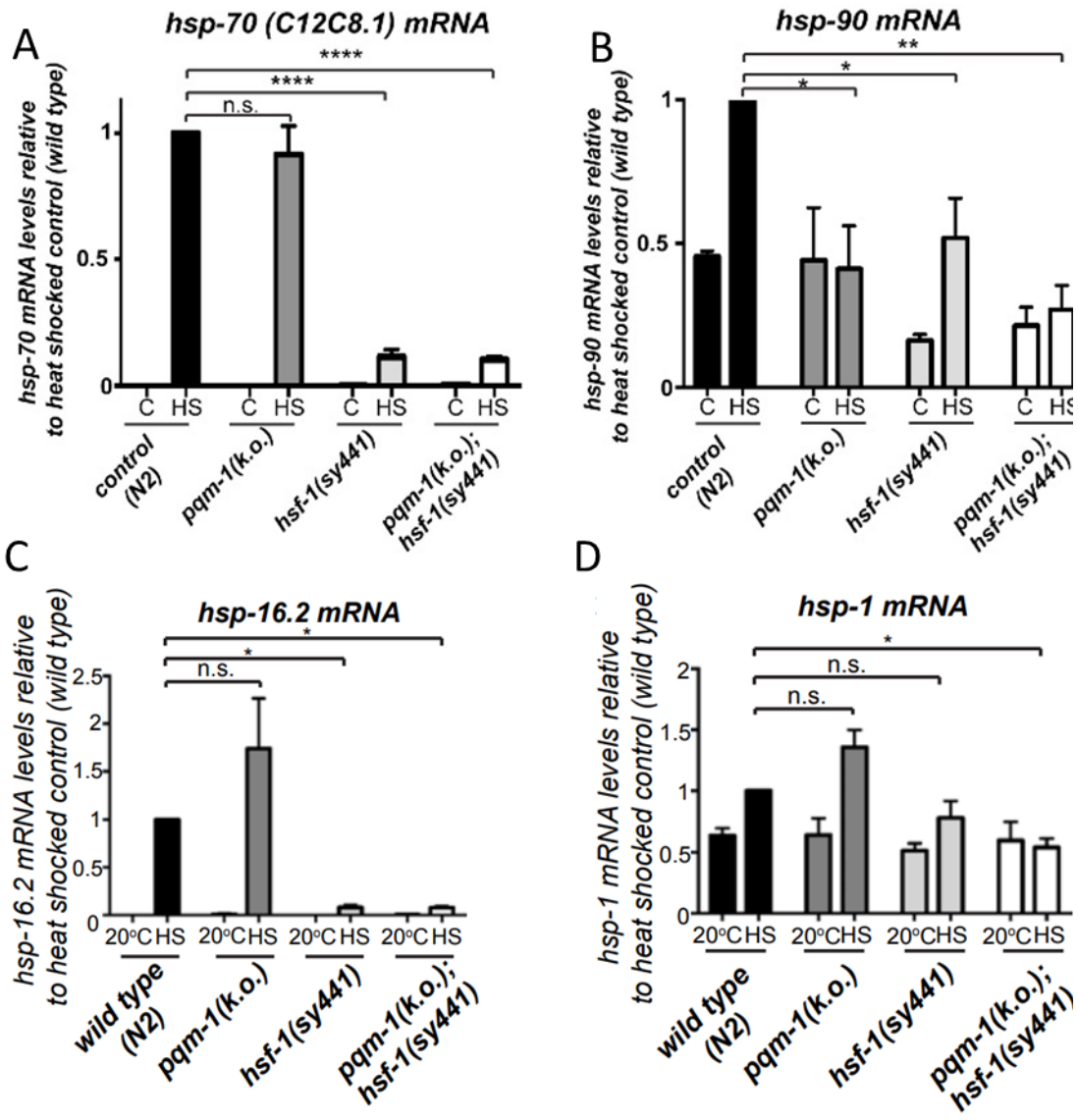

Figure 2.3. In *C. elegans, hsp-90* is differentially regulated during heat stress in the absence of *pqm-1.*

Quantitative RT-PCR analysis to measure differential chaperone expression transcripts. (A) Expression levels of *hsp-70 (C12C8.1)* mRNA relative to control animals. (B) Expression levels of *hsp-90* transcripts during heat shock relative to control animals. (C) Expression levels of *hsp-16.2* transcripts during HS relative control. (D) Expression levels of *hsp-1* mRNA transcripts during HS control animals.

2.5.2 Chaperone expression is altered after heat shock exposure in *C. elegans* lacking *pqm-1*.

To understand a potential mechanism for the inferior thermotolerance of the *pqm-1* (ko) we investigated the induction of several key molecular chaperones by qRT-PCR analysis. The major molecular chaperone *hsp-90*, and heat responsive *hsp-70 (C12C8.1)* were chosen as they have previously been shown to be required for stress survival (Taipale et al., 2010; Mayer, 2013; Kim et al., 2013). Furthermore, both have been implicated in PQM-1 mediated TCS (van Oosten-Hawle et al., 2013; O'Brien et al., 2018). The induction of the heat responsive *hsp-70* was not affected by *pqm-1* (ko) as it is induced to wildtype levels upon heat stress (Figure 2.3A). As expected in the *hsf-1* mutant strain *hsp-70* was not induced, with expression levels ten times lower than the wildtype under the same conditions, nor was it induced when the *pqm-1* (ko); *hsf-1* double mutant is subject to heat stress. The major molecular chaperone *hsp-90* was regulated by *pqm-1* under these conditions – although at ambient temperatures (20°C) there was no difference in *hsp-90* mRNA levels between the wildtype and *pqm-1* (ko) (Figure 2.3B). After exposure to acute heat stress for an hour (35°C), *hsp-90* mRNA levels in the *pqm-1* (ko) mutant remained at a level similar to ambient conditions. In the *hsf-1* mutant, there were low levels of *hsp-90* under ambient conditions and heat shock did not fully induce the expression of *hsp*-90, with levels then reaching the background level that is seen in the wildtype at 20°C. In the *pqm-1* (ko); *hsf-1 (sy441)* mutant strain there was no induction of *hsp-90* mRNA levels under heat stress conditions, indicating that both transcription factors are required for proper *hsp-90* induction.

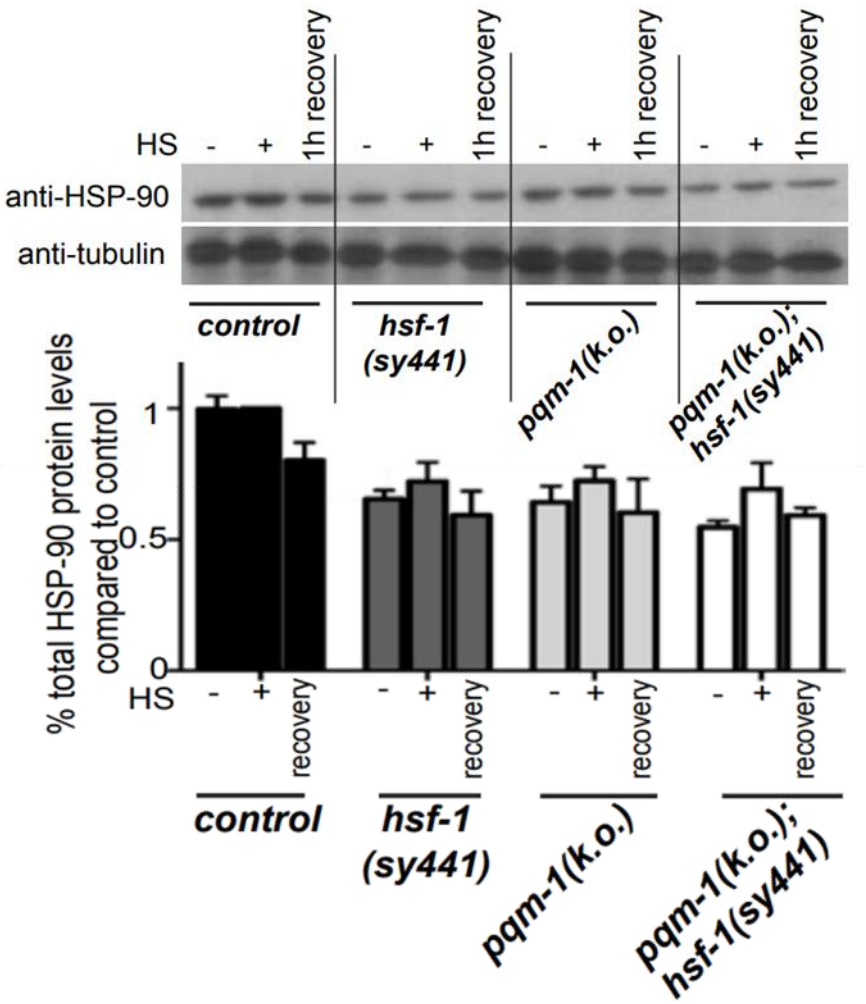

Figure 2.4. The major molecular chaperone HSP-90 is differentially regulated during stress in the absence of *pqm-1.*

Western blot analysis of HSP-90 protein expression at 20°C (-), immediately after a 1h 35°C HS (+), and after a 1h recovery period at 20°C in young adult control animals, *hsf-1(sy441)* mutant, *pqm-1*(ko) mutant and *pqm-1*(ko);*hsf-1(sy441)* double mutants.

The small heat shock protein *hsp-16.2* has been previously reported to be an important factor for stress resistance (Prahlad et al., 2008). Therefore we investigated whether its expression was influenced by *pqm-1*. Although it appears there is an induction of *hsp-16.2* mRNA levels after heat stress in the *pqm-1* (ko) mutant, the difference is not statistically significant when compared to control animals (Figure 2.3C). As expected, the induction of *hsp-16.2* mRNA levels was severely restricted in the *hsf-1* mutant, as well as in the double mutant *pqm-1* (ko); *hsf-1 (sy441).*

Constitutively expressed *Hsc70* (*hsp-1*) is a major chaperone which is expressed under ambient conditions in *C. elegans* (Heschl and Baillie, 1990). After heat stress *hsp-1* levels are induced by 50% (Figure 2.3D). The induction of *hsp-1* does not seem to be affected in the *pqm-1* (ko) strain, as transcript levels are similar to wildtype animals at both 20°C and after 35°C. The induction of *hsp-1* mRNA was not significantly altered in the *hsf-1 (sy441)* mutant, or in the double mutant above the wildtype basal expression levels at the permissive temperature (20°C). After heat shock, however, in the double *pqm-1* (ko); *hsf-1 (sy441*) mutant, there was a significant reduction in *hsp-1* levels (50% of wildtype), which is a further indication of the interplay between these two stress responsive factors.

To confirm whether the decreased mRNA expression of *hsp*-90 is reflected in a similarly reduced expression of protein levels, we examined HSP-90 protein levels by Western Blot analysis using an anti-HSP-90 antibody. HSP-90 expression is reduced in the *hsf-1* mutant *(sy441)* compared to the wildtype when samples are collected at 20°C, immediately following heat shock, and after a 1-hour recovery post heat shock (Figure 2.4). A similar pattern was observed for the *pqm-1* (ko) mutant strain with HSP-90

proteins levels reduced to approximately 70% compared to control animals at each time point. The *pqm-1* (ko); *hsf-1 (sy441)* mutant strain also exhibited reduced HSP-90 protein expression, indicating that both *pqm-1* and *hsf*-1 are required for heat-stress dependent expression of HSP-90.

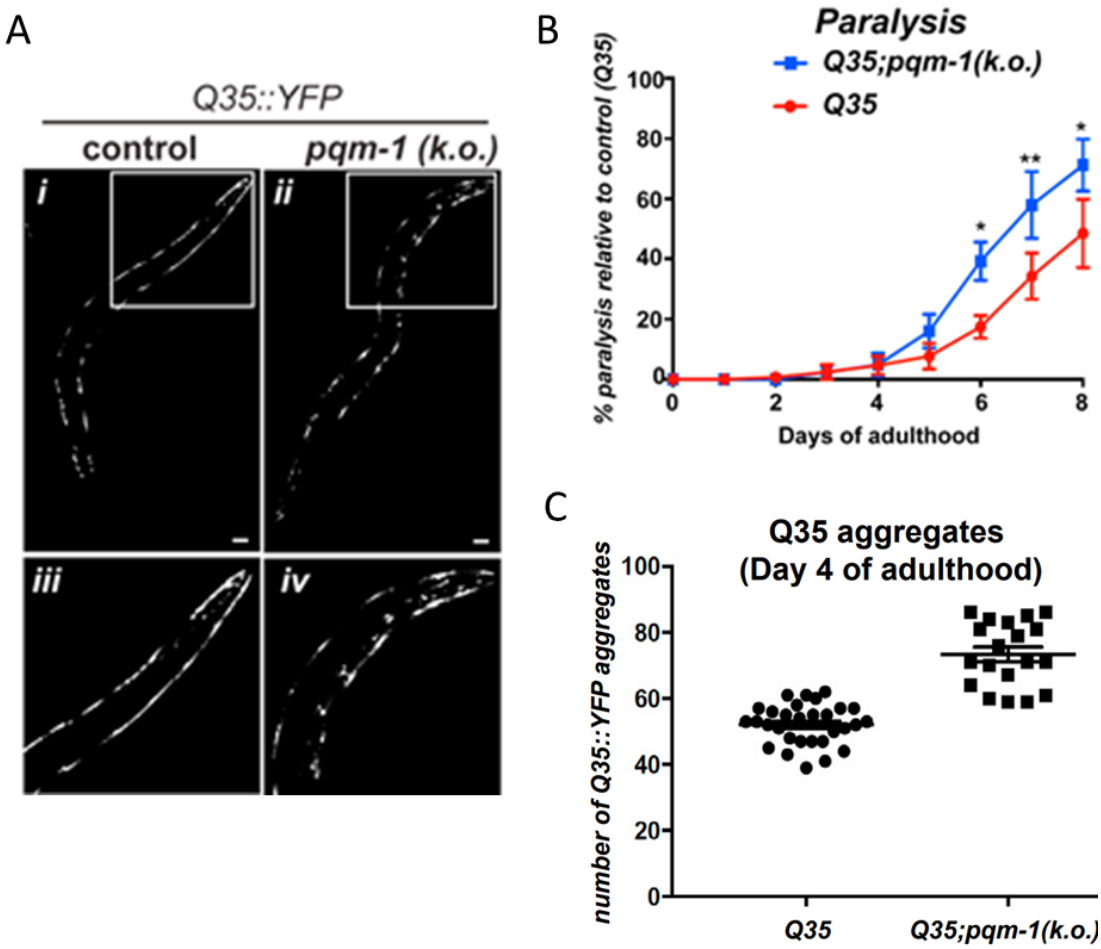

Figure 2.5. The proteostasis sensor Q35 model reveals that *pqm-1* is required to maintain proteostasis throughout aging.

(A) Day 4 adult *C. elegans* which express Q35::YFP in the body wall muscle: control animals (i and iii) and *pqm-1* (ko) mutants (ii and iv). 20x magnification of anterior (head) region of control and *pqm-1* (ko) mutants (ii and iv). Scale bar, 50 µm. (B) Paralysis was measured in age-synchronized nematodes expressing *Q35::YFP* in the body wall muscle (Q35) in wildtype (control) background and *pqm-1*(ko) mutant background animals at the indicated time points (100 animals per biological replicate, N = 3). ∗p < 0.05; ∗∗p < 0.01; paired t test. Error bars represent ± SEM. (C) *Q35::YFP* aggregation is enhanced in *pqm-1*(ko) mutants. Quantification of accumulated Q35 foci in age-synchronized day 4 adults of *pqm-1*(ko) mutants and control animals. *p < 0.05.

2.5.3 Polyglutamine aggregation is more severe in a *pqm-1* (ko) background

In order to gain an understanding of whether *pqm-1* plays a role in proteostasis during aging, we used the *C.elegans* Huntington's Disease model expressing Q35::YFP in the body wall muscle and crossed it into the genetic background of *pqm-1* (ko) mutants. As shown in Figure 2.5, there are higher numbers of Q35::YFP aggregates when *pqm-1* is knocked out compared to control animals. At day 4 of adulthood *Q35;pqm-1 (ko)* exhibit 70 aggregates per nematode compared to control animals which have 50 visible aggregates per nematode (Figure 2.5C). This can also be seen in the representative images of the animals (Figure 2.5A) which show the difference in aggregation level between the two backgrounds. Additionally, when the motility of the animals is scored in a paralysis assay, it is clear that there is a significantly higher proportion of paralysis in *Q35;pqm-1* (ko) animals compared to control. At day 6, 20% of control animals (*Q35::YFP)* are paralysed, and 40% of *Q35;pqm-1* (ko) animals are paralysed (Figure 2.5B). At day 8, 50% of the control animals are paralysed compared to 70% of the *Q35*;*pqm-1* (ko) nematodes.

2.5.4 Transcellular chaperone signalling is protective against Aβ aggregation

We had previously established HSP-90::RFP overexpression in the neurons or intestine protects against $A\beta_{(3-42)}$-mediated toxicity when expressed in muscle cells via TCS (Figure 2.6). This figure was provided by Sarah Good (O'Brien et al., 2018). Expression of human amyloid Beta (Aβ) in the body wall muscle of *C. elegans* leads to a severe paralysis phenotype, with approx. 50% of nematodes paralysed by day 8 of adulthood, while only 15% of wildtype *C. elegans* are paralysed at the same time point. Aβ induced paralysis

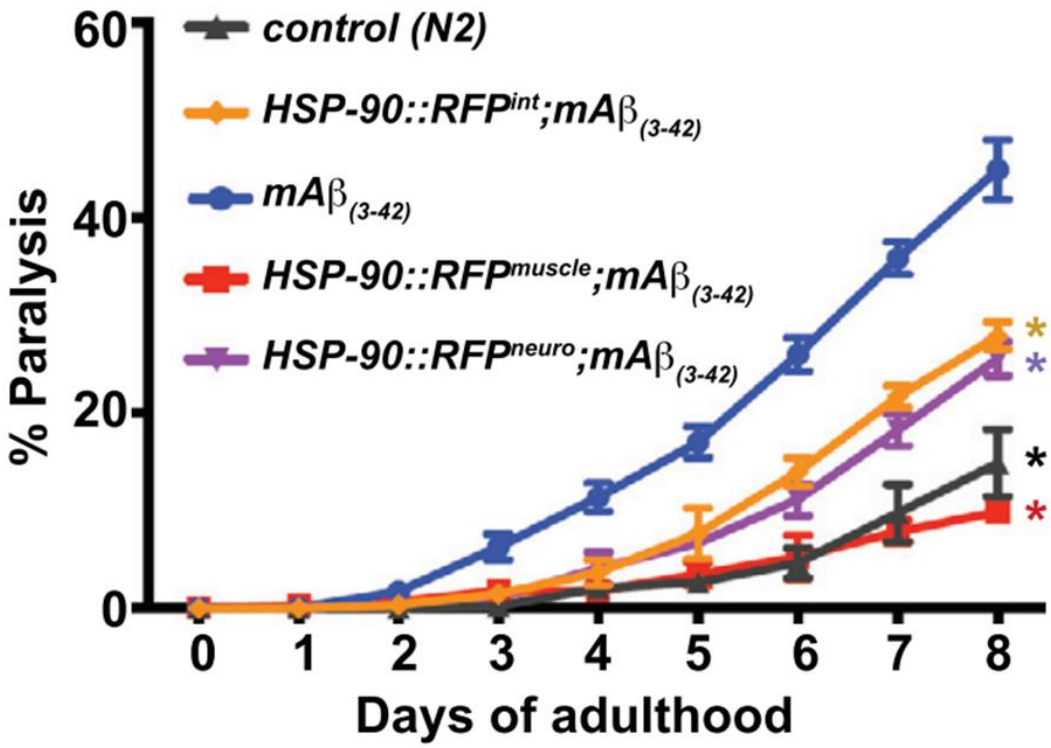

Figure 2.6. TCS driven by tissue specific HSP-90 overexpression protects against Aβ(3-42) Protein Toxicity in muscle.

Paralysis assays of *C. elegans* expressing Aβ(3-42) in the body wall muscle (CL2006) compared to wildtype control or HSP-90::RFP^{neuro}; Aβ(3-42), HSP-90::RFP^{int}; Aβ(3-42), or HSP-90:: RFP^{muscle}; Aβ(3-42). Paralysis data represent SEM of 3 biological replicates (n = 100 animals). Statistical significance was determined by Wilcoxon matched-pairs signed-rank test. *p < 0.05. Figure provided by Sarah Good (O'Brien et al 2018).

can be combatted by the expression of HSP-90::RFP in specific tissues. When HSP-90::RFP was expressed in the body wall muscle, the same tissue also expressing Aβ, paralysis was prevented, with only 10% of nematodes paralysed at day 8 of adulthood (Figure 2.6). Similarly, expression of HSP-90::RFP in distal tissues can protect against Aβ induced paralysis via TCS – as in these cases the Aβ and HSP-90::RFP do not directly interact as they are expressed in different tissues. When HSP-90::RFP was expressed in the intestine, paralysis at day 8 of adulthood was less than 30%. Likewise when HSP-90::RFP was expressed in the neurons, the paralysis levels in day 8 adults were about 30%. In each case this shows that there is a significant reduction in paralysis when TCS is activated, protecting the nematodes from Aβ aggregation and its associated toxicity. Having established that TCS reduces the severity of paralysis that is caused by the expression of the toxic Aβ polypeptide; we sought to characterise the underlying mechanism(s) for the phenotype displayed. Western blotting against the Aβ species revealed that TCS suppresses some of the larger oligomers that could be visualised by the 6E10 antibody (Mccoll et al., 2012) (Figure 2.7A). There were a reduced number of oligomers in the 26 kDa range when HSP-90::RFP is expressed specifically in the neurons or intestine, improving the effectiveness of the proteostasis network in the muscle by TCS. There was also a large reduction in oligomeric species when HSP-90::RFP is overexpressed in the muscle – a cell autonomous effect as HSP-90 is expressed in the same cell-type as Aβ.

To visualise Aβ aggregates in the body wall muscle we used the amyloid-specific dye, X-34 (Styren et al., 2000; Link et al., 2001). This revealed that there is a build-up of amyloid deposits from day 1 of adulthood to day 5 (Figure 2.7B). Control animals (N2) expressing no Aβ showed no X-34 stained build-up of aggregates. When HSP-90 was expressed in

the muscle, there was a drastic reduction in visible Aβ aggregates (Figure 2.7B), consistent with the Western blot and paralysis data (Fig 2.5; Fig 2.6A; O'Brien et al., 2018). The imaging also revealed that when HSP-90 is expressed in distal tissues, there is still a reduction in the amount of visible amyloid in the body wall muscle. HSP-90^{neuro} animals have a reduced amount of Aβ that can be seen in the body wall muscle, and the same is true for HSP-90^{intestine} nematodes (Figure 2.7B).

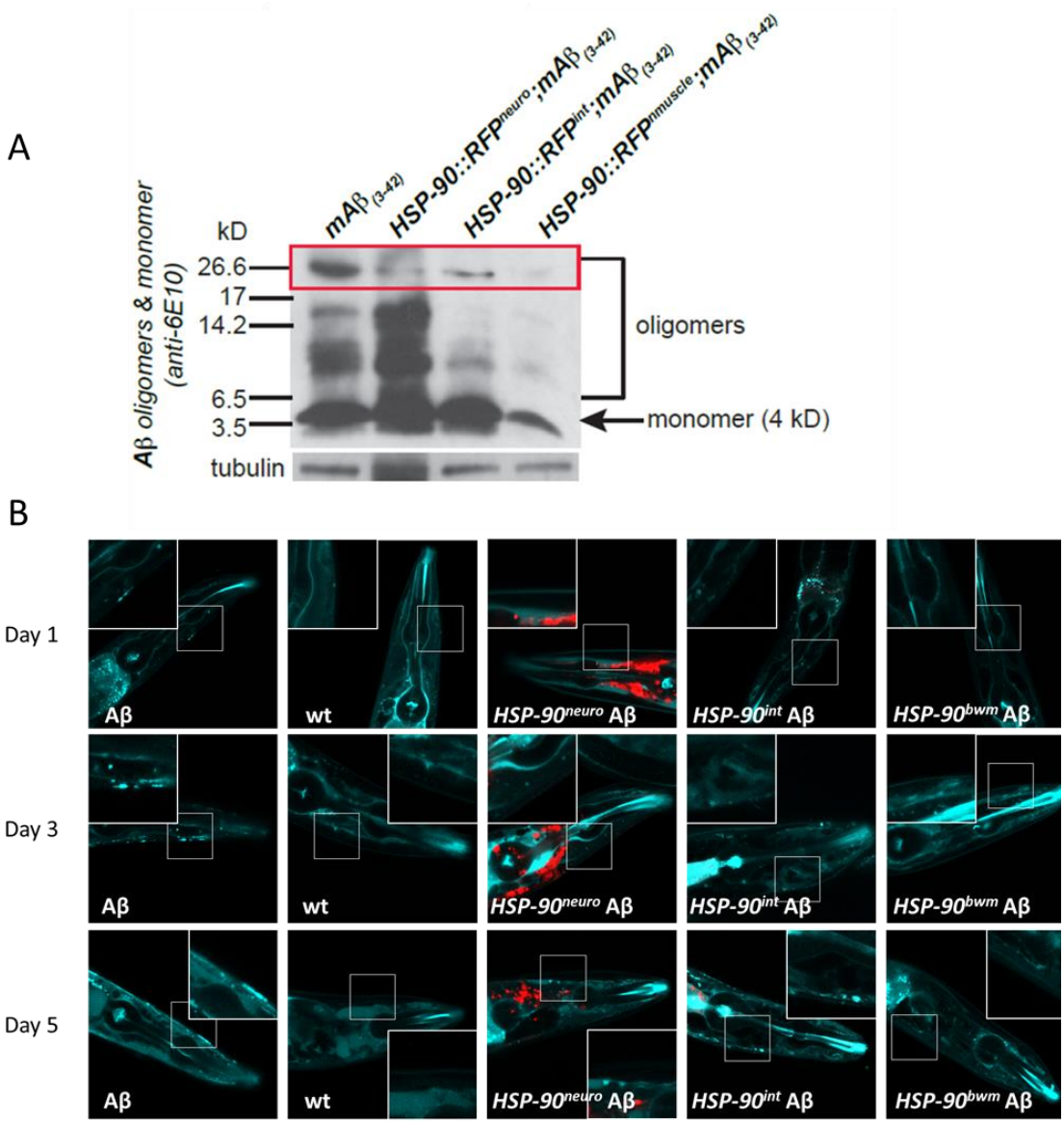

Figure 2.7. Transcellular Chaperone signalling prevents Aβ oligomer build up and toxicity in *C. elegans* body wall muscle.

(A) Western blotting using anti-6E10 antibody to probe for Aβ species when $A\beta_{(3\text{-}42)}$ is expressed in the body wall muscle in wildtype; HSP-90::RFP^{neuro}; HSP-90::$RFP^{intestine}$; or HSP-90::RFP^{muscle} background. Loading control anti-tubulin. (B) Confocal microscopy images of *C. elegans* on day 1; day 3; day 5 of adulthood. The nematodes imaged express Amyloid $Beta_{(3\text{-}42)}$ in the body wall muscle (Aβ), except for the wildtype (wt) negative control. The imaged individuals also express HSP-90::RFP in the neurons; intestine; or body wall muscle, as indicated.

2.6 Discussion

2.6.1 Role of PQM-1 in stress tolerance

The work detailed in this chapter has revealed that PQM-1 is an important stress responsive transcription factor that is required for proper thermotolerance and chronic stress resistance in *C. elegans*. This builds upon previous work which has shown that PQM-1 is a transcription factor that is upregulated during oxidative stress (Tawe et al., 1998) and required for surviving pathogenic infection with *P. aeruginosa* (Shapira et al., 2006). This work shows that PQM-1 is also crucial for *C. elegans* heat stress survival, complementing the requirement for HSF-1 and DAF-16. The discovery of PQM-1 as an important component of the PN demonstrates that there are factors that control proteostasis under some circumstances to complement the canonical stress transcription factors. For example, this is reflected in the regulation of HSP-90 in the establishment of proteostasis by the myogenic transcription factor HLH-1 during muscle development in *C. elegans* (Bar-Lavan et al., 2016). A further example is the regulation of HSP-90 during TCS by the FOXA protein PHA-4 (van Oosten-Hawle et al., 2013). It may be that overall responsibility for proteostasis falls to HSF-1 and DAF-16, but this is complemented by other stress responsive transcription factors, such as PQM-1, that fine tune responses to stress to ensure the PN is safeguarding the proteome.

Moreover, a role for PQM-1 in proteostasis to combat chronic stress ties in to the requirement for PQM-1 for the extended lifespan of *daf-2* mutants (Tepper et al., 2013). Indeed, Tepper et al. observed that the PQM-1 subcellular localisation shifted with age from 80% nuclear to 90% cytoplasmic. This suggested that the large transcriptional

changes that arise throughout aging may be caused by the loss of PQM-1 from the nucleus. It was furthermore demonstrated that the nuclear localisation of PQM-1 and DAF-16 was anticorrelated – they each exclude the other from the nucleus (Tepper et al., 2013). During acute heat stress, PQM-1 leaves the nucleus while DAF-16 enters it (Tepper et al., 2013). Once animals are returned to 20˚C, however, PQM-1 re-enters the nucleus (Chapter 4). It has also been found that PQM-1 functions to antagonise intestinal fat transport to the germline in an mTORC2 regulated manner (Dowen et al., 2016). It may be that during this recovery period PQM-1 is required to promote transcription of genes that are important for heat stress recovery and therefore survival. An alternative is that PQM-1 is required in the nucleus to suppress the allocation of metabolic resources to the germline in times of stress, as misallocation of resources that could be spent repairing the soma could be damaging to organismal health.

It would be interesting to look at the stress resistance of *C. elegans* lacking *sgk-1*, which promotes PQM-1's nuclear export when active (Dowen et al., 2016). Increased PQM-1 localisation to the nucleus might suppress the extent of Q35::YFP aggregation, as we have shown *pqm-1* loss to be deleterious.

2.6.2 Role of PQM-1 in proteostasis in chronic stress conditions

PQM-1 influences chaperone expression under conditions that give rise to TCS (Fig 2.2) and is important for *C. elegans* heat stress survival (Figure 2.2). Therefore, it is not unexpected, that the absence of *pqm-1* can have deleterious effects on the efficacy of proteostasis in *C. elegans* as the animal ages. It is clear that when *C. elegans* express the Huntington's model protein in the body wall muscle there is an increase in the rate of

paralysis compared to wildtype nematodes (Morley et al., 2002). The paralysis worsens as the organism ages and proteostasis decline takes hold (Ben-Zvi et al., 2009) the exhaustion of the PN's resources to combat the toxic aggregation-prone protein lead to a premature breakdown in proteostasis. *C. elegans* lacking *pqm-1* succumbed to proteostasis collapse, protein aggregation and paralysis earlier in adulthood (Figure 2.5) indicating that *pqm-1* is important for the PN's defence against chronic stress. Dietary restriction through either bacterial deprivation or the use of an *eat-2* mutant, which rescues the decline in quality control of proteostasis in early adulthood, has been shown to require PQM-1 (Shpigel et al., 2018). Interestingly, Shpigel et al found that the recruitment of PQM-1 requires an intact germline, as when it is compromised through a *glp-1* mutation, DAF-16 is recruited instead.

The loss of *pqm-1* has both deleterious effects on short term survival of acute proteostasis stress via heat shock and long term consequences for the proteostasis network as the organism ages to defend against chronic stress. The effect of *pqm-1* loss on chaperone expression, specifically *hsp-90 (daf-21)* in *C. elegans* can provide one potential explanation for the wide-ranging effects on proteostasis.

The lower levels of expression of *hsp-90* in the *pqm-1* (ko) strain demonstrates that *pqm-1* can influence the expression of major molecular chaperones, thus indicating that *pqm-1* is an important transcription factor in stress survival. The underlying mechanism for the regulation of *hsp-90* by *pqm-1* remains unknown. Attempts by other members of the lab to investigate the regulation of *hsp-90* by mutagenesis of a potential *pqm-1* binding site in its promoter proved not to alter its expression in the presence and absence of *pqm-1* (O'Brien et al., 2018). It may be that *pqm-1* affects the expression of

hsp-90 through indirect means. PQM-1 is expressed only in neuronal and intestinal tissues (Reece-Hoyes et al., 2007), whereas HSP-90 is expressed in the entire organism (van Oosten-Hawle et al., 2013). Furthermore, PQM-1 is not required in muscle cells to upregulate HSP-90 during TCS (O'Brien et al., 2018). Downstream effectors of PQM-1 are required for TCS: *clec-41* and *asp-12* depending if HSP-90 overexpression is in the neurons or intestine respectively (O'Brien et al., 2018). Therefore, as PQM-1 indirectly regulates *hsp-90* expression in distal tissues, it may be the case that the same is true cell-autonomously.

2.6.3 Protective effects of TCS

The work done in this chapter adds further evidence that TCS enhances organismal proteostasis by activating *hsp-90* expression in the body wall muscle and other tissues. The expression of the $A\beta_{(3-42)}$ peptide in the *C. elegans* body wall muscle is known to cause an array of deleterious effects on the organism including paralysis (Link, 1995).

There is a much greater level of $A\beta_{(3-42)}$ oligomers as shown by Western blotting in the Aβ control strain than when *HSP-90::RFP* is overexpressed in the neurons or intestine, and the level of amyloid seen in the body wall muscle in much lower TCS is activated. The loss in particular of certain oligomeric species could be an underlying reason for the less severe phenotype seen in these animals, as Aβ oligomers are causing toxicity (Kayed et al., 2003; Cline et al., 2018).

There is a beneficial effect to the overexpression of HSP-90 in the same tissue as $A\beta_{(3-42).}$ When both are expressed in the body wall muscle, there are lower levels of $A\beta_{(3-42}$ monomers and small oligomers present in the cells (Figure 2.7A). Furthermore, there

are fewer visible aggregates present in muscle cells overexpressing HSP-90, compared to control animals (Figure 2.7B).

This provides evidence that HSP-90 can prevent the build-up of toxic Aβ species – and provides a potential mechanism for TCS to be protective, as *HSP-90::RFP* expressed specifically in the neurons or intestine upregulates *hsp-90* in other tissues, including the body wall muscle (van Oosten-Hawle et al., 2013). It was also demonstrated that the overexpression of HSP-90 in the neurons and intestine could be protective against the misfolding of a metastable myosin (ts) mutant, indicating that TCS can improve the capacity of the proteostasis network of distal tissues, something that has been corroborated in these results. The result also more generally demonstrates that disease-causing proteins can be defended against in *C. elegans* through induction of TCS by distal tissues. In principal this also opens the door to the possibility that the activity of small molecules in a certain tissue can affect distal tissue environments through a similar mechanism. This is particularly pertinent for neurodegenerative diseases as the blood-brain barrier is often a tricky block to drug development that must be overcome when directly treating neurons (Daneman and Prat, 2015). If we could leverage TCS we could avoid this by in built, cell-non-autonomous signalling pathways then it could be beneficial for the prospects of future treatments.

It is also of interest that PQM-1 has been linked to the innate immune response and survival of pathogenic bacteria (Shapira et al., 2006), as it's knockdown by RNAi led to greatly reduced survival of *C. elegans* fed on *Pseudomonas aeruginosa.* DAF-16 has also been linked with innate immunity in *C. elegans*. In fact enhanced activity of DAF-16 enhances susceptibility to bacterial infection by *P. aeruginosa* (Singh and Aballay, 2009).

It may be that the susceptibility of nematodes with overactive DAF-16 to *P. aeruginosa* is linked to nuclear localised DAF-16 preventing the nuclear entry of PQM-1, and hence removing the protective effects of PQM-1's transcriptional targets when the *C. elegans* are confronted with the stress of pathogenic bacteria. DAF-16 is also a known regulator of the small heat shock proteins *hsp-16.1, hsp-16.49,* and *hsp-12.6* (Hsu et al., 2003). This information combined offers one possible route through which the expression and activity of PQM-1 could influence chaperone expression in a *wildtype* organism. Shpigel et al. have predicted bioinformatically that PQM-1 could regulate a number of chaperones including *F44E5.4*, the heat inducible *hsp-70*; and a number of other sHSPs and HSP-90 co-chaperones.

PQM-1 is thought to belong to the family of B2B-ZF transcription factors, which contain both a leucine zipper motif a C-terminal C2H2 zinc-finger domain responsible for specific DNA interactions (Wolfe et al., 2000) and are also able to make protein-protein interactions (Brayer and Segal, 2008). PQM-1 has been shown to make protein-protein complexes with CEH-60 (Dowen, 2019), and it may be that it associates with other proteins for diverse functions. It has also been implicated in mTORC2 signalling, mediating the cell-non-autonomous crosstalk between developmental cues in the hypodermis to the intestine where it regulates vitellogenesis and fat transport to the germline (Dowen et al., 2016).

The closest human orthologue of *pqm-1* is SALL2 *(spalt like transcription factor 2)* (23.7% identity) which is a transcription factor that has been implicated in eye-formation, neurogenesis and tumorigenesis (Li et al., 2004; Sung and Yim, 2017). It may be that

there is a conserved role for transcription factors in the niche of PQM-1 in higher metazoans, despite the lack of conservation of sequence.

Chapter 3 The Role of PQM-1 in gene expression after heat shock

3.1 Introduction

C. elegans expresses all the same chaperone functional families as humans, albeit fewer chaperones in total (219 in *C. elegans* compared to 332 in humans) (Brehme et al., 2014). Both chaperones and the master regulator of the heat shock response (HSR), HSF-1 are conserved from *C. elegans* to mammals - so nematodes are well placed as a model for stress response, proteostasis and associated diseases such as Parkinson's disease.

In *C. elegans,* heat stress induces a specific heat shock program which is mediated by the master regulator of the heat shock response, HSF-1 (Morley and Morimoto, 2004). Under heat stress conditions HSF-1 effects the expression of a number of heat responsive genes including molecular chaperones (Akerfelt et al., 2010; Vihervaara and Sistonen, 2014; Mantione et al., 2014) which are required for survival of heat stress. HSF-1 also has wider reaching effects on the transcriptional programme of the whole organism including development (Anckar and Sistonen, 2007; Brunquell et al., 2016) and as such HSF-1 is essential in *C. elegans*. Therefore, the *hsf-1 (sy441)* mutant strain, which can develop to adulthood despite a temperature-sensitive developmental defect was used as a control for the experimental conditions. Although the *hsf-1 (sy441)* mutant develops to adulthood it cannot properly activate the HSR due to the truncation of the DNA-binding HR-C, a hydrophobic heptad repeat (Hajdu-Cronin et al., 2004). DAF-16 is also known to be important for stress survival and it too can induce expression of certain heat shock proteins such as *hsp-16* (Walker and Lithgow, 2003).

The previous chapter demonstrates that *pqm-1* is necessary for heat stress survival in *C. elegans*. The loss of *pqm-1* leads to reduced survival after heat stress, comparable to the *hsf-1 (sy441)* mutant (Chapter 2). This result revealed a novel role for *pqm-1* in stress tolerance, it is not generally considered an important transcription factor for stress survival, but has been linked with insulin-like signalling (Tepper et al., 2014), transport of fats to the oocytes (Dowen et al., 2016) and the innate immune response (Shapira et al., 2006). To that end we sought to understand whether *pqm-1* regulates a transcriptional programme that is specifically activated in response to heat stress. For example, what are the genes that are regulated by PQM-1 in response to acute heat shock; and which of these are required for survival? To answer this question, the transcriptional profile of both the wildtype *C. elegans* and *pqm-1* (*ok485*) strain (henceforth referred to as *pqm-1* (ko)) were examined at 20˚C and after acute heat shock (1 hour at 35˚C). Gene expression profiles were then compared in order to identify the genes that are differentially regulated between the conditions. The data generated revealed which genes were regulated by PQM-1 response to acute heat stress. Our aim was to identify important genes that are required for heat stress survival, other than the molecular chaperones that could potentially be regulated by the established stress responsive transcription factors HSF-1 and DAF-16.

To that end, we used microarrays to explore the different transcriptomes in response to acute heat stress in wildtype (N2) *C. elegans* and the *pqm-1* (ko) and *hsf-1 (sy441)* mutants. Microarrays are a tool which can be used to analyse RNA expression. Briefly, total RNA is reverse transcribed into DNA which is then amplified multiple times by PCR. Fluorescent probes are attached to the end of each strand of DNA and the library is then exposed to a chip which has oligonucleotides that correspond to every gene annotated

in the organism. Amplified DNA anneals to complementary fixed oligonucleotides on the chip and the chip is imaged. The fluorescence is quantified and this is what is used to measure the change in expression between genes, and samples once the data has been normalised (Churchill, 2002).

Microarrays have been used for many years in *C. elegans* to identify differential gene regulation between conditions, and have been applied to proteostasis, aging and the heat shock response to gain an insight into the mechanisms underlying these phenomena (Kim et al., 2001; GuhaThakurta, 2002; Golden and Melov, 2004). Although recently RNAseq has become much more widespread in its use to investigate the gene expression profiles of many organisms (Malone and Oliver, 2011), microarrays remain a useful technique to measure global gene expression in *C. elegans* in differing conditions– particularly as the genome is so well annotated (Mantione et al., 2014). The genes identified by the microarray as being differentially regulated during heat stress depending on the presence of *pqm-1* provide insight into the role of PQM-1 in transcriptional regulation under these stress conditions.

3.2 Materials and Methods

3.2.1 Nematode strains and maintenance

Nematodes were grown on NGM plates supplemented with streptomycin and seeded with OP50-1 bacteria, and maintained as previously described (Brenner, 1974). The following strains were used: N2 Bristol (wildtype strain); PS3551 (*hsf-1 (sy441) I);* RB711 (*pqm-1 (ok485) II);* some strains were provided by the CGC, which is funded by NIH Office of Research Infrastructure Programs (P40 OD010440).

3.2.2 Heat stress conditions

Nematodes were bleach synchronised (hypochlorite treatment followed by rotation overnight in M9 buffer (Sulston and Hodgkin, 1988)) then grown from arrested L1s to L4 stage at a density of 1000 nematodes per 9cm plate. At L4 stage the nematodes were placed in an incubator at 35˚C for an hour. The nematodes were returned to 20 ˚C for an hour before being rapidly washed off with ice cold M9 and snap frozen.

RNA was extracted from nematodes that had recovered for 1 hour at 20˚C from an acute 1 hour heat shock at 35˚C. Alongside the wildtype, which has an intact copy of *pqm-1*, a *pqm-1* (ko), and an *hsf-1 (sy441)* mutant were also subject to heat stress and their gene expression analysed. The nematode strains were analysed both at 20˚C and after recovery from heat shock, giving 6 conditions analysed. To increase the fidelity of the data output of the microarray, all experiments were performed in duplicate.

Nematodes were assayed at the L4 stage. This stage was selected for several reasons: the previous heat stress tolerance assays had been performed on *C. elegans* at L4 stage; nematodes at adult stage would also have eggs or L1 larvae on the plate, introducing RNA transcripts from non-staged *C. elegans*. Furthermore, once nematodes have become adults the heat shock response becomes weaker so the effect of *pqm-1* on survival may be harder to discern against higher background death (Ben-Zvi et al., 2009).

3.2.3 RNA Extraction

Nematodes sufficient to yield 5mg total RNA were grown from L1 on standard NGM plates supplemented with streptomycin and seeded with OP50-1 bacteria as described previously (Brenner, 1974). Following heat shock (35˚C) or control (20˚C) treatment of synchronised L4 animals' total RNA was prepared by mixing of frozen nematode pellets with an equal volume of TRIzol Reagent (Ambion) and then subjecting the nematodes to grinding with a pellet grinder for 3 x 30 seconds over ice. The RNA was then extracted using RNA miniprep kit (Zymo) as instructed. The extracted and purified RNA was then assayed for its RIN (RNA integrity number) score using an Agilent Tapestation (Schroeder et al., 2006). The RNA samples assayed had a RIN score >9 and as such we proceeded with the microarray (Appendix Figure A.1). The RIN score gives a measure of RNA integrity as it measures the ratio of 28S to 18S rRNA. The RNA was sent to EMBL where it underwent reverse transcription to cDNA followed by hybridisation and microarray analysis took place.

3.2.4 Microarray Analysis

Extracted RNA was sent to EMBL for microarray analysis using Affymetrix array GeneChip ST 1.0 for *C. elegans*. Results were preprocessed and analysed in R version 3.4.3. Preprocessing of arrays was done using oligo package, normalisation was done using rma (Irizarry et al., 2003). Differential expression analysis was performed with limma version 3.34.9 (Ritchie et al., 2015; Phipson et al., 2016). Batch effects among biological repeats were removed using mFit; ebayes; contrasts.fit; removeBatchEffect in limma (version 3.34.9). The linear model was defined using the generic design matrix given below. In each case comparison was made between a 'control' or 'normal' condition and a treated (e.g. heat shocked) or mutant sample, with 2 samples (replicates) in each condition.

Sample Number	**Control/Normal**	**Treated/Mutated**
1	1	0
2	1	0
3	0	1
4	0	1

The linear model specified by the design matrix fits a mean expression level for each gene in each condition, and differential gene expression between conditions was assessed using a defined contrast in LIMMA and employing the default empirical Bayes derived t statistics with false discovery rate adjustment.

The analysis of the microarray focused on the transcripts which are in each condition, compared to the wildtype at 20 ˚C, significantly differentially regulated (-1.5< FC > 1.5,

p.adj < 0.05). P-values were adjusted for FDR using the BH method (Benjamini and Hochberg, 1995).

I would like to thank to Chulin Sha for the R script which was used to analyse the Affymetrix data.

3.2.5 Comparison to ChIP analysis of PQM-1 binding

The microarray dataset was compared to a ChIPseq data set which was generated as part of the modENCODE project (Niu et al., 2011).

3.2.6 GO biological process

GO term analysis for differentially regulated genes following acute heat shock in wildtype (N2); *pqm-1* (ko); and *hsf-1 (sy441) C. elegans* was performed using PANTHER version 14.1; GO Ontology database Released 2019-02-02 (Mi et al., 2013; Mi, Muruganujan, Huang, et al., 2019). The GO terms with a FDR <0.05 were selected.

3.2.7 Graphing

Statistical analysis and graphing were performed using GraphPad Prism version 7 for Windows, GraphPad Software, La Jolla California USA, www.graphpad.com.

3.3 Results

3.3.1 Experimental design to determine the transcriptional response elicited by PQM-1 following heat stress

We had previously shown that *pqm-1* is required for heat stress survival at 35˚C (Chapter 2), therefore we set out to determine the transcriptional programme that depends on the presence of PQM-1 during heat stress and normal growth conditions. For this we used the *pqm-1 (ok485)* knockout mutant that shows reduced survival rates after a 6 hour heat shock at 35˚C. Because the heat stress survival rates of *pqm-1* (ko) are comparable to the *hsf-1 (sy441)* mutant we wanted to compare different gene expression patterns of the two transcription factor mutants during stress to see if the same genes were being affected by the loss of the two transcription factors during stress.

3.3.2 Initial Verification of heat shock conditions

As an internal control and to verify that the heat shock conditions used were sufficient to induce a HSR, we have contrasted gene expression between 20 ˚C and 35˚C that are expressed in the control (N2) strain. The genes which are most upregulated in response to acute heat shock are shown in Table 3.1 (show in full in Appendix Table A.1) and mirror previous datasets investigating transcriptional profiles in response to heat stress (Brunquell et al., 2016). These genes include the *hsp70*s *C12C8.1* (log_2FC 5.24), *F44E5.4* (log_2FC 2.54), and *F44E5.5* (log2FC 5.31), and *hsp-16.11* (log_2FC 5.56) giving us

confidence in our microarray dataset (Table 3.1). The *hsf-1 (sy441)* mutant strain was used as a negative control as this mutant is deficient in the upregulation of key heat shock response proteins – including key molecular chaperones

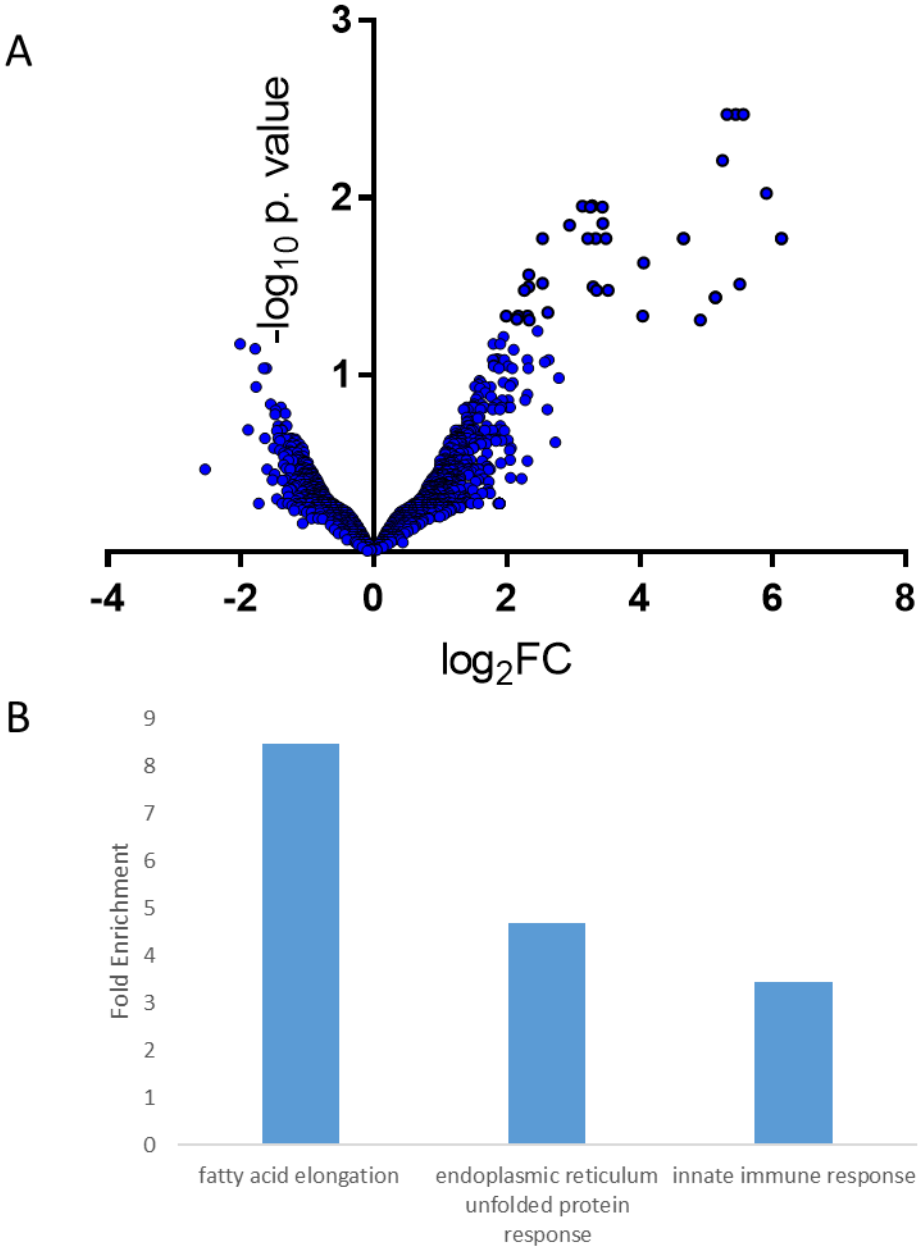

Figure 3.1. Genes that are differentially regulated post-acute heat shock in wildtype *C. elegans*.

A) Volcano plot comparing gene expression between a wildtype at 20˚C and after heat stress, with $-\log_{10}$ p value on the y axis vs $\log_2$FC on the x axis. Individual genes are represented by single points on the plot. B) Top processes normally differentially regulated in wildtype (N2) *C. elegans* following acute heat stress. The genes that were differentially regulated following heat stress are arranged by Gene Ontology terms that were determined using PANTHER.

Gene Name	*Transcript ID*	log_2FC *pqm-1(+);* HS vs control	Description (Wormbase)
F33H12.6	*F33H12.6*	6.44	
R11A5.3	*R11A5.3*	6.23	
hsp-16.11	*T27E4.2*	5.83	*hsp-16.11* encodes a 16-kD heat shock protein (HSP) that is a member of the hsp16/hsp20/alphaB-crystallin (HSP16) family of heat shock proteins, and that is identical to the protein encoded by *hsp-16.1*; *hsp-16.11* expression is induced in response to heat shock or other environmental stresses.
F44E5.5	*F44E5.5*	5.52	*F44E5.5* encodes a member of the Hsp70 family of heat shock proteins.
hsp-70	*C12C8.1*	5.38	*hsp-70* encodes a heat-shock protein that is a member of the Hsp70 family of molecular chaperones.
hsp-16.48	*T27E4.3*	4.64	hsp-16.48 encodes a 16-kD heat shock protein (HSP) that is a member of the Hsp16/Hsp20/alphaB-crystallin (HSP16) family of heat shock proteins
hsp-12.6	*F38E11.2*	4.62	*hsp-12.6* encodes a small heat-shock protein with very short N- and C-terminal domains flanking its central region of similarity to alpha-crystallins; HSP-12.6 is required in vivo for normal lifespan; the *hsp-12.6* promoter is predicted to have both DAF-16 and HSF-1 binding sites
C25F9.2	C25F9.2	4.31	*C25F9.2* is predicted to have 3'-5' exonuclease activity, DNA binding activity, DNA-directed DNA polymerase activity, endonuclease activity, and nucleotide binding activity, based on protein domain information.
hsp-16.2	*Y46H3A.3*	3.95	*hsp-16.2* encodes a 16-kD heat shock protein (HSP) that is a member of the Hsp16/Hsp20/alphaB-crystallin (HSP16) family of heat shock proteins; *hsp-16.2* is induced in response to heat shock or other environmental stresses.
tts-1	*F09E10*.11a	3.79	The lncRNA *tts-1* functions in longevity pathways to reduce ribosome levels to promote life extension (Essers et al., 2015)

Table 3.1. Top 10 Genes upregulated in wildtype following acute heat shock.

(Hajdu-Cronin et al., 2004). Although the *hsf-1 (sy441)* mutant does upregulate some heat-inducible heat shock protein genes, including the *hsp-70s C12C8.1* and *F44E5.4* upon heat stress, they are induced to a much lower level (2.4 log_2FC and 2.2 log_2FC) above baseline expression (Appendix Table A.3). These results indicate that the heat shock was sufficient to induce *hsps*, and that the induction of the HSR is compromised in the *hsf-1 (sy441)* strain.

3.3.3 Upregulated genes in the wildtype, *pqm-1* (ko) and *hsf-1 (sy441)* mutant.

In the wildtype (N2) *C. elegans*, there are 281 genes that are upregulated when the animals are subject to acute heat stress (1 hour 35˚C), and 52 genes which are downregulated. The differential expression is also visualised in a volcano plot (Figure 3.1A). The top GO term processes differentially regulated by acute heat stress are fatty acid elongation (8.5 fold enrichment), ER unfolded protein response (4.7 fold enrichment) and innate immune response (3.4 fold enrichment) (Figure 3.1B; Appendix Table A.4).

In the *pqm-1* (ko) there are 278 genes which are upregulated following acute heat shock (1 hour 35˚C) and 101 genes which are downregulated (Appendix Table A.2). This information is also displayed in a volcano plot (Figure 3.2A). The most differentially regulated processes, as determined by GO term analysis using PANTHER (Mi et al., 2019) are ER unfolded protein response (4.4 fold enrichment) and innate immune response (2.9 fold enrichment) (Figure 3.2B; Appendix Table A.5).

In the *hsf-1 (sy441)* strain there are 198 genes which are upregulated following acute heat stress (1 hour 35˚C) and 39 genes which are downregulated under the same

Gene Name	Transcript ID	log_2FC *pqm-1(+);* HS vs control	Description (Wormbase)
fipr-26	F53B6.8	1.96	Fungus induced protein related; *fipr-26* is enriched in the cephalic sheath cell, excretory cell, hypodermis, and intestine and in the dopaminergic neurons
F55B12.10	F55B12.10	1.92	F55B12.10 is thought to be enriched in the cephalic sheath cell, hypodermis, germ line, pharyngeal-intestinal valve cell and in the dopaminergic, PVD, and OLL neurons.
ZK970.7	ZK970.7	1.91	ZK970.7 encodes, along with C06A8.3, one of two *C. elegans* proteins with similarity to the Onchocerca volvulus Ov17 hypodermal antigen.
C27B7.9	C27B7.9	1.87	C27B7.9 is enriched in the cephalic sheath cell, excretory cell, hypodermis, and germ line and in the dopaminergic neurons.
catp-3	C09H5.2a	1.80	*catp-3* is an ortholog of members of the human ATPase H+/K+ transporting family; *catp-3* is predicted to have nucleotide binding activity, based on protein domain information.
F23F1.2	F23F1.2	1.75	F23F1.2 is predicted to have calcium ion binding activity, based on protein domain information.
T10E10.4	T10E10.4	1.73	T10E10.4 encodes a large (966-residue) protein, predicted to be secreted, with two N-terminal chitin-binding peritrophin-A domains followed by 14 cysteine-rich domains and one C-terminal EB module; T10E10.4 has no obvious function in mass RNAi assays but, might participate in chitin synthesis.
F48D6.4	F48D6.4	1.66	F48D6.4 is enriched in the intestine, pharyngeal muscle cell, and muscle cell and in the ASER neurons.
K01A6.7	K01A6.7	1.54	RNA sequencing and microarray studies indicate that K01A6.7 is affected by daf-2 and daf-16, and ethanol and colistin; K01A6.7 is enriched in the amphid sheath cell.
nlp-25	Y43F8C.1	1.50	Neuropeptide Like Protein; *nlp-25* is expressed in the embryonic cell.

Table 3.2. Top 10 Genes upregulated by PQM-1 during heat shock

conditions. These genes are displayed in a Volcano plot shown in Figure 3.3 and significantly differentially regulated genes are listed in Appendix Table A.3. GO term analysis reveals that the most differentially regulated processes are exogenous drug catabolic process (6 fold enrichment); xenobiotic metabolic process (5.7 fold); innate immune response (3.2 fold); detection of stimuli involved in the perception of smell (3.16 fold); olfactory behaviour (2.9 fold); and G-protein coupled receptor signalling pathways (2 fold) (Figure 3.3B; Appendix Table A.6).

3.3.4 Differential expression of genes after acute heat stress between wildtype and *pqm-1* (ko) and *hsf-1 (sy441)* strains

When a *pqm-1* (ko) strain of *C. elegans* is exposed to acute heat stress, the resulting gene expression varies greatly from the heat stress response in the wildtype (Figure 3.4A). The Volcano plot demonstrates that there are 87 with significantly different expression levels under each condition – indicating that many genes have their heat-responsive expression altered by the presence of PQM-1. When the same plot is applied to the *hsf-1 (sy441)* after heat stress compared to wildtype post heat stress, no genes are significantly differentially regulated (Figure 3.4B). It could be the case that the *hsf-1 (sy441)* can still regulate the majority of genes in a wildtype manner, but is unable to regulate key heat shock genes, whereas the full *pqm-1* (ko) affects gene expression of background genes to a greater extent.

3.3.5 Genes that are normally regulated by PQM-1 in response to HS

To visualise the subset of genes that is upregulated only when *pqm-1* is expressed, a Venn diagram was constructed which details all the significantly upregulated genes for each condition tested (Appendix Table A.8). There are 53 transcripts that are normally upregulated in the wildtype during heat stress (Figure 3.5A, red; Appendix Table A.10) that are expressed but not upregulated in the *pqm-1* (ko) strain under ambient permissive temperature or following heat stress. Therefore, we can conclude that these 53 genes are dependent on PQM-1 activity to be upregulated following heat stress exposure.

A heat map has been constructed to highlight fold-expression changes of the 53 genes upregulated during HS in the wildtype but not in the *pqm-1* (ko) strains (Figure 3.5B). The ten most upregulated genes following heat stress that are controlled by PQM-1 are listed in Table 3.2. Among the genes most strongly upregulated by PQM-1 following heat stress is *fipr-26* (FIP (Fungus-Induced Protein) Related) (1.96 $\log_2$fold) which is a gene that is upregulated in response to UV stress in a *glp-1* background (Boyd et al., 2010). The transcript *ZK970.7* is also significantly upregulated (1.91 $\log_2$fold). *ZK970.7* is a protein of uncharacterised function that is upregulated in *aak-2* (AMP-Activated Kinase) mutants subjected to oxidative stress (Shin et al., 2011). These genes may be related to *C. elegans* stress and immune response, which has been linked to the activity of *pqm-1* previously - the knockdown of *pqm-1* has been shown to be deleterious to *C. elegans* survival on pathogenic bacteria (Shapira et al., 2006), and data from our group reveals that under TCS, which is mediated by PQM-1, many immune genes are upregulated (O'Brien et al., 2018).

Gene Name	Transcript ID	log_2FC *pqm-1(+);* HS vs control	Description (Wormbase)
K12B6.11	K12B6.11	-1.89	RNA sequencing studies indicate that K12B6.11 is affected by *hsf-1*, *daf-12*, *daf-16*, Multi-walled carbon nanotubes and Zidovudine; and that K12B6.11 is enriched in the intestine.
F21C10.9	F21C10.9	-1.55	F21C10.9 is enriched in the hypodermis and intestine and in the PVD, OLL, ASER, and PLM neurons
T20D4.3	T20D4.3	-1.52	RNA sequencing studies indicate that T20D4.3 is enriched in the PLM neurons.
math-40	T08E11.3	-1.50	Microarray and RNA sequencing studies indicate that *math-40* is affected by *lin-15B*, *hsf-1*, *mir-34*, *sma-4*; *math-40* is affected by RNA sequencing studies indicate that *math-40* is enriched in the intestine and in the PVD, OLL, GABAergic, and FLP neurons.
clec-7	F10G2.3	-1.49	*clec-7* is an ortholog of human CLEC3B (C-type lectin domain family 3 member B) and CLEC3A (C-type lectin domain family 3 member A); *clec-7* is involved in defence response to Gram-positive bacterium.
elt-2	C33D3.1	-1.44	*elt-2* encodes a GATA-type transcription factor most like the vertebrate GATA4-6 transcription factors required for cardiac and endoderm development
drd-1	F49E12.9	-1.41	(Dietary Restriction Down regulated) *drd-1* is an ortholog of human FAXDC2 (fatty acid hydroxylase domain containing 2); drd-1 is predicted to have iron ion binding activity and oxidoreductase activity, based on protein domain information; *drd-1* is expressed in the intestine.
C47G2.16	C47G2.16	-1.39	RNA sequencing studies indicate that C47G2.16 is affected by *let-418* (component of NURD complex).
T24E12.14	T24E12.14	-1.35	Unknown function
nduo-3	MTCE.34	-1.35	The *nduo-3* gene resides on the mitochondrial chromosome, and encodes the protein NADH-ubiquinone oxidoreductase chain 3; this is the *C. elegans* homolog of the core MT-ND3 of mitochondrial NADH:ubiquinone oxidoreductase (Complex I).

Table 3.3. Top 10 Genes downregulated by PQM-1 during heat shock

There are 26 transcripts that are downregulated in the wildtype after heat stress (when PQM-1 is present in the organism) relative to the *pqm-1* (ko) either at 20˚C or after heat stress (Figure 3.6A, blue; Appendix Table A.9; Appendix Table A.10). These 26 genes are also less downregulated in the *pqm-1* (ko) than the wildtype (Figure 3.6B). Indeed, several of the genes down regulated by *pqm-1* following heat stress are upregulated in its absence. This suggests that PQM-1 represses these 26 genes during heat stress. A closer examination of the transcripts reveals that the GATA-transcription factor *elt-2* is repressed by PQM-1 during heat stress conditions (Table 3.3). ELT-2 is required for intestinal differentiation and maintenance (Sommermann et al., 2010). It may be the case that in times of stress PQM-1 mediates the diversion of resources away from long term cellular differentiation to combat the more immediate threat to the organism. Interestingly the mitochondrial gene, *nduo-3*, is also repressed by PQM-1 during heat stress. The *nduo-3* transcript encodes the protein NADH-ubiquinone oxidoreductase chain 3 of Complex 1 of the mitochondrial transport chain (ETC) (Davis and Van Auken, 2014). The suppression of the transcription of components of the mitochondrial transport chain by PQM-1 suggests that PQM-1 could help manage oxidative stress on the cells during heat stress by reducing the production of reactive oxygen species (ROS) which occurs concurrently with the generation of ATP by the electron transport chain (Murphy, 2009; Dancy et al., 2014). It has previously been reported that perturbation of components of the ETC, such as *cco-1* and *nuo-2* leads to extended lifespan (Dillin et al., 2002). This is compatible with results that show PQM-1 is upregulated when *C. elegans* are exposed to oxidative stress response (Tawe et al., 1998). Data from my postdoctoral colleague, Laura Jones, revealed that upon exposure of the nematodes to the oxidative agent paraquat, PQM-1 localises to the intestinal nuclei (not shown).

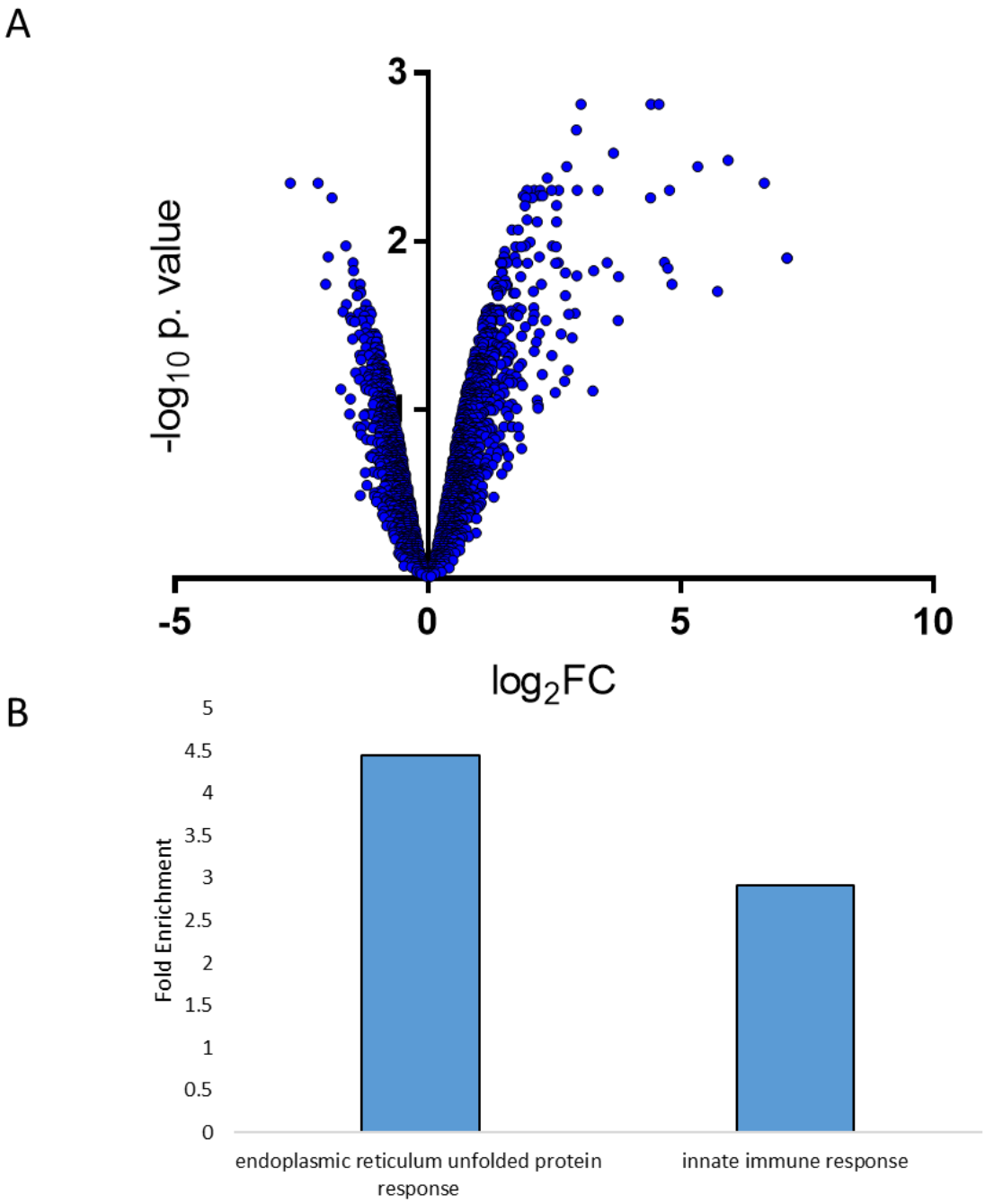

Figure 3.2. Genes that are differentially regulated post-acute heat stress in *pqm-1* (ko) *C. elegans*.

A) Volcano plot comparing gene expression between a *pqm-1* (ko) at 20˚C and after acute heat stress, $-\log_{10}$ p value on the y axis vs $\log_2$FC on the x axis. Individual genes are represented by single points on the plot . B) Top processes normally differentially regulated in *pqm-1* (ko) *C. elegans* following acute heat stress. The genes that were differentially regulated following heat stress are arranged by Gene Ontology terms that were determined using PANTHER.

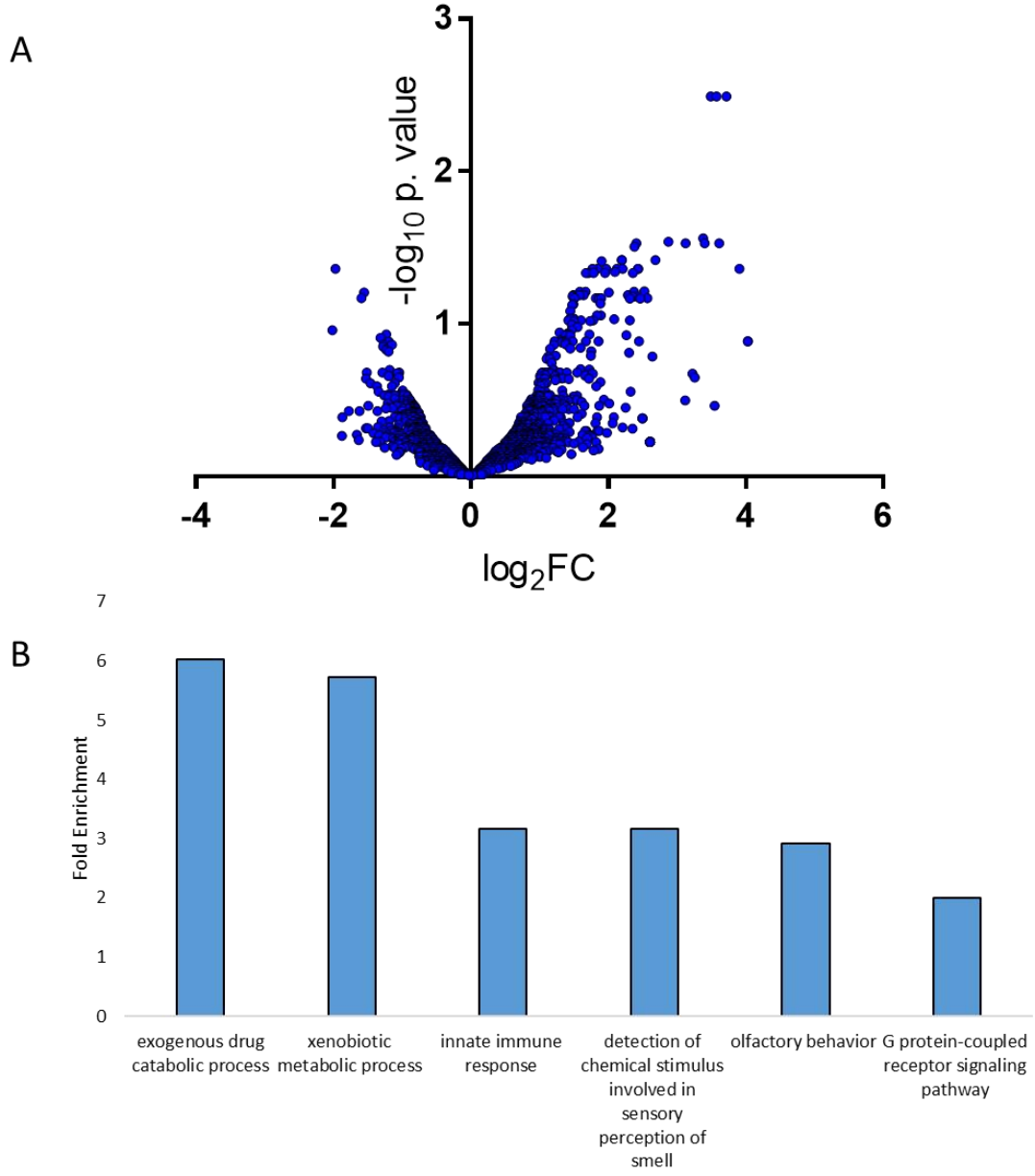

Figure 3.3. Genes that are differentially regulated post-acute heat shock in *hsf-1 (sy441)* mutant *C. elegans*

A) Volcano plot comparing gene expression between an *hsf-1* (sy441) mutant at 20˚C and after acute heat stress, with $-\log_{10}$ p value on the y axis vs $\log_2$FC on the x axis. Individual genes are represented by single points on the plot. B) Top processes normally differentially regulated in *hsf-1* (sy441) *C. elegans* following acute heat stress. The genes that were differentially regulated following heat stress are arranged by Gene Ontology terms that were determined using PANTHER.

3.3.6 Genes that are normally regulated by PQM-1 independent of HS

From the Venn diagrams that have been constructed it can be interpreted that there are not only the transcripts that are up and down regulated in a PQM-1 dependent manner after acute heat stress, but also genes whose expression levels depend on PQM-1 independent of heat stress. We can infer that genes which are up regulated in the *pqm-1* (ko) strain both at 20°C and after heat stress relative to wildtype at 20°C are repressed by PQM-1 during normal growth conditions and HS (Figure 3.7A, blue). Relative expression levels of these 258 genes reveals they are highly downregulated compared to the wildtype at 20°C in both cases (Figure 3.7B). A closer examination of these genes reveals that a number of the most downregulated genes are the *dumpy* genes: *dpy-9*; *dpy-3* and *dpy-2* which encode for cuticle collagen proteins (Appendix Table A.11). Collagen proteins are important structural proteins that fall into two classes in *C. elegans* functioning in either the cuticle or basement membrane (Kramer, 1994). Collagens are highly conserved, and in humans approximately 1/3 of all expressed proteins are collagens (Di Lullo et al., 2002). Furthermore, collagen genes have also been found to be upregulated by the stress responsive transcription factor, SKN-1 (Ewald et al., 2015).

There are 138 genes identified from the analysis which are induced in the presence of PQM-1 at both 20˚C and after heat stress (independent of heat shock conditions) (Figure 3.8A, red). These genes are down regulated in the *pqm-1* (ko) at both 20°C and following exposure to heat stress relative to wildtype at 20°C. As can be seen from the heat map (Figure 3.8B), these genes are strongly upregulated by PQM-1 in all conditions tested. The genes most strongly upregulated by PQM-1 include *vit-5* (3.15 fold) a vitellogenin gene that is important for fat transport from the intestine to the yolk of oocytes

(Appendix Table A.11). The collagen gene, *col-8*, is also highly upregulated (2.5 fold) by PQM-1 in all conditions, indicating that the cuticle structure of *C. elegans* might be perturbed in a *pqm-1* mutant, with the phenotype only presenting when higher levels of stress are experienced such as exposure to heat shock conditions.

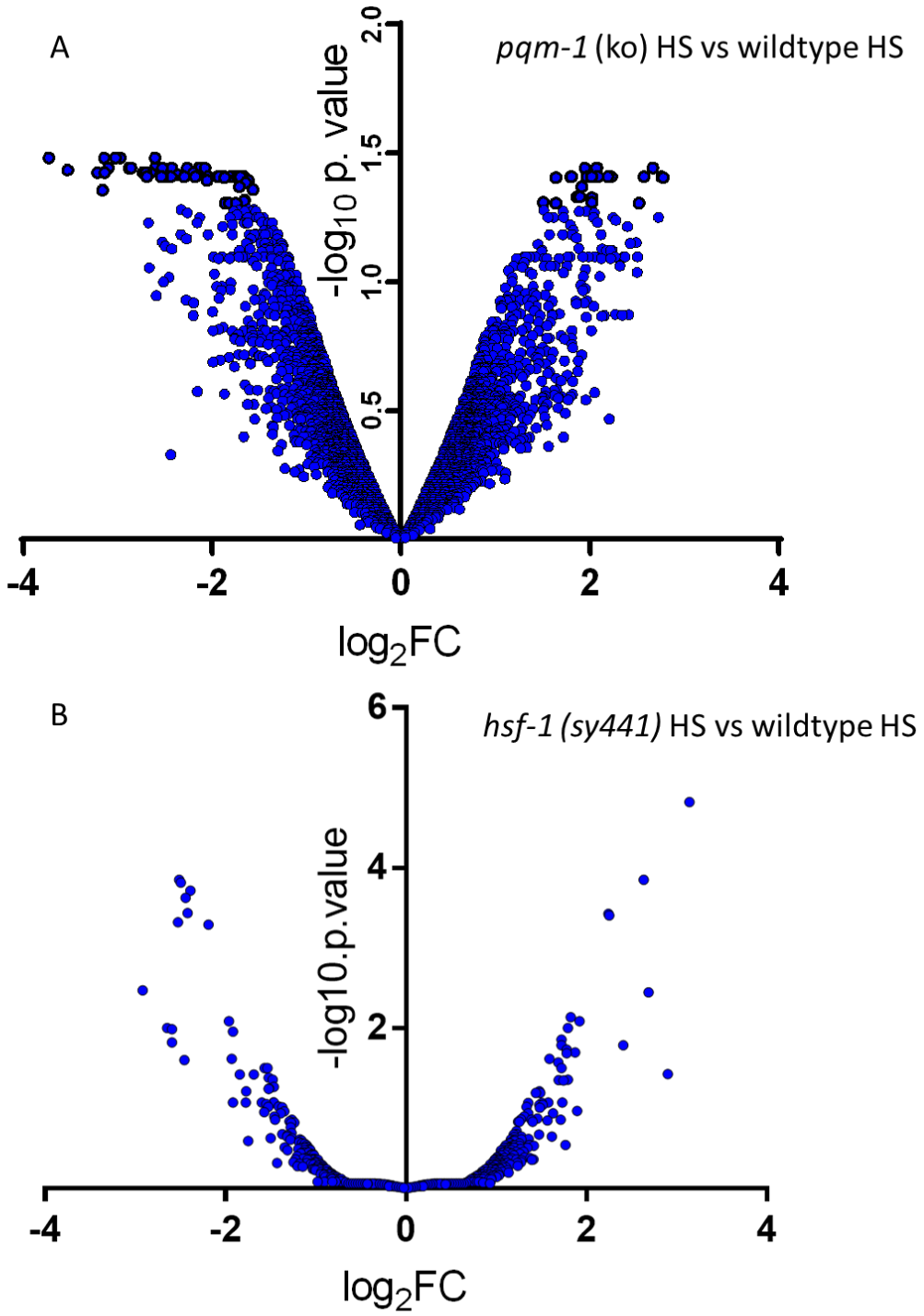

Figure 3.4. Differentially regulated genes in heat sensitive mutants and wildtype *C. elegans* after acute heat stress.

A) Volcano plot comparing gene expression between a *pqm-1* (ko) strain and N2 wildtype after heat stress. B) Volcano plot comparing gene expression between an *hsf-1 (sy441)* mutant and wildtype during heat stress. Individual genes are represented by single points on the plots.

3.4 Discussion

3.4.1 Differentially regulated genes in wildtype *C. elegans* following acute heat shock

In the wildtype there are 333 genes which we found to be differentially regulated following heat stress by microarray (Figure 3.1; Appendix Table A.1). Using GO term analysis these genes were screened for enrichment of biological processes. As expected, genes related to the unfolded protein response of the ER (UPR^{ER}) were found to be upregulated (4.68 fold enrichment) – it makes sense to find an enrichment of genes pertaining to unfolded proteins as heat stress causes metastable proteins to misfold (Walter, 2006; Gidalevitz et al., 2011). We also, however, found that there is an enrichment of genes involved in fatty acid elongation (8.46 fold enrichment) and the innate immune response (3.45 fold enrichment). Heat shock has previously been shown to stimulate the immune response and improve survival of *C.* elegans exposed to pathogens (Prithika et al., 2016). Interestingly, this study also linked SGK-1 to stress survival and pathogen response, and SGK-1 is thought to be a key regulator of PQM-1 activity (Dowen et al., 2016), indeed this finding is mirrored in my own results (Figure 4.7).

3.4.2 Differentially regulated genes in a *pqm-1* (ko) strain following acute heat shock

There are 379 differentially regulated genes in the *pqm-1* (ko) following exposure to acute heat stress (Figure 3.2; Appendix Table A.2). GO term analysis revealed that the most upregulated genes in these conditions were those pertaining to the UPR^{ER} (4.44 fold enrichment) and the innate immune response (2.92 fold enrichment). Compared to the wildtype GO term analysis, there is no fatty acid elongation gene enrichment – potentially an indication that PQM-1 plays a role in fatty acid elongation regulation during heat stress. A closer look at the differentially regulated genes reveals that there are 183 genes which are differentially regulated in both conditions (Appendix Table A.7). These genes include the chaperones *C12C8.1*, *hsp-16.2* and *hsp-12.6* indicating that many core components of the HSR are still upregulated following heat stress in the *pqm-1* (ko).

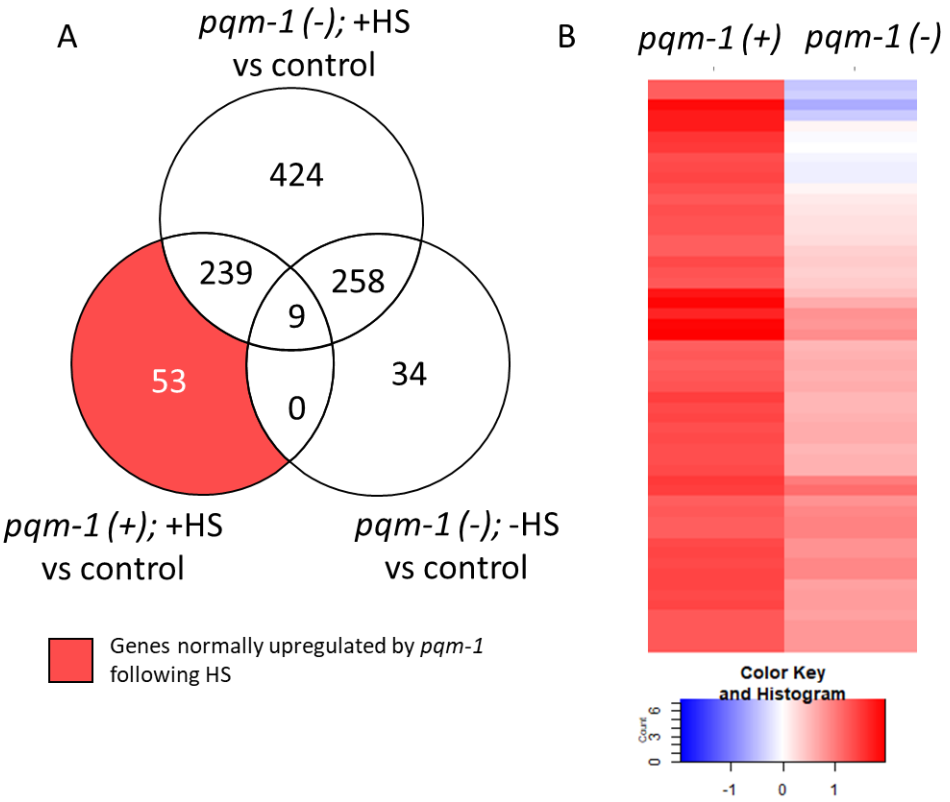

Figure 3.5. Genes that are normally upregulated by PQM-1 after heat stress.

A) The Venn diagram indicates the genes that are significantly upregulated (adj. p-value < 0.05) for each of the indicated comparisons between the samples and the wildtype control at 20°C. The shaded area indicates the genes that are upregulated after heat stress in the wildtype, but which are not upregulated in the *pqm-1* (ko) at 20°C or after heat stress. B) A heatmap which compares the previously mentioned genes which are upregulated by PQM-1 after heat stress to their values in the *pqm-1* (ko) after heat stress.

3.4.3 PQM-1 regulated genes following heat shock

We performed microarray analysis of the global mRNA state in *C. elegans* following heat stress to gain an understanding of why PQM-1 is required for heat stress survival. The results reveal that when *pqm-1* is not present in *C. elegans* under conditions of heat stress, there are 827 differentially regulated genes (435 upregulated; 392 downregulated) compared to wildtype. 79 (53 upregulated and 26 downregulated) genes were found to be differentially regulated in the wildtype (*pqm-1 (+))* compared to the *pqm-1 (ko)* mutant, either at the permissive temperature or after heat stress. The microarray also reveals that there are 397 genes which are regulated by *pqm-1* independent of HS conditions. Therefore, we have established that depletion of *pqm-1* has a significant effect on the landscape of the transcriptome in both a heat shock dependent and independent manner. Plotting the relative fold change of genes in wildtype vs *pqm-1* (ko) nematodes following heat shock provides insight into how differently genes are regulated in the 2 conditions (Figure 3.4A).

3.4.4 Differentially regulated genes in a *hsf-1 (sy441)* strain following acute heat shock

There are 237 differentially regulated genes when *C. elegans* with an *hsf-1 (sy441)* mutation are exposed to acute heat shock. GO term analysis reveals a much wider array of upregulated processes following heat stress: exogenous drug catabolic process (6. 06 fold enrichment); xenobiotic metabolic process (5.73 fold enrichment); innate immune response (3.16 fold enrichment); detection of chemical stimuli involved in sensory

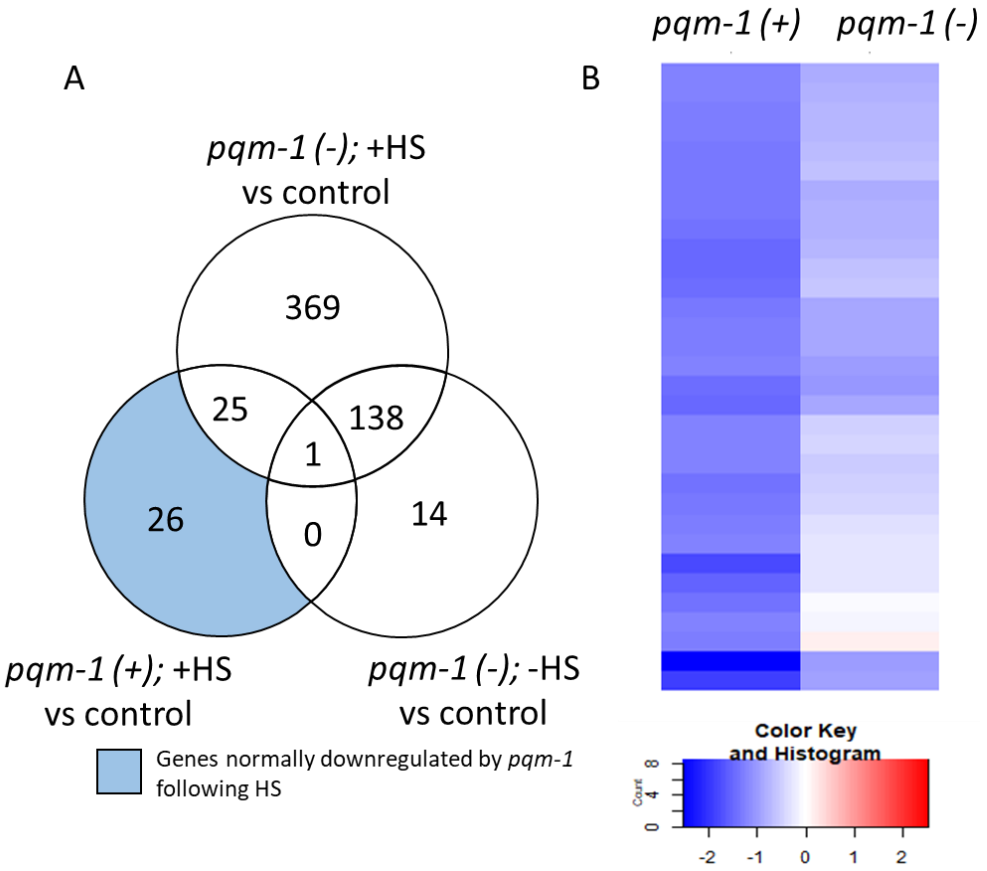

Figure 3.6. Genes that are normally downregulated by PQM-1 after heat stress.

A) The Venn diagram indicates the genes that are significantly downregulated (adj. p-value < 0.05) for each of the indicated comparisons between the samples and the wildtype control at 20°C. The shaded area indicates the genes that are upregulated after heat stress in the wildtype, but which are not upregulated in the *pqm-1* (ko) at 20°C or after heat stress. B) A heatmap which compares the previously mentioned genes which are upregulated by PQM-1 after heat stress to their values in the *pqm-1* (ko) after heat stress.

perception of smell (3.16 fold enrichment); olfactory behaviour (2.92 fold enrichment); G protein-coupled receptor (GPCR) signalling pathway (2.00 fold enrichment). Compared to wildtype, only the enrichment of innate immune genes persists – with the upregulation of metabolic processes related to external factors (xenobiotics; exogenous drugs) enriched more than 5-fold in these conditions. There is also an enrichment of genes related to olfactory environmental sensing and response – the olfactory AWC neurons modulate behaviour in response to heat stress (Biron et al., 2008). It may be that in the absence of functional HSF-1, heat avoidance pathways are upregulated. It has previously been demonstrated that the GPCR, *gtr-1,* is required for induction of the HSR in in *C. elegans* (Maman et al., 2013), demonstrating the importance of GPCRs for the HSR – and offering a potential explanation for the >3 fold enrichment of GPCR signalling pathways found. Interestingly, in all three cases the innate immune response is enriched above background levels, suggesting both that it is an important process to upregulate in the event of heat stress, and that it is upregulated regardless of the presence of PQM-1 or HSF-1, despite both transcription factors being associated with the innate immune response (Shapira et al., 2006; Prithika et al., 2016).

3.4.5 Genes regulated by PQM-1 independent of temperature

As well as revealing the gene expression profile of a *pqm-1* mutant following acute heat stress, the experiments also revealed a potential role of *pqm-1* under normal growth conditions (20˚C). 397 genes are differentially regulated in the *pqm-1* (ko) strain independent of HS, indicating that PQM-1 regulates these genes under both ambient and stress conditions. It may be that one or several of these genes are responsible for the thermosensitive phenotype exhibited by the *pqm-1* (ko) strain. As the *pqm-1* (ko)

strain presents with a developmental delay (Tepper et al., 2013), it could be the case that some of these 397 genes are involved in *C. elegans* development. Indeed, PQM-1 is localised to intestinal nuclei during development and only leaves once the nematode reaches reproductive adulthood (Tepper et al., 2013; O'Brien et al., 2018). It might also be valuable to conduct a similar experiment to look at transcription profiles of the *pqm-1* (ko) mutant during adulthood. In adult animals, PQM-1 re-localises to the nucleus following HS (Laura Jones, unpublished). In this case, nuclearly localised PQM-1 would be there as a result of the HS and have no developmental role to fill, so it would be interesting to see which of the genes upregulated are the same as in L4s.

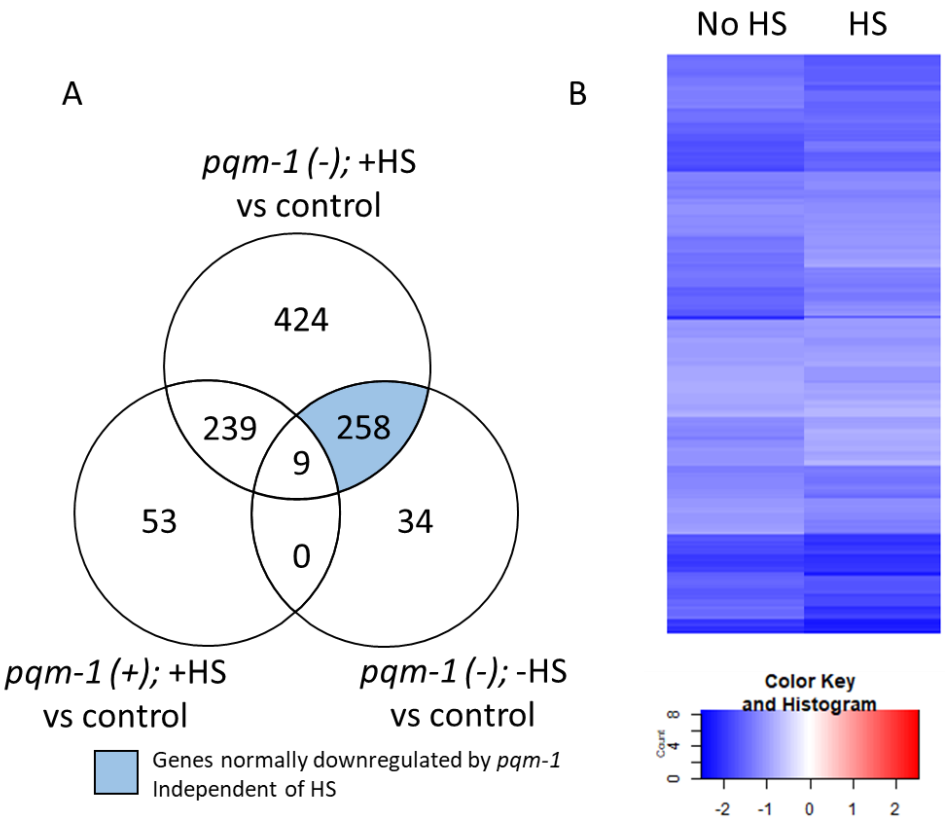

Figure 3.7. Genes that are normally downregulated by PQM-1 independent of heat stress.

A) The Venn diagram indicates the genes that are significantly downregulated (adj. p-value < 0.05) for each of the indicated comparisons between the samples and the wildtype control at 20°C. The shaded area indicates the genes that are upregulated after heat stress in the wildtype, but which are not upregulated in the *pqm-1* (ko) at 20°C or after heat stress. B) A heatmap which compares the previously mentioned genes which are upregulated by PQM-1 after heat stress to their values in the *pqm-1* (ko) after heat stress.

One of the genes that was identified to be most upregulated by *pqm-1* independent of HS was *vit-5*, a vitellogenin which is involved in yolk transport to oocytes. This is unexpected as it has been previously reported that *vit* genes are negatively regulated by PQM-1 in an mTORC2/SGK-1 dependent manner (Dowen et al., 2016). The study principally used a *Pvit-3::GFP* reporter construct, but also looked at the induction of other vitellogenins including *vit-2.* The transcript levels of *vit-5* were also measured by qPCR to show that loss of *pqm-1* suppresses defects in *vit* gene expression. One explanation for this discrepancy is the fact that the animals used in the study by *Dowen et al.* were adults and not L4 larvae and the role of PQM-1 in vitellogenin expression may simply shift as the animal ages. Indeed PQM-1 becomes less localised to the nucleus after *C. elegans* has reached adulthood (Tepper et al., 2013; O'Brien et al., 2018). Furthermore, *vit-3, vit-4* and *vit-5* were found to be among the top 5 most upregulated genes by *hsf-1* independent of heat stress (Brunquell et al., 2016) so it may be that the roles of HSF-1 and PQM-1 in stress tolerance converge on the germline. Vitellogenins are produced in the intestine before being transported to the oocytes to provide yolk (Kimble and Sharrock, 1983) – therefore provide a conduit for intestinal conditions to influence reproduction.

Indeed recent studies have shown that signals from the reproductive system influence PQM-1 localisation and activation (Dowen et al., 2016; Shpigel et al., 2018). The collagen genes *dpy-9; dpy-3*; and *dpy-2* are downregulated by PQM-1 in the wildtype at 20˚C (Appendix Table A.11), indicating that PQM-1 may contribute towards proper cuticle composition during development. Furthermore *nhr-74* which has predicted DNA-binding transcription factor activity and is expressed in the seam cell is also

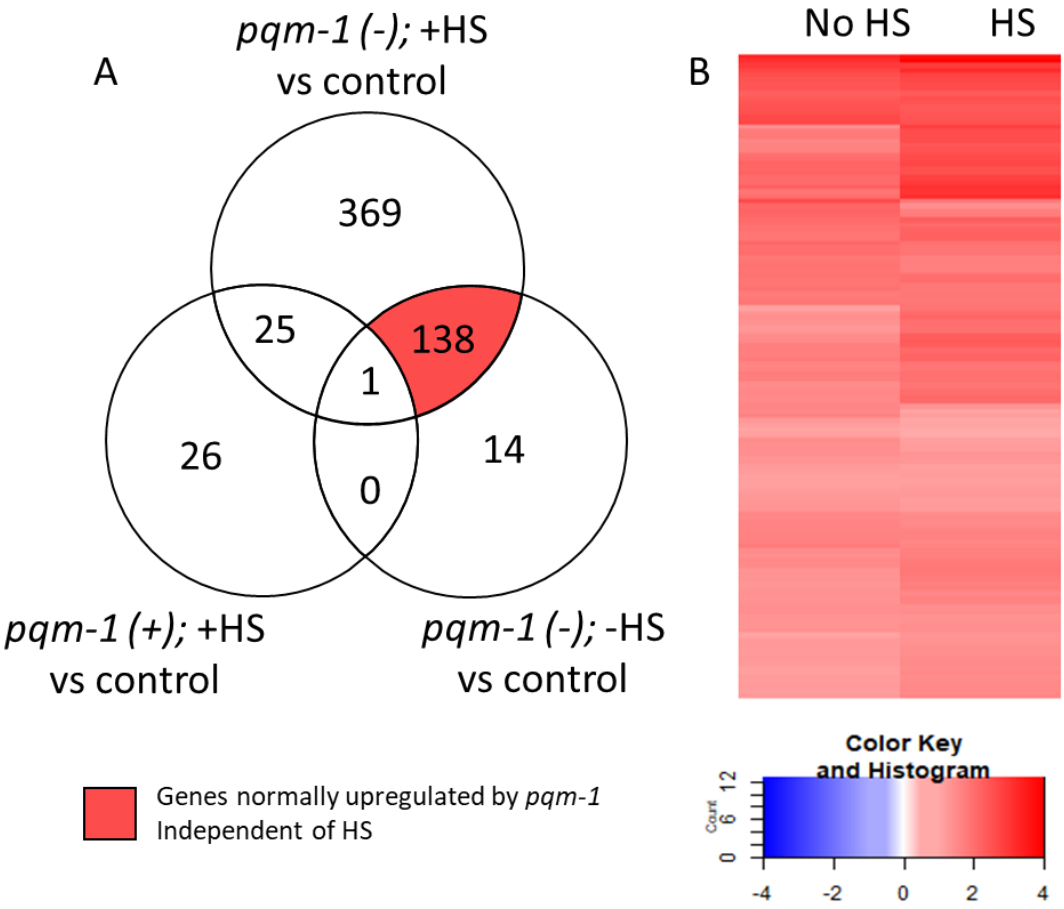

Figure 3.8. Genes that are normally upregulated by PQM-1 independent of heat stress.

A) The Venn diagram indicates the genes that are significantly downregulated (adj. p-value < 0.05) for each of the indicated comparisons between the samples and the wildtype control at 20°C. The shaded area indicates the genes that are upregulated after heat stress in the wildtype, but which are not upregulated in the *pqm-1* (ko) at 20°C or after heat stress. B) A heatmap which compares the previously mentioned genes which are upregulated by PQM-1 after heat stress to their values in the *pqm-1* (ko) after heat stress.

downregulated by PQM-1, so it may be the case that PQM-1 has a role to play in seam cell development.

3.4.6 ChIPseq analysis to complement transcriptome analysis

The microarray dataset informs about gene expression differences between wildtype and *pqm-1* (k.o.) mutant animals, and therefore highlights gene expression outputs that likely depend on the presence of the transcription factor PQM-1. The here investigated gene expression profiles however do not provide any information on whether PQM-1 directly or indirectly regulates identified gene datasets. In order to ascertain whether PQM-1 directly binds to the genes in question ChIPseq would need to be undertaken after heat stress. To determine whether the differentially regulated transcripts identified in our study could be directly controlled by PQM-1 we compared our dataset to an existing ChIPseq data set, that was previously performed in L3 larvae at 20C (Niu et al., 2011). A comparison of the genes that were discovered in the microarray study to be regulated by PQM-1 to the genes which were bound by PQM-1 during L3 stage under permissive conditions revealed only a few genes in common between the data sets (Figure 3.9A). Of the 79 genes differentially regulated by PQM-1 during heat stress (53 upregulated, 26 downregulated) only 11 are found in common with the almost 3000 gene that were identified as being bound by PQM-1 during L3 (Appendix Table A.12). There are 396 genes which we found to be driven by PQM-1 independent of HS conditions. When we compared this gene list to the transcripts identified in the ChIPseq, we found only 7 which were present in both (Figure 3.9B; Appendix Table A.13), indicating that PQM-1 might not regulate the same targets in L3 and L4 stages. In general, the gene lists generated in this study have only a small

overlap with the ChIPseq data from *Niu et al*. However, there are several reasons why this may be the case. First, not all of the loci that were found to be bound by PQM-1 during L3 map directly to genes – only 2014/2979, eliminating around a third of the binding sites.

Furthermore, the availability of DNA to be bound by transcription factors is controlled by chromatin structure, many transcription factors will only bind to open chromatin (Felsenfeld et al., 1996; Grossman et al., 2017)In *C. elegans* chromatin structure is altered by both development and organismal stress (Matilainen et al., 2017), both of which are relevant here – therefore there may be a very different chromatin structure in heat shocked L4s compared to L3s under ambient conditions. Furthermore, the binding of transcription factors to DNA has been shown to be highly cell type specific (Heintzman et al., 2009; Wiench et al., 2011). It is therefore likely that the binding sites found in a whole animal study at a different larval stage with a different mix of cell types are not representative of PQM-1 binding to the relevant cells in an L4 animal during heat stress. Finally, although the microarray study has identified genes whose expression post-heat stress depend on PQM-1, it cannot reveal whether or not PQM-1 directly binds to the promoters of all the genes which it regulates. A ChIPseq experiment performed under conditions mirroring the microarray – L4 stage nematodes subjected to 35°C heat stress for an hour – could shed light on which of these genes are directly regulated by PQM-1 following heat stress.

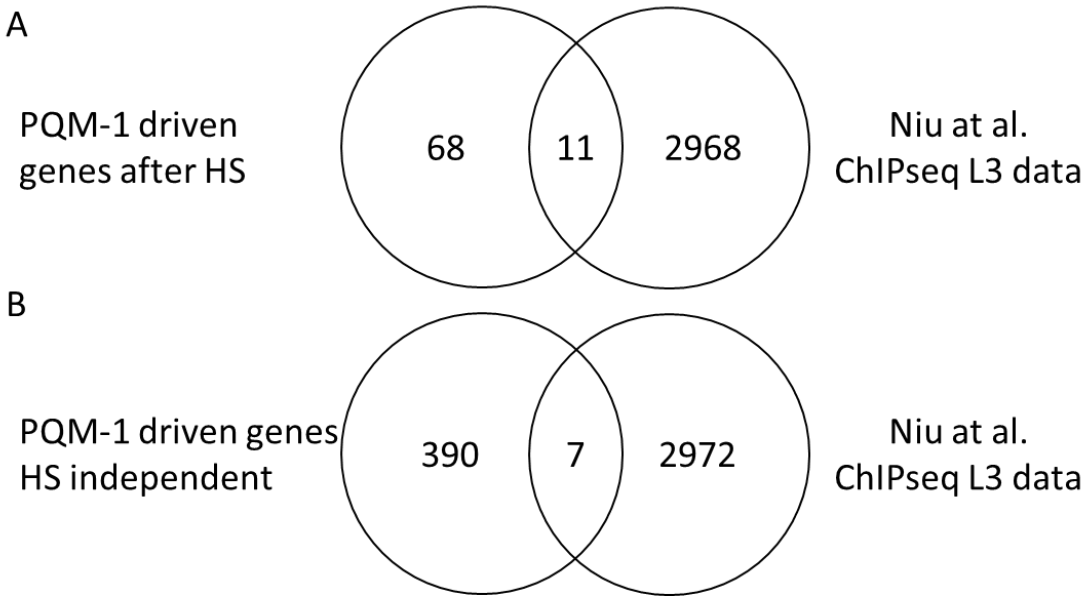

Figure 3.9. Comparison of transcripts regulated by PQM-1 with modENCODE L3 PQM-1 ChIP dataset.

A) Venn Diagram showing the genes whose expression is driven by PQM-1 after heat stress against genetic loci bound by PQM-1 in L3 stage nematodes as found by Niu et al. B) Venn Diagram showing the genes whose expression is driven by PQM-1 independent of heat stress vs. genetic loci bound by PQM-1 in L3 stage nematodes.

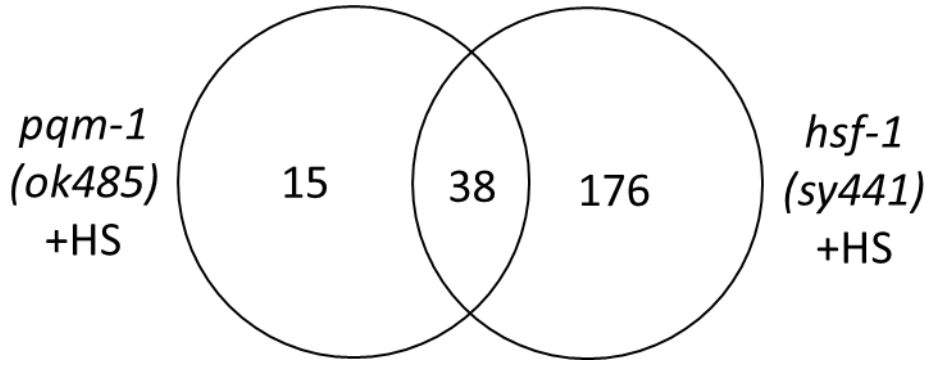

Figure 3.10. Genes controlled by both PQM-1 and HSF-1 post-acute heat stress.

Venn Diagram showing the overlap of genes found by this study to be regulated by PQM-1 following heat stress and genes regulated by HSF-1 following heat stress.

3.4.7 What are the roles of PQM-1 and HSF-1 following heat shock and do they overlap?

At the outset of the microarray we sought to understand whether the *pqm-1* (ko) was thermosensitive for the same reasons that an *hsf-1 (sy441)* mutant is thermosensitive – an inability to effectively upregulate components of the canonical HSR. As we do not see the heat shock responsive chaperones among the 53 genes upregulated by PQM-1 (Figure 3.5; Appendix Table A.10) we can conclude that the sensitivity to heat stress is not caused by an inability to enact the HSR. This evidence is compatible with data seen in the previous chapter, where the inhibited activity of both *pqm-1* and *hsf-1* has an additive effect on heat stress survival – suggesting separate pathways are regulated by each. Our analysis identified 53 PQM-1 dependent genes following acute HS and 214 HSF-1 dependent genes. 38 genes are shared between these two datasets (Figure 3.10; Appendix Table A.14). There are a few interesting genes to examine more closely from the shared list of genes that require both *hsf-1* and *pqm-1* for upregulation following acute heat stress including ubiquitin conjugating enzyme *ubc-23,* an ortholog of human FAF1 (Fas associated factor 1) (Shaye and Greenwald, 2011), which is expressed in the intestine. This enzyme is involved in protein degradation via the UPS and it is possible that post heat stress the UPS is upregulated to clear the abundant misfolded protein present in the organism, as it has been shown that the upregulation of the UPS can confer resistance to oxidative stress (Chondrogianni et al., 2015). Furthermore, the RNA binding protein LIN-28, was found to have its transcript upregulated by both HSF-1 and PQM-1 following heat stress – this gene has previously been associated with increased resistance to heat stress when knocked down by RNAi (Wang et al., 2017), so its upregulation during heat stress is unexpected. However, *lin-28* is associated with

longevity by the LIN-28 regulated microRNA *let-7* reducing the protein levels of AKT-1/2, tying *lin-28* to DAF-16 and PQM-1 through ILS. Finally, *pqm-1* mRNA is upregulated in the *hsf-1 (sy441)* mutant at 20˚C (3.16 fold) (Appendix Table A.15), a result which was mirrored in a comparable RNAi-driven study (Brunquell et al., 2016) which could be indicative of a compensatory mechanism in action in response to depleted levels of functional HSF-1.

The transcript datasets produced by the microarray analysis are not sufficient to be able to narrow down the thermosensitivity of *pqm-1* (ko) to a single gene or group of genes, but it does provide the basis for further research into the phenotype. A mini RNAi screen could be used to investigate some of the more likely candidates for thermosensitivity revealed by the microarray: growing wildtype nematodes on RNAi to specifically knock down candidate genes and then scoring heat stress survival could reveal novel genes required for heat stress survival, from the smaller pool revealed in this study.

3.5 Conclusions

It is clear that a subset of genes is regulated by *pqm-1* following heat stress as there is a distinct transcriptional profile following heat stress in the *pqm-1* (ko) compared the wildtype. There are questions remaining as to whether the affected genes are directly regulated by PQM-1, but if ChIPseq were used to look at PQM-1 binding to DNA at this time it could illuminate its binding targets. The study has also provided evidence that PQM-1 may affect thermotolerance of *C. elegans* through non-canonical pathways such as cuticle integrity and regulation of electron transport chain components of the mitochondria.

Chapter 4 Characterisation of PQM-1 in response to stress

4.1 Introduction

Stress transcription factors respond to a variety of stresses in C. elegans. For example, DAF-16/FOXO localises to the nucleus when *C. elegans* is exposed to heat shock (HS) (Tepper et al., 2013), whereas SKN-1 has been shown to accumulate in intestinal nuclei when nematodes are exposed to oxidative stress (An and Blackwell, 2003). HSF-1 localises to the nucleus constitutively, but forms sub-nuclear "stress granules" during heat stress in *C. elegans* (Morton and Lamitina, 2013; Sampuda et al., 2017; Ooi and Prahlad, 2017). In Chapter 2 I have shown that PQM-1 is required for heat stress survival in *C. elegans*. We therefore wanted to investigate the nuclear localisation pattern of PQM-1 in response to heat stress. PQM-1 is believed to be regulated through phosphorylation by the serum/glucocorticoid-regulated kinase (SGK-1), which lies downstream of PDK-1 in the ILS pathway (Dowen et al., 2016). Therefore, I investigated whether RNAi mediated knockdown of *sgk-1* affects PQM-1 protein levels and subcellular localisation during normal growth conditions or acute heat stress. I also speculated on whether PQM-1 was regulated by protein degradation by the Ubiquitin-proteasome-system in a manner analogous to SKN-1 (Choe et al., 2009). In order to investigate whether PQM-1 is post-translationally modified during heat stress we decided to immunoprecipitate PQM-1 and analyse potential posttranslational modifications by mass spectrometry. This would also allow us to identify potential PQM-1 interacting proteins during normal growth conditions as well as during heat stress, and so provide a clearer picture of the role of PQM-1 in heat stress resistance.

One of the most conserved and ancient stress responsive transcription factors is HSF-1, which is activated upon exposure of cells to heat stress (Morimoto, 1998). The stress-induced increase of misfolded proteins in the cell requires that the molecular chaperones, including the major molecular chaperones HSP-90 and HSP-70, be upregulated to combat the further protein aggregation and promote proteostasis (Anckar and Sistonen, 2011). HSF-1 activation requires that it be converted from a relatively inert monomeric state to a trimeric state which is able to bind to DNA (Bharadwaj et al., 1999; Anckar and Sistonen, 2007). The HSF-1 trimer enters the nucleus where it binds to stretches of DNA which have the canonical heat shock element (HSE) motif nGAAnnTTCn (Amin et al., 1988). The transcriptional targets of HSF-1 include major molecular chaperones including *hsp-70* and *hsp-90* and important structural genes (Anckar and Sistonen, 2011).

The FOXO transcription factor DAF-16, originally discovered as a regulator of dauer formation (Albert et al., 1981), is recruited to the nucleus during heat stress to combat the deleterious effects of stress on the survival of the nematodes (Murphy et al., 2003; Tepper et al., 2013; Hesp et al., 2015). Cellular stress is communicated to DAF-16 by a variety of stress-related kinases that activate the FOXO transcription factor by phosphorylation. These kinases include the AMP activated protein kinase AAK-2 (Apfeld et al., 2004); JUN kinase JNK-1 which is involved in oxidative stress response (Oh et al., 2005); and the p38 MAP kinase pathway which is implicated in *C. elegans* innate immunity (Troemel et al., 2006). Furthermore, DAF-16 regulates pro-longevity genes which lie downstream of *daf-2* signalling including the sHSPs *hsp-16.1* and *hsp-12.6* and *sod-3*. This is one example of how stress responsive transcription factors can have broader roles pertaining to the incidence and severity of age-related disease.

The nuclear localisation of DAF-16 anti-correlates with PQM-1 in *C. elegans* intestinal cells during development and heat stress (Tepper et al., 2013). PQM-1 functions alongside DAF-16 as a transcription factor downstream of *daf-2* and the ILS pathway. Similar to DAF-16, PQM-1 regulated by SGK-1, as well as AKT-1 and AKT-2 (Baumeister et al., 2006; Dowen et al., 2016).

SKN-1/Nrf-2 is a transcription factor which has a role in specifying mesoendodermal fate during development (Bowerman et al., 1992). SKN-1 is highly comparable to mammalian NRF-1 and 2 with which it shares the DIDLID motif, but lacks the ZIP domain – SKN-1 binds to DNA strongly as a monomer (An and Blackwell, 2003). SKN-1 has been shown to direct the response to oxidative stress and aging in *C. elegans* (An and Blackwell, 2003; Blackwell et al., 2015). Furthermore, SKN-1 is an important direct target of ILS, when ILS is active it blocks SKN-1 nuclear accumulation (Tullet et al., 2008). SKN-1 nuclear localisation is inhibited by phosphorylation by the kinases AKT-1 and AKT-2, which function downstream of DAF-2 and AGE-1 in the ILS signalling cascade (Tullet et al., 2008).

PQM-1 is a transcription factor which is known to be transcriptionally active during development (Tepper et al., 2013; Dowen et al., 2016) and accordingly localised to the nuclei in the intestine from L1 to L4 stage (O'Brien et al., 2018). PQM-1 was initially discovered as an oxidative stress responsive protein, as its RNA transcript was strongly upregulated in response to oxidative stress (Tawe et al., 1998). Since then it has also been demonstrated to be required for *C. elegans* resistance to the pathogenic bacteria *P. aeruginosa* (Shapira et al., 2006). Efforts were made by the modENCODE Consortium to analyse the genome binding sites of multiple transcription factors by ChIP-seq, among

which PQM-1 was included (Niu et al., 2011). This study revealed that at L3 stage PQM-1 primarily binds to genes involved in lipid metabolism, but alludes to PQM-1 as a stress sensor shifting from a development role to an environmental sensor, like PHA-4 (Zhong et al., 2010).

In the previous chapter we discovered that PQM-1 is necessary for *C. elegans* to survive acute heat stress events. *C. elegans* harbouring a null deletion of PQM-1 have reduced thermotolerance relative to wildtype (Chapter 2). Furthermore, when *C. elegans* are exposed to an elevated temperature, PQM-1 drives a specific transcriptional program, as determined by gene expression analysis using microarray (Chapter 3). Because PQM-1 is necessary for heat stress survival, the genes regulated by PQM-1 in response to acute heat stress are likely crucial for stress survival.

As PQM-1 is a stress responsive transcription factor, I set out to investigate whether PQM-1 localises to the nucleus in the event of heat stress, to drive the transcription of genes. Furthermore, I was interested in how PQM-1 is regulated during stress and whether it interacts with different proteins before, during and after heat stress. I approached this biochemically by immunoprecipitation of PQM-1 via a FLAG tag, using a strain expressing PQM-1::GFP::FLAG (OP201; *unc-119(tm4063) III; wgIs201*). The construct was integrated by microparticle bombardment and is expressed at a low copy number, therefore the strain reproducibly expresses the transgene without variations in expression level (Praitis et al., 2001; Sarov et al., 2006; Zhong et al., 2010).

I also looked at this problem using the powerful genetic techniques available to *C. elegans* researchers though RNAi mediated knockdown of genes that had been reported in the literature to interact with and regulate PQM-1. Confocal fluorescence microscopy

was used to visualise the localisation of PQM-1 following heat stress by its C-terminal GFP tag.

4.2 Materials and Methods

4.2.1 Nematode maintenance and strains

Nematodes were maintained as previously described (Brenner, 1974), except using OP50-1 *E. coli* and supplementing the growth media with 1 mg streptomycin per litre. The following strains were used: N2 Bristol (wildtype strain) OP201 (*unc-119(tm4063) III; wgIs201*) - generated as part of the Regulatory Elements Project, part of ModEncode (Celniker et al., 2009). The strain expresses PQM-1::GFP::FLAG under the control of the *pqm-1* promoter. The DNA binding profile of AMA-1::GFP, generated in an analogous manner, is the same as the native protein (Zhong et al., 2010); which were obtained from the *Caenorhabditis* Genetics Center. OP201 (PQM-1::TY1::GFP::FLAG) was crossed into the following strains overexpressing HSP-90::RFP in the neurons (AM987); intestine (AM986) or muscle (AM988) to result in strains PVH58 (*rmIs345[F25B3.3p::DAF-21::RFP]; wgIs201*) and PVH64 (*rmIs346[vha-6p::DAF-21::RFP]; wgIs201*) and PVH145 (*rmIs346[unc-54p::DAF-21::RFP]; wgIs201*).

4.2.2 Immunoprecipitation

Frozen nematode pellets were ground with a pestle and mortar under liquid N_2 until reaching a consistency of a fine powder. Crushed nematodes were transferred into a 50 mL falcon tube on ice. 1 mL of IP buffer (50 mM Tris pH 7.5; 150 mM NaCl; 1 mM EDTA; 0.1% NP-40; 5% Glycerol; 20mM N-Ethylmaleimide; PhosSTOP (Merck); cOmplete™ ULTRA Tablets protease inhibitor (Merck)) was added to the ground nematodes pellet and the pellet was resuspended by vortexing. 1.5 ml of ice cold suspension was

transferred to a micro centrifuge tube and spun 5 min at 10,000 x g to pellet debris. The protein concentration was determined by Bradford assay. 50 µl of Anti-FLAG® M2 Magnetic Beads (Merck) slurry was washed 3 times with the Wash buffer (Wash buffer consists of IP buffer supplemented with 1% NP-40) before use. 5 mg total protein of nematode extract was added to the FLAG bead slurry. A sample was taken for SDS-PAGE of the nematode extract ("Input") 10% of input. The whole protein extract was incubated with FLAG M2 beads at 4˚C for 3hrs rotating. Beads were pelleted, and a sample of the supernatant was taken for SDS-PAGE (10% of supernatant). The beads were washed 3x by adding 500 µL Wash Buffer and rotated for 5min at 4C before the beads were pelleted gently with a magnet. Samples were taken of the wash for analysis by SDS-PAGE. The bound proteins were eluted by adding 50 µL Elution buffer (Wash buffer supplemented with 3xFLAG Peptide (Merck) to a final volume of 500 µg/ml) and rotated for 30 minutes at 4˚C. The beads were pelleted at 4°C and the supernatant (FLAG eluate) was transferred to a fresh tube. 12.5 µl 5x SDS sample buffer was added and samples were boiled for 5 min at 95˚C. A second elution was performed with 50 µl Elution buffer and rotated for 30 minutes at 4C. The beads were pelleted at 4˚C and the supernatant was transferred (2nd FLAG eluate) to a fresh tube. 12.5 µl 5x SDS sample buffer was added and samples boiled for 5 min at 95˚C.

4.2.3 Western Blot

For Western Blot analysis, cell extracts were prepared of 1,000 age-synchronised animals grown on 10 cm NGM plates at a population density of 1,000 nematodes per plate. Nematodes were collected by washing off plates with ice cold M9 buffer and flash frozen in liquid nitrogen. The frozen pellet was supplemented with an equal volume of

Nematode Lysis Buffer (10 mM Tris pH 7.5; 150 mM NaCl; 0.5 mM EDTA; 0.5% NP-40), supplemented with EDTA-free protease inhibitor cocktail tablet (cOmplete™ ULTRA Tablets protease inhibitor, Merck) and ground with a pestle. The cell extract was prepared by centrifugation at 10,000 x g for 5 minutes at 4°C and protein concentration was determined using the Bio Rad protein assay kit (Bradford assay). Cell extracts were mixed with 5x SDS sample buffer and boiled for 5 min. 25 µg total protein was loaded onto a 10 % SDS-PAGE and western blot analysis was performed as described previously (van Oosten-Hawle et al., 2013). A monoclonal anti-FLAG antibody (Sigma) was used to detect PQM-1::GFP::FLAG. The gel analysis tool of ImageJ software was used to quantify anti-FLAG relative to endogenous tubulin levels. HRP-conjugated anti-mouse or anti-rabbit antibodies were used as secondary antibodies and Pierce ECL Western Blotting Substrate (Thermo Fisher Scientific) was used for detection.

4.2.4 Confocal Microscopy

Nematodes were imaged using a Zeiss LSM880 confocal microscope through a 10x 1.0 or a 20x 1.0 numerical aperture objective with a 488 nm line for excitation of GFP and 561nm line for excitation of mCherry (RFP). For imaging, age-synchronised animals were immobilised using 5 mM Levamisole solution in M9 buffer and mounted on 2% agarose pads.

4.2.5 Fluorescence intensity scoring

Nuclear fluorescence intensity of PQM-1::GFP::FLAG was determined by measuring the intensity of the fluorescence detected at 488 nm (GFP) in confocal microscopy images captured at 20x numerical aperture using ImageJ software (Schneider et al., 2012).

4.2.6 RNAi

In order to knockdown the indicated genes by RNAi, L4 nematodes were placed onto NGM plates supplemented with Ampicillin and IPTG seeded with *E. coli* strain HT115(DE3) transformed with RNAi vectors (J. Ahringer, University of Cambridge, Cambridge, UK) and allowed to lay eggs, adult nematodes were removed, and the progeny was grown until L4 stage. Nematodes were then collected into ice cold M9 and flash frozen in liquid nitrogen. When it was not possible to grow nematodes in this way, starved L1s from bleached populations were deposited onto plates to generate synchronous populations.

Primers used:

sgk-1*For:* ACATTCTTATTGGAACCAACCCT *Rev:* CTTTAAGCACCCTTTCCTTGTTT

uba-1 *For:* ACGGTGATTTTGAGTGGCTC *Rev:* AGTTGTTTCTTTGCCTGCGT

4.2.7 Mass Spectrometry

Eluates from the immunoprecipitation using Anti-FLAG® M2 Magnetic Beads (Merck) were run on a SDS-PAGE Gel. The gel was then subjected to silver staining (Rabilloud, 2012), to visualise protein bands.

To prepare samples for Mass spectrometry analysis, the eluates were run on a 10% Mini-PROTEAN® TGX™ Precast Gel (Bio-Rad) and stained with InstantBlue™ Protein Stain (Expedeon). Bands were excised and electrospray time-of-flight mass spectrometry was performed to identify proteins present as well as possible post-translational

modifications. Mass spectrometry analysis was performed by the University of Leeds Biomolecular Mass Spectrometry facility.

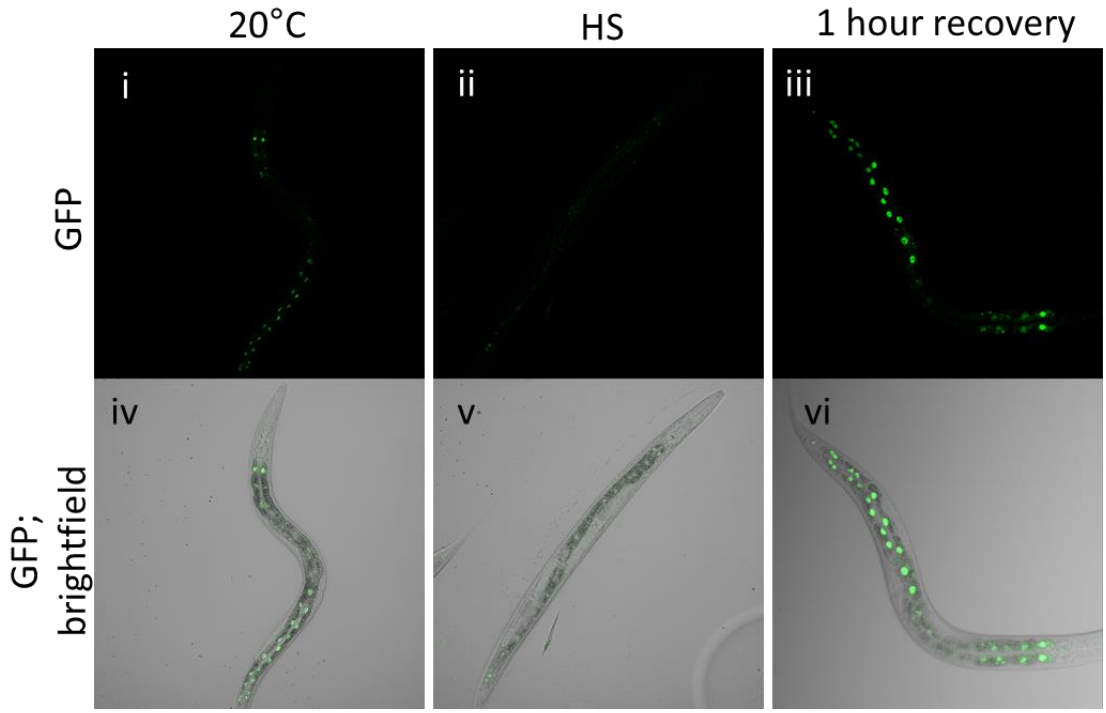

Figure 4.1. PQM-1 localises to the nucleus during recovery from heat stress

PQM-1::GFP::FLAG is localised to intestinal nuclei at L4 stage under normal growth conditions (20˚C). During heat stress conditions PQM-1::GFP::FLAG exits the nucleus and only faint GFP expression can be visualised. 1 hour post heat stress, strong nuclear localisation of PQM-1::GFP::FLAG is once again visible in the intestine. (i – iii) show GFP; (iv – vi) show GFP combined with brightfield. (i; iv) L4 *C. elegans* expressing PQM-1::GFP::FLAG at 20˚C. (ii;v) L4 *C. elegans* expressing PQM-1::GFP::FLAG during heat stress (35˚C). (iii; vi) L4 *C. elegans* expressing PQM-1::GFP::FLAG recovered for 1 hour at 20˚C from a 1 hour 35˚C heat shock.

4.3 **Results**

I was interested in the role of PQM-1 during stress and investigated its nuclear localisation following heat stress and conditions inducing TCS. To identify when PQM-1 is present in the nucleus I have made use of a strain which expresses a PQM-1::GFP::FLAG fusion protein (Sarov et al., 2006). When PQM-1 is present in the nucleus and presumably influencing gene expression, such as during development, GFP can be visualised in intestinal nuclei (Tepper et al., 2013; O'Brien et al., 2018).

4.3.1 Localisation of PQM-1 to intestinal nuclei following heat stress

PQM-1 localises to the intestinal nuclei of *C. elegans* during development from L1 to L4 stage (O'Brien et al., 2018). PQM-1 nuclear localisation becomes diffuse at the L4 stage and this continues as the animal enters early adulthood (Tepper et al., 2013; O'Brien et al., 2018). As soon as *C. elegans* enters reproductive adulthood, the nuclear localisation of PQM-1 disappears completely. Figure 4.1 shows representative confocal images of L4 larvae expressing PQM-1::GFP::FLAG at 20˚C (Figure 4.1, i and iv) when nuclear localisation can be seen. During a 1 hour HS at 35˚C PQM-1 exits the nucleus (Fig. 1, ii and v) and after 1 hour recovery at 20˚C, i.e. post HS (Figure 4.1, iii and vi) PQM-1 re-enters the nucleus. By comparison, nuclear localisation of PQM-1::GFP::FLAG cannot be observed in day 1 adults at 20C (Figure 4.2, i and iv) or during HS (Figure 4.2, ii and v). Interestingly, PQM-1::GFP::FLAG re-localises to the nucleus after 1 hour recovery at 20C post HS (Figure 4.2, iii and vi). This result was surprising, as PQM-1 was originally described as a developmentally active transcription factor that regulates genes involved in dauer formation (Tepper et al., 2013) and pathogen response (Shapira et al., 2006).

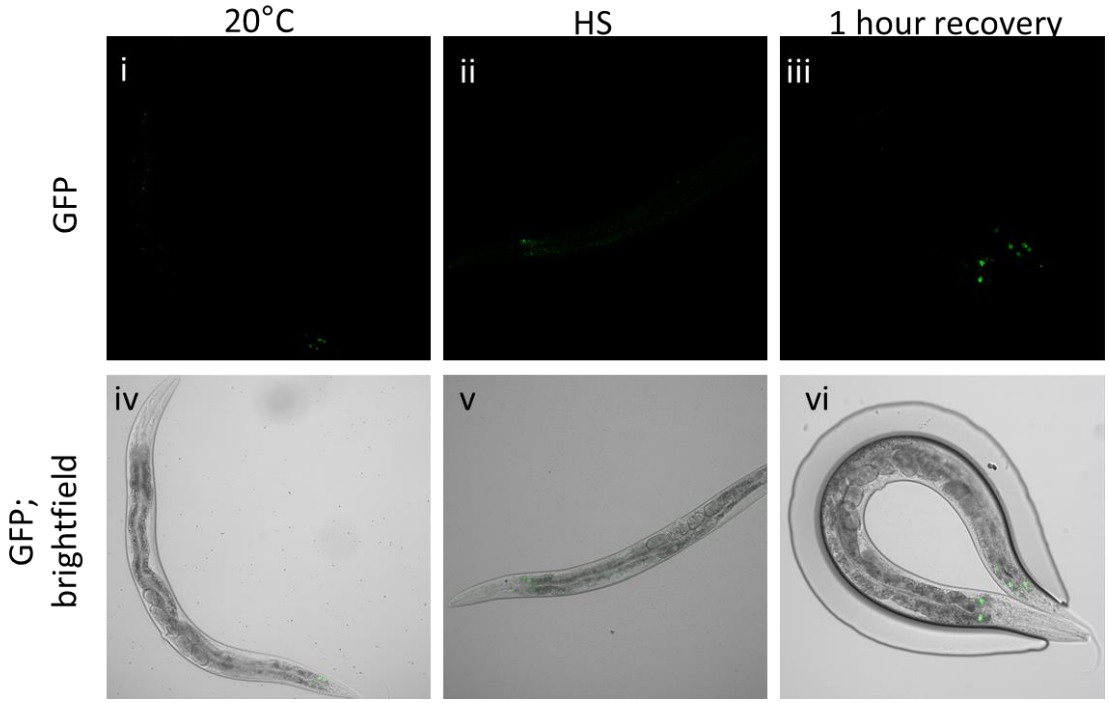

Figure 4.2. PQM-1 localises to the nucleus during recovery from heat stress even in adult *C. elegans.*

PQM-1::GFP::FLAG is not visible in the intestinal nuclei in adult stage *C. elegans* under normal growth conditions (20˚C). During heat stress conditions PQM-1::GFP::FLAG exits the nucleus and only faint GFP expression can be visualised. After a 1 hour recovery period at 20˚C post heat shock, strong localisation of PQM-1::GFP::FLAG is visible in the intestinal nuclei. (i – iii) show GFP; (iv – vi) show GFP combined with brightfield filters. (i; iv) Adult *C. elegans* expressing PQM-1::GFP::FLAG at 20˚C. (ii;v) Adult *C. elegans* expressing PQM-1::GFP::FLAG during heat stress (35˚C). (iii; vi) Adult *C. elegans* expressing PQM-1::GFP::FLAG recovered for 1 hour at 20˚C from a 1 hour 35˚C heat shock.

4.3.2 PQM-1 expression is increased during heat stress recovery

To determine whether the increased localisation of PQM-1 to intestinal nuclei in day 1 *C. elegans* adults post HS was related to the abundance of the protein, we analysed protein expression levels by Western blot. As can be seen in Figure 4.3, protein expression levels of PQM-1 rise following heat stress and continue to increase during recovery. PQM-1 expression levels increase 2-fold after a 1-hour recovery period post heat shock. 2 hours post HS, PQM-1 levels further increase by 6-fold, compared to expression levels at 20C before HS (Figure 4.3). The peak of PQM-1 expression appears to be reached at 2-hour post HS, after which PQM-1 expression levels steadily decrease until they reach expression levels comparable to control conditions, 12 hours post HS (Figure 4.3).

4.3.3 PQM-1 localises to the intestinal nuclei when TCS is active

Transcellular chaperone signalling (TCS) occurs when molecular chaperones are either overexpressed or knocked down tissue specifically (van Oosten-Hawle et al., 2013; van Oosten-Hawle and Morimoto, 2014). In the model used in this thesis, HSP-90 was overexpressed tissue-specifically in the neurons, intestine, or body wall muscle, which in turn upregulates *hsp-90* expression in distal tissues. This cell-non-autonomous response that transcellularly triggers increased *hsp-90* expression in muscle cells, is mediated by PQM-1 (O'Brien et al., 2018).

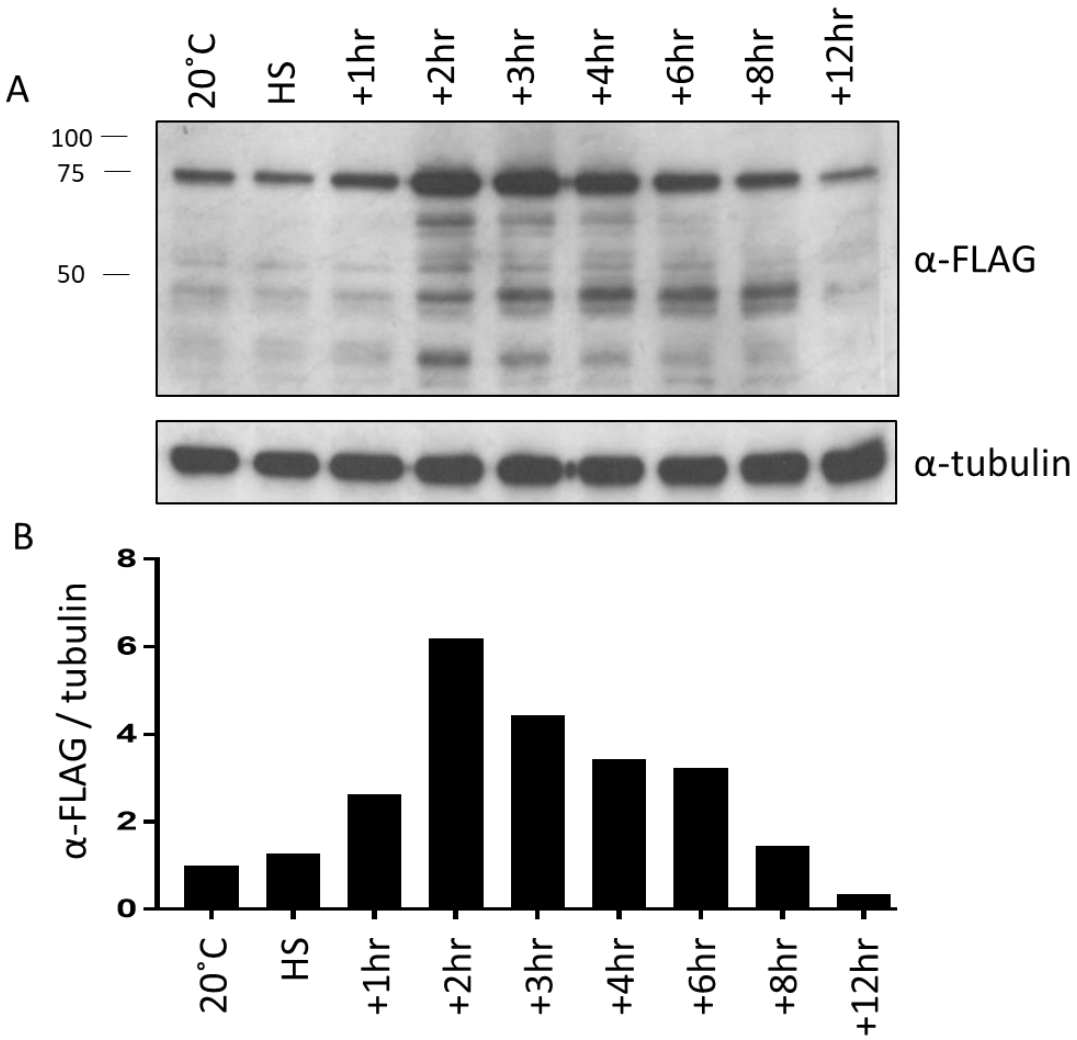

Figure 4.3. PQM-1 levels increase during the recovery phase after heat shock.

(A) Western blot analysis of PQM-1::GFP::FLAG expression before (20˚C), during (HS), and at 1hr, 2hr, 3hr, 4hr, 6hr, 8hr and 12 hour recovery time points post HS, using an anti-FLAG antibody. Anti-tubulin antibody was used as a loading control. (B) Quantification of the intensity of (PQM-1::GFP::FLAG) 75kDa, normalised to the tubulin control for each sample.

While PQM-1::GFP::FLAG is normally not observed in the nucleus in day 1 adult *C. elegans* (Figure 4.2, i, v), activation of TCS in either the neurons or the intestine by tissue-specific overexpression of HSP-90 induces PQM-1 nuclear localisation in adult animals (Figure 4.4; O'Brien et al., 2018).

If HSP-90::RFP is overexpressed in the body wall muscle (Figure 4.4, ii, vi), localisation of PQM-1::GFP::FLAG to the intestinal nuclei can be observed. Furthermore, if HSP-90 is overexpressed in the intestine, triggering TCS from the gut of the animal, there is an increase in the localisation of PQM-1 to the intestinal nuclei (Figure 4.4). When HSP-90::RFP is overexpressed in the *C. elegans* nervous system, PQM-1 localises to the intestinal nuclei much more strongly than in a wildtype background (Figure 4.4, iv, viii). Therefore, it is clear that TCS driven by HSP-90 overexpression in the intestine, body wall muscle or neurons activates nuclear localisation of PQM-1. Quantification of PQM-1::GFP::FLAG subcellular localisation shows greater nuclear localisation in the TCS *C. elegans* models(Figure 4; Laura Jones, O'Brien et al., 2018), with a significantly higher nuclear localisation in both HSP-90^{int} (15%) and HSP-90^{neuro} (20%) nematodes compared to wildtype (5%), although nuclear localisation appears increased for PQM-1 in an HSP-90^{bwm} background (10%), it does not reach statistical significance.

The nuclear localisation of PQM-1 under these conditions implies that it is directing transcriptional activity when TCS is activated. Interestingly, Western blot analysis revealed that TCS does not lead to increased PQM-1 expression levels (Figure 5; O'Brien et al., 2018).

4.3.4 Knockdown of *sgk-1* results in increased nuclear localisation of PQM-1

The observation that PQM-1::GFP::FLAG localises to the nucleus during the recovery period post HS as well as during TCS indicates that it may be transcriptionally active during these stress conditions. We however do not know how PQM-1 is regulated during these stress conditions that triggers its nuclear localisation. We therefore sought to uncover regulators of PQM-1 activity.

The serine/threonine kinase *sgk-1,* which is required for oxidative stress response, regulation of lifespan through its function in the insulin like signalling pathway (Baumeister et al., 2006) has been identified as a regulator of PQM-1 (Dowen et al., 2016). SGK-1 forms a protein complex with the AKT kinases, and is activated by and dependent on the kinase PDK-1 (Hertweck et al., 2004). SGK-1, AKT-1 and PDK-1 are all able to phosphorylate DAF-16, yet have different roles within the ILS pathway (Kimura, 1997; Murphy et al., 2003; Hertweck et al., 2004).

Dowen et al. had previously shown that SGK-1 acts as a suppressor of PQM-1 transcriptional activity (Dowen et al., 2016). RNAi mediated knockdown of sgk-1 indeed confirmed this finding as this led to nuclear localisation of PQM-1::GFP::FLAG in day 1 adult, but not L4 stage *C. elegans* (Figure 4.6; Figure 4.7). In L4 *C. elegans*, when sgk-1 is knocked down by RNAi, there is no change of GFP intensity in the intestinal nuclei at 20˚C (Figure 4.6). Thus, the localisation of PQM-1 to intestinal nuclei during sgk-1 RNAi does not differ from control conditions. During the recovery phase following heat stress, a strong nuclear localisation of PQM-1 can be observed as shown by the 2.5-fold increased GFP fluorescence intensity (Figure 4.6). RNAi-mediated knockdown of *sgk-1*

leads to a 3-fold increase of GFP fluorescence intensity post HS compared to control (Figure 4.6B).

In day 1 adult *C. elegans* the effects of RNAi-mediated *sgk-1* knock-down are much more pronounced (Figure 4.7). The nuclear intensity of GFP is 3-fold higher in the *sgk-1* knock-down than the control at 20˚C (Figure 4.7B). The increased GFP fluorescence in intestinal nuclei persists through heat stress during sgk-*1* RNAi, with nuclear GFP fluorescence intensity being 3.5-fold higher, compared to control conditions (Figure 4.7B). Additionally, after recovery from the heat stress, GFP fluorescence intensity during sgk-*1* RNAi are more than 6-fold higher, compared to control nematodes (Figure 4.7B).

This result indicates that *sgk-1* plays a role in the transport of PQM-1 from the nucleus during heat stress. These results seem to suggest that *sgk-1* acts as a repressor of PQM-1 (Dowen et al., 2016).

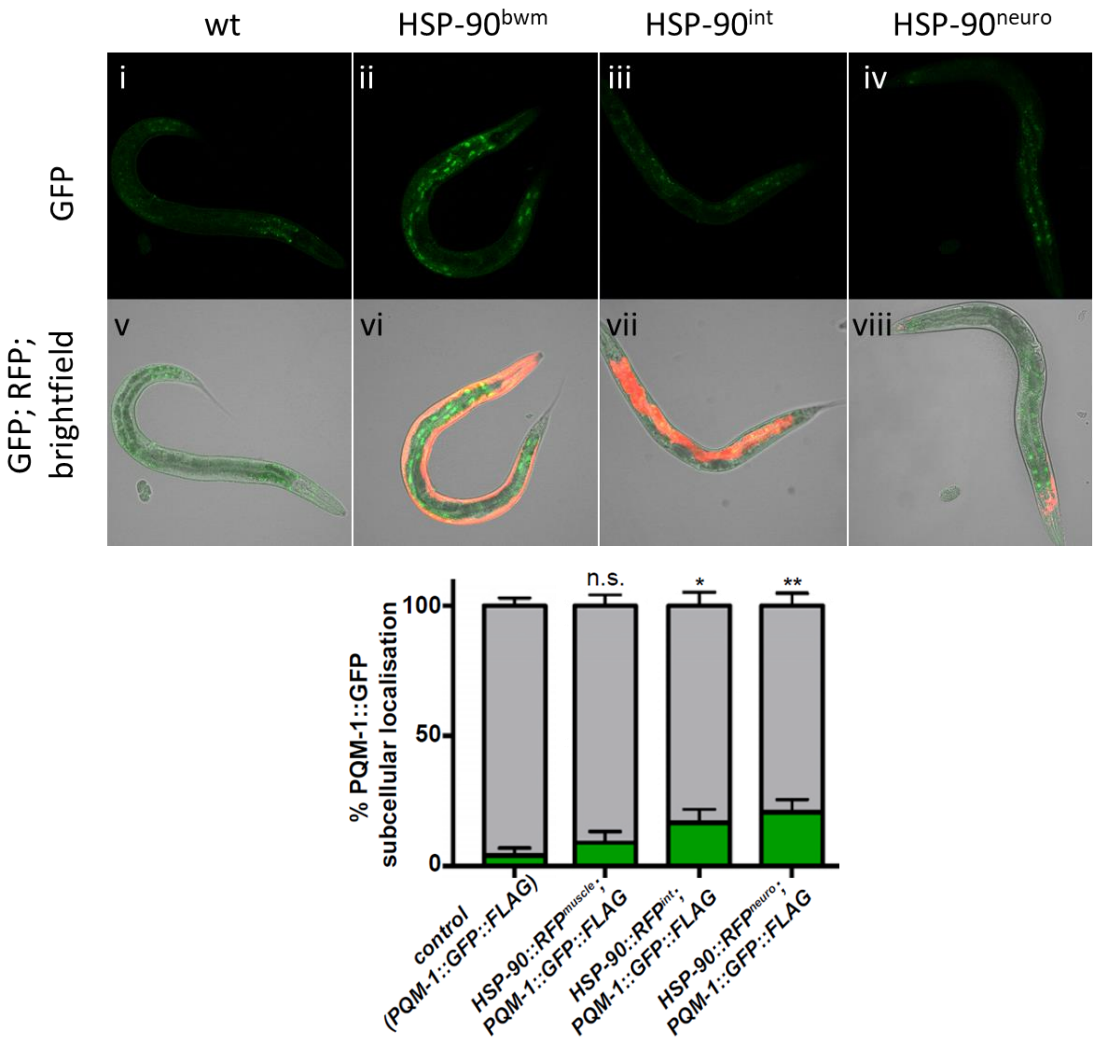

Figure 4.4. Transcellular chaperone signalling promotes PQM-1 nuclear localisation.

Adult nematodes expressing PQM-1::GFP::FLAG in a control background (i; v); and in strains overexpressing HSP-90::RFP in the body wall muscle (HSP-90^{bwm})(ii; vi); in the intestine (HSP-90^{int}) (iii; vii); and in the neurons (HSP-90^{neuro})(iv; viii). i and v: PQM-1::GFP::FLAG is cytoplasmic in adult stage *C. elegans* under normal growth conditions at 20˚C. During TCS when HSP-90::RFP is tissue-specifically overexpressed, PQM-1::GFP::FLAG is retained in the nucleus, even in day 1 adults. i – iv shows GFP; v – viii shows GFP overlayed with RFP and brightfield filters. The subcellular localisation (cytosolic or nuclear) of PQM-1::GFP::FLAG in the intestine of strains expressing HSP-90::RFP in the neurons (HSP-90::RFP^{neuro}), the intestine (HSP-90::RFP^{int}), or the muscle (HSP-90::RFP^{muscle})was scored and compared to the control strain (n > 20 per strain). *p < 0.05; **p < 0.01; Kruskal-Wallis test. Error bars represent ± SEM. Graph provided by Laura Jones (O'Brien et al., 2018).

4.3.5 Knockdown of *uba-1* results in increased nuclear localisation of PQM-1

To test potential links between PQM-1 activity and the UPS – an integral component of the PN (Labbadia and Morimoto, 2015), *uba-1,* the sole ubiquitin E1 ligase in *C. elegans* was knocked down by RNAi. Under these conditions GFP fluorescence intensity in intestinal nuclei is even higher. In L4-stage animals*, uba-1* RNAi promotes localisation of PQM-1::GFP::FLAG to intestinal nuclei at 20˚C, and the localisation is continued throughout and post heat stress (Figure 4.6A). When the localisation of PQM-1::GFP::FLAG in L4 *C. elegans* is quantified by measuring GFP fluorescence intensity in the intestinal nuclei, it reveals that at 20˚C, RNAi-mediated knock-down of *uba-1* results in a 1.5-fold increase in nuclear intensity relative to control RNAi (Figure 4.6B). Furthermore, the nuclear intensity persists through heat shock, and levels are approximately 2-fold higher in nematodes subjected to *uba-1* RNAi (Figure 4.6B). During recovery from heat stress, the levels of nuclear intensity remain constant in *uba-1* RNAi treated nematodes (Figure 4.6B), although they are 2.5-fold higher control animals at 20˚C.

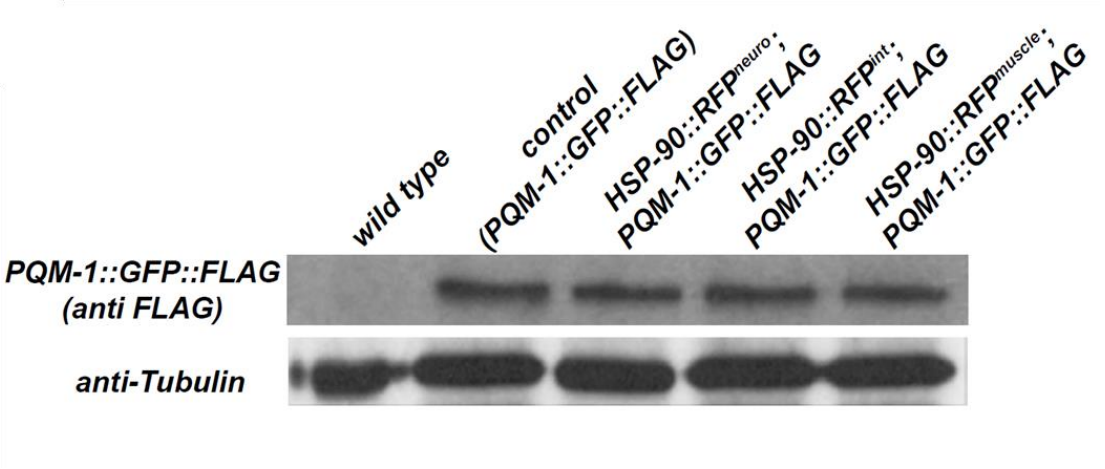

Figure 4.5. TCS does not affect PQM-1 protein levels in *C. elegans*.

Western blot analysis of PQM-1::GFP::FLAG in TCS-activated strains compared to control animals using an anti-FLAG antibody. Tubulin was used as a loading control.

Uba-1 RNAi in day 1 adult nematodes led to increased levels of PQM-1::GFP::FLAG in the nucleus, as analysed by quantification of GFP fluorescence intensity during all conditions tested (20˚C; HS and recovery post heat shock) (Figure 4.7A). RNAi-mediated knockdown of *uba-1* in *C. elegans* adults increased the GFP fluorescence intensity in intestinal nuclei by 5-fold compared to control conditions (Figure 4.7B). The nuclear intensity was 3-fold higher during HS (35 ˚C) compared to the control at 20˚C, and 2-fold higher than the control during HS (35˚C) (Figure 4.7B). During the recovery phase post-HS, GFP fluorescence intensity was 2-fold higher compared to control animals (Figure 4.7B).

4.3.6 Knockdown of *sgk-1* increases PQM-1 protein levels

To understand how PQM-1 is regulated by SGK-1, PQM-1::GFP::FLAG protein expression levels were examined by Western Blot in cell extracts of L4 nematodes grown on *sgk-1* or control RNAi at 20°C; or treated with a 1-hour HS at 35°C ; or 2-hours recovery at 20C post HS (Figure 4.8A). PQM-1 expression levels are elevated 2-fold during *sgk-1* RNAi at 20˚C compared to control RNAi (Figure 4.8B). This indicates that *sgk-1* negatively regulates PQM-1 protein expression, even under normal growth conditions (Figure 4.8). During HS, PQM-1 expression is upregulated approximately 1.2-fold in both, animals treated with *sgk-1* RNAi or control RNAi (Figure 4.8B). PQM-1 expression is upregulated 5-fold 2 hours post-HS compared to 20°C; whereas PQM-1 expression levels are upregulated 4-fold when treated with *sgk-1* RNAi (Figure 4.8B).

4.3.7 Knockdown of *uba-1* increases PQM-1 protein levels

To investigate whether PQM-1 protein levels are regulated by the UPS, knocked down *uba-1* by RNAi to block targeting of proteins for degradation by ubiquitin. RNAi-mediated knockdown of *uba-1* in L4 stage animals resulted in a 4-fold increase of PQM-1::GFP::FLAG expression levels at 20°C compared to control RNAi (Figure 4.8B). During HS, PQM-1::GFP::FLAG expression was approximately 4-fold higher compared to the control at 20°C. During recovery, PQM-1 expression continued to be elevated in nematodes treated with *uba-1* RNAi, albeit levels appear slightly lower (4-fold) when compared to PQM-1 expression at the same timepoint during control RNAi (5-fold) (Figure 4.8B). The fact that RNAi-mediated knockdown of *uba-1* results in increased expression of PQM-1 even during control conditions (20˚C), suggests that *uba-1* negatively regulates PQM-1. This indicates that PQM-1 may be turned over via the UPS to repress its transcriptional activity during normal growth conditions. Thus, interference with the UPS by RNAi mediated knockdown of one of its components (*uba-1*) leads to an increase in PQM-1 protein levels and increased nuclear localisation.

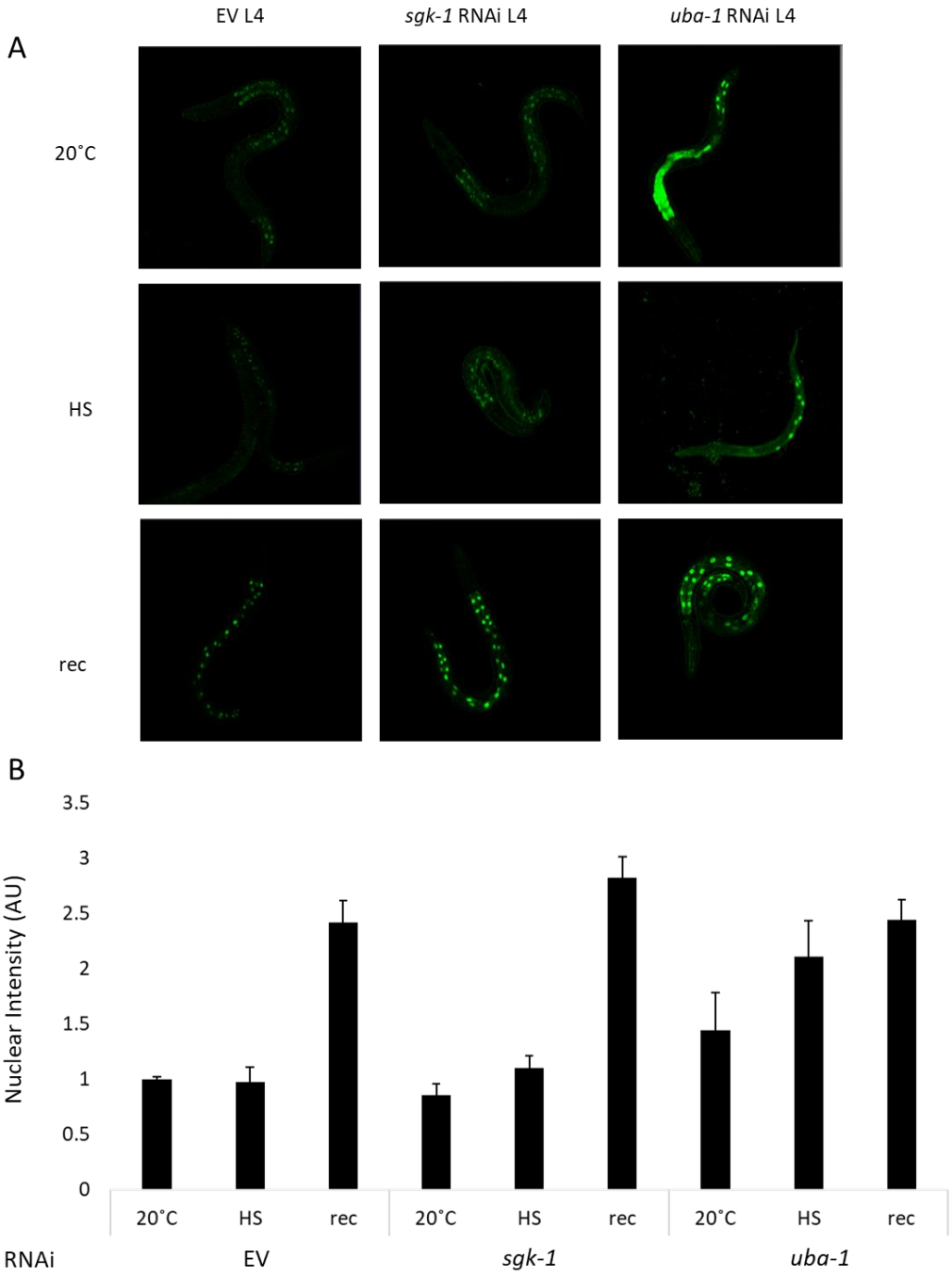

Figure 4.6. RNAi-mediated knockdown of *sgk-1* or *uba-1* results in PQM-1::GFP::FLAG nuclear localisation.

(A) L4 nematodes expressing *pqm-1p::PQM-1::GFP::FLAG* fed with bacteria expressing control RNAi (E.V.) (I; iv; vii); *sgk-1* (ii; v; viii); or *uba-1* (iii; vi; ix) RNAi were imaged by confocal microscopy at 20°C (i-iii); immediately after heat shock (iv-vi), and 2 hours post HS (recovery) (vii-ix). (B) Graph shows quantification of fluorescence intensity of nuclei relative to background, normalised to EV (control) RNAi at 20˚C (n > 4). Analysis was performed using ImageJ software. Error bars represent ± SEM.

4.3.8 **Immunoprecipitation of PQM-1**

To gain a more detailed understanding of how PQM-1 could be regulated during HS, we aimed to examine potential protein-protein interactions that take place during the recovery period 2 hours post HS. Therefore, we sought to purify PQM-1 from whole nematode extracts by immunoprecipitation and analyse the samples by mass spectrometry. This would allow us to identify any potential post translational modifications of PQM-1; and to identify any proteins that directly interact with PQM-1. The strain used (OP201 *unc-119(tm4063) III; wgIs201*) expressed a PQM-1::GFP::FLAG construct. The 3xFLAG tag, is a peptide highly amenable to immunoprecipitation with an anti-FLAG antibody. The nematodes were collected after a 2 hour recovery at 20˚C post-HS, as we had previously observed that PQM-1::GFP::FLAG expression levels peak at this time point by both Western Blot (Figure 4.3) and confocal microscopy (Figure 4.1). Immunoprecipitation of PQM-1::GFP::FLAG from whole animal extract is shown in Figure 4.9A: PQM-1::GFP::FLAG protein is present in the input samples, and enriched in the eluates after immunoprecipitation.

The eluates were analysed on an SDS-PAGE by silver stain (Figure 4.9B) as well as MS-compatible Coomassie staining. Protein bands appearing at different molecular weights in the eluate were excised and further processed by the Leeds Biomolecular Mass Spectrometry Facility. The samples were analysed by electrospray time-of-flight mass spectrometry to determine the identity of PQM-1-interacting proteins as well as potential post-translational modifications of PQM-1 itself. Mass spectrometry analysis identified five PQM-1 protein interactors (Table 4.1). These were Y37E3.17, which is

predicted to have oxidoreductase activity (Shaye and Greenwald, 2011); HSP-90, a highly conserved and highly expressed major molecular chaperone (Taipale et al., 2010); ACLY-1, predicted to have ATP citrate synthase activity (Shaye and Greenwald, 2011); EEF-2, eukaryotic elongation factor 2 ; and GLDC-1, predicted to have glycine dehydrogenase activity (Shaye and Greenwald, 2011).

We were however unable to identify PQM-1 protein by mass spectrometry in the co-immunoprecipitated sample, despite the fact that it is detected by Western Blot analysis using an anti-FLAG antibody (Figure 4.9A). Peptide fragment mapping to the proteins can be found in Appendix B.

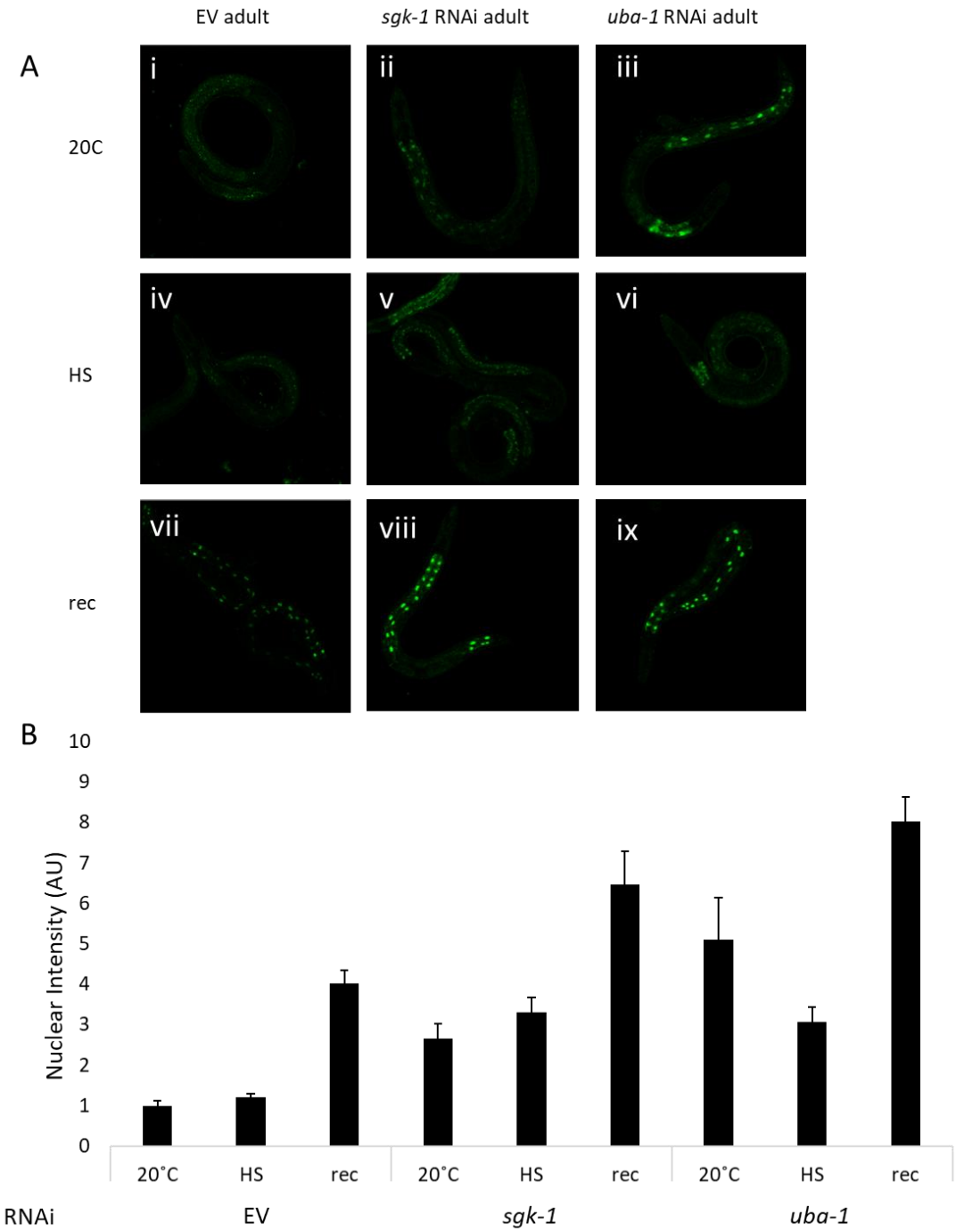

Figure 4.7. *sgk-1* or *uba-1* RNAi leads to nuclear localisation of PQM-1::GFP::FLAG.

(A) Day 1 adult nematodes expressing *pqm-1p::PQM-1::GFP::FLAG* grown on control RNAi (E.V.) (I; iv; vii); *sgk-1* (ii; v; viii); or*uba-1* (iii; vi; ix) RNAi were imaged by confocal microscopy at 20°C (i-iii); immediately after heat shock (iv-vi), and after a 2 hour recovery post HS (vii-ix). (B) Graph shows quantification of fluorescence intensity of nuclei relative to background normalised to EV (control) RNAi at 20˚C (n > 8) . Analysis was performed using ImageJ software. Error bars represent ± SEM.

4.4 Discussion

4.4.1 PQM-1 localises to the nucleus during heat stress recovery

Nuclear localisation of PQM-1 during development is indicative of its active role in regulating transcription during this time (Tepper et al., 2013). Here we discovered that PQM-1 localises to the nucleus after heat shock in both L4 and adult *C. elegans.* This indicates that it plays a role in regulating gene expression in response to heat stress. Indeed, this localisation ties in with the thermosensitive phenotype of the *pqm-1(ok485)* deletion mutant strain. Thus, the nuclear translocation of PQM-1 during HS recovery suggests that it could promote a specific transcriptional programme post-HS that is required for survival.

The elevated protein levels of PQM-1, as investigated by Western Blot analysis, during the recovery phase post HS reveal that PQM-1 is upregulated during HS and after the nematodes are removed from the heat stress environment (Figure 4.8). The co-ordination of both upregulation of protein expression and nuclear localisation of PQM-1 in response to heat stress indicates that the transcription factor is important at this time. It is worth considering this result in light of the localisation pattern of the stress responsive transcription factors DAF-16 and SKN-1. DAF-16 localises to the intestinal nuclei when *C. elegans* is exposed to heat stress (Tepper et al., 2013). Moreover, the relationship between DAF-16 and PQM-1 is thought to be mutually antagonistic – whereby each excludes the other from the nucleus. Tepper et al. (2013) described the interplay of DAF-16 and PQM-1 (Tepper et al., 2013). The nuclear localisation of each is regulated in opposite ways by the DAF-2/ILS pathway. In *daf-2* mutants, DAF-16

influences the expression of the DAE (DAF-16-associated element) target genes, which are regulated by PQM-1. Further evidence of the link between PQM-1 and ILS is shown by the reduced lifespan of the long lived *daf-2* mutants lacking *pqm-1* (Tepper et al., 2013).

Our observations that PQM-1 localises to the nucleus once the nematodes are removed from heat stress seem to agree with the observations made by Tepper et al. whereby DAF-16 and PQM-1 nuclear localisation is anticorrelated (Figure 4.1; Figure 4.2). PQM-1 is excluded from the nucleus during HS, reflecting the result reported by Tepper et al that DAF-16 is localised to the nucleus during heat stress. It is only after the nematodes are returned to 20˚C that PQM-1 nuclear accumulation occurs. Furthermore PQM-1, like SKN-1, is a transcription factor which responds to oxidative stress that also plays a role in development of the organism (An and Blackwell, 2003). Also, like SKN-1, PQM-1 is expressed mostly in the intestine of the nematode – and localises to the nuclei as a result of *C. elegans* exposure to stressful conditions. All three of these transcription factors are regulated by ILS (Ogg et al., 1997; Tullet et al., 2008; Dowen et al., 2016)which is responsible for regulation of lifespan and response to heat stress (McColl et al., 2010). As each of these stress responsive transcription factors can be regulated by ILS, it may be the case that there are multiple outcomes from the signalling pathway to fine tune the cellular stress response to particular insults to the proteome.

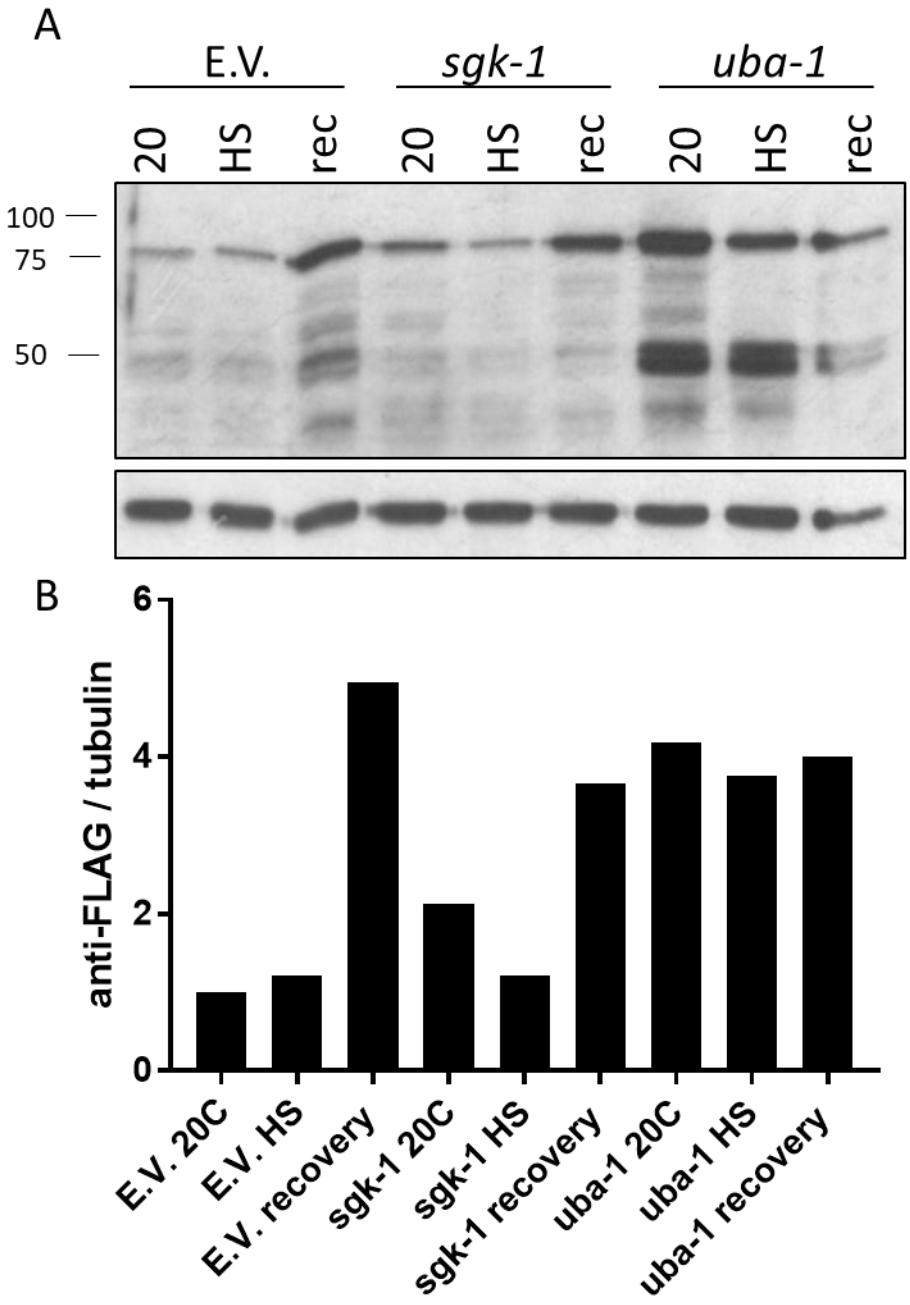

Figure 4.8. PQM-1 protein expression levels are elevated when *sgk-1* or *uba-1* is knocked down by RNAi.

(A)Western blot analysis of *C. elegans* expressing PQM-1::GFP::FLAG. Whole nematode extracts were prepared from nematodes treated with control RNAi (Empty Vector; EV); *sgk-1* or *uba-1* RNAi at 20°C; or treated with HS for 1 hour at 35°C (HS); or HS plus 2 hours recovery at 20˚C (rec). (B) Quantification of the intensity of the PQM-1::GFP::FLAG protein bands (75kDa), normalised to the tubulin control for each sample.

C. elegans mutants of *skn-1* have aberrant fat metabolism, with yolk accumulation in the head of the animal occurring prematurely (An and Blackwell, 2003). The accumulation of fat occurs naturally as *C. elegans* traverse old age, but it seems to be mis-regulated in a *pqm-1* mutant. Indeed, PQM-1 has been heavily implicated in yolk transport through its influence on vitellogenin gene expression (Dowen et al., 2016).

It has been shown that PQM-1 acts, albeit indirectly, to inhibit vitellogenin genes which are required for production of healthy oocytes (Dowen et al., 2016). While the transcriptional programme directed by PQM-1 post HS may be required for its survival (described in Chapter 2), a repressive role of PQM-1 during and post HS is of equal importance. For example, it may be that in the aftermath of heat stress the soma of the nematode is not in a state of repair such that the animal can safely allocate resources to reproduction. Perhaps at this time, PQM-1 is required to suppress a reproductive transcriptional programme until the body of the animal is recovered to such an extent that it would not be deleterious to organismal survival. Thus, it may be that the disruption of these stress responsive transcription factors leads to mismanagement of resources to reproduction and the associated decline of somatic function.

4.4.2 PQM-1 localises to the nucleus during TCS

Tissues that experience local proteotoxic stress, such as the tissue-specific overexpression of a major molecular chaperone HSP90, induce TCS which activates molecular chaperones in distal tissues (van Oosten-Hawle et al., 2013). The tissue that experiences the insult to its proteome is designated the “sensor” tissue, and the tissues which respond by upregulating their molecular chaperones are the “receiving” tissues.

Overexpression of HSP90 in a particular “sensor” tissue, such as the neurons or intestine induces TCS (van Oosten-Hawle et al., 2013; O’Brien et al., 2018).

PQM-1 facilitates TCS by mediating *hsp-90* expression in the muscle when HSP-90 is overexpressed in the neurons or the intestine. In concordance with this finding which indicates an increased transcriptional activity during TCS, PQM-1 is also retained in intestinal nuclei in adult nematodes, indicating increased transcriptional activity during TCS (O’Brien et al., 2018). It is, however, surprising that PQM-1 localises to the intestinal nuclei regardless of the “sensor” tissue (O’Brien et al., 2018). For example, it would be expected that PQM-1 localises to the nuclei of the intestine when HSP-90 is overexpressed in the intestine (Figure 4.4, iii, vii). However, PQM-1 localisation to the intestinal nuclei is also seen when HSP-90 is overexpressed in the body wall muscle or neurons (Figure 4.4, ii, vi & iv, viii respectively). There is no alteration in PQM-1 levels under these conditions when compared with a PQM-1::GFP::FLAG background (Figure 4.5; O’Brien et al., 2018). It is therefore possible, at least in the case of TCS, that the increase of PQM-1 in the intestinal nuclei is not due to an increase in the abundance of the protein, but due to PQM-1 being targeted to and retained in the nucleus in these circumstances. While *pqm-1* expression was observed in neurons by the use of a fluorescent reporter (Reece-Hoyes et al., 2007), and by single cell transcriptional profiling (Cao et al., 2017), we have not been able to detect the expression of PQM-1::GFP::FLAG in neurons by confocal fluorescence microscopy. However, knockdown of *pqm-1* specifically in neurons interferes with TCS originating from overexpression of HSP-90 in the neurons (O’Brien et al., 2018), indicating that PQM-1 is required in the neurons to enact TCS.

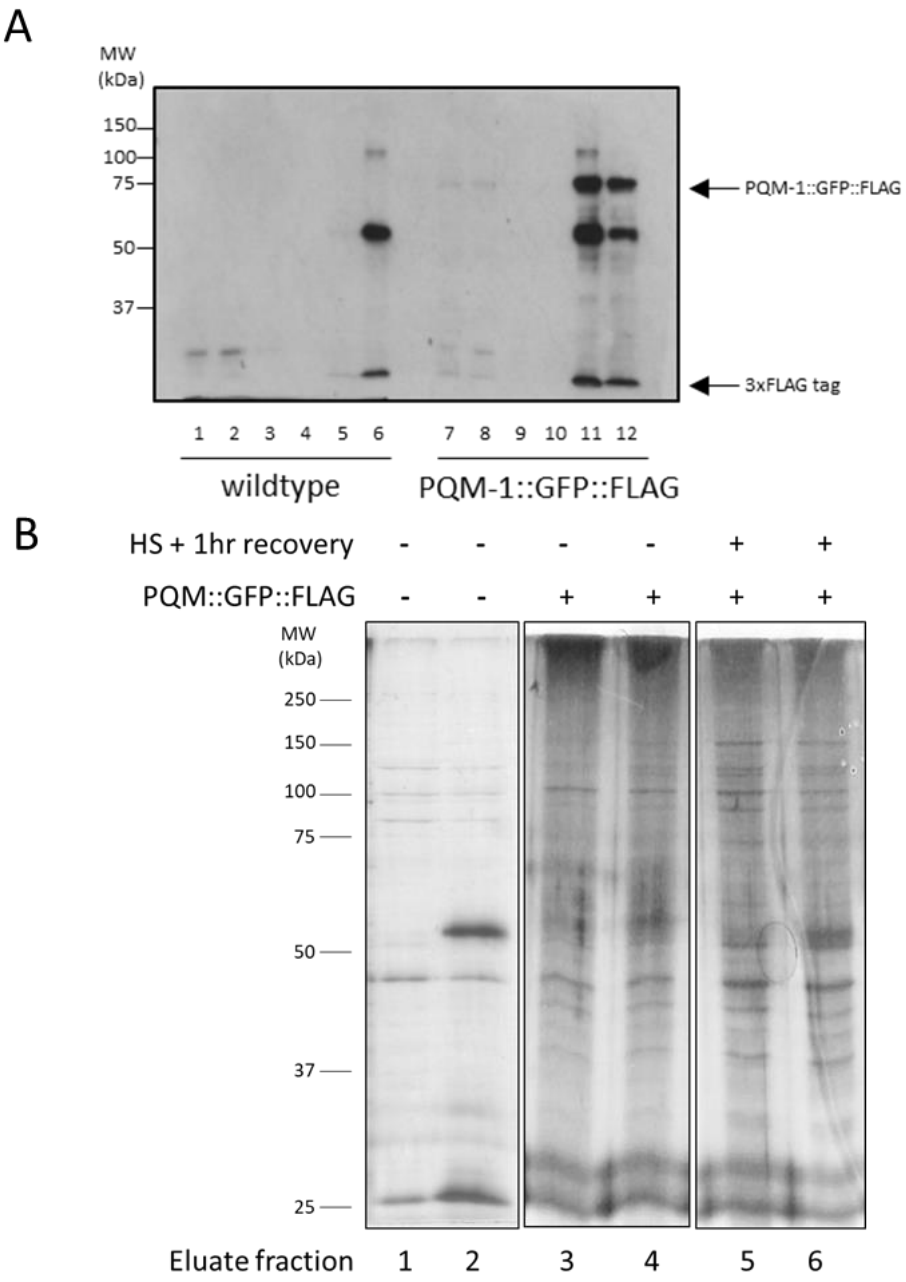

Figure 4.9. Immunoprecipitation of PQM-1::GFP::FLAG using anti-FLAG beads.

(A) Western blot analysis of immunoprecipitation. Wildtype (negative control) is on the left (1-6), nematodes which express PQM-1::GFP::FLAG transgene are on the right (7-12). 1+7: protein extract prior to immunoprecipitation (Input); 2+8: supernatant of the FLAG beads; 3+9: wash 1; 4+10: wash 2; 5+11: first elution; 6+12: second elution (B) Silver stained gel showing eluted samples from magnetic anti-FLAG agarose beads. Wildtype (left panel; lanes 1+2); PQM-1::GFP::FLAG expressing nematodes at 20˚C (middle panel; lanes 3+4); PQM-1::GFP::FLAG expressing nematodes 1 hour recovery at 20˚C post-HS (35˚C, 1 hour) (right panel lanes 5+6).

4.4.3 Localisation of PQM-1 to the nucleus is influenced by the kinase SGK-1

There is speculation that SGK-1 phosphorylates PQM-1 on one or several sites and this could hypothetically prevent its nuclear entry (Dowen et al., 2016). Dowen et al. note that PQM-1 possesses a SGK consensus phosphorylation motif (RERTSTI) in a conserved region at the C terminus of the protein (Kobayashi et al. 1999); but that the mutation of this site to a non-phosphorylatable residue was not sufficient to constitutively repress *vit-3* expression, which is a reported PQM-1 target (Dowen et al., 2016). The authors also hypothesise that other phosphorylation sites may compensate when this residue is removed. The nuclear localisation of PQM-1 is increased when *sgk-1* is knocked down by RNAi at 20˚C in adult *C. elegans* (Figure 4.7). This implies that the subcellular localisation of PQM-1 is indeed regulated by SGK-1. It is however also possible that PQM-1 is indirectly regulated via SGK-1, through another *sgk-1* dependent kinase for example. When *sgk-1* is knocked down by RNAi, PQM-1 protein levels are elevated in L4 nematodes above the control levels (Figure 4.8). Furthermore, it was previously demonstrated that *pqm-1* mRNA levels are upregulated 2.5 fold in *sgk-1* mutant nematodes (Dowen et al., 2016). It therefore appears that *sgk-1* may regulate the activity of PQM-1 by suppressing its expression at the transcript level.

4.4.4 Disruption of the UPS causes increased PQM-1 nuclear localisation and expression

There are increased levels of PQM-1::GFP::FLAG in the nucleus when *uba-1* is knocked down by RNAi, as shown by increased fluorescence intensity in the nuclei under these conditions (Figure 4.6B; Figure 4.7B). PQM-1 protein levels under these conditions are also increased (Figure 4.8B). The higher abundance of PQM-1 may therefore be an underlying factor in the increased nuclear localisation that is seen. One possibility is that the nuclear localisation of PQM-1 may be concentration dependent, i.e. it needs to be present in a sufficient quantity in the cell for it to be localised to the nucleus. When PQM-1 protein levels are higher, such as when the UPS pathway is blocked, the protein reaches a threshold concentration and localises to the nucleus. Alternatively, it could be that interfering with the UPS *uba*-1 RNAi has broad effects on proteostasis in the nematodes resulting in stress. As PQM-1 is a stress responsive transcription factor it is therefore recruited to the nucleus in response to the resultant imbalance in proteostasis.

Gene name	Gene	Length (amino acids)	Mol. Weight (kDa)	Description (WormBase)
Y37E3.17	Y37E3.17	830/837	92	Ortholog of human DMGDH (dimethylglycine dehydrogenase); is predicted to have oxidoreductase activity (Shaye and Greenwald, 2011)
hsp-90	C47E8.5	702	80	Highly conserved major molecular chaperone
acly-1 (Probable ATP-citrate synthase)	D1005.1	1106	122	Predicted to have ATP citrate synthase activity
*eef-2 (*elongation factor 2)	F25H5.4	840/852	94	Ortholog of human EEF2; is predicted to have GTPase activity, and translation elongation factor activity; is involved in negative regulation of gene expression
gldc-1 (glycine cleavage system P protein)	R12C12.1	979/915	101/109	Ortholog of human GLDC; is predicted to have glycine dehydrogenase (decarboxylating) activity

Table 4.1. Potential interactors of PQM-1 identified by MS. Proteins co-immunoprecipitating with PQM-1::GFP::FLAG, identified by ESI-TOF mass spectrometry.

4.4.5 PQM-1 and its interacting partners

Eluate samples obtained from the PQM-1::GFP::FLAG co-immunoprecipitation were analysed by mass spectrometry to identify its interacting partners after HS (Table 4.1). HSP-90 was found to co-immunoprecipitate with PQM-1::GFP::FLAG, and it may be that there is an interaction between the two proteins, with the transcription factor regulated by the chaperone in a manner analogous to HSF-1 (Zou et al., 1998). Furthermore, the protein EEF-2, which is a *C. elegans* ortholog of human eukaryotic translation elongation factor, was co-immunoprecipitated. EEF-2 has been found to be downregulated when *C. elegans* are infected with *P. aeruginosa,* and Exotoxin A of *P. aeruginosa* can directly bind to EEF-2. PQM-1 has been shown to be required for *C. elegans* survival when infected with *P. aeruginosa* (Shapira et al., 2006). It is possible that the protein-protein interaction of PQM-1 and EEF-2 is important for *C. elegans* innate immunity. EEF-2 has also been identified in a co-immunoprecipitation of STI-1, the stress inducible co-chaperone which facilitates handing over of client proteins from HSP-70 to HSP-90 (Song et al., 2009). The proteins Y37E3.17, ACLY-1, and GLDC-1 were also found to co-immunoprecipitate with PQM-1::GFP::FLAG. Y37E3.17 is an enzyme predicted to have oxidoreductase activity; ACLY-1 exhibits ATP citrate synthase activity; and GLDC-1 is an enzyme harbouring glycine dehydrogenase activity, respectively (Shaye and Greenwald, 2011). Interestingly, both *Y37E3.17* (DMGDH) and *GLDC-1* are localised to the mitochondria in mammals (Binzak et al., 2000; Bravo-Alonso et al., 2017), which implies that PQM-1 may too be localised to mitochondria in some conditions. If this is indeed the case, it has implications for PQM-1's role in thermotolerance and contribution to

maintenance of the PN. The mitochondria influence *C. elegans* stress tolerance and lifespan (Dillin et al., 2002; Labbadia et al., 2017).

We were however unable to identify PQM-1 protein by mass spectrometry in the co-immunoprecipitated sample, despite the fact that it is detected by Western Blot analysis using an anti-FLAG antibody (Figure 4.9A). In future work it would be valuable to immunoprecipitate PQM-1 by scaling up nematode growth cultures in order to isolate greater amounts of the protein for analysis. Greater amounts of material would improve the odds of detection (and determination of possible post-translational modifications) of the protein by mass spectrometry.

Chapter 5 Conclusion

In Chapter 2, I described the importance of *pqm-1* for heat stress survival in *C. elegans* and demonstrated its importance for resistance to chronic stress induced by the expression of aggregation prone proteins. In Chapter 3, I analysed the transcriptome of *C. elegans* after heat stress in a *pqm-1* (ko) mutant compared to the wildtype to identify genes upregulated by PQM-1 during heat stress conditions. Finally, in Chapter 4, I explored the localisation and protein expression levels of PQM-1 during heat stress. In addition, an immunoprecipitation was performed to isolate PQM-1 and its interactors.

My studies aimed to further elucidate the role of PQM-1 in *C. elegans*. I have found that PQM-1 is required in *C. elegans* for survival of prolonged heat stress exposure. The thermotolerance assays conducted in this thesis demonstrate the necessity of PQM-1 for *C. elegans* survival of extended heat stress. Furthermore PQM-1 is required for the protective effects of TCS against Aβ aggregation in the muscle tissue (O'Brien et al., 2018). PQM-1 mediates TCS from the tissue with the perceived insult of proteostasis, to the responsive, distal tissue in *C. elegans*. For example, when the perturbation of proteostasis occurs in the neurons, PQM-1 induces TCS-mediated *hsp-90* expression via c-type lectin protein CLEC-41, which contains 2 CUB domains. CUB domains are beta-barrel forming domains which are found primarily in extracellular and plasma-membrane associated proteins (Bork and Beckmann, 1993). Furthermore, *clec-41* is enriched in the neurons and intestine (Reece-Hoyes et al., 2007; Spencer et al., 2011). Therefore, we investigated whether *clec-41* could participate in glutamergic signalling like other neuronally expressed protein with CUB domains, such as *sol-1* (Zheng et al.,

2006). Our results showed that TCS was reduced in a *glr-1* mutant relative to controls, suggesting that the TCS signal may be relayed by glutamatergic signalling (O'Brien et al., 2018).

Alternatively, when the proteomic insult is localised to the intestine, PQM-1 mediates TCS via *asp-12*, which encodes an aspartic protease. In either case the signal is relayed to distal tissues, including the body wall muscle which enacts a cytoprotective *hsp-90* chaperone upregulation. RNAi mediated knockdown of *hsp-90* exacerbates Aβ toxicity in a *C. elegans* model (Brehme et al., 2014). Our results demonstrate that HSP-90 overexpression is protective against $A\beta_{(3-42)}$ toxicity and aggregation. Furthermore, we have demonstrated that TCS upregulates *hsp-90* in distal tissues and that TCS is protective against $A\beta_{(3-42)}$ toxicity as well as aggregation in the muscle (O'Brien et al., 2018).

Our results also showed that depletion of *pqm-1* results in increased aggregation and toxicity of the polyglutamine protein – therefore *pqm-1* is required for proteostasis in this model to protect against the Huntington's model's aggregation and the accompanying paralysis in *C. elegans.* It is however difficult to propose a mechanism for the protective effects of PQM-1 in this context, as we have not yet analysed PQM-1 - regulated genes in the background of this disease model. *Hsp-90* may also be a potential protective component in the Huntington's disease model, as *hsp-90* expression is reduced in a *pqm-1* (ko) mutant.

In addition, using microarrays I found that there is a set of genes which are specifically upregulated by PQM-1 following heat stress. These genes are not molecular chaperones – and as such probably promote survival through alternate means than rectifying protein

misfolding. Even though we were unable to categorise the identified genes into a specific GO term, several genes of interest were found. For example, the putative immune genes *ZK970.7* and *fipr-26* were found to be upregulated by PQM-1 after heat stress exposure. PQM-1 has previously been reported to be important for immune function in terms of survival of *P. aeruginosa* infection (Shapira et al., 2006), and it may be the case that its contribution to the immune response are also important for stress survival. For example, the transcription factor SKN-1 is a stress responsive transcription factor that is also important in the *C. elegans* immune response (Papp et al., 2012).

It has previously been found that HSF-1 regulates many more genes than chaperones during heat stress, including genes involved in cuticle structure such as *col-149* and the chromatin remodelling gene *nurf-1* (Brunquell et al., 2016). It is somewhat surprising that HSF-1, the master regulator of the HSR, would modify the expression of genes that do not have obvious cytoprotective roles (such as molecular chaperones) to such a large extent – but may exemplify how non-canonical heat responsive genes protect an organism from heat stress.

It may be that PQM-1 is protective against heat stress in an indirect manner, rather than through the promotion of chaperone expression. I did, however, record a dependence for *hsp-90* expression on PQM-1 in heat stress conditions – and PQM-1 regulates *hsp-90* expression during TCS. This regulation may however be indirect, as was shown by my colleague Dr Laura Jones. Her data indicated that deletion of the predicted PQM-1 consensus site in the promoter region of *hsp-90* has no effect on *hsp-90* during condition that activate TCS (O'Brien et al., 2018).

In this study I attempted to identify how PQM-1 could be regulated during heat stress. I found that PQM-1 protein levels increase following heat stress and that the protein localises to the *C. elegans* intestinal nuclei post heat shock. The knockdown of *sgk-1*, or the proteasome (*uba-1)* leads to increased PQM-1 protein levels under ambient conditions, as well as localisation to the nucleus. This implies that PQM-1 could be regulated both at the translational level as well as via post translational modification to determine its subcellular localisation. A search of the literature reveals that PQM-1 is predicted to be phosphorylated on the TST *sgk-1* consensus site (Dowen et al., 2016), which is also a consensus site for AKT-1 (Kobayashi et al., 1999).

Mass spectrometry analysis of an immunoprecipitation of PQM-1 identified several interacting partners that associate with PQM-1 during heat stress recovery, including the major molecular chaperone *hsp-90*, which also seems to be regulated by PQM-1.

PQM-1 is required for heat stress survival in *C. elegans*, which adds a layer of complexity to stress responses, demonstrating that in metazoans non-canonical transcription factors which act in a complementary manner to *hsf-1* and *daf-16* to promote proteostasis. In our models, when both *hsf-1* and *pqm-1* were compromised, the heat stress survival of nematodes was worse than when either was individually lost. This more complex web of regulatory transcription factors allows fine-tuning of the stress response to different insults to the proteome.

PQM-1 also has a role in chronic stress resistance, preventing build-up of polyglutamine aggregates and the resulting early paralysis of the nematodes. PQM-1 acting as an important factor in chronic stress conditions has been previously demonstrated, as it is required for dietary restriction mediated rescue from proteostasis collapse (Shpigel et

al., 2018). Furthermore, Shpigel et al. showed bioinformatic data promoting the idea that DAF-16 has a more prominent role during acute stress response, and PQM-1 in chronic stress. This observation coincides with the nuclear localisation of DAF-16 during acute heat stress (Tepper et al., 2013) and relatively rapid exit during recovery and PQM-1 then entering the nucleus during the recovery phase (Figure 4.1; Figure 4.2; O'Brien et al., 2018). This could explain the important, but distinct, role that each of the transcription factors contribute to heat stress tolerance. PQM-1 has been linked to the mitochondrial chaperones *tomm-70* (HSP-90 co-chaperone); *Y22D7AL.10* (HSP-60); and *dnj-10* (HSP-40) as was revealed by bioinformatic analysis (Shpigel et al., 2018). The immunoprecipitation data we collected found that PQM-1 was associated with the metabolic enzymes *acly-1* which is cytoplasmic in humans (Chypre et al., 2012), and *Y37E3.17* (DMGDH) and *gldc-1* which are localised to the mitochondria in mammals (Binzak et al., 2000; Bravo-Alonso et al., 2017). This posits the possibility that PQM-1 is involved in respiration, which is mediated by the mitochondria. Mitochondria have been shown to influence *C. elegans* lifespan and stress tolerance (Dillin et al., 2002; Labbadia et al., 2017) and this can also occur cell-non-autonomously (Durieux et al., 2011). Therefore, it would be interesting to explore if there are any functional links between PQM-1 and the mitochondria as it might explain the effect of *pqm-1* on stress resistance and longevity.

Stress responsive transcription factors have been implicated in tumorigenesis and proliferation. HSF-1, the master regulator of the major cytosolic chaperones has been implicated in malignant transformation and the progression of cancers (Bell et al., 2012; Scherz-Shouval et al., 2014). DAF-16 has been shown to induce germline tumour formation through activation of mTORC1 (Qi et al., 2017), and furthermore despite being

typically thought of as a suppressor of tumour formation, FOXO transcription factors in some circumstances support tumour progression by maintaining cellular homeostasis and inducing therapy resistance (Hornsveld et al., 2018). It is therefore important to fully understand the induction and roles that PQM-1 plays in *C. elegans*, as much of the research may be translated into higher organisms. SALL2 the closest human ortholog of PQM-1, has pro-apoptotic and growth arrest functions, that has also been implicated in cancer (Sung and Yim, 2017). It may be that the role PQM-1 plays in nematodes is mirrored in mammals by SALL2.

Further research into the roles and regulation of PQM-1 could be fruitful to enhance our understanding of the complex regulation of stress response pathways in *C. elegans.* For example, a ChIP-seq experiment to examine the DNA binding sites of PQM-1 during heat stress recovery. It would be interesting to find out whether these sites mirror the genes regulated by PQM-1 post heat stress that were identified by our microarray. Or whether the sites match the DAE found to be bound by PQM-1 (Tepper et al., 2013). Although I was unable to identify post-translational modifications to PQM-1 via mass spectrometry, a more refined immunoprecipitation protocol may be able to produce a greater amount of protein and therefore increase the likelihood of detection. As I have touched upon, PQM-1 seems to direct the response of many signalling pathways – it might be prudent therefore to look at PQM-1 in response to other stresses such as oxidative, osmotic and cold stress.

PQM-1 is probably regulated by ILS through the kinases AKT-1/-2 and SGK-1 (Dowen et al., 2016). As well as being regulated by signalling from the hypodermis via mTORC and SGK-1 (Dowen et al., 2016). As PQM-1 is also a DAF-16 antagonist (Tepper et al., 2013),

it is influenced by (and may influence) the localisation of DAF-16 – which gives further scope for PQM-1 regulation. In addition, PQM-1 is required for dietary-restriction mediated rescue of proteostasis collapse in adult *C. elegans* (Shpigel et al., 2018). PQM-1 is also localised to the nucleus and transcriptionally active during development under ambient growth conditions, before exiting upon the transition to adulthood (Niu et al., 2011; Tepper et al., 2013; O'Brien et al., 2018).

PQM-1 therefore seems to lie at a junction between stress response pathways – pathogen response (Shapira et al., 2006), heat stress (O'Brien et al., 2018), chronic protein misfolding (O'Brien et al., 2018; Shpigel et al., 2018), regulating longevity and integrating ILS (Tepper et al., 2013) and reproduction control (Dowen et al., 2016; Dowen, 2019). Integrating this data leads to the model shown in Figure 5.1, whereby PQM-1 is regulated by multiple pathways and acts protectively against acute and chronic stresses.

In summary, this study has demonstrated that PQM-1 influences many aspects of proteostasis from heat stress survival to suppression of aggregation prone proteins in chronic stress conditions. The discovery of PQM-1 as a non-canonical stress responsive transcription factor reveals that the regulation of cytoplasmic stress response may be more complicated and nuanced than previously thought.

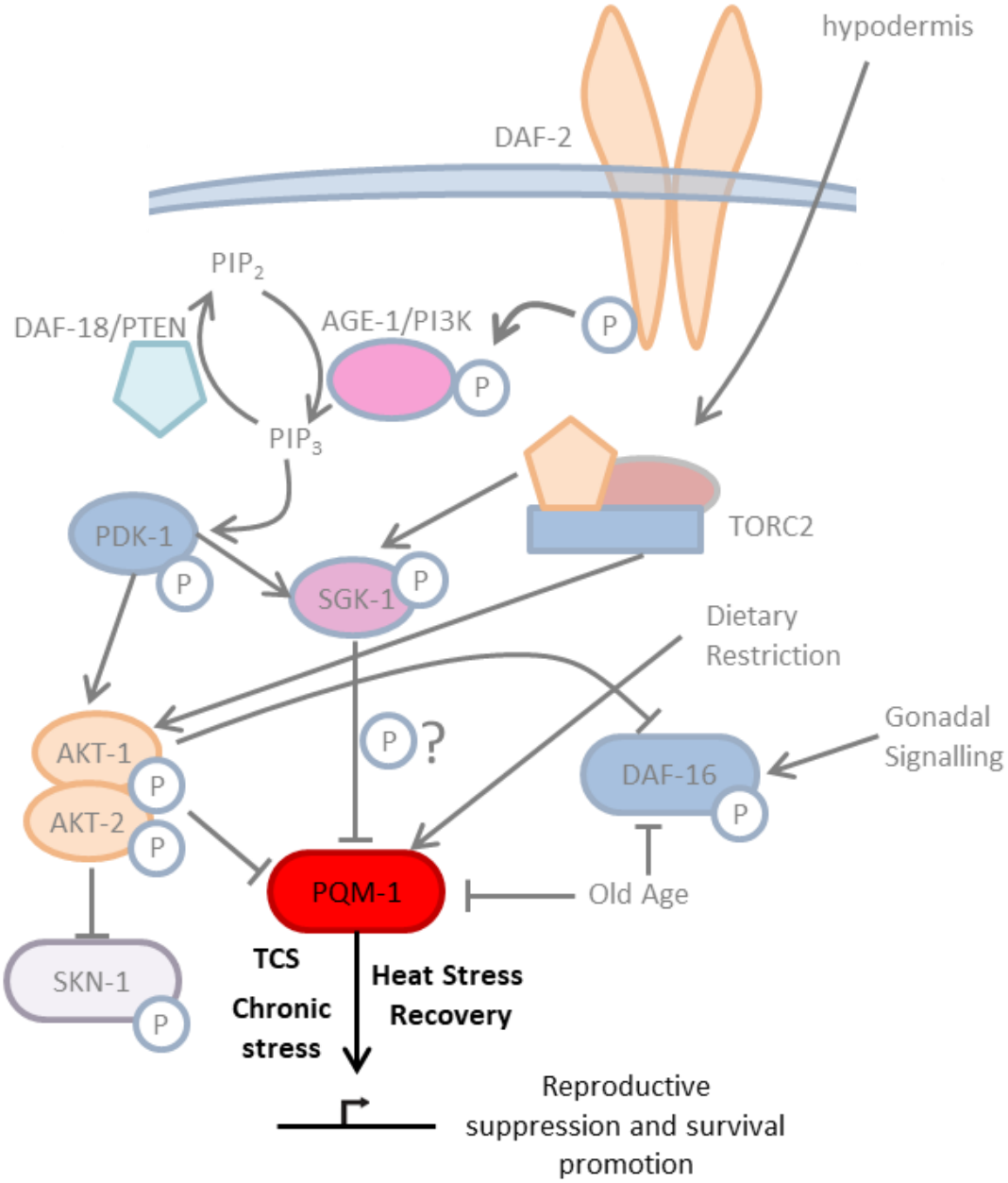

Figure 5.1. Model of PQM-1 regulation and transcriptional output.

PQM-1 is regulated by diverse pathways including ILS; mTORC2 and dietary restriction to integrate stress response and reproductive activity. These pathways control PQM-1 sub-cellular localisation, most likely via inhibitory phosphorylation. Highlighted is the contribution to the model that this thesis has added.

Bibliography

Abravaya, K., Myers, M.P., Murphy, S.P. and Morimoto, R.I. 1992. The human heat shock protein hsp70 interacts with HSF, the transcription factor that regulates heat shock gene expression. *Genes & development*. **6**(7), pp.1153–64.

Akerfelt, M., Morimoto, R.I. and Sistonen, L. 2010. Heat shock factors: integrators of cell stress, development and lifespan. *Nature reviews. Molecular cell biology*. **11**(8), pp.545–55.

Albert, P.S., Brown, S.J. and Riddle, D.L. 1981. Sensory control of dauer larva formation in Caenorhabditis elegans. *Journal of Comparative Neurology*. **198**(3), pp.435–451.

Amin, J., Ananthan, J. and Voellmy, R. 1988. Key features of heat shock regulatory elements. *Molecular and cellular biology*. **8**(9), pp.3761–9.

An, J.H. and Blackwell, T.K. 2003. SKN-1 links *C. elegans* mesendodermal specification to a conserved oxidative stress response. *Genes & development*. **17**(15), pp.1882–93.

An, J.H., Vranas, K., Lucke, M., Inoue, H., Hisamoto, N., Matsumoto, K. and Blackwell, T.K. 2005. Regulation of the Caenorhabditis elegans oxidative stress defense protein SKN-1 by glycogen synthase kinase-3. *Proceedings of the National Academy of Sciences*. **102**(45), pp.16275–16280.

Anckar, J. and Sistonen, L. 2007. Heat shock factor 1 as a coordinator of stress and developmental pathways. *Advances in Experimental Medicine and Biology*. **594**, pp.78–88.

Anckar, J. and Sistonen, L. 2011. Regulation of HSF1 Function in the Heat Stress Response: Implications in Aging and Disease. *Annual Review of Biochemistry*. **80**(1), pp.1089–1115.

Anon n.d. nduo-3 (gene) - WormBase : Nematode Information Resource. [Accessed 20 October 2018]. Available from: https://www.wormbase.org/species/c_elegans/gene/WBGene00010966#0e-9gcb-3.

Apfeld, J., O'Connor, G., McDonagh, T., DiStefano, P.S. and Curtis, R. 2004. The AMP-activated protein kinase AAK-2 links energy levels and insulin-like signals to lifespan in C. elegans. *Genes and Development*. **18**(24), pp.3004–3009.

Balch, W.E., Morimoto, R.I., Dillin, A. and Kelly, J.W. 2008. Adapting proteostasis for disease intervention. *Science*. **319**(5865), pp.916–919.

Ballinger, C.A., Connell, P., Wu, Y., Hu, Z., Thompson, L.J., Yin, L.Y. and Patterson, C. 1999. Identification of CHIP, a novel tetratricopeptide repeat-containing protein that interacts with heat shock proteins and negatively regulates chaperone

functions. *Molecular and cellular biology*. **19**(6), pp.4535–45.

Bar-Lavan, Y., Shemesh, N., Dror, S., Ofir, R., Yeger-Lotem, E. and Ben-Zvi, A. 2016. A Differentiation Transcription Factor Establishes Muscle-Specific Proteostasis in Caenorhabditis elegans. *PLoS genetics*. **12**(12), p.e1006531.

Bardwell, J.C. and Craig, E.A. 1987. Eukaryotic Mr 83,000 heat shock protein has a homologue in Escherichia coli. *Proceedings of the National Academy of Sciences of the United States of America*. **84**(15), pp.5177–81.

Bates, G.P., Dorsey, R., Gusella, J.F., Hayden, M.R., Kay, C., Leavitt, B.R., Nance, M., Ross, C.A., Scahill, R.I., Wetzel, R., Wild, E.J. and Tabrizi, S.J. 2015. Huntington disease. *Nature Reviews Disease Primers*. **1**(1), p.15005.

Baumeister, R., Schaffitzel, E. and Hertweck, M. 2006. Endocrine signaling in Caenorhabditis elegans controls stress response and longevity. *Journal of Endocrinology*. **190**, pp.191–202.

Bell, G.W., Tamimi, R.M., Santagata, S., Ince, T.A., Koeva, M., Fraenkel, E., Lindquist, S., Hu, R., Whitesell, L. and Mendillo, M.L. 2012. HSF1 Drives a Transcriptional Program Distinct from Heat Shock to Support Highly Malignant Human Cancers. *Cell*. **150**(3), pp.549–562.

Ben-Zvi, A., Miller, E. a and Morimoto, R.I. 2009. Collapse of proteostasis represents an early molecular event in Caenorhabditis elegans aging. *Proceedings of the National Academy of Sciences of the United States of America*. **106**(35), pp.14914–14919.

Benjamini, Y. and Hochberg, Y. 1995. Controlling the false discovery rate: a practical and powerful approach to multiple testing. *Developmental Cell*. **57**(1), pp.289–300.

Berdichevsky, A., Viswanathan, M., Horvitz, H.R. and Guarente, L. 2006. C. elegans SIR-2.1 Interacts with 14-3-3 Proteins to Activate DAF-16 and Extend Life Span. *Cell*. **125**(6), pp.1165–1177.

Bharadwaj, S., Ali, A. and Ovsenek, N. 1999. Multiple components of the HSP90 chaperone complex function in regulation of heat shock factor 1 In vivo. *Mol Cell Biol*. **19**(12), pp.8033–8041.

Binzak, B.A., Vockley, J.G., Jenkins, R.B. and Vockley, J. 2000. Structure and analysis of the human dimethylglycine dehydrogenase gene. *Molecular Genetics and Metabolism*. **69**(3), pp.181–187.

Biron, D., Wasserman, S., Thomas, J.H., Samuel, A.D.T. and Sengupta, P. 2008. An olfactory neuron responds stochastically to temperature and modulates Caenorhabditis elegans thermotactic behavior. *Proceedings of the National Academy of Sciences*. **105**(31), pp.11002–11007.

Blackwell, T.K., Steinbaugh, M.J., Hourihan, J.M., Ewald, C.Y. and Isik, M. 2015. SKN-1/Nrf, stress responses, and aging in Caenorhabditis elegans. *Free Radical Biology and Medicine*. **88**(Part B), pp.290–301.

Bork, P. and Beckmann, G. 1993. The CUB domain. A widespread module in developmentally regulated proteins. *Journal of molecular biology*. **231**(2), pp.539–

45.

Bowerman, B., Eaton, B.A. and Priess, J.R. 1992. skn-1, a maternally expressed gene required to specify the fate of ventral blastomeres in the early C. elegans embryo. *Cell*. **68**(6), pp.1061–1075.

Boyd, W.A., Crocker, T.L., Rodriguez, A.M., Leung, M.C.K., Wade Lehmann, D., Freedman, J.H., Van Houten, B. and Meyer, J.N. 2010. Nucleotide excision repair genes are expressed at low levels and are not detectably inducible in Caenorhabditis elegans somatic tissues, but their function is required for normal adult life after UVC exposure. *Mutation Research - Fundamental and Molecular Mechanisms of Mutagenesis*. **683**(1–2), pp.57–67.

Bravo-Alonso, I., Navarrete, R., Arribas-Carreira, L., Perona, A., Abia, D., Couce, M.L., García-Cazorla, A., Morais, A., Domingo, R., Ramos, M.A., Swanson, M.A., Van Hove, J.L.K., Ugarte, M., Pérez, B., Pérez-Cerdá, C. and Rodríguez-Pombo, P. 2017. Nonketotic hyperglycinemia: Functional assessment of missense variants in GLDC to understand phenotypes of the disease. *Human Mutation*. **38**(6), pp.678–691.

Brayer, K.J. and Segal, D.J. 2008. Zinc fingers in protein-protein interactions. *Journal Cell Biochemistry and Biophysics*. **50**(3).

Brehme, M., Voisine, C., Rolland, T., Wachi, S., Soper, J.H., Zhu, Y., Orton, K., Villella, A., Garza, D., Vidal, M., Ge, H. and Morimoto, R.I. 2014. A chaperome subnetwork safeguards proteostasis in aging and neurodegenerative disease. *Cell reports*. **9**(3), pp.1135–50.

Brenner, S. 1974. The genetics of Caenorhabditis elegans. *Genetics*. **77**(1), pp.71–94.

Brignull, H.R., Morley, J.F. and Morimoto, R.I. 2007. The Stress of Misfolded Proteins *In*: P. Csermely and L. Vígh, eds. *Molecular Aspects of the Stress Response: Chaperones, Membranes and Networks* [Online]. New York, NY: Springer New York, pp.167–189. Available from: https://doi.org/10.1007/978-0-387-39975-1_15.

Brunet, A., Sweeney, L.B., Sturgill, J.F., Chua, K.F., Greer, P.L., Lin, Y., Tran, H., Ross, S.E., Mostoslavsy, R., Cohen, H.Y., Hu, L.S., Cheng, H.L., Jedrychowski, M.P., Gygi, S.P., Sinclair, D.A., Alt, F.W. and Greenberg, M.E. 2004. Stress-Dependent Regulation of FOXO Transcription Factors by the SIRT1 Deacetylase. *Science*. **303**(5666), pp.2011–2015.

Brunquell, J., Morris, S., Lu, Y., Cheng, F. and Westerheide, S.D. 2016. The genome-wide role of HSF-1 in the regulation of gene expression in Caenorhabditis elegans. *BMC Genomics*. **17**(1), p.559.

Calfon, M., Zeng, H., Urano, F., Till, J.H., Hubbard, S.R., Harding, H.P., Clark, S.G. and Ron, D. 2002. IRE1 couples endoplasmic reticulum load to secretory capacity by processing the XBP-1 mRNA. *Nature*. **415**(6867), pp.92–96.

Cao, J., Packer, J.S., Ramani, V., Cusanovich, D.A., Huynh, C., Daza, R., Qiu, X., Lee, C., Furlan, S.N., Steemers, F.J., Adey, A., Waterston, R.H., Trapnell, C. and Shendure, J. 2017. Comprehensive single-cell transcriptional profiling of a multicellular organism. *Science (New York, N.Y.)*. **357**(6352), pp.661–667.

Celniker, S.E., Dillon, L.A.L., Gerstein, M.B., Gunsalus, K.C., Henikoff, S., Karpen, G.H., Kellis, M., Lai, E.C., Lieb, J.D., MacAlpine, D.M., Micklem, G., Piano, F., Snyder, M., Stein, L., White, K.P. and Waterston, R.H. 2009. Unlocking the secrets of the genome. *Nature*. **459**(7249), pp.927–930.

Choe, K.P., Przybysz, A.J. and Strange, K. 2009. The WD40 Repeat Protein WDR-23 Functions with the CUL4/DDB1 Ubiquitin Ligase To Regulate Nuclear Abundance and Activity of SKN-1 in Caenorhabditis elegans. *Molecular and Cellular Biology*. **29**(10), pp.2704–2715.

Chondrogianni, N., Georgila, K., Kourtis, N., Tavernarakis, N. and Gonos, E.S. 2015. 20S proteasome activation promotes life span extension and resistance to proteotoxicity in Caenorhabditis elegans. *FASEB journal : official publication of the Federation of American Societies for Experimental Biology*. **29**(2), pp.611–22.

Churchill, G.A. 2002. Fundamentals of experimental design for cDNA microarrays. *Nature Genetics*. **32**(S4), pp.490–495.

Chypre, M., Zaidi, N. and Smans, K. 2012. ATP-citrate lyase: A mini-review. *Biochemical and Biophysical Research Communications*. **422**(1), pp.1–4.

Cline, E.N., Bicca, M.A., Viola, K.L. and Klein, W.L. 2018. The Amyloid-β Oligomer Hypothesis: Beginning of the Third Decade G. Perry, J. Avila, P. I. Moreira, A. A. Sorensen, & M. Tabaton, eds. *Journal of Alzheimer's Disease*. **64**(s1), pp.S567–S610.

Dancy, B.M., Sedensky, M.M. and Morgan, P.G. 2014. Effects of the mitochondrial respiratory chain on longevity in C. elegans. *Experimental Gerontology*. **56**, pp.245–255.

Daneman, R. and Prat, A. 2015. The blood-brain barrier. *Cold Spring Harbor perspectives in biology*. **7**(1), p.a020412.

Davis, P. and Van Auken, K. 2014. nduo-3 (gene). *Wormbase*. [Online]. Available from: http://wormbase.org/db/get?name=WBGene00010966;class=Gene.

DiFiglia, M., Sapp, E., Chase, K., Schwarz, C., Meloni, A., Young, C., Martin, E., Vonsattel, J.P., Carraway, R., Reeves, S.A., Boyce, F.M. and Aronin, N. 1995. Huntingtin is a cytoplasmic protein associated with vesicles in human and rat brain neurons. *Neuron*. **14**(5), pp.1075–1081.

Dillin, A., Hsu, A.-L., Arantes-Oliveira, N., Lehrer-Graiwer, J., Hsin, H., Fraser, A.G., Kamath, R.S., Ahringer, J. and Kenyon, C. 2002. Rates of behavior and aging specified by mitochondrial function during development. *Science (New York, N.Y.)*. **298**(5602), pp.2398–401.

Dowen, R.H. 2019. CEH-60/PBX and UNC-62/MEIS Coordinate a Metabolic Switch that Supports Reproduction in C. elegans. *Developmental Cell*. **49**(2), pp.235-250.e7.

Dowen, R.H., Breen, P.C., Tullius, T., Conery, A.L. and Ruvkun, G. 2016. A microRNA program in the C. elegans hypodermis couples to intestinal mTORC2/PQM-1 signaling to modulate fat transport. *Genes and Development*. **30**(13), pp.1515–1528.

Dresen, A., Finkbeiner, S., Dottermusch, M., Beume, J.S., Li, Y., Walz, G. and Neumann-

Haefelin, E. 2015. Caenorhabditis elegans OSM-11 signaling regulates SKN-1/Nrf during embryonic development and adult longevity and stress response. *Developmental Biology*. **400**(1), pp.118–131.

Durieux, J., Wolff, S. and Dillin, A. 2011. The cell-non-autonomous nature of electron transport chain-mediated longevity. *Cell*. **144**(1), pp.79–91.

Essers, P.B., Nonnekens, J., Goos, Y.J., Betist, M.C., Viester, M.D., Mossink, B., Lansu, N., Korswagen, H.C., Jelier, R., Brenkman, A.B. and MacInnes, A.W. 2015. A Long Noncoding RNA on the Ribosome Is Required for Lifespan Extension. *Cell Reports*. **10**(3), pp.339–345.

Ewald, C.Y., Landis, J.N., Abate, J.P., Murphy, C.T. and Blackwell, T.K. 2015. Dauer-independent insulin/IGF-1-signalling implicates collagen remodelling in longevity. *Nature*. **519**(7541), pp.97–101.

Felsenfeld, G., Boyes, J., Chung, J., Clark, D. and Studitsky, V. 1996. Chromatin structure and gene expression. *Proceedings of the National Academy of Sciences*. **93**(18), pp.9384–9388.

Finka, A. and Goloubinoff, P. 2013. Proteomic data from human cell cultures refine mechanisms of chaperone-mediated protein homeostasis. *Cell Stress and Chaperones*. **18**(5), pp.591–605.

Fiorese, C.J., Schulz, A.M., Lin, Y.-F., Rosin, N., Pellegrino, M.W. and Haynes, C.M. 2016. The Transcription Factor ATF5 Mediates a Mammalian Mitochondrial UPR. *Current Biology*., pp.1–7.

Fonte, V., Kipp, D.R., Yerg, J., Merin, D., Forrestal, M., Wagner, E., Roberts, C.M. and Link, C.D. 2008. Suppression of in vivo beta-amyloid peptide toxicity by overexpression of the HSP-16.2 small chaperone protein. *The Journal of biological chemistry*. **283**(2), pp.784–91.

Friedberg, I. and Margalit, H. 2002. Persistently conserved positions in structurally similar, sequence dissimilar proteins: roles in preserving protein fold and function. *Protein science*. **11**(2), pp.350–60.

Furuyama, T., Nakazawa, T., Nakano, I. and Mori, N. 2000. Identification of the differential distribution patterns of mRNAs and consensus binding sequences for mouse DAF-16 homologues. *Biochemical Journal*. **349**(2), pp.629–634.

Gardner, B.M., Pincus, D., Gotthardt, K., Gallagher, C.M. and Walter, P. 2013. Endoplasmic reticulum stress sensing in the unfolded protein response. *Cold Spring Harb Perspect Biol*. **5**(3), p.a013169.

Gidalevitz, T., Ben-Zvi, A., Ho, K.H., Brignull, H.R. and Morimoto, R.I. 2006. Progressive Disruption of Cellular Protein Folding in Models of Polyglutamine Diseases. *Science*. **311**(5766), pp.1471–1474.

Gidalevitz, T., Prahlad, V. and Morimoto, R.I. 2011. The stress of protein misfolding: From single cells to multicellular organisms. *Cold Spring Harbor Perspectives in Biology*. **3**(6), pp.1–18.

Golden, T.R. and Melov, S. 2004. Microarray analysis of gene expression with age in individual nematodes. *Aging Cell*. **3**(3), pp.111–124.

Grossman, S.R., Zhang, X., Wang, L., Engreitz, J., Melnikov, A., Rogov, P., Tewhey, R., Isakova, A., Deplancke, B., Bernstein, B.E., Mikkelsen, T.S. and Lander, E.S. 2017. Systematic dissection of genomic features determining transcription factor binding and enhancer function. *Proceedings of the National Academy of Sciences of the United States of America*. **114**(7), pp.E1291–E1300.

GuhaThakurta, D. 2002. Identification of a Novel cis-Regulatory Element Involved in the Heat Shock Response in Caenorhabditis elegans Using Microarray Gene Expression and Computational Methods. *Genome Research*. **12**(5), pp.701–712.

Hajdu-Cronin, Y.M., Chen, W.J. and Sternberg, P.W. 2004. The L-Type Cyclin CYL-1 and the Heat-Shock-Factor HSF-1 Are Required for Heat-Shock-Induced Protein Expression in Caenorhabditis elegans. *Genetics*. **168**(4), pp.1937–1949.

Halaschek-Wiener, J., Khattra, J.S., McKay, S., Pouzyrev, A., Stott, J.M., Yang, G.S., Holt, R.A., Jones, S.J.M., Marra, M.A., Brooks-Wilson, A.R. and Riddle, D.L. 2005. Analysis of long-lived C. elegans daf-2 mutants using serial analysis of gene expression. *Genome Research*. **15**(5), pp.603–615.

Haynes, C.M., Yang, Y., Blais, S.P., Neubert, T.A. and Ron, D. 2010. The matrix peptide exporter HAF-1 signals a mitochondrial UPR by activating the transcription factor ZC376.7 in C. elegans. *Molecular cell*. **37**(4), pp.529–40.

Heintzman, N.D., Hon, G.C., Hawkins, R.D., Kheradpour, P., Stark, A., Harp, L.F., Ye, Z., Lee, L.K., Stuart, R.K., Ching, C.W., Ching, K.A., Antosiewicz-Bourget, J.E., Liu, H., Zhang, X., Green, R.D., Lobanenkov, V. V., Stewart, R., Thomson, J.A., Crawford, G.E., Kellis, M. and Ren, B. 2009. Histone modifications at human enhancers reflect global cell-type-specific gene expression. *Nature*. **459**(7243), pp.108–112.

Heinz, S., Benner, C., Spann, N., Bertolino, E., Lin, Y.C., Laslo, P., Cheng, J.X., Murre, C., Singh, H. and Glass, C.K. 2010. Simple Combinations of Lineage-Determining Transcription Factors Prime cis-Regulatory Elements Required for Macrophage and B Cell Identities. *Molecular Cell*. **38**(4), pp.576–589.

Hertweck, M., Göbel, C. and Baumeister, R. 2004. C. elegans SGK-1 is the critical component in the Akt/PKB kinase complex to control stress response and life span. *Developmental cell*. **6**(4), pp.577–88.

Heschl, M.F.P. and Baillie, D.L. 1990. The HSP70 multigene family of Caenorhabditis elegans. *Comparative Biochemistry and Physiology Part B: Comparative Biochemistry*. **96**(4), pp.633–637.

Hesp, K., Smant, G. and Kammenga, J.E. 2015. Caenorhabditis elegans DAF-16/FOXO transcription factor and its mammalian homologs associate with age-related disease. *Experimental Gerontology*. **72**, pp.1–7.

Hipp, M.S., Park, S.H. and Hartl, F.U. 2014. Proteostasis impairment in protein-misfolding and -aggregation diseases. *Trends in Cell Biology*. **24**(Figure 2), pp.1–9.

Honda, Y. and Honda, S. 2002. Oxidative stress and life span determination in the nematode Caenorhabditis elegans. *Annals of the New York Academy of Sciences*. **959**(1), pp.466–74.

Honda, Y. and Honda, S. 1999. The daf-2 gene network for longevity regulates

oxidative stress resistance and Mn-superoxide dismutase gene expression in Caenorhabditis elegans. *FASEB Journal*. **13**(11), pp.1385–1393.

Hoogewijs, D., Houthoofd, K., Matthijssens, F., Vandesompele, J. and Vanfleteren, J.R. 2008. Selection and validation of a set of reliable reference genes for quantitative sod gene expression analysis in *C. elegans*. *BMC molecular biology*. **9**(1), p.9.

Hornsveld, M., Dansen, T.B., Derksen, P.W. and Burgering, B.M.T. 2018. Re-evaluating the role of FOXOs in cancer. *Seminars in Cancer Biology*. **50**(November 2017), pp.90–100.

Hsu, A.-L., Murphy, C.T. and Kenyon, C. 2003. Regulation of Aging and Age-Related Disease by DAF-16 and Heat-Shock Factor. *Science*. **300**(5622), pp.1142–1145.

Imanikia, S., Özbey, N.P., Krueger, C., Casanueva, M.O. and Taylor, R.C. 2019. Neuronal XBP-1 Activates Intestinal Lysosomes to Improve Proteostasis in C. elegans. *Current Biology*., pp.2322–2338.

Inglis, P.N. et al. 2007. The sensory cilia of Caenorhabditis elegans. *WormBook, ed. The C. elegans Research Community, WormBook*. [Online]. Available from: http://www.wormbook.org.

Irizarry, R.A., Bolstad, B.M., Collin, F., Cope, L.M., Hobbs, B. and Speed, T.P. 2003. Summaries of Affymetrix GeneChip probe level data. *Nucleic acids research*. **31**(4), p.e15.

Kahn, N.W., Rea, S.L., Moyle, S., Kell, A. and Johnson, T.E. 2008. Proteasomal dysfunction activates the transcription factor SKN-1 and produces a selective oxidative-stress response in Caenorhabditis elegans. *Biochemical Journal*. **409**(1), pp.205–213.

Kaplan, J.M. and Horvitz, H.R. 1993. A dual mechanosensory and chemosensory neuron in Caenorhabditis elegans. . **90**(March), pp.2227–2231.

Kayed, R., Head, E., Thompson, J.L., McIntire, T.M., Milton, S.C., Cotman, C.W. and Glabe, C.G. 2003. Common structure of soluble amyloid oligomers implies common mechanism of pathogenesis. *Science*. **300**(5618), pp.486–9.

Kenyon, C., Chang, J., Gensch, E., Rudner, A. and Tabtlang, R. 1993. A C.elegans mutant that lives twice as long as wild type. *Nature*. **366**, p.462.

Kim, S.K., Lund, J., Kiraly, M., Duke, K., Jiang, M., Stuart, J.M., Eizinger, A., Wylie, B.N. and Davidson, G.S. 2001. A Gene Expression Map for Caenorhabditis elegans. *Science*. **293**(5537), pp.2087–2092.

Kim, Y.E., Hipp, M.S., Bracher, A., Hayer-Hartl, M. and Ulrich Hartl, F. 2013. *Molecular Chaperone Functions in Protein Folding and Proteostasis* [Online]. Available from: http://www.annualreviews.org/doi/abs/10.1146/annurev-biochem-060208-092442.

Kimble, J. and Sharrock, W.J. 1983. Tissue-specific synthesis of yolk proteins in Caenorhabditis elegans. *Developmental Biology*. **96**(1), pp.189–196.

Kimura, K.D. 1997. *daf-2*, an Insulin Receptor-Like Gene That Regulates Longevity and Diapause in Caenorhabditis elegans. *Science*. **277**(5328), pp.942–946.

Kobayashi, T., Deak, M., Morrice, N. and Cohen, P. 1999. Characterization of the structure and regulation of two novel isoforms of serum- and glucocorticoid-induced protein kinase. *The Biochemical journal*. **344 Pt 1**(1), pp.189–97.

Kramer, J.M. 1994. Structures and functions of collagens in Caenorhabditis elegans. *The FASEB Journal*. **8**(3), pp.329–336.

Labbadia, J., Brielmann, R.M., Neto, M.F., Lin, Y.F., Haynes, C.M. and Morimoto, R.I. 2017. Mitochondrial Stress Restores the Heat Shock Response and Prevents Proteostasis Collapse during Aging. *Cell Reports*. **21**(6), pp.1481–1494.

Labbadia, J. and Morimoto, R.I. 2015. The Biology of Proteostasis in Aging and Disease. *Annual Review of Biochemistry*. **84**(1), pp.435–464.

Lackie, R.E., Maciejewski, A., Ostapchenko, V.G., Marques-Lopes, J., Choy, W.Y., Duennwald, M.L., Prado, V.F. and Prado, M.A.M. 2017. The Hsp70/Hsp90 chaperone machinery in neurodegenerative diseases. *Frontiers in Neuroscience*. **11**(MAY), p.254.

Li, D., Tian, Y., Ma, Y. and Benjamin, T. 2004. p150(Sal2) is a p53-independent regulator of p21(WAF1/CIP). *Molecular and cellular biology*. **24**(9), pp.3885–93.

Li, J., Ebata, A., Dong, Y., Rizki, G., Iwata, T. and Siu, S.L. 2008. Caenorhabditis elegans HCF-1 functions in longevity maintenance as a DAF-16 regulator. *PLoS Biology*. **6**(9), pp.1870–1886.

Li, J., Tewari, M., Vidal, M. and Sylvia Lee, S. 2007. The 14-3-3 protein FTT-2 regulates DAF-16 in Caenorhabditis elegans. *Developmental Biology*. **301**(1), pp.82–91.

Li, W., Gao, B., Lee, S.M., Bennett, K. and Fang, D. 2007. RLE-1, an E3 Ubiquitin Ligase, Regulates C. elegans Aging by Catalyzing DAF-16 Polyubiquitination. *Developmental Cell*. **12**(2), pp.235–246.

Lin, K., Dorman, J.B., Rodan, A. and Kenyon, C. 1997. daf-16: An HNF-3/forkhead Family Member That Can Function to Double the Life-Span of Caenorhabditis elegans. *Science*. **278**(5341), pp.1319–1322.

Lin, K., Hsin, H., Libina, N. and Kenyon, C. 2001. Regulation of the Caenorhabditis elegans longevity protein DAF-16 by insulin/IGF-1 and germline signaling. *Nature genetics*. **28**(2), pp.139–45.

Lindquist, S. and Craig, E.A. 1988. The Heat-Shock Proteins. *Annual Review of Genetics*. **22**(1), pp.631–677.

Link, C.D. 1995. Expression of human beta-amyloid peptide in transgenic Caenorhabditis elegans. *Proceedings of the National Academy of Sciences*. **92**(20), pp.9368–9372.

Link, C.D., Johnson, C.J., Fonte, V., Paupard, M.C., Hall, D.H., Styren, S., Mathis, C.A. and Klunk, W.E. 2001. Visualization of fibrillar amyloid deposits in living, transgenic Caenorhabditis elegans animals using the sensitive amyloid dye, X-34. *Neurobiology of Aging*. **22**(2), pp.217–226.

Lithgow, G.J., White, T.M., Hinerfeld, D.A. and Johnson, T.E. 1994. Thermotolerance of a Long-lived Mutant of Caenorhabditis elegans. *Journal of Gerontology*. **49**(6),

pp.B270–B276.

Di Lullo, G.A., Sweeney, S.M., Korkko, J., Ala-Kokko, L. and San Antonio, J.D. 2002. Mapping the ligand-binding sites and disease-associated mutations on the most abundant protein in the human, type I collagen. *The Journal of biological chemistry*. **277**(6), pp.4223–31.

MacDonald, M.E., Ambrose, C.M., Duyao, M.P., Myers, R.H., Lin, C., Srinidhi, L., Barnes, G., Taylor, S.A., James, M., Groot, N., MacFarlane, H., Jenkins, B., Anderson, M.A., Wexler, N.S., Gusella, J.F., Bates, G.P., Baxendale, S., Hummerich, H., Kirby, S., North, M., Youngman, S., Mott, R., Zehetner, G., Sedlacek, Z., Poustka, A., Frischauf, A.-M., Lehrach, H., Buckler, A.J., Church, D., Doucette-Stamm, L., O'Donovan, M.C., Riba-Ramirez, L., Shah, M., Stanton, V.P., Strobel, S.A., Draths, K.M., Wales, J.L., Dervan, P., Housman, D.E., Altherr, M., Shiang, R., Thompson, L., Fielder, T., Wasmuth, J.J., Tagle, D., Valdes, J., Elmer, L., Allard, M., Castilla, L., Swaroop, M., Blanchard, K., Collins, F.S., Snell, R., Holloway, T., Gillespie, K., Datson, N., Shaw, D. and Harper, P.S. 1993. A novel gene containing a trinucleotide repeat that is expanded and unstable on Huntington's disease chromosomes. *Cell*. **72**(6), pp.971–983.

Malone, J.H. and Oliver, B. 2011. Microarrays, deep sequencing and the true measure of the transcriptome. *BMC Biology*. **9**(1), p.34.

Maman, M., Carvalhal Marques, F., Volovik, Y., Dubnikov, T., Bejerano-Sagie, M. and Cohen, E. 2013. A Neuronal GPCR is Critical for the Induction of the Heat Shock Response in the Nematode C. elegans. *Journal of Neuroscience*. **33**(14), pp.6102–6111.

Mantione, K.J., Kream, R.M., Kuzelova, H., Ptacek, R., Raboch, J., Samuel, J.M. and Stefano, G.B. 2014. Comparing bioinformatic gene expression profiling methods: microarray and RNA-Seq. *Medical science monitor basic research*. **20**(6), pp.138–42.

Matilainen, O., Sleiman, M.S.B., Quiros, P.M., Garcia, S.M.D.A. and Auwerx, J. 2017. The chromatin remodeling factor ISW-1 integrates organismal responses against nuclear and mitochondrial stress. *Nature Communications*. **8**(1).

Mayer, M.P. 2013. Hsp70 chaperone dynamics and molecular mechanism. *Trends in Biochemical Sciences*. **38**(10), pp.507–514.

Mayer, M.P. and Bukau, B. 2005. Hsp70 chaperones: Cellular functions and molecular mechanism. *Cellular and Molecular Life Sciences*. **62**(6), pp.670–684.

McColgan, P. and Tabrizi, S.J. 2018. Huntington's disease: a clinical review. *European Journal of Neurology*. **25**(1), pp.24–34.

Mccoll, G., Roberts, B.R., Pukala, T.L., Kenche, V.B., Roberts, C.M., Link, C.D., Ryan, T.M., Masters, C.L., Barnham, K.J., Bush, A.I. and Cherny, R.A. 2012. Utility of an improved model of amyloid-beta (Aβ1-42) toxicity in Caenorhabditis elegans for drug screening for Alzheimer's disease. *Molecular Neurodegeneration*. **7**(1), pp.1–9.

McColl, G., Rogers, A.N., Alavez, S., Hubbard, A.E., Melov, S., Link, C.D., Bush, A.I., Kapahi, P. and Lithgow, G.J. 2010. Insulin-like signaling determines survival during

stress via posttranscriptional mechanisms in C. elegans. *Cell Metabolism*. **12**(3), pp.260–272.

McDonough, H. and Patterson, C. 2003. CHIP: a link between the chaperone and proteasome systems. *Cell stress & chaperones*. **8**(4), pp.303–8.

Meimaridou, E., Gooljar, S.B. and Chapple, J.P. 2009. From hatching to dispatching: the multiple cellular roles of the Hsp70 molecular chaperone machinery. *Journal of Molecular Endocrinology*. **42**(1), pp.1–9.

Mi, H., Muruganujan, A., Casagrande, J.T. and Thomas, P.D. 2013. Large-scale gene function analysis with the panther classification system. *Nature Protocols*. **8**(8), pp.1551–1566.

Mi, H., Muruganujan, A., Ebert, D., Huang, X. and Thomas, P.D. 2019. PANTHER version 14: more genomes, a new PANTHER GO-slim and improvements in enrichment analysis tools. *Nucleic acids research*. **47**(D1), pp.D419–D426.

Mi, H., Muruganujan, A., Huang, X., Ebert, D., Mills, C., Guo, X. and Thomas, P.D. 2019. Protocol Update for large-scale genome and gene function analysis with the PANTHER classification system (v.14.0). *Nature Protocols*. **14**(3), pp.703–721.

Miles, J., Scherz-Shouval, R. and van Oosten-Hawle, P. 2019. Expanding the Organismal Proteostasis Network: Linking Systemic Stress Signaling with the Innate Immune Response. *Trends in Biochemical Sciences*. **xx**(xx), pp.1–16.

Mori, I. and Ohshima, Y. 1995. Neural regulation of thermotaxis in Caenorhabditis elegans. *Nature*. **376**(6538), pp.344–348.

Morimoto, R.I. 1993. Cells in stress: Transcriptional activation of heat shock genes. *Science*. **259**(5100), pp.1409–1410.

Morimoto, R.I. 1998. Regulation of the heat-shock transcriptional response: cross talk between a family of heat-shock factors, molecular chaperones, and negative regulators. *Genes Dev*. **12**, pp.3788–3796.

Morley, J.F., Brignull, H.R., Weyers, J.J. and Morimoto, R.I. 2002. The threshold for polyglutamine-expansion protein aggregation and cellular toxicity is dynamic and influenced by aging in Caenorhabditis elegans. *Proceedings of the National Academy of Sciences*. **99**(16), pp.10417–10422.

Morley, J.F. and Morimoto, R.I. 2004. Regulation of Longevity in Caenorhabditis elegans by Heat Shock Factor and Molecular Chaperones. *Molecular Biology of the Cell*. **15**(2), pp.657–664.

Morton, E.A. and Lamitina, T. 2013. C. elegans HSF-1 is an essential nuclear protein that formsstress granule-like structures following heat shock. *Aging Cell*. **12**(1), pp.112–120.

Motta, M.C., Divecha, N., Lemieux, M., Kamel, C., Chen, D., Gu, W., Bultsma, Y. and Mcburney, M. 2004. Mammalian SIRT1 Represses Forkhead Transcription Factors. *Cell*. **116**, pp.551–563.

Murphy, C.T., McCarroll, S.A., Bargmann, C.I., Fraser, A., Kamath, R.S., Ahringer, J., Li, H. and Kenyon, C. 2003. Genes that act downstream of DAF-16 to influence the

lifespan of Caenorhabditis elegans. *Nature*. **424**(6946), pp.277–283.

Murphy, M.P. 2009. How mitochondria produce reactive oxygen species. *Biochemical Journal*. **417**(1), pp.1–13.

Niu, W., Lu, Z.J., Zhong, M., Sarov, M., Murray, J.I., Brdlik, C.M., Janette, J., Chen, C., Alves, P., Preston, E., Slightham, C., Jiang, L., Hyman, A.A., Kim, S.K., Waterston, R.H., Gerstein, M., Snyder, M. and Reinke, V. 2011. Diverse transcription factor binding features revealed by genome-wide ChIP-seq in C. elegans. *Genome Research*. **21**(2), pp.245–254.

O'Brien, D., Jones, L.M., Good, S., Miles, J., Vijayabaskar, M.S., Aston, R., Smith, C.E., Westhead, D.R. and van Oosten-Hawle, P. 2018. A PQM-1-Mediated Response Triggers Transcellular Chaperone Signaling and Regulates Organismal Proteostasis. *Cell Reports*. **23**(13), pp.3905–3919.

O'Brien, D. and van Oosten-Hawle, P. 2016. Regulation of cell-non-autonomous proteostasis in metazoans. *Essays In Biochemistry*. **60**(2), pp.133–142.

Ogg, S., Paradis, S., Gottlieb, S., Patterson, G.I., Lee, L., Tissenbaum, H.A. and Ruvkun, G. 1997. The Fork head transcription factor DAF-16 transduces insulin-like metabolic and longevity signals in C. elegans. *Nature*. **389**(6654), pp.994–999.

Oh, S.W., Mukhopadhyay, A., Svrzikapa, N., Jiang, F., Davis, R.J. and Tissenbaum, H.A. 2005. JNK regulates lifespan in Caenorhabditis elegans by modulating nuclear translocation of forkhead transcription factor/DAF-16. *Proceedings of the National Academy of Sciences*. **102**(12), pp.4494–4499.

Ooi, F.K. and Prahlad, V. 2017. Olfactory experience primes the heat shock transcription factor HSF-1 to enhance the expression of molecular chaperones in C. elegans. *Science Signaling*. **10**(501), p.eaan4893.

van Oosten-Hawle, P. and Morimoto, R.I. 2014. Transcellular chaperone signaling: an organismal strategy for integrated cell stress responses. *The Journal of experimental biology*. **217**(Pt 1), pp.129–36.

Owusu-ansah, E., Song, W. and Perrimon, N. 2013. Muscle Mitohormesis Promotes Longevity via Systemic Repression of Insulin Signaling. *Cell*. **155**(3), pp.699–712.

Papp, D., Csermely, P. and Soti, C. 2012. A role for SKN-1/Nrf in pathogen resistance and immunosenescence in caenorhabditis elegans. *PLoS Pathogens*. **8**(4).

Pearl, L.H. and Prodromou, C. 2006. Structure and Mechanism of the Hsp90 Molecular Chaperone Machinery. *Annual Review of Biochemistry*. **75**(1), pp.271–294.

Pellegrino, M.W., Nargund, A.M. and Haynes, C.M. 2013. Signaling the mitochondrial unfolded protein response. *Biochimica et biophysica acta*. **1833**(2), pp.410–6.

Petrucelli, L., Dickson, D., Kehoe, K., Taylor, J., Snyder, H., Grover, A., De Lucia, M., McGowan, E., Lewis, J., Prihar, G., Kim, J., Dillmann, W.H., Browne, S.E., Hall, A., Voellmy, R., Tsuboi, Y., Dawson, T.M., Wolozin, B., Hardy, J. and Hutton, M. 2004. CHIP and Hsp70 regulate tau ubiquitination, degradation and aggregation. *Human Molecular Genetics*. **13**(7), pp.703–714.

Phipson, B., Lee, S., Majewski, I.J., Alexander, W.S. and Smyth, G.K. 2016. ROBUST

HYPERPARAMETER ESTIMATION PROTECTS AGAINST HYPERVARIABLE GENES AND IMPROVES POWER TO DETECT DIFFERENTIAL EXPRESSION. *The annals of applied statistics*. **10**(2), pp.946–963.

Prahlad, V., Cornelius, T. and Morimoto, R.I. 2008. Regulation of the Cellular Heat Shock Response in Caenorhabditis elegans by Thermosensory Neurons. *Science*. **320**(5877), pp.811–814.

Praitis, V., Casey, E., Collar, D. and Austin, J. 2001. Creation of low-copy integrated transgenic lines in Caenorhabditis elegans. *Genetics*. **157**(3), pp.1217–1226.

Prince, M., Albanese, E., Guerchet, M. and Prina, M. 2014. *World Alzheimer Report 2014: Dementia and Risk Reduction. An Analysis of Protective and Modifiable Factors*.

Prithika, U., Deepa, V. and Balamurugan, K. 2016. External induction of heat shock stimulates the immune response and longevity of Caenorhabditis elegans towards pathogen exposure. *Innate Immunity*. **22**(6), pp.466–478.

Qi, W., Yan, Y., Pfeifer, D., Donner v. Gromoff, E., Wang, Y., Maier, W. and Baumeister, R. 2017. C. elegans DAF-16/FOXO interacts with TGF-ß/BMP signaling to induce germline tumor formation via mTORC1 activation. *PLoS Genetics*. **13**(5), pp.1–25.

Rabilloud, T. 2012. Silver Staining of 2D Electrophoresis Gels *In*: K. Marcus, ed. *Quantitative Methods in Proteomics* [Online]. Totowa, NJ: Humana Press, pp.61–73. Available from: http://link.springer.com/10.1007/978-1-61779-885-6.

Reece-Hoyes, J.S., Shingles, J., Dupuy, D., Grove, C.A., Walhout, A.J.M., Vidal, M. and Hope, I.A. 2007. Insight into transcription factor gene duplication from Caenorhabditis elegans Promoterome-driven expression patterns. *BMC Genomics*. **8**, pp.1–17.

Richardson, C.E., Kooistra, T. and Kim, D.H. 2010. An essential role for XBP-1 in host protection against immune activation in C. elegans. *Nature*. **463**(7284), pp.1092–1095.

Richmond, J.E., Davis, W.S. and Jorgensen, E.M. 1999. UNC-13 is required for synaptic vesicle fusion in C. elegans. *Nature Neuroscience*. **2**(11), pp.959–964.

Ritchie, M., Phipson, B., Wu, D., Hu, Y., Law, C., Shi, W. and Smyth, G. 2015. limma powers differential expression analyses for RNA-sequencing and microarray studies. *Nucleic Acids Research*. **43**(7), p.e47.

Rizki, G., Iwata, T.N., Li, J., Riedel, C.G., Picard, C.L., Jan, M., Murphy, C.T. and Lee, S.S. 2011. The evolutionarily conserved longevity determinants HCF-1 and SIR-2.1/SIRT1 collaborate to regulate DAF-16/FOXO. *PLoS Genetics*. **7**(9).

Rodriguez, M., Basten Snoek, L., De Bono, M. and Kammenga, J.E. 2013. Worms under stress: C. elegans stress response and its relevance to complex human disease and aging. *Trends in Genetics*. **29**(6), pp.367–374.

Rüdiger, S., Germeroth, L., Schneider-Mergener, J. and Bukau, B. 1997. Substrate specificity of the DnaK chaperone determined by screening cellulose-bound peptide libraries. *The EMBO journal*. **16**(7), pp.1501–7.

Runkel, E.D., Liu, S., Baumeister, R. and Schulze, E. 2013. Surveillance-Activated Defenses Block the ROS-Induced Mitochondrial Unfolded Protein Response. *PLoS Genetics*. **9**(3).

Sampuda, K.M., Riley, M. and Boyd, L. 2017. Stress induced nuclear granules form in response to accumulation of misfolded proteins in Caenorhabditis elegans. *BMC Cell Biology*. **18**(1), pp.1–18.

Sarov, M., Schneider, S., Pozniakovski, A., Roguev, A., Ernst, S., Zhang, Y., Hyman, A.A. and Stewart, A.F. 2006. A recombineering pipeline for functional genomics applied to Caenorhabditis elegans. *Nature Methods*. **3**(10), pp.839–844.

Scherz-Shouval, R., Santagata, S., Mendillo, M.L., Sholl, L.M., Ben-Aharon, I., Beck, A.H., Dias-Santagata, D., Koeva, M., Stemmer, S.M., Whitesell, L. and Lindquist, S. 2014. The reprogramming of tumor stroma by HSF1 is a potent enabler of malignancy. *Cell*. **158**(3), pp.564–578.

Schneider, C.A., Rasband, W.S. and Eliceiri, K.W. 2012. NIH Image to ImageJ: 25 years of image analysis. *Nature Methods*. **9**(7), pp.671–675.

Schroeder, A., Mueller, O., Stocker, S., Salowsky, R., Leiber, M., Gassmann, M., Lightfoot, S., Menzel, W., Granzow, M. and Ragg, T. 2006. The RIN: An RNA integrity number for assigning integrity values to RNA measurements. *BMC Molecular Biology*. **7**, pp.1–14.

Schulz, A.M. and Haynes, C.M. 2015. UPR(mt)-mediated cytoprotection and organismal aging. *Biochimica et biophysica acta*. **1847**, pp.1448–1456.

Schuster, E., McElwee, J.J., Tullet, J.M.A., Doonan, R., Matthijssens, F., Reece-Hoyes, J.S., Hope, I.A., Vanfleteren, J.R., Thornton, J.M. and Gems, D. 2010. DamID in C. elegans reveals longevity-associated targets of DAF-16/FoxO. *Molecular Systems Biology*. **6**(399), pp.1–6.

Seah, N.E., de Magalhaes Filho, C.D., Petrashen, A.P., Henderson, H.R., Laguer, J., Gonzalez, J., Dillin, A., Hansen, M. and Lapierre, L.R. 2016. Autophagy-mediated longevity is modulated by lipoprotein biogenesis. *Autophagy*. **12**(2), pp.261–272.

Serrano-Pozo, A., Frosch, M.P., Masliah, E. and Hyman, B.T. 2011. Neuropathological alterations in Alzheimer disease. *Cold Spring Harbor Perspectives in Medicine*. **1**(1), pp.1–23.

Shapira, M., Hamlin, B.J., Rong, J., Chen, K., Ronen, M. and Tan, M.-W. 2006. A conserved role for a GATA transcription factor in regulating epithelial innate immune responses. *Proceedings of the National Academy of Sciences*. **103**(38), pp.14086–14091.

Shaye, D.D. and Greenwald, I. 2011. Ortholist: A compendium of C. elegans genes with human orthologs. *PLoS ONE*. **6**(5).

Shin, H., Lee, H., Fejes, A.P., Baillie, D.L., Koo, H.S. and Jones, S.J. 2011. Gene expression profiling of oxidative stress response of C. elegans aging defective AMPK mutants using massively parallel transcriptome sequencing. *BMC Research Notes*. **4**.

Shpigel, N., Shemesh, N., Kishner, M. and Ben-Zvi, A. 2018. Dietary restriction and

gonadal signaling differentially regulate post-development quality control functions in Caenorhabditis elegans. *Aging Cell*. (September 2018).

Shpilka, T. and Haynes, C.M. 2018. The mitochondrial UPR: Mechanisms, physiological functions and implications in ageing. *Nature Reviews Molecular Cell Biology*. **19**(2), pp.109–120.

Singh, V. and Aballay, A. 2009. Regulation of DAF-16-mediated innate immunity in Caenorhabditis elegans. *Journal of Biological Chemistry*. **284**(51), pp.35580–35587.

Sommermann, E.M., Strohmaier, K.R., Maduro, M.F. and Rothman, J.H. 2010. Endoderm development in Caenorhabditis elegans: The synergistic action of ELT-2 and -7 mediates the specification→differentiation transition. *Developmental Biology*. **347**(1), pp.154–166.

Song, H.-O., Lee, W., An, K., Lee, H., Cho, J.H., Park, Z.-Y. and Ahnn, J. 2009. C. elegans STI-1, the Homolog of Sti1/Hop, Is Involved in Aging and Stress Response. *Journal of Molecular Biology*. **390**(4), pp.604–617.

Spencer, W.C., Zeller, G., Watson, J.D., Henz, S.R., Watkins, K.L., McWhirter, R.D., Petersen, S., Sreedharan, V.T., Widmer, C., Jo, J., Reinke, V., Petrella, L., Strome, S., Von Stetina, S.E., Katz, M., Shaham, S., Rätsch, G. and Miller, D.M. 2011. A spatial and temporal map of C. elegans gene expression. *Genome research*. **21**(2), pp.325–41.

Styren, S.D., Hamilton, R.L., Styren, G.C. and Klunk, W.E. 2000. X-34, a fluorescent derivative of Congo red: A novel histochemical stain for Alzheimer's disease pathology. *Journal of Histochemistry and Cytochemistry*. **48**(9), pp.1223–1232.

Sulston, J. and Hodgkin, J. 1988. Methods *In*: W. B. Wood, ed. *The Nematode Caenorhabditis elegans*. Cold Spring Harbor: Cold Spring Harbor Laboratory, pp.587–606.

Sun, J., Liu, Y. and Aballay, A. 2012. Organismal regulation of XBP-1-mediated unfolded protein response during development and immune activation. *EMBO reports*. **13**(9), pp.855–860.

Sun, J., Singh, V., Kajino-sakamoto, R. and Aballay, A. 2011. Neuronal GPCR Controls Innate Immunity by Regulating Noncanonical Unfolded Protein Response Genes. . **1**(May), pp.729–732.

Sung, C.K. and Yim, H. 2017. Roles of SALL2 in tumorigenesis. *Archives of Pharmacal Research*. **40**(2), pp.146–151.

Taipale, M., Jarosz, D.F. and Lindquist, S. 2010. HSP90 at the hub of protein homeostasis: emerging mechanistic insights. *Nature Reviews Molecular Cell Biology*. **11**(7), pp.515–528.

Takahashi, R.H., Nagao, T. and Gouras, G.K. 2017. Plaque formation and the intraneuronal accumulation of β-amyloid in Alzheimer's disease. *Pathology International*. **67**(4), pp.185–193.

Takeda, K., Wada, A., Yamamoto, K., Moriyama, Y. and Aoki, K. 1989. Conformational change of bovine serum albumin by heat treatment. *Journal of Protein Chemistry*.

8(5), pp.653–659.

Tanford, C. and Roxby, R. 1972. Interpretation of protein titration curves. Application to lysozyme. *Biochemistry*. **11**(11), pp.2192–2198.

Tatum, M.C., Ooi, F.K., Chikka, M.R., Chauve, L., Martinez-Velazquez, L.A., Steinbusch, H.W.M., Morimoto, R.I. and Prahlad, V. 2015. Neuronal Serotonin Release Triggers the Heat Shock Response in C. elegans in the Absence of Temperature Increase. *Current Biology*. **25**(2), pp.163–174.

Tawe, W.N., Eschbach, M.-L.M.L., Walter, R.D., Henkle-Dührsen, K. and Henkle-Duhrsen, K. 1998. Identification of stress-responsive genes in Caenorhabditis elegans using RT-PCR differential display. *Nucleic Acids Research*. **26**(7), pp.1621–1627.

Taylor, R.C., Berendzen, K.M. and Dillin, A. 2014. Systemic stress signalling: understanding the cell non-autonomous control of proteostasis. *Nature Reviews Molecular Cell Biology*. **15**(3), pp.211–217.

Taylor, R.C. and Dillin, A. 2013. XBP-1 Is a cell-nonautonomous regulator of stress resistance and longevity. *Cell*. **153**(7), pp.1435–1447.

Tepper, R.G., Ashraf, J., Kaletsky, R., Kleemann, G., Murphy, C.T. and Bussemaker, H.J. 2013. PQM-1 Complements DAF-16 as a Key Transcriptional Regulator of DAF-2-Mediated Development and Longevity. *Cell*. **154**(3), pp.676–690.

Tepper, R.G., Murphy, C.T. and Bussemaker, H.J. 2014. DAF-16 and PQM-1: Partners in longevity. *Aging*. **6**(1), pp.5–6.

Troemel, E.R., Chu, S.W., Reinke, V., Lee, S.S., Ausubel, F.M. and Kim, D.H. 2006. p38 MAPK regulates expression of immune response genes and contributes to longevity in C. elegans. *PLoS Genetics*. **2**(11), pp.1725–1739.

Tullet, J.M.A., Hertweck, M., An, J.H., Baker, J., Hwang, J.Y., Liu, S., Oliveira, R.P., Baumeister, R. and Blackwell, T.K. 2008. Direct Inhibition of the Longevity-Promoting Factor SKN-1 by Insulin-like Signaling in C. elegans. *Cell*.

van Oosten-Hawle, P., Porter, R.S. and Morimoto, R.I. 2013. Regulation of Organismal Proteostasis by Transcellular Chaperone Signaling. *Cell*. **153**(6), pp.1366–1378.

Vihervaara, A. and Sistonen, L. 2014. HSF1 at a glance. *Journal of cell science*. **127**(Pt 2), pp.261–6.

Walker, A.K., See, R., Batchelder, C., Kophengnavong, T., Gronniger, J.T., Shi, Y. and Blackwell, T.K. 2000. A conserved transcription motif suggesting functional parallels between Caenorhabditis elegans SKN-1 and Cap'n'Collar-related basic leucine zipper proteins. *Journal of Biological Chemistry*. **275**(29), pp.22166–22171.

Walker, G.A. and Lithgow, G.J. 2003. Lifespan extension in C. elegans by a molecular chaperone dependent upon insulin-like signals. *Aging cell*. **2**(2), pp.131–139.

Walter, P. 2006. The unfolded protein response. *Mol Biotechnol*. **34**(2), pp.279–290.

Walter, P. and Ron, D. 2011. The Unfolded Protein Response: From Stress Pathway to Homeostatic Regulation. *Science*. **334**(6059), pp.1081–1086.

Wang, D., Hou, L., Nakamura, S., Su, M., Li, F., Chen, W., Yan, Y., Green, C.D., Chen, D.,

Zhang, H., Antebi, A. and Han, J.D.J. 2017. LIN-28 balances longevity and germline stem cell number in Caenorhabditis elegans through let-7/AKT/DAF-16 axis. *Aging Cell*. **16**(1), pp.113–124.

Westwood, J.T., Clos, J. and Wu, C. 1991. Stress-induced oligomerization and chromosomal relocalization of heat-shock factor. *Nature*. **353**(6347), pp.822–827.

Wiench, M., John, S., Baek, S., Johnson, T.A., Sung, M.H., Escobar, T., Simmons, C.A., Pearce, K.H., Biddie, S.C., Sabo, P.J., Thurman, R.E., Stamatoyannopoulos, J.A. and Hager, G.L. 2011. DNA methylation status predicts cell type-specific enhancer activity. *EMBO Journal*. **30**(15), pp.3028–3039.

Williams, G.T. and Morimoto, R.I. 1990. Maximal Stress-Induced Transcription from the Human HSP70 Promoter Requires Interactions with the Basal Promoter Elements Independent of Rotational Alignment. *Molecular and cellular biology*. **10**(6), pp.3125–3136.

Williams, K.W., Liu, Tiemin, Kong, X., Fukuda, M., Deng, Y., Berglund, E.D., Deng, Z., Gao, Y., Liu, Tianya, Sohn, J.-W., Jia, L., Fujikawa, T., Kohno, D., Scott, M.M., Lee, S., Lee, C.E., Sun, K., Chang, Y., Scherer, P.E. and Elmquist, J.K. 2014. Xbp1s in Pomc Neurons Connects ER Stress with Energy Balance and Glucose Homeostasis. *Cell metabolism*. **3**(3), pp.1–12.

Wolfe, S.A., Nekludova, L. and Pabo, C.O. 2000. DNA recognition by Cys2His2 zinc finger proteins. *Annual review of biophysics and biomolecular structure*. **29**, pp.183–212.

Wu, Y. and Luo, Y. 2005. Transgenic C . Elegans As a Model Organism for Investigations on Alzheimer ' S Disease. *Current Alzeihmer Research*. **2**, pp.37–45.

Xiao, H., Perisic, O. and Lis, J.T. 1991. Cooperative Binding of Drosophila Heat Shock Factor to Arrays of a Conserved 5 bp Unit. *Cell*. **64**, pp.585–593.

Yoneda, T., Benedetti, C., Urano, F., Clark, S.G., Harding, H.P. and Ron, D. 2004. Compartment-specific perturbation of protein handling activates genes encoding mitochondrial chaperones. *Journal of cell science*. **117**(Pt 18), pp.4055–66.

Young, J.C., Obermann, W.M.J. and Hartl, F.U. 1998. Specific binding of tetratricopeptide repeat proteins to the C-terminal 12-kDa domain of hsp90. *Journal of Biological Chemistry*. **273**(29), pp.18007–18010.

Zhang, Q., Wu, X., Chen, P., Liu, L., Xin, N., Tian, Y. and Dillin, A. 2018. The Mitochondrial Unfolded Protein Response Is Mediated Cell-Non-autonomously by Retromer-Dependent Wnt Signaling. *Cell*. **174**(4), pp.870-883.e17.

Zheng, Y., Brockie, P.J., Mellem, J.E., Madsen, D.M., Walker, C.S., Francis, M.M. and Maricq, A. V. 2006. SOL-1 is an auxiliary subunit that modulates the gating of GLR-1 glutamate receptors in Caenorhabditis elegans. *Proceedings of the National Academy of Sciences of the United States of America*. **103**(4), pp.1100–1105.

Zhong, M., Niu, W., Lu, Z.J., Sarov, M., Murray, J.I., Janette, J., Raha, D., Sheaffer, K.L., Lam, H.Y.K., Preston, E., Slightham, C., Hillier, L.D.W., Brock, T., Agarwal, A., Auerbach, R., Hyman, A.A., Gerstein, M., Mango, S.E., Kim, S.K., Waterston, R.H., Reinke, V. and Snyder, M. 2010. Genome-wide identification of binding sites

defines distinct functions for Caenorhabditis elegans PHA-4/FOXA in development and environmental response. *PLoS Genetics*. **6**(2).

Zou, J., Guo, Y., Guettouche, T., Smith, D.F. and Voellmy, R. 1998. Repression of heat shock transcription factor HSF1 activation by HSP90 (HSP90 complex) that forms a stress-sensitive complex with HSF1. *Cell*. **94**(4), pp.471–480.

Zuiderweg, E.R.P., Hightower, L.E. and Gestwicki, J.E. 2017. The remarkable multivalency of the Hsp70 chaperones. *Cell Stress and Chaperones*. **22**(2), pp.173–189.

Appendix A

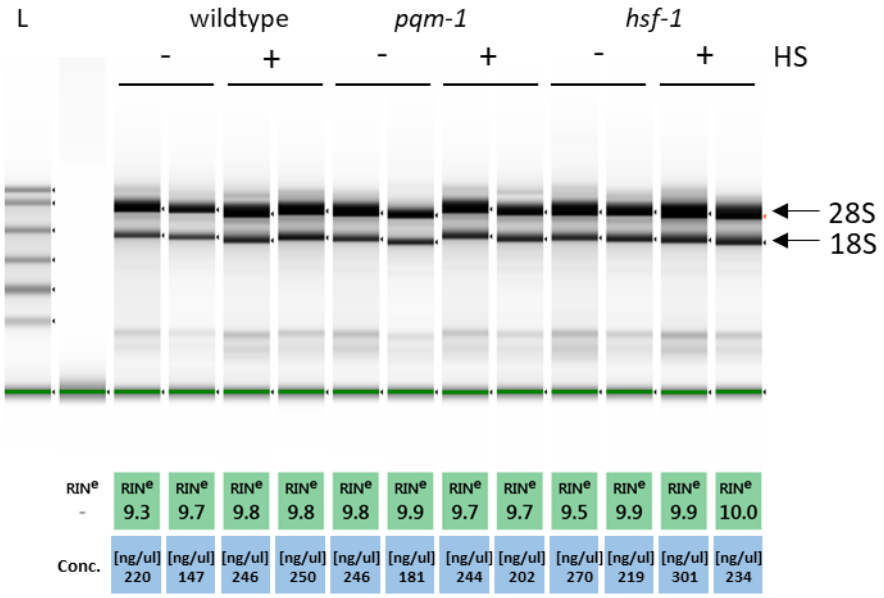

Figure A.1 Total RNA run on an Agilent 4200 Tapestation for RNA. The automatically determined RINe values are shown below the gel-like image, alongside the concentration of RNA measured for each sample.

Table A.1 N2 (wt) vs N2 (wt) +HS

Gene	transcript	log2FC	adj.P.Val
F33H12.6	F33H12.6	6.131403	1.39E-59
R11A5.3	R11A5.3	5.906352	2.57E-55
hsp-16.11	T27E4.2	5.556136	7.47E-49
F44E5.5	F44E5.5	5.310143	1.05E-44
hsp-70	C12C8.1	5.241761	1.41E-43
hsp-16.48	T27E4.3	4.65425	2.99E-34
hsp-12.6	F38E11.2	4.057357	1.06E-25
C25F9.2	C25F9.2	4.044943	1.46E-25
hsp-16.2	Y46H3A.3a	3.524687	4.5E-19
tts-1	F09E10.11a	3.492651	1E-18
K10G4.3	K10G4.3	3.441215	3.7E-18
hsp-16.41	Y46H3A.2	3.434331	4.21E-18
F59C12.4	F59C12.4	3.351373	3.45E-17
mtl-1	K11G9.6	3.338137	4.62E-17
numr-1	F08F8.5	3.296486	1.27E-16
Y17D7C.2	Y17D7C.2	3.28488	1.63E-16
F19B10.13	F19B10.13	3.25576	3.24E-16
cnc-11	R09B5.13	3.21765	8E-16
R03H10.6	R03H10.6	3.139878	5.11E-15
F08H9.4a	F08H9.4a	2.943322	4.81E-13
clec-196	F26D10.12a	2.781142	1.64E-11
sri-39	F33H12.2	2.727045	4.98E-11
R09E10.13	R09E10.13	2.631721	3.44E-10
ttll-12	D2013.9.1	2.615747	4.6E-10
gem-4	T12A7.1.1	2.612475	4.77E-10
C25F9.12	C25F9.12	2.572946	1.02E-09
ZC21.10.2	ZC21.10.2	2.537306	1.94E-09
F44E5.4	F44E5.4	2.535992	1.94E-09
tos-1	K07B1.8	2.46601	7.28E-09
ipla-2	F47A4.5	2.33834	7.59E-08
F31D5.6	F31D5.6	2.331743	8.34E-08
C54F6.5	C54F6.5	2.32672	8.9E-08
C49G7.6	C49G7.6	2.324179	9.1E-08
Y94H6A.10	Y94H6A.10	2.311157	1.08E-07
M106.6	M106.6	2.3111	1.08E-07
ugt-13	H23N18.1	2.311011	1.08E-07
C17F4.12	C17F4.12	2.309208	1.09E-07
F15B9.6	F15B9.6	2.279674	1.8E-07
C54F6.15	C54F6.15	2.261679	2.42E-07
smy-9	Y45F10B.16	2.226191	4.39E-07
str-118	F57A8.3a	2.172453	1.08E-06
NA	NA	2.147981	1.59E-06

cdr-4	K01D12.11	2.101566	3.36E-06
C08F11.13a.1	C08F11.13a.1	2.090328	3.95E-06
ZC47.13a	ZC47.13a	2.081437	4.48E-06
T22B7.3	T22B7.3	2.064138	5.82E-06
C50F7.5	C50F7.5	2.057694	6.34E-06
F53A9.1	F53A9.1	2.051621	6.86E-06
T25D10.1	T25D10.1	2.0491	7.02E-06
C44B12.3	C44B12.3	2.047032	7.13E-06
F08H9.3	F08H9.3	2.044347	7.32E-06
asic-2	T28F4.2	2.025524	9.71E-06
srg-34	Y51A2D.12	2.024133	9.76E-06
C18D11.6	C18D11.6	2.022072	9.92E-06
Y51A2D.13a	Y51A2D.13a	2.019576	1.02E-05
F08G2.5	F08G2.5	1.993249	1.49E-05
cnc-4	R09B5.9	1.960183	2.41E-05
fipr-26	F53B6.8	1.960146	2.41E-05
srr-6	C13D9.1	1.949493	2.79E-05
sqst-1	T12G3.1a.1	1.948562	2.79E-05
irg-2	C49G7.5	1.931603	3.56E-05
M60.7	M60.7	1.922966	3.99E-05
F55B12.10	F55B12.10	1.91831	4.22E-05
oac-14	F09B9.1	1.912672	4.51E-05
ZK970.7	ZK970.7	1.91212	4.51E-05
pgp-8	T21E8.3	1.906025	4.88E-05
W09D6.7	W09D6.7	1.904858	4.9E-05
tli-1	F25H2.1	1.895954	5.01E-05
Y102A5D.13	Y102A5D.13	1.892847	5.01E-05
B0403.3	B0403.3	1.891612	5.04E-05
hsp-4	F43E2.8a.1	1.882128	5.68E-05
C27B7.9	C27B7.9	1.867216	6.99E-05
B0205.13	B0205.13	1.855884	8.16E-05
C05B5.8	C05B5.8	1.850285	8.76E-05
nhr-154	C13C4.2	1.838858	0.000102
Y47H10A.5	Y47H10A.5	1.833674	0.000109
F53C3.6b	F53C3.6b	1.812199	0.000147
C54C6.7	C54C6.7	1.803707	0.000164
Y43F8B.2a	Y43F8B.2a	1.803092	0.000164
catp-3	C09H5.2a	1.802434	0.000164
cebp-1	D1005.3	1.794558	0.000181
C06B3.7	C06B3.7	1.791042	0.000189
tbb-6	T04H1.9	1.789461	0.000191
C49A9.6	C49A9.6	1.786213	0.000198
Y75B8A.28	Y75B8A.28	1.781442	0.000208
C25H3.15	C25H3.15	1.760155	0.000274
ckb-2	B0285.9	1.754774	0.000292

ugt-24	C49A9.8.1	1.754327	0.000292
F23F1.2	F23F1.2	1.752565	0.000297
F22B7.9	F22B7.9	1.746989	0.000317
F59C6.15	F59C6.15	1.730636	0.00039
T10E10.4	T10E10.4	1.727283	0.000405
T27F6.8	T27F6.8	1.725462	0.000412
linc-22	F47E1.17	1.719668	0.000441
gst-7	F11G11.2	1.716831	0.000455
Y22D7AL.15	Y22D7AL.15	1.707898	0.000509
C41C4.11	C41C4.11	1.704976	0.000525
T14G8.4	T14G8.4	1.702729	0.000537
srsx-7	Y97E10B.4	1.694982	0.000591
T23F11.6	T23F11.6	1.694046	0.000593
R02E4.3	R02E4.3	1.692276	0.000603
F16B12.4	F16B12.4	1.679713	0.000707
fbxa-66	Y54F10BM.11	1.67329	0.000763
fbxa-163	C08E3.6	1.667381	0.000819
F17C11.11a	F17C11.11a	1.657807	0.000921
F48D6.4a	F48D6.4a	1.656268	0.000926
K01F9.2	K01F9.2	1.644087	0.001077
C33A12.19a	C33A12.19a	1.63081	0.001256
C07A9.12	C07A9.12	1.630419	0.001256
ttr-26	Y51A2D.11.1	1.62993	0.001256
nex-2	T07C4.9a	1.616174	0.001477
arrd-8	Y17G7B.14	1.609847	0.00159
fbxa-59	T12B5.8	1.60882	0.0016
W01D2.7	W01D2.7	1.604601	0.001676
fis-2	F13B9.8a	1.600619	0.001738
K02G10.15	K02G10.15	1.597488	0.001796
fbxa-48	Y54F10BM.7	1.596708	0.001802
F45B8.6	F45B8.6	1.591333	0.001909
pek-1	F46C3.1	1.591043	0.001909
nmur-4	C30F12.6	1.58854	0.001957
W09D6.8	W09D6.8	1.585182	0.002028
C34D10.1	C34D10.1	1.581976	0.002097
Y58A7A.5	Y58A7A.5	1.576332	0.002226
gst-36	R07B1.4	1.576157	0.002226
T28D6.10	T28D6.10	1.574912	0.002247
C30B5.6b	C30B5.6b	1.572026	0.002314
T23F2.4	T23F2.4	1.567116	0.002444
tsp-1	C02F5.8	1.566246	0.002455
Y82E9BL.18	Y82E9BL.18	1.563276	0.002531
K01A6.7	K01A6.7	1.535364	0.003524
nhr-247	ZK1037.5	1.532929	0.003608
F45D3.4a.1	F45D3.4a.1	1.532227	0.003617

C49G7.10	C49G7.10	1.521992	0.004022
F53B2.8	F53B2.8	1.521959	0.004022
F19B2.5.1	F19B2.5.1	1.521475	0.004022
aly-1	C01F6.5	1.512893	0.004418
gly-8	Y66A7A.6.2	1.512609	0.004418
R09A1.3	R09A1.3	1.512221	0.004418
ugt-25	C10H11.3	1.509903	0.004514
bus-18	F55A11.5	1.509444	0.004514
K08B4.7	K08B4.7	1.50559	0.004701
ZC443.3	ZC443.3	1.504459	0.00471
nlp-25	Y43F8C.1	1.499081	0.004994
Y38E10A.14	Y38E10A.14	1.498114	0.005024
rap-3	C08F8.7	1.493695	0.005266
Y6G8.5b	Y6G8.5b	1.490679	0.005397
ZC168.2	ZC168.2	1.489996	0.005411
memb-1	B0272.2	1.487844	0.00552
K02C4.8	K02C4.8	1.482767	0.005798
C49A9.9a.1	C49A9.9a.1	1.470551	0.006624
F01F1.14	F01F1.14	1.46584	0.006962
F12A10.1	F12A10.1	1.465147	0.006981
C50F4.6	C50F4.6	1.459953	0.007379
Y38E10A.22a	Y38E10A.22a	1.457363	0.007565
T13C5.6	T13C5.6	1.454615	0.007724
fbxa-27	Y82E9BL.17	1.449368	0.008129
M04F3.4a	M04F3.4a	1.446052	0.008403
swt-6	R10D12.9.2	1.433188	0.009522
efhd-1	Y48B6A.6a.2	1.43299	0.009522
ubc-23	C28G1.1	1.429083	0.009908
K09D9.1	K09D9.1	1.425246	0.010301
ttr-30	T08A9.2	1.42217	0.010616
fipr-22	C37A5.2	1.420667	0.010699
C52A10.1	C52A10.1	1.41811	0.010937
C04F12.1	C04F12.1	1.417827	0.010937
gst-20	Y48E1B.10	1.414213	0.01134
Y58A7A.4	Y58A7A.4	1.411757	0.011548
Y71F9AM.7	Y71F9AM.7	1.409764	0.011738
F41B4.3	F41B4.3	1.409056	0.011738
dnj-27	Y47H9C.5a	1.408178	0.011799
Y44A6C.1	Y44A6C.1	1.405838	0.012058
F27D9.7	F27D9.7	1.401089	0.012661
R11F4.1.2	R11F4.1.2	1.399174	0.012877
C34C6.7a	C34C6.7a	1.395952	0.013289
daf-8	R05D11.1	1.395179	0.013343
tyr-6	Y73B6BL.1	1.393677	0.013446
T01B7.8	T01B7.8	1.393048	0.013465

tag-234	F55C12.7.1	1.39274	0.013465
F21C10.10.2	F21C10.10.2	1.391217	0.013635
best-5	C07A9.8	1.387555	0.01414
F52H3.5	F52H3.5	1.386811	0.014144
F47B10.9	F47B10.9	1.385807	0.014144
magu-2	C01B7.4	1.385467	0.014144
F09F7.6	F09F7.6	1.385158	0.014144
cutl-14	B0511.5	1.381481	0.014664
F37C4.5a.1	F37C4.5a.1	1.381126	0.014664
Y37H2A.12a	Y37H2A.12a	1.37967	0.014839
Y15E3A.5.2	Y15E3A.5.2	1.378363	0.014928
faah-2	B0218.2	1.371876	0.015969
F28H1.1	F28H1.1	1.370577	0.016066
F25G6.1	F25G6.1	1.364559	0.017075
nlp-34	B0213.17	1.361069	0.017505
syx-2	F48F7.2.2	1.360956	0.017505
T28F4.5.2	T28F4.5.2	1.360865	0.017505
W03F9.1	W03F9.1	1.358434	0.017903
Y38H6C.8	Y38H6C.8	1.356991	0.01804
R03E9.9	R03E9.9	1.355475	0.018267
F53A9.7	F53A9.7	1.348651	0.019362
T27A1.2	T27A1.2	1.347643	0.019454
fbxa-31	ZC47.5	1.347211	0.019454
K03A1.4a	K03A1.4a	1.347122	0.019454
C06B3.6.1	C06B3.6.1	1.343313	0.020194
cyp-43A1	E03E2.1.2	1.342724	0.020244
Y58A7A.3	Y58A7A.3	1.34212	0.020297
nipi-3	K09A9.1	1.34087	0.020482
sri-36	F33H12.5	1.340564	0.020482
F01D5.6	F01D5.6	1.33847	0.02087
F18H3.4	F18H3.4	1.334971	0.02159
C29F3.3	C29F3.3	1.333988	0.021733
C16D9.1	C16D9.1	1.333644	0.021733
C55C3.1	C55C3.1	1.33234	0.021957
clp-4	Y39A3CL.5a	1.329784	0.022398
abhd-5.1	C37H5.2	1.328868	0.022535
lin-28	F02E9.2a	1.32699	0.022901
C10C6.8	C10C6.8	1.326668	0.022901
ZK1290.5	ZK1290.5	1.325139	0.022971
F08G2.4	F08G2.4	1.324834	0.022971
F09C6.1	F09C6.1	1.324606	0.022971
ZK637.14	ZK637.14	1.323981	0.022971
nhr-241	Y69H2.8	1.323397	0.023031
Y46H3A.5	Y46H3A.5	1.321786	0.023346
T09F5.12a	T09F5.12a	1.320247	0.023593

cnp-3	T23C6.3	1.32013	0.023593
ikb-1	C04F12.3	1.311465	0.025435
F25B3.5a	F25B3.5a	1.311457	0.025435
Y54G9A.12	Y54G9A.12	1.31139	0.025435
fbxb-14	W08F4.9	1.310419	0.025608
phg-1	F27E5.4	1.305518	0.026783
F28C6.5	F28C6.5	1.305101	0.026808
C01A2.4	C01A2.4	1.300166	0.028045
T28F4.4	T28F4.4	1.299219	0.028228
F44E2.4	F44E2.4	1.298233	0.028425
F44A6.5	F44A6.5	1.29769	0.02849
glod-4	C16C10.10	1.295384	0.029036
F28H7.8	F28H7.8	1.293839	0.029314
ptr-8	F44F4.4	1.293683	0.029314
unc-23	H14N18.1a	1.29097	0.029957
K06H7.2	K06H7.2	1.28712	0.031019
Y45F10B.8	Y45F10B.8	1.286994	0.031019
T24B8.5	T24B8.5	1.285277	0.031269
R07B1.5	R07B1.5	1.284499	0.03142
F21D9.8	F21D9.8	1.283018	0.0317
skr-3	F44G3.6.2	1.2814	0.032133
atg-11	T08A9.1	1.278965	0.032849
E01G6.1	E01G6.1	1.278249	0.032987
F56C3.9	F56C3.9	1.276628	0.033438
F41E6.12	F41E6.12	1.275632	0.033677
Y38C1AA.6	Y38C1AA.6	1.273499	0.034209
ubc-8	Y94H6A.6	1.272982	0.034283
F57B10.9	F57B10.9	1.269681	0.035247
W06B11.9	W06B11.9	1.264398	0.036785
fbxa-37	ZC47.14	1.264292	0.036785
C34C12.9	C34C12.9	1.263671	0.036785
F33D11.8	F33D11.8	1.262655	0.036956
Y54G2A.52	Y54G2A.52	1.26232	0.03697
F53A2.9	F53A2.9	1.260888	0.037368
comt-3	Y40B10A.2	1.260678	0.037368
ZK355.8	ZK355.8	1.256246	0.038874
C44H9.5	C44H9.5	1.254891	0.039286
T13C2.6a	T13C2.6a	1.252872	0.039981
F18C5.10.1	F18C5.10.1	1.246059	0.042552
C33A12.3b	C33A12.3b	1.245852	0.042552
igeg-2	F48C5.1	1.241777	0.044068
F08C6.5	F08C6.5	1.239326	0.044919
grl-4	F42C5.7	1.236526	0.045856
Y55F3BR.13	Y55F3BR.13	1.234607	0.046263
epg-9	Y69A2AR.7a	1.234393	0.046263

F20D1.3	F20D1.3	1.234373	0.046263
Y73B6BL.27	Y73B6BL.27	1.233616	0.046428
R107.5a	R107.5a	1.231887	0.046892
Y102A11A.9.1	Y102A11A.9.1	1.231148	0.047106
wht-1	C05D10.3	1.227517	0.048437
C34D10.2a.1	C34D10.2a.1	1.227149	0.048473
F20B6.4	F20B6.4	1.226675	0.048473
F19C6.2a	F19C6.2a	1.22634	0.048473
tps-1	ZK54.2a.1	1.226044	0.048473
ippk-1	Y17G7B.13	1.225686	0.048512
F26G1.5	F26G1.5	1.225009	0.048706
Y58A7A.7	Y58A7A.7	1.223007	0.04928
M60.4a	M60.4a	1.222674	0.049309
C07H6.10	C07H6.10	-1.2213	0.049716
cyp-33C3	F41B5.4	-1.22145	0.049716
K01D12.8	K01D12.8	-1.22458	0.048781
pqn-37	F40F4.8	-1.22629	0.048473
C37C3.10	C37C3.10	-1.22806	0.04831
gcsh-1	D1025.2	-1.23345	0.046428
W01A11.16	W01A11.16	-1.23534	0.046213
nhr-114	Y45G5AM.1a.1	-1.2364	0.045856
ZC416.6a	ZC416.6a	-1.24472	0.042915
K06C4.10	K06C4.10	-1.24715	0.04225
F08A8.4.2	F08A8.4.2	-1.25622	0.038874
scav-4	F11C1.3	-1.26341	0.036785
oac-54	W07A12.6	-1.2638	0.036785
Y102A11A.1	Y102A11A.1	-1.26879	0.03535
pept-1	K04E7.2.1	-1.26911	0.035345
T05B4.12	T05B4.12	-1.27144	0.034722
R08E5.1.1	R08E5.1.1	-1.27505	0.033772
F35D2.1	F35D2.1	-1.28338	0.031684
drd-1	F49E12.9a	-1.28549	0.031269
C40H1.7	C40H1.7	-1.28623	0.031166
acp-6	Y73B6BL.24	-1.29148	0.029897
aat-6	T11F9.4a	-1.29524	0.029036
plep-1	Y52E8A.4	-1.3014	0.027777
ugt-62	M88.1.1	-1.30914	0.025867
ZC116.3	ZC116.3	-1.31192	0.025435
F23F12.3	F23F12.3	-1.31877	0.023853
clec-165	F38A1.10	-1.32405	0.022971
F01D5.2	F01D5.2	-1.32405	0.022971
str-233	C06C6.2	-1.33181	0.022
MTCE.34	MTCE.34	-1.34918	0.019328
T24E12.14	T24E12.14	-1.35171	0.018878
F56H11.9	F56H11.9	-1.35426	0.018435

nas-27	T23F4.4	-1.37057	0.016066
C47G2.16	C47G2.16	-1.38537	0.014144
elo-6	F41H10.8	-1.39372	0.013446
rhy-1	W07A12.7	-1.40927	0.011738
ugt-22	C08F11.8.1	-1.43478	0.009423
elt-2	C33D3.1	-1.43725	0.009206
T08B6.9	T08B6.9	-1.43936	0.009032
asp-10	C15C8.3a	-1.45581	0.007662
Y71A12B.18	Y71A12B.18	-1.48456	0.005708
clec-7	F10G2.3	-1.4917	0.005362
math-40	T08E11.3	-1.505	0.004707
T20D4.3	T20D4.3	-1.522	0.004022
F21C10.9.1	F21C10.9.1	-1.55325	0.002847
trx-3	M01H9.1	-1.60211	0.001718
pcp-3	F23B2.11.1	-1.61808	0.001452
T10B9.13	T10B9.13	-1.65632	0.000926
T20D4.5	T20D4.5	-1.73333	0.000379
ifc-1	F37B4.2	-1.76941	0.000243
K12B6.11	K12B6.11	-1.89049	5.07E-05
R193.2	R193.2	-2.00983	1.17E-05

Table A.2 *pqm-1* (ko) vs *pqm-1* (ko) +HS

Gene	transcript	log_2FC	P.Value
F33H12.6	F33H12.6	7.100037	3.49E-06
R11A5.3	R11A5.3	6.652959	2.23E-07
F44E5.5	F44E5.5	5.937192	7.94E-08
hsp-70	C12C8.1	5.337239	1.2E-07
C25F9.2	C25F9.2	4.776743	3.64E-07
hsp-12.6	F38E11.2	4.679077	4.34E-06
hsp-16.11	T27E4.2	4.570536	1.87E-08
hsp-16.41	Y46H3A.2	4.404912	8.71E-07
hsp-16.2	Y46H3A.3a	3.772139	8.72E-06
ZC21.10.2	ZC21.10.2	3.759966	4.1E-05
K10G4.3	K10G4.3	3.674175	1.09E-07
F44E5.4	F44E5.4	3.548659	5.48E-06
hsp-16.48	T27E4.3	3.363321	7.91E-07
F59C12.4	F59C12.4	3.277806	7.95E-06
sri-39	F33H12.2	3.262079	0.000499
R03H10.6	R03H10.6	3.027338	6.65E-08
Y15E3A.5.2	Y15E3A.5.2	2.950577	7.45E-07
srr-6	C13D9.1	2.949713	9.94E-06
F31D5.6	F31D5.6	2.935764	1.17E-07
smy-9	Y45F10B.16	2.914228	3.26E-05
C06B3.7	C06B3.7	2.852363	8.25E-05
F33H12.7	F33H12.7	2.784579	3.61E-05
Y102A5D.13	Y102A5D.13	2.773643	0.000252
tts-1	F09E10.11a	2.74773	3.61E-07
F08H9.3	F08H9.3	2.721916	2.11E-05
M106.6	M106.6	2.718686	1.01E-05
F17C11.11a	F17C11.11a	2.706607	0.000375
C44B12.3	C44B12.3	2.589065	1.01E-06
F53A9.1	F53A9.1	2.575353	8.13E-06
F19B10.13	F19B10.13	2.54954	2.04E-06
clec-196	F26D10.12a	2.542089	2.83E-06
M60.7	M60.7	2.541619	4.67E-06
C50F7.5	C50F7.5	2.528306	8.56E-06
C49G7.6	C49G7.6	2.518585	0.000575
irg-2	C49G7.5	2.458386	4.56E-06
str-118	F57A8.3a	2.453286	0.000151
C25F9.12	C25F9.12	2.445316	1.32E-06
arrd-8	Y17G7B.14	2.362076	6.7E-07
sri-36	F33H12.5	2.341481	5.49E-05
nhr-247	ZK1037.5	2.273607	1.96E-06
C06B3.6.1	C06B3.6.1	2.264065	0.00032
Y17D7C.2	Y17D7C.2	2.243524	1.77E-05

C33A12.19a	C33A12.19a	2.221815	1.68E-06
ZK355.8	ZK355.8	2.220778	1.95E-05
cnp-3	T23C6.3	2.20522	8.16E-05
ttll-12	D2013.9.1	2.20341	2.11E-06
Y46H3A.5	Y46H3A.5	2.201893	7.61E-06
C50F4.6	C50F4.6	2.164635	0.000764
C04F12.1	C04F12.1	2.158772	3.81E-06
Y47H10A.5	Y47H10A.5	2.149677	0.000109
fbxa-48	Y54F10BM.7	2.10659	1.52E-06
cebp-1	D1005.3	2.103629	4.85E-05
C49G7.10	C49G7.10	2.101512	0.000145
W01D2.7	W01D2.7	2.095209	3.45E-05
Y43F8B.2a	Y43F8B.2a	2.088597	2.46E-05
T25D10.1	T25D10.1	2.075423	6.26E-05
nhr-241	Y69H2.8	2.060572	2.83E-06
asic-2	T28F4.2	2.023432	6.05E-06
ipla-2	F47A4.5	1.968143	1.29E-05
R09E10.13	R09E10.13	1.962375	2.44E-06
tos-1	K07B1.8	1.959388	4.51E-06
fbxb-14	W08F4.9	1.939257	3.39E-06
Y38H6C.8	Y38H6C.8	1.933143	7.35E-06
Y75B8A.39	Y75B8A.39	1.92756	7.62E-05
sqst-1	T12G3.1a.1	1.923341	3.97E-06
F28H1.1	F28H1.1	1.888068	3.18E-06
ZK1240.8	ZK1240.8	1.870628	0.000503
cdr-4	K01D12.11	1.86672	0.000114
srsx-7	Y97E10B.4	1.85321	0.00024
Y58A7A.3	Y58A7A.3	1.850009	0.000106
W09D6.8	W09D6.8	1.843435	4.28E-05
Y6G8.5b	Y6G8.5b	1.842391	8.97E-06
oac-14	F09B9.1	1.840315	1.95E-05
Y94H6A.10	Y94H6A.10	1.832665	0.000472
ZK1290.5	ZK1290.5	1.79177	0.000273
F53B2.8	F53B2.8	1.788582	6.98E-06
Y75B8A.28	Y75B8A.28	1.777191	6.17E-05
F53A9.7	F53A9.7	1.776369	4.3E-05
F53C3.6b	F53C3.6b	1.764561	1.39E-05
numr-1	F08F8.5	1.746819	6.17E-05
unc-23	H14N18.1a	1.745723	0.000403
R11F4.1.2	R11F4.1.2	1.729424	3.56E-05
C08F11.13a.1	C08F11.13a.1	1.716878	1.28E-05
hsp-4	F43E2.8a.1	1.699092	3.63E-05
F45B8.6	F45B8.6	1.680509	0.000505
F08H9.4a	F08H9.4a	1.674158	6.31E-05
F45D3.4a.1	F45D3.4a.1	1.672467	0.000195

srt-42	Y46H3A.1b	1.660681	8.54E-06
F16B12.4	F16B12.4	1.646493	5.49E-05
Y58A7A.5	Y58A7A.5	1.646031	0.000387
B0205.13	B0205.13	1.643903	0.000415
F15B9.6	F15B9.6	1.633148	0.000164
gem-4	T12A7.1.1	1.62709	0.000486
T28D6.10	T28D6.10	1.604243	0.000529
F48G7.13	F48G7.13	1.601851	0.00023
C14F11.11	C14F11.11	1.596817	0.000103
nipi-3	K09A9.1	1.577613	0.000265
F08G2.5	F08G2.5	1.568485	3.41E-05
pek-1	F46C3.1	1.568041	2.02E-05
C13G3.1	C13G3.1	1.559813	0.000492
Y71G12B.18a	Y71G12B.18a	1.549559	0.000275
M03D4.77	M03D4.77	1.546359	0.000396
egrh-1	C27C12.2	1.54333	0.000188
T28F4.5.2	T28F4.5.2	1.54187	3.63E-05
ckb-2	B0285.9	1.541158	0.000169
tsp-1	C02F5.8	1.5273	0.000116
E01G4.5	E01G4.5	1.526429	3.09E-05
C49A9.9a.1	C49A9.9a.1	1.519559	1.6E-05
F11A6.6	F11A6.6	1.51534	0.000784
F19B2.5.1	F19B2.5.1	1.508285	1.83E-05
F22B7.9	F22B7.9	1.503992	2.13E-05
clec-221	F17C11.5	1.493312	0.000208
try-5	K07B1.1.1	1.478941	0.000674
K09D9.1	K09D9.1	1.474019	0.000499
F52H3.5	F52H3.5	1.472841	4.06E-05
ZK1010.10	ZK1010.10	1.468684	2.9E-05
clp-4	Y39A3CL.5a	1.459969	3.02E-05
cnc-4	R09B5.9	1.459494	2.59E-05
Y58A7A.7	Y58A7A.7	1.454152	0.00023
tag-234	F55C12.7.1	1.449598	0.000152
nex-2	T07C4.9a	1.448842	4.68E-05
C06G1.t4	C06G1.t4	1.447973	6.71E-05
gst-36	R07B1.4	1.446328	4.86E-05
linc-22	F47E1.17	1.445845	0.0001
F22E12.13	F22E12.13	1.445652	0.0002
ptr-8	F44F4.4	1.441125	6.88E-05
F18H3.4	F18H3.4	1.438959	2.47E-05
T23F11.6	T23F11.6	1.437162	0.000323
Y51A2D.13a	Y51A2D.13a	1.418052	0.000109
fbxa-52	F07G6.6	1.410359	7.71E-05
faah-2	B0218.2	1.408564	8.83E-05
B0222.5	B0222.5	1.394989	0.000204

dct-1	C14F5.1a	1.390919	5.9E-05
C17F4.12	C17F4.12	1.38111	8.15E-05
T27F6.8	T27F6.8	1.378479	5.37E-05
R03E9.9	R03E9.9	1.373352	5.76E-05
T13C5.6	T13C5.6	1.367514	7.7E-05
nmur-4	C30F12.6	1.364827	0.000207
C18D11.6	C18D11.6	1.360989	5.2E-05
Y38E10A.22a	Y38E10A.22a	1.355473	0.000228
fbxa-59	T12B5.8	1.353416	4.28E-05
fis-2	F13B9.8a	1.347446	0.000258
C27B7.9	C27B7.9	1.331602	0.000176
cnc-11	R09B5.13	1.327842	0.00066
T13H10.5	T13H10.5	1.326947	0.000715
aip-1	F58E10.4	1.324979	0.000155
igeg-2	F48C5.1	1.323832	8.96E-05
fil-2	K12B6.3	1.321915	0.000273
Y54G2A.10b	Y54G2A.10b	1.321787	0.000772
ttr-30	T08A9.2	1.319243	0.000277
gst-7	F11G11.2	1.310905	0.000301
Y69A2AL.2	Y69A2AL.2	1.30704	0.000122
K02B9.3a	K02B9.3a	1.30203	5.23E-05
hsp-43	C14F11.5a	1.298263	0.000105
Y56A3A.33	Y56A3A.33	1.296881	9.44E-05
pqm-1	F40F8.7.2	1.291835	0.000116
C34C6.7a	C34C6.7a	1.289871	0.000167
K05C4.9	K05C4.9	1.287747	0.000106
T09F5.12a	T09F5.12a	1.285641	5.68E-05
F37C4.5a.1	F37C4.5a.1	1.284164	0.000173
C54F6.5	C54F6.5	1.283493	0.000259
Y22D7AL.15	Y22D7AL.15	1.279358	0.000225
F29G9.14	F29G9.14	1.274184	0.000384
epg-9	Y69A2AR.7a	1.27299	9.65E-05
fbxa-37	ZC47.14	1.269266	0.000268
F41B4.3	F41B4.3	1.268183	0.000134
K08B4.7	K08B4.7	1.26299	0.000283
crb-3	C35B8.4	1.262086	0.000104
Y54G2A.t2	Y54G2A.t2	1.2585	0.00046
T28B8.1.2	T28B8.1.2	1.255153	8.91E-05
C34D10.1	C34D10.1	1.250198	9.59E-05
F26F12.3a	F26F12.3a	1.247844	0.000161
K02G10.15	K02G10.15	1.244829	0.000143
F53C3.5	F53C3.5	1.244716	0.000375
F54D5.22	F54D5.22	1.24466	0.000186
T14G8.4	T14G8.4	1.239654	0.000232
C34C12.9	C34C12.9	1.235719	0.00018

F21C10.10.2	F21C10.10.2	1.222901	0.000326
gst-20	Y48E1B.10	1.220218	0.000376
C01A2.4	C01A2.4	1.219126	0.00012
B0035.7	B0035.7	1.217787	0.00024
F13C5.1.1	F13C5.1.1	1.215474	0.000184
K01F9.6	K01F9.6	1.208511	0.000124
C14B1.3	C14B1.3	1.204688	0.000755
T21F4.1a	T21F4.1a	1.20228	0.000518
M04F3.4a	M04F3.4a	1.201315	0.000185
T14G8.2	T14G8.2	1.198427	0.000224
cpi-1	K08B4.6	1.197633	0.000135
F37A8.5	F37A8.5	1.188412	0.000478
B0303.7a	B0303.7a	1.185262	0.000255
C54G10.1	C54G10.1	1.183927	0.000109
F11A6.4	F11A6.4	1.182577	0.00021
C30E1.9a	C30E1.9a	1.179719	0.00078
tli-1	F25H2.1	1.171869	0.000565
F20C5.6	F20C5.6	1.17094	0.000679
F37B12.7	F37B12.7	1.169435	0.000137
R03E9.7	R03E9.7	1.164574	0.000823
VF15C11L.2	VF15C11L.2	1.162118	0.000273
C10C5.2	C10C5.2	1.159564	0.000165
F11A5.20	F11A5.20	1.156724	0.000423
T13C2.6a	T13C2.6a	1.15538	0.000129
Y22D7AR.6.1	Y22D7AR.6.1	1.14762	0.000399
Y116A8C.465	Y116A8C.465	1.145888	0.00021
zig-4	C09C7.1	1.144237	0.000247
B0416.7a	B0416.7a	1.14149	0.000244
W02A11.5	W02A11.5	1.131273	0.000227
Y102A11A.9.1	Y102A11A.9.1	1.130092	0.000238
swt-1	K02D7.5	1.128941	0.000194
F55H2.8	F55H2.8	1.127463	0.000163
Y44A6C.1	Y44A6C.1	1.125988	0.000222
T24C4.4	T24C4.4	1.119527	0.00048
F54B11.5	F54B11.5	1.115715	0.000504
K06H6.5	K06H6.5	1.115526	0.000767
nhr-154	C13C4.2	1.115358	0.000181
F47B8.3	F47B8.3	1.113959	0.000204
F20D1.3	F20D1.3	1.113087	0.000178
ZK131.5	ZK131.5	1.111519	0.000442
efhd-1	Y48B6A.6a.2	1.108112	0.000211
F43H9.4	F43H9.4	1.107988	0.00048
C33A11.2	C33A11.2	1.107713	0.000545
F25B3.5a	F25B3.5a	1.107449	0.000304
F08F1.4a	F08F1.4a	1.100783	0.000677

K01F9.2	K01F9.2	1.099174	0.000255
C11G10.1	C11G10.1	1.095	0.000191
C06A12.18	C06A12.18	1.093128	0.000381
pho-9	Y71H2AM.16	1.091848	0.0007
pqn-44	F55A12.9a	1.088427	0.000283
dct-10	Y38H6C.5	1.083919	0.00021
rbg-1	F20D1.6	1.08307	0.000342
cyp-43A1	E03E2.1.2	1.082417	0.000346
T04H1.2.1	T04H1.2.1	1.078434	0.00023
ZK1240.1	ZK1240.1	1.07752	0.000401
F22E5.6	F22E5.6	1.076176	0.000746
T05A8.2.1	T05A8.2.1	1.076041	0.000374
ugt-14	H23N18.2	1.074593	0.000203
frm-7	C51F7.1	1.072725	0.000318
clec-144	T27D12.3	1.06116	0.000707
F20B6.4	F20B6.4	1.060374	0.000601
str-31	C54F6.10	1.057569	0.000471
ZK418.7	ZK418.7	1.054791	0.00079
ippk-1	Y17G7B.13	1.051744	0.000687
F57B10.9	F57B10.9	1.046852	0.000467
nhr-147	C03G6.8	1.038889	0.000546
tbc-1	F20D1.2	1.037831	0.000565
R02E4.3	R02E4.3	1.037697	0.000662
sod-4	F55H2.1b	1.03553	0.000662
vhp-1	F08B1.1a.2	1.035133	0.000714
C05B5.8	C05B5.8	1.032751	0.000607
sir-2.3	F46G10.3	1.019682	0.000352
ikke-1	R107.4a	1.018652	0.000537
F38B7.2b	F38B7.2b	1.008364	0.000764
F01F1.14	F01F1.14	1.005188	0.000707
atg-11	T08A9.1	1.003401	0.000357
Y73B6BL.27	Y73B6BL.27	0.995629	0.000544
T23F4.2	T23F4.2	0.98401	0.00062
R102.5a	R102.5a	0.982761	0.000661
atg-13	D2007.5.1	0.982225	0.000544
R03G5.6a	R03G5.6a	0.980183	0.000491
F46G10.2	F46G10.2	0.980181	0.000588
C52E12.8	C52E12.8	0.97447	0.000582
tag-120	F40F9.2	0.972013	0.000482
ZK154.6a	ZK154.6a	0.952502	0.000616
ceh-74	ZC376.4	0.950895	0.000624
H03A11.7	H03A11.7	0.944501	0.000693
ZC504.3	ZC504.3	0.942778	0.000633
K08D8.11	K08D8.11	0.942757	0.000788
pcm-1	C10F3.5a	0.942154	0.000573

W02A2.9	W02A2.9	0.94082	0.000676
T07E3.4a	T07E3.4a	0.940684	0.000535
Y53H1B.2	Y53H1B.2	0.935053	0.000527
C15H11.16	C15H11.16	0.92845	0.000599
T24B8.5	T24B8.5	0.925202	0.000584
H25K10.4	H25K10.4	0.924786	0.000782
hsp-17	F52E1.7b	0.920963	0.000641
F08G2.4	F08G2.4	0.896468	0.000818
mdl-1	R03E9.1	0.885023	0.000797
dhs-9	Y32H12A.3	0.884031	0.000756
skr-16	C42D4.6	0.868914	0.000863
Y52B11B.1	Y52B11B.1	-0.87028	0.000849
B0222.11	B0222.11	-0.90032	0.000775
Y106G6D.3	Y106G6D.3	-0.90112	0.000854
gln-5	F26D10.10	-0.91465	0.000612
catp-4	C01G12.8	-0.91607	0.000765
egg-6	K07A12.2	-0.92299	0.000784
clec-73	Y46C8AL.1	-0.9258	0.000587
Y51H4A.22	Y51H4A.22	-0.93569	0.000582
lys-4	F58B3.1	-0.94391	0.000575
C38D4.4	C38D4.4	-0.95639	0.000558
ZK1225.4	ZK1225.4	-0.9617	0.000598
let-355	T05E8.3	-0.96202	0.000628
egg-3	F44F4.2.1	-0.96367	0.000474
C31H1.5	C31H1.5	-0.96498	0.000453
glc-1	F11A5.10	-0.99261	0.000814
B0238.13	B0238.13	-0.9939	0.000383
gln-6	C28D4.3.1	-0.9985	0.000646
Y32F6B.1	Y32F6B.1	-1.00205	0.000326
T05G5.4	T05G5.4	-1.00425	0.0006
B0244.9	B0244.9	-1.00673	0.000329
K08C7.1	K08C7.1	-1.00732	0.000461
mboa-4	C08F8.4a	-1.01184	0.000511
rme-2	T11F8.3a.1	-1.01739	0.000327
cyb-2.2	H31G24.4.2	-1.01933	0.000863
klp-15	M01E11.6	-1.02143	0.000359
puf-3	Y45F10A.2	-1.02337	0.000756
nasp-2	C50B6.2	-1.02394	0.000323
Y24D9A.10	Y24D9A.10	-1.03553	0.00083
Y106G6H.1	Y106G6H.1	-1.03843	0.000381
cbd-1	H02I12.1	-1.04765	0.000275
C44B7.11	C44B7.11	-1.05105	0.000372
clec-91	ZK858.3	-1.05452	0.000486
Y48E1B.8	Y48E1B.8	-1.05654	0.000415
F38B6.4	F38B6.4	-1.05682	0.000721

F01D5.1	F01D5.1	-1.06306	0.000644
T28D6.3	T28D6.3	-1.06409	0.000579
elo-7	F56H11.3a	-1.06736	0.000351
Y119D3B.13	Y119D3B.13	-1.06767	0.000509
btb-21	F47C10.2	-1.08309	0.00027
nep-23	Y116A8C.4.1	-1.08576	0.000582
ugt-47	R04B5.9	-1.08895	0.000254
F35C12.3a.1	F35C12.3a.1	-1.0903	0.000864
B0252.1	B0252.1	-1.09319	0.000687
drd-1	F49E12.9a	-1.1031	0.000484
W05F2.3	W05F2.3	-1.10658	0.000295
clec-79	F47C12.4	-1.11943	0.000361
ent-4	C47A4.2a	-1.12293	0.000153
T10B10.8	T10B10.8	-1.1301	0.000865
scav-5	R07B1.3	-1.1427	0.000528
T11G6.4	T11G6.4	-1.14373	0.000131
elo-6	F41H10.8	-1.15112	0.000168
clec-227	F08H9.5	-1.1517	0.00062
ncx-7	C07A9.11	-1.1527	0.000712
F32D8.12a.1	F32D8.12a.1	-1.15346	0.000558
col-157	T11F9.9	-1.16139	0.000237
lon-3	ZK836.1	-1.17547	0.000611
Y55F3BR.13	Y55F3BR.13	-1.17623	0.000643
F55C10.4	F55C10.4	-1.20823	0.000174
T08B6.4	T08B6.4	-1.2141	0.000143
T16G12.1	T16G12.1	-1.22088	9.16E-05
ZC116.3	ZC116.3	-1.22091	0.000268
nas-27	T23F4.4	-1.22249	0.000856
F37A4.4	F37A4.4	-1.2245	0.000164
nep-22	T25B6.2	-1.23037	0.000102
clec-64	F35C5.7	-1.23164	0.000183
K01D12.9	K01D12.9	-1.23887	0.000762
cpg-2	B0280.5	-1.25204	0.000213
puf-5	F54C9.8	-1.25806	0.000119
C35A5.5	C35A5.5	-1.26958	9.76E-05
cpr-8	W07B8.1	-1.28225	0.000482
rhy-1	W07A12.7	-1.2871	0.000304
prg-2	C01G5.2a	-1.29821	0.000115
Y62H9A.15b	Y62H9A.15b	-1.30558	0.000128
ugt-22	C08F11.8.1	-1.31768	0.00032
Y69A2AR.19a	Y69A2AR.19a	-1.33081	6.14E-05
C33G3.4	C33G3.4	-1.33876	4.85E-05
C42D4.2	C42D4.2	-1.34102	5.7E-05
MTCE.34	MTCE.34	-1.34489	0.000273
Y14H12A.1	Y14H12A.1	-1.35084	0.000585

cpg-1	C07G2.1a	-1.35253	0.000162
oma-2	ZC513.6	-1.37342	8.77E-05
B0410.3	B0410.3	-1.39358	5.88E-05
F23F12.3	F23F12.3	-1.42584	0.000437
scav-4	F11C1.3	-1.44601	0.000107
ugt-16	ZC443.6	-1.46299	3.74E-05
aat-6	T11F9.4a	-1.46319	4.08E-05
C04E12.5	C04E12.5	-1.46729	2.85E-05
T01D3.6a	T01D3.6a	-1.48136	2.35E-05
F31C3.6b	F31C3.6b	-1.48287	2.34E-05
gfat-2	F22B3.4	-1.4902	0.000157
F35D2.2	F35D2.2	-1.5162	9.6E-05
C15B12.1	C15B12.1	-1.533	8.17E-05
acp-6	Y73B6BL.24	-1.61586	4.82E-05
T08B6.9	T08B6.9	-1.61859	1.17E-05
ugt-62	M88.1.1	-1.68235	5.76E-05
trx-3	M01H9.1	-1.71741	0.000611
pcp-3	F23B2.11.1	-1.89901	3.58E-06
F35D2.1	F35D2.1	-1.97103	9.33E-06
R193.2	R193.2	-2.02059	2.04E-05
asp-13	F28A12.4.1	-2.17292	1.11E-06
asp-10	C15C8.3a	-2.72394	5.63E-07

Table A.3 *hsf-1 (sy441)* vs *hsf-1 (sy441)* +HS

Gene	transcript	log_2FC	adj.P.Val
F33H12.6	F33H12.6	4.032085	1.37E-05
F44E5.5	F44E5.5	3.909668	4.52E-07
hsp-16.11	T27E4.2	3.71777	6.29E-08
cnc-11	R09B5.13	3.613719	3E-07
C25F9.2	C25F9.2	3.547835	0.000537
R03H10.6	R03H10.6	3.490097	6.47E-08
F59C12.4	F59C12.4	3.40104	4.52E-07
K10G4.3	K10G4.3	3.382785	3E-07
F08H9.3	F08H9.3	3.259272	0.000128
numr-1	F08F8.5	3.123323	9.68E-07
R11A5.3	R11A5.3	3.120566	0.000441
C25F9.12	C25F9.12	2.87523	1.95E-06
F19B10.13	F19B10.13	2.686555	1.02E-05
hsp-12.6	F38E11.2	2.642419	0.000155
Y102A5D.13	Y102A5D.13	2.609914	0.033069
Y58A7A.5	Y58A7A.5	2.571332	4.92E-05
F17C11.11a	F17C11.11a	2.522263	3.9E-05
tts-1	F09E10.11a	2.464527	6.31E-05
hsp-70	C12C8.1	2.44484	0.000161
tbb-6	T04H1.9	2.433427	3.49E-05
C49G7.10	C49G7.10	2.429236	3.54E-05
ugt-13	H23N18.1	2.408085	2.13E-05
cdr-4	K01D12.11	2.407021	6.31E-05
catp-3	C09H5.2a	2.382779	2.66E-05
B0205.13	B0205.13	2.373897	6.31E-05
F53C3.6b	F53C3.6b	2.359841	5.85E-05
C06B3.7	C06B3.7	2.357925	7.61E-05
sri-39	F33H12.2	2.351851	0.008785
M106.6	M106.6	2.323951	0.000983
fipr-22	C37A5.2	2.314491	0.000136
ZK970.7	ZK970.7	2.311717	0.000102
irg-2	C49G7.5	2.304354	0.000323
C49G7.6	C49G7.6	2.285984	9.31E-05
F44E5.4	F44E5.4	2.266206	0.000226
C16D9.1	C16D9.1	2.253713	0.002903
F31D5.6	F31D5.6	2.208233	6.86E-05
hsp-16.48	T27E4.3	2.196152	6.31E-05
tos-1	K07B1.8	2.124042	9.31E-05
C17F4.12	C17F4.12	2.096571	0.000127
ckb-2	B0285.9	2.088121	0.000128
C29F3.3	C29F3.3	2.08648	0.000298
C27B7.9	C27B7.9	2.081274	0.00631

srh-179	ZK228.7	2.062818	0.009189
asic-2	T28F4.2	2.016553	0.003469
M60.7	M60.7	2.014507	0.003442
ugt-14	H23N18.2	2.010794	0.000241
fil-2	K12B6.3	1.980458	0.020065
F48D6.4a	F48D6.4a	1.967754	0.000212
T22B7.3	T22B7.3	1.955449	0.000242
clec-221	F17C11.5	1.938208	0.003412
nlp-25	Y43F8C.1	1.903979	0.000241
C04F12.1	C04F12.1	1.899756	0.00051
mtl-1	K11G9.6	1.88966	0.000617
CD4.14	CD4.14	1.886451	0.002587
C05B5.8	C05B5.8	1.884548	0.000584
far-3	F15B9.1	1.872032	0.005344
T23E7.6	T23E7.6	1.869991	0.020353
pgp-8	T21E8.3	1.863648	0.000594
hsp-16.2	Y46H3A.3a	1.85721	0.001172
jmjd-3.3	C29F7.6	1.84325	0.000407
NA	NA	1.841969	0.020801
C52A10.1	C52A10.1	1.838323	0.000804
C17C3.24.1	C17C3.24.1	1.827056	0.003412
ttr-30	T08A9.2	1.819137	0.00071
sri-36	F33H12.5	1.812134	0.014587
C50F7.5	C50F7.5	1.786265	0.000603
hsp-12.3	F38E11.1	1.780074	0.001152
cnc-4	R09B5.9	1.775384	0.003036
F45B8.6	F45B8.6	1.769189	0.000596
C17C3.21	C17C3.21	1.763607	0.036866
C25H3.15	C25H3.15	1.750112	0.002327
gst-14	F37B1.3	1.746547	0.03406
Y58A7A.3	Y58A7A.3	1.746157	0.002467
F40F11.3a	F40F11.3a	1.739661	0.003422
sdz-28	R52.1	1.735338	0.001472
nhr-247	ZK1037.5	1.735314	0.032835
F38B7.11	F38B7.11	1.724257	0.003129
zig-4	C09C7.1	1.723583	0.001882
tli-1	F25H2.1	1.721106	0.00394
arrd-3	M176.1a	1.718226	0.033069
K10H10.5	K10H10.5	1.712801	0.000894
nspe-8	Y38E10A.29	1.69357	0.044531
F53A9.1	F53A9.1	1.689368	0.029621
C54F6.5	C54F6.5	1.684026	0.001092
F53C3.5	F53C3.5	1.681492	0.025988
K01A6.7	K01A6.7	1.675656	0.001137
linc-22	F47E1.17	1.675175	0.002637

T20D4.12	T20D4.12	1.667838	0.001353
C07A9.12	C07A9.12	1.661468	0.004339
ZC21.10.2	ZC21.10.2	1.661161	0.027673
dct-8	F56D6.10	1.654254	0.009936
gem-4	T12A7.1.1	1.639711	0.001684
CD4.5	CD4.5	1.623325	0.035356
K08B4.7	K08B4.7	1.615132	0.009189
K09D9.1	K09D9.1	1.612174	0.015743
best-5	C07A9.8	1.60058	0.002878
C06B3.6.1	C06B3.6.1	1.596554	0.00394
C54C6.7	C54C6.7	1.594692	0.004814
Y37F4.1	Y37F4.1	1.588142	0.005132
F52H3.5	F52H3.5	1.583731	0.002264
ttr-26	Y51A2D.11.1	1.581787	0.002456
spp-2	T08A9.12	1.561225	0.003639
F19H8.2	F19H8.2	1.552005	0.003667
srr-6	C13D9.1	1.551532	0.021003
C54F6.15	C54F6.15	1.547119	0.010878
rap-3	C08F8.7	1.546294	0.006506
Y43F8B.12	Y43F8B.12	1.545912	0.009936
nlp-28	B0213.3	1.506415	0.003662
igeg-2	F48C5.1	1.503874	0.003667
Y39B6A.9	Y39B6A.9	1.503112	0.004339
ZC47.13a	ZC47.13a	1.502435	0.019186
C08F11.13a.1	C08F11.13a.1	1.501774	0.004183
T28F4.5.2	T28F4.5.2	1.493865	0.003667
K02G10.15	K02G10.15	1.490088	0.012836
F57B1.9b	F57B1.9b	1.489479	0.004067
W09D6.7	W09D6.7	1.483074	0.013756
cebp-1	D1005.3	1.480047	0.005962
F26F12.3a	F26F12.3a	1.47818	0.004015
oac-14	F09B9.1	1.472849	0.004443
C49A9.9a.1	C49A9.9a.1	1.466668	0.005404
F23F1.2	F23F1.2	1.463743	0.005787
cyp-43A1	E03E2.1.2	1.448768	0.005344
Y51A2D.13a	Y51A2D.13a	1.447214	0.006699
ugt-25	C10H11.3	1.445298	0.00803
C33A12.3b	C33A12.3b	1.441888	0.005787
srw-71	F18E3.6	1.434128	0.033069
F33H12.7	F33H12.7	1.43387	0.044774
eol-1	T26F2.3.1	1.425463	0.023154
T14G8.4	T14G8.4	1.425296	0.012836
F08G2.8	F08G2.8	1.418327	0.006801
T01B4.3	T01B4.3	1.417825	0.007832
nhr-154	C13C4.2	1.413333	0.01893

Y75B8A.28	Y75B8A.28	1.405532	0.041161
F21C10.10.2	F21C10.10.2	1.404485	0.00823
ZK1290.5	ZK1290.5	1.39957	0.012704
clc-2	C01C10.1	1.382701	0.010232
skr-21	K08H2.1	1.382283	0.010351
T27F6.8	T27F6.8	1.378107	0.024771
sqst-1	T12G3.1a.1	1.376961	0.009733
C25F9.11.1	C25F9.11.1	1.367189	0.04582
C49A9.6	C49A9.6	1.364127	0.022679
T24A6.7	T24A6.7	1.361871	0.022936
Y38E10A.14	Y38E10A.14	1.356759	0.024751
K05C4.9	K05C4.9	1.355185	0.040227
ipla-2	F47A4.5	1.34792	0.044531
F53A9.7	F53A9.7	1.343523	0.024751
F22B7.9	F22B7.9	1.343412	0.012574
F26G1.2a	F26G1.2a	1.342931	0.022044
C41C4.11	C41C4.11	1.338643	0.031798
F43H9.4	F43H9.4	1.333689	0.043548
T20D4.10	T20D4.10	1.33356	0.019259
Y105C5A.12	Y105C5A.12	1.329964	0.021756
F53A2.9	F53A2.9	1.325693	0.018493
asns-2	M02D8.4a	1.324353	0.018493
B0403.3	B0403.3	1.322431	0.014084
Y75B8A.39	Y75B8A.39	1.321517	0.025181
C34C6.7a	C34C6.7a	1.320724	0.014084
F01F1.14	F01F1.14	1.320611	0.020243
F08G2.13	F08G2.13	1.308137	0.041161
ippk-1	Y17G7B.13	1.302111	0.020065
tyr-6	Y73B6BL.1	1.300428	0.022044
nex-2	T07C4.9a	1.300309	0.015143
W05H9.3.1	W05H9.3.1	1.291884	0.014979
nlp-29	B0213.4	1.288111	0.044282
F31F7.1a	F31F7.1a	1.285745	0.021032
C08E3.1	C08E3.1	1.285325	0.022936
F25A2.1	F25A2.1	1.284931	0.023053
Y43F8B.2a	Y43F8B.2a	1.252036	0.038949
gst-24	F37B1.1	1.249931	0.022475
bus-18	F55A11.5	1.241919	0.037366
R07E3.4	R07E3.4	1.241694	0.033639
nlp-34	B0213.17	1.236176	0.029713
comt-3	Y40B10A.2	1.234652	0.023587
ceh-74	ZC376.4	1.233845	0.037366
F35E12.5	F35E12.5	1.231344	0.041795
F26G1.5	F26G1.5	1.230559	0.029322
cpt-4	K11D12.4	1.229403	0.034329

F15B9.6	F15B9.6	1.227828	0.031072
swt-6	R10D12.9.2	1.221748	0.023053
C53A3.2	C53A3.2	1.220808	0.023052
F33D11.8	F33D11.8	1.207698	0.029741
dct-1	C14F5.1a	1.206977	0.025636
ZC443.1	ZC443.1	1.206084	0.041724
hsp-16.41	Y46H3A.2	1.201586	0.049264
B0238.12	B0238.12	1.194547	0.031798
sod-4	F55H2.1b	1.175528	0.033069
fipr-26	F53B6.8	1.174432	0.033069
pho-6	F52E1.8	1.17171	0.034579
nhr-147	C03G6.8	1.167642	0.048301
fbxa-37	ZC47.14	1.153722	0.033069
F25B3.5a	F25B3.5a	1.152304	0.034579
C01C10.2b	C01C10.2b	1.151499	0.045321
C17G1.5	C17G1.5	1.14939	0.039323
cpi-1	K08B4.6	1.136824	0.041161
F27D9.7	F27D9.7	1.122953	0.040387
Y106G6H.9	Y106G6H.9	1.102462	0.049151
F37C4.5a.1	F37C4.5a.1	1.102063	0.044816
ugt-53	T03D3.1	-1.14157	0.048301
F59D8.1	F59D8.1	-1.14683	0.044308
C30G12.2	C30G12.2	-1.14861	0.033069
T06A1.5	T06A1.5	-1.17997	0.033069
F01D5.1	F01D5.1	-1.18065	0.03406
nep-23	Y116A8C.4.1	-1.1901	0.027713
acox-3	F08A8.3	-1.19467	0.033069
sra-17	F28C12.1	-1.19487	0.028979
pept-1	K04E7.2.1	-1.19747	0.038845
clec-10	C03H5.1.1	-1.20032	0.036448
asp-10	C15C8.3a	-1.21086	0.041161
F07H5.9a	F07H5.9a	-1.21339	0.044352
T24E12.14	T24E12.14	-1.22858	0.023587
gcsh-1	D1025.2	-1.233	0.021032
cyp-34A2	T10H4.11	-1.23614	0.041795
F13B6.2	F13B6.2	-1.26991	0.019259
K12B6.11	K12B6.11	-1.27251	0.019259
clec-4	Y38E10A.5	-1.2765	0.022538
T08B6.9	T08B6.9	-1.28676	0.021032
C40H1.7	C40H1.7	-1.29504	0.047032
dsc-4	K02D7.4	-1.31532	0.013852
F31D5.1	F31D5.1	-1.34025	0.021032
pho-8	R13H4.3	-1.35285	0.044801
ZK1025.2	ZK1025.2	-1.36041	0.031072
C30H6.5a	C30H6.5a	-1.36401	0.018738

K01D12.9	K01D12.9	-1.45799	0.011717
nspb-7	C01G12.2	-1.48987	0.017411
str-168	Y9C9A.6	-1.49949	0.033069
ugt-62	M88.1.1	-1.51307	0.007826
Y38H6C.21	Y38H6C.21	-1.52285	0.008464
T10B9.13	T10B9.13	-1.52403	0.031798
clec-7	F10G2.3	-1.55439	0.002644
pcp-3	F23B2.11.1	-1.59227	0.002467
R193.2	R193.2	-1.62176	0.013852
C37C3.10	C37C3.10	-1.65807	0.033069
T20D4.4	T20D4.4	-1.77378	0.009189
T20D4.5	T20D4.5	-1.86962	0.009189
nas-27	T23F4.4	-1.97086	0.00021
ifc-1	F37B4.2	-2.01393	0.000503

Table A.4 N2 (wt) vs N2 (wt) HS GO term Analysis

Analysis Type:	PANTHER Overrepresentation Test (Released 20190606)						
Annotation Version and Release Date:	GO Ontology database Released 2019-02-02						
Analyzed List:	Client Text Box Input (Caenorhabditis elegans)						
Reference List:	Caenorhabditis elegans (all genes in database)						
Test Type:	FISHER						
Correction:	FDR						
GO biological process complete	**Caenorhabditis elegans - REFLIST (19921)**	**Client Text Box Input**	**expected**	**Client Text Box Input (over/under)**	**Fold Enrichment**	**raw P-value**	**FDR**
fatty acid elongation (GO:0030497)	17	7	0.83	+	8.46	7.86E-05	3.23E-02
endoplasmic reticulum unfolded protein response (GO:0030968)	57	13	2.78	+	4.68	1.74E-05	7.68E-03
cellular response to unfolded protein (GO:0034620)	70	15	3.41	+	4.4	7.70E-06	4.75E-03

response to unfolded protein (GO:0006986)	74	15	3.6	+	4.16	1.37E-05	6.52E-03
cellular response to topologically incorrect protein (GO:0035967)	81	16	3.94	+	4.06	9.52E-06	5.34E-03
response to topologically incorrect protein (GO:0035966)	91	17	4.43	+	3.84	9.66E-06	4.96E-03
innate immune response (GO:0045087)	220	37	10.71	+	3.45	9.34E-10	2.88E-06
immune response (GO:0006955)	222	37	10.81	+	3.42	1.16E-09	1.79E-06
immune system process (GO:0002376)	227	37	11.05	+	3.35	1.99E-09	2.46E-06
defense response (GO:0006952)	277	43	13.49	+	3.19	3.80E-10	2.35E-06
cellular response to chemical stimulus (GO:0070887)	365	40	17.77	+	2.25	6.98E-06	4.79E-03
response to stress (GO:0006950)	831	85	40.46	+	2.1	9.60E-10	1.97E-06
response to chemical (GO:0042221)	1000	78	48.69	+	1.6	1.01E-04	3.90E-02

response to stimulus (GO:0050896)	2693	189	131.13	+	1.44	5.05E-07	5.19E-04
biological_process (GO:0008150)	9106	521	443.39	+	1.18	1.20E-06	9.22E-04
Unclassified (UNCLASSIFIED)	10815	449	526.61	-	0.85	1.20E-06	1.05E-03

Table A.5 *pqm-1* (ko) vs *pqm-1* (ko) +HS GO term Analysis

Analysis Type:	PANTHER Overrepresentation Test (Released 20190606)						
Annotation Version and Release Date:	GO Ontology database Released 2019-02-02						
Analyzed List:	Client Text Box Input (Caenorhabditis elegans)						
Reference List:	Caenorhabditis elegans (all genes in database)						
Test Type:	FISHER						
Correction:	FDR						
GO biological process complete	Caenorhabditis elegans - REFLIST (19921)	1023	expected	over/under	fold Enrichment	raw P-value	FDR
endoplasmic reticulum unfolded protein response (GO:0030968)	57	13	2.93	+	4.44	2.96E-05	1.83E-02
response to unfolded protein (GO:0006986)	74	15	3.8	+	3.95	2.49E-05	1.70E-02
cellular response to unfolded protein (GO:0034620)	70	14	3.59	+	3.89	5.23E-05	2.93E-02
response to topologically incorrect protein (GO:0035966)	91	17	4.67	+	3.64	1.86E-05	1.43E-02

cellular response to topologically incorrect protein (GO:0035967)	81	15	4.16	+	3.61	6.20E-05	3.19E-02
innate immune response (GO:0045087)	220	33	11.3	+	2.92	2.76E-07	3.40E-04
immune response (GO:0006955)	222	33	11.4	+	2.89	3.31E-07	3.41E-04
immune system process (GO:0002376)	227	33	11.66	+	2.83	5.19E-07	4.58E-04
defense response (GO:0006952)	277	40	14.22	+	2.81	3.89E-08	8.01E-05
response to stress (GO:0006950)	831	82	42.67	+	1.92	9.98E-08	1.54E-04
biological_process (GO:0008150)	9106	573	467.62	+	1.23	1.39E-10	4.30E-07
cellular process (GO:0009987)	6798	411	349.1	+	1.18	8.93E-05	4.24E-02
Unclassified (UNCLASSIFIED)	10815	450	555.38	-	0.81	1.39E-10	8.60E-07

Table A.6 *hsf-1 (sy441)* vs *hsf-1 (sy441)* +HS GO term Analysis

Analysis Type:	PANTHER Overrepresentation Test (Released 20190606)						
Annotation Version and Release Date:	GO Ontology database Released 2019-02-02						
Analyzed List:	Client Text Box Input (Caenorhabditis elegans)						
Reference List:	Caenorhabditis elegans (all genes in database)						
Test Type:	FISHER						
Correction:	FDR						
GO biological process complete	Caenorhabditis elegans - REFLIST (19921)	Client Text Box Input (745)	expected	over/under	Fold Enrichment	raw P-value	FDR
exogenous drug catabolic process (GO:0042738)	40	9	1.5	+	6.02	5.52E-05	1.79E-02
xenobiotic metabolic process (GO:0006805)	42	9	1.57	+	5.73	7.66E-05	2.36E-02
cellular response to xenobiotic stimulus (GO:0071466)	42	9	1.57	+	5.73	7.66E-05	2.25E-02
response to xenobiotic stimulus (GO:0009410)	43	9	1.61	+	5.6	8.97E-05	2.52E-02

innate immune response (GO:0045087)	220	26	8.23	+	3.16	1.01E-06	7.76E-04
detection of chemical stimulus involved in sensory perception of smell (GO:0050911)	271	32	10.13	+	3.16	5.91E-08	3.65E-04
immune response (GO:0006955)	222	26	8.3	+	3.13	1.17E-06	8.05E-04
detection of chemical stimulus involved in sensory perception (GO:0050907)	274	32	10.25	+	3.12	7.44E-08	2.29E-04
immune system process (GO:0002376)	227	26	8.49	+	3.06	1.71E-06	9.60E-04
sensory perception of smell (GO:0007608)	280	32	10.47	+	306	1.17E-07	2.40E-04
detection of chemical stimulus (GO:0009593)	281	32	10.51	+	3.05	1.26E-07	1.94E-04
defense response (GO:0006952)	277	31	10.36	+	2.99	2.79E-07	2.87E-04
detection of stimulus involved in sensory perception (GO:0050906)	289	32	10.81	+	2.96	2.24E-07	2.76E-04
olfactory behavior (GO:0042048)	192	21	7.18	+	2.92	3.11E-05	1.07E-02

chemosensory behavior (GO:0007635)	226	24	8.45	+	2.84	1.36E-05	5.23E-03
detection of stimulus (GO:0051606)	319	32	11.93	+	2.68	1.62E-06	9.97E-04
sensory perception of chemical stimulus (GO:0007606)	465	39	17.39	+	2.24	8.46E-06	3.73E-03
sensory perception (GO:0007600)	487	39	18.21	+	2.14	2.36E-05	8.55E-03
G protein-coupled receptor signaling pathway (GO:0007186)	787	59	29.43	+	2	1.74E-06	8.93E-04
response to stress (GO:0006950)	831	58	31.08	+	1.87	1.26E-05	5.20E-03
response to chemical (GO:0042221)	1000	68	37.4	+	1.82	6.28E-06	2.98E-03
response to stimulus (GO:0050896)	2693	152	100.71	+	1.51	4.12E-07	3.63E-04
biological_process (GO:0008150)	9106	395	340.54	+	1.16	9.66E-05	2.48E-02
Unclassified (UNCLASSIFIED)	10815	350	404.46	-	0.87	9.66E-05	2.59E-02

Table A.7 Genes differentially regulated both in wt +HS; wt -HS and *pqm-1* +HS; *pqm-1 -HS*

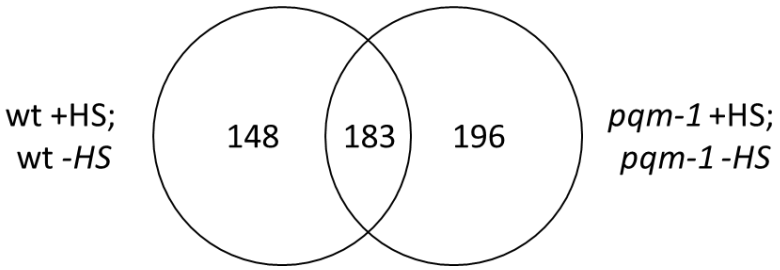

Transcript	Gene
F33H12.6	*F33H12.6*
R11A5.3	*R11A5.3*
F44E5.5	*F44E5.5*
C12C8.1	*hsp-70*
C25F9.2	*C25F9.2*
F38E11.2	*hsp-12.6*
T27E4.2	*hsp-16.11*
Y46H3A.2	*hsp-16.41*
Y46H3A.3a	*hsp-16.2*
ZC21.10.2	*ZC21.10.2*
K10G4.3	*K10G4.3*
F44E5.4	*F44E5.4*
T27E4.3	*hsp-16.48*
F59C12.4	*F59C12.4*
F33H12.2	*sri-39*
R03H10.6	*R03H10.6*
Y15E3A.5.2	*Y15E3A.5.2*
C13D9.1	*srr-6*
F31D5.6	*F31D5.6*
Y45F10B.16	*smy-9*
C06B3.7	*C06B3.7*
Y102A5D.13	*Y102A5D.13*
F09E10.11a	*tts-1*
F08H9.3	*F08H9.3*
M106.6	*M106.6*
F17C11.11a	*F17C11.11a*

C44B12.3	*C44B12.3*
F53A9.1	*F53A9.1*
F19B10.13	*F19B10.13*
F26D10.12a	*clec-196*
M60.7	*M60.7*
C50F7.5	*C50F7.5*
C49G7.6	*C49G7.6*
C49G7.5	*irg-2*
F57A8.3a	*str-118*
C25F9.12	*C25F9.12*
Y17G7B.14	*arrd-8*
F33H12.5	*sri-36*
ZK1037.5	*nhr-247*
C06B3.6.1	*C06B3.6.1*
Y17D7C.2	*Y17D7C.2*
C33A12.19a	*C33A12.19a*
ZK355.8	*ZK355.8*
T23C6.3	*cnp-3*
D2013.9.1	*ttll-12*
Y46H3A.5	*Y46H3A.5*
C50F4.6	*C50F4.6*
C04F12.1	*C04F12.1*
Y47H10A.5	*Y47H10A.5*
Y54F10BM.7	*fbxa-48*
D1005.3	*cebp-1*
C49G7.10	*C49G7.10*
W01D2.7	*W01D2.7*
Y43F8B.2a	*Y43F8B.2a*
T25D10.1	*T25D10.1*
Y69H2.8	*nhr-241*
T28F4.2	*asic-2*
F47A4.5	*ipla-2*
R09E10.13	*R09E10.13*

K07B1.8	*tos-1*
W08F4.9	*fbxb-14*
Y38H6C.8	*Y38H6C.8*
T12G3.1a.1	*sqst-1*
F28H1.1	*F28H1.1*
K01D12.11	*cdr-4*
Y97E10B.4	*srsx-7*
Y58A7A.3	*Y58A7A.3*
W09D6.8	*W09D6.8*
Y6G8.5b	*Y6G8.5b*
F09B9.1	*oac-14*
Y94H6A.10	*Y94H6A.10*
ZK1290.5	*ZK1290.5*
F53B2.8	*F53B2.8*
Y75B8A.28	*Y75B8A.28*
F53A9.7	*F53A9.7*
F53C3.6b	*F53C3.6b*
F08F8.5	*numr-1*
H14N18.1a	*unc-23*
R11F4.1.2	*R11F4.1.2*
C08F11.13a.1	*C08F11.13a.1*
F43E2.8a.1	*hsp-4*
F45B8.6	*F45B8.6*
F08H9.4a	*F08H9.4a*
F45D3.4a.1	*F45D3.4a.1*
F16B12.4	*F16B12.4*
Y58A7A.5	*Y58A7A.5*
B0205.13	*B0205.13*
F15B9.6	*F15B9.6*
T12A7.1.1	*gem-4*
T28D6.10	*T28D6.10*
K09A9.1	*nipi-3*
F08G2.5	*F08G2.5*

F46C3.1	*pek-1*
T28F4.5.2	*T28F4.5.2*
B0285.9	*ckb-2*
C02F5.8	*tsp-1*
C49A9.9a.1	*C49A9.9a.1*
F19B2.5.1	*F19B2.5.1*
F22B7.9	*F22B7.9*
K09D9.1	*K09D9.1*
F52H3.5	*F52H3.5*
Y39A3CL.5a	*clp-4*
R09B5.9	*cnc-4*
Y58A7A.7	*Y58A7A.7*
F55C12.7.1	*tag-234*
T07C4.9a	*nex-2*
R07B1.4	*gst-36*
F47E1.17	*linc-22*
F44F4.4	*ptr-8*
F18H3.4	*F18H3.4*
T23F11.6	*T23F11.6*
Y51A2D.13a	*Y51A2D.13a*
B0218.2	*faah-2*
C17F4.12	*C17F4.12*
T27F6.8	*T27F6.8*
R03E9.9	*R03E9.9*
T13C5.6	*T13C5.6*
C30F12.6	*nmur-4*
C18D11.6	*C18D11.6*
Y38E10A.22a	*Y38E10A.22a*
T12B5.8	*fbxa-59*
F13B9.8a	*fis-2*
C27B7.9	*C27B7.9*
R09B5.13	*cnc-11*
F48C5.1	*igeg-2*

T08A9.2	*ttr-30*
F11G11.2	*gst-7*
C34C6.7a	*C34C6.7a*
T09F5.12a	*T09F5.12a*
F37C4.5a.1	*F37C4.5a.1*
C54F6.5	*C54F6.5*
Y22D7AL.15	*Y22D7AL.15*
Y69A2AR.7a	*epg-9*
ZC47.14	*fbxa-37*
F41B4.3	*F41B4.3*
K08B4.7	*K08B4.7*
C34D10.1	*C34D10.1*
K02G10.15	*K02G10.15*
T14G8.4	*T14G8.4*
C34C12.9	*C34C12.9*
F21C10.10.2	*F21C10.10.2*
Y48E1B.10	*gst-20*
C01A2.4	*C01A2.4*
M04F3.4a	*M04F3.4a*
F25H2.1	*tli-1*
T13C2.6a	*T13C2.6a*
Y102A11A.9.1	*Y102A11A.9.1*
Y44A6C.1	*Y44A6C.1*
C13C4.2	*nhr-154*
F20D1.3	*F20D1.3*
Y48B6A.6a.2	*efhd-1*
F25B3.5a	*F25B3.5a*
K01F9.2	*K01F9.2*
E03E2.1.2	*cyp-43A1*
F20B6.4	*F20B6.4*
Y17G7B.13	*ippk-1*
F57B10.9	*F57B10.9*
R02E4.3	*R02E4.3*

C05B5.8	*C05B5.8*
F01F1.14	*F01F1.14*
T08A9.1	*atg-11*
Y73B6BL.27	*Y73B6BL.27*
T24B8.5	*T24B8.5*
F08G2.4	*F08G2.4*
F49E12.9a	*drd-1*
F41H10.8	*elo-6*
Y55F3BR.13	*Y55F3BR.13*
ZC116.3	*ZC116.3*
T23F4.4	*nas-27*
W07A12.7	*rhy-1*
C08F11.8.1	*ugt-22*
MTCE.34	*MTCE.34*
F23F12.3	*F23F12.3*
F11C1.3	*scav-4*
T11F9.4a	*aat-6*
Y73B6BL.24	*acp-6*
T08B6.9	*T08B6.9*
M88.1.1	*ugt-62*
M01H9.1	*trx-3*
F23B2.11.1	*pcp-3*
F35D2.1	*F35D2.1*
R193.2	*R193.2*
C15C8.3a	*asp-10*

Table A.8 Genes upregulated in wt and *pqm-1* (ko) ± HS

Upregulated genes

Adj. p value <0.05

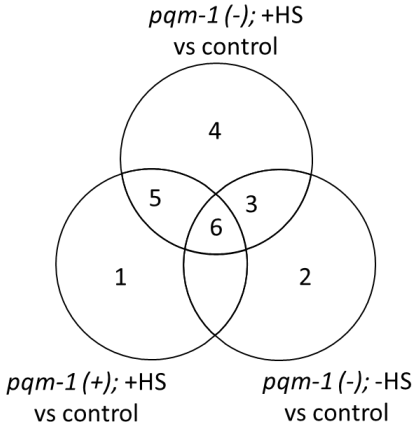

1	2	3	4	5	6
F53B6.8	F35D2.1	R57.2	F07G6.6	F33H12.6	T04H1.9
F55B12.10	F55C10.4	Y37A1B.7	M176.1a	F33H12.6	F59C6.15
ZK970.7	Y48E1B.8	T21D12.2a	F33H12.7	R11A5.3	C30B5.6b
C27B7.9	C04E12.5	T14B4.6	C33D3.3	T27E4.2	R09A1.3
C09H5.2a	F35D2.2	C27C7.3	R05H11.2.1	F33H12.6	F55A11.5
F23F1.2	ZK836.1	R05H10.6	F17E9.10	T27E4.2	Y47H9C.5a
T10E10.4	F35C12.3a.1	T14B4.7a	Y46H3A.1b	F44E5.5	F28C6.5
F48D6.4a	F31C3.6b	Y102A11A.5	C09C7.1	C12C8.1	F44E2.4
K01A6.7	C35A5.5	Y64H9A.2	F48G7.13	F33H12.6	
Y43F8C.1	F01G10.6	ZC328.1	B0035.7	F33H12.6	
ZC168.2	VZK822L.2	C14A4.9	F43H9.4	F33H12.6	
F01F1.14	T23F6.5	C29E6.1a.2	C14F5.2	F33H12.6	
F12A10.1	W09G12.10	W04G3.3	ZK1240.8	T27E4.3	
Y82E9BL.17	F35C5.7	ZK783.1a	F13G3.2	T27E4.3	
C28G1.1	C04F1.1	B0365.9	K02B9.3a	F38E11.2	
C37A5.2	T01B7.7	Y73E7A.8	F10B5.3	C25F9.2	
C52A10.1	C50F2.6a.1	C15F1.2	T19B4.8	Y46H3A.3a	
Y58A7A.4	C38C6.3	Y71D11A.1	C09F5.1	F09E10.11a	
F27D9.7	C34H3.1	C09F9.2	K11C4.6	K10G4.3	
Y73B6BL.1	F37A4.3	F30A10.2	ZK265.10	Y46H3A.2	
T01B7.8	K09B11.10	Y43D4A.5a	D1046.6	F59C12.4	
C07A9.8	C52D10.1	F55F8.1.2	Y56A3A.33	K11G9.6	
F47B10.9	Y38A10A.2	ZK1025.9	C26D10.5a	F08F8.5	
F09F7.6	JC8.16	K08B12.1	C27C12.2	Y17D7C.2	
B0511.5	F08G5.5a	Y46G5A.29	F52E1.7b	F19B10.13	
Y37H2A.12a	ZC513.1	W09C2.7	F41C3.2	R09B5.13	
F25G6.1	F42G9.2	T03G6.1	C37E2.2b	R03H10.6	
B0213.17	T28A11.6	B0205.4	T10E10.5	F08H9.4a	
T27A1.2	ZC373.6	W04G3.1a	F54B11.5	F26D10.12a	
K03A1.4a	Y39G10AR.29	Y105E8A.13a	F54D8.1	F33H12.2	
C29F3.3	F41E6.14	W04G3.2	T23E7.6	R09E10.13	

C16D9.1	F36H2.3a	M03B6.3	C03G6.8	D2013.9.1	
C55C3.1	F56C11.2a	F46C8.6	C17D12.8	T12A7.1.1	
F02E9.2a	F44B9.1a	U61235	ZK546.18	C25F9.12	
T28F4.4		C01F1.5	C34F6.10	ZC21.10.2	
F28H7.8		C17G1.6a	D2013.8a	F44E5.4	
F44F4.4		W01F3.3a	C54G10.1	K07B1.8	
T24B8.5		H04M03.4	F37A8.5	F47A4.5	
F21D9.8		R09B5.8	F53A9.2	F31D5.6	
E01G6.1		Y75B8A.20	C44C8.6.1	C54F6.5	
F56C3.9		H19M22.3a	F47B8.3	C49G7.6	
Y38C1AA.6		F19H8.4	C54F6.10	Y94H6A.10	
W06B11.9		T26C5.2	F25H5.9	M106.6	
F33D11.8		Y39A1A.9	Y75B8A.39	H23N18.1	
C44H9.5		F49D11.6	H23N18.2	C17F4.12	
F08C6.5		R10H1.4	C09B8.3	F15B9.6	
F42C5.7		T13F2.4	F18E9.5b	C54F6.15	
Y55F3BR.13		Y38H8A.1	M88.6b	Y45F10B.16	
C05D10.3		Y38H6C.16	F55C9.3.1	F57A8.3a	
C34D10.2a.1		C44H4.2	Y32H12A.3	K01D12.11	
F19C6.2a		F49C5.12	Y69A2AL.2	C08F11.13a.1	
ZK54.2a.1		C44H4.10	K12G11.3	ZC47.13a	
F26G1.5		K02E10.4a	F11A6.1a.1	T22B7.3	
		R07E3.6	Y49A3A.4	C50F7.5	
		C01F1.3a	F20C5.6	F53A9.1	
		H03E18.1	C14F5.1a	T25D10.1	
		C45G7.5	F25A2.1	C44B12.3	
		F08A8.2	F08B12.4a	F08H9.3	
		F31B9.4	F53E10.1	T28F4.2	
		F17A9.3	R12E2.17	Y51A2D.12	
		T05C1.3	K11E4.4b	C18D11.6	
		F22F4.1	T27D12.3	Y51A2D.13a	
		ZK1290.8	F45D3.2a	F08G2.5	
		F59E12.12	M03A1.8	R09B5.9	
		F32E10.3a	ZK131.5	C13D9.1	
		F20G2.3a	F32A5.4a.2	T12G3.1a.1	
		C44H4.3	K09A9.2.1	C49G7.5	
		F32A11.7	F20D1.6	M60.7	
		F32D1.11	F33E2.2a	F09B9.1	
		ZC449.6	Y41G9A.5a	T21E8.3	
		T06G6.6b	C12D12.5	W09D6.7	
		Y80D3A.5	C04F6.5	F25H2.1	
		C30G12.4	F40F9.2	Y102A5D.13	
		F15H10.8	C38C6.8	Y102A5D.13	
		F35G2.5a	C14B1.3	Y102A5D.13	

		F18C5.5	T03D8.4a	Y102A5D.13	
		C14F11.6.1	F47F2.3	Y102A5D.13	
		T19C4.1	R09H10.7	Y102A5D.13	
		C32E12.3	T23F4.2	Y102A5D.13	
		F01G10.9	F08F1.8	Y102A5D.13	
		F11E6.9	F25H9.4	Y102A5D.13	
		F09F9.2	F53H4.5	Y102A5D.13	
		Y55F3AM.14	C13G3.1	Y102A5D.13	
		T20F5.4	C54E4.5	Y102A5D.13	
		F52B11.3	M01A8.1a	B0403.3	
		C11H1.5	K05C4.9	F43E2.8a.1	
		C26B9.7	H06O01.3a	B0205.13	
		C32D5.12	T24E12.5	C05B5.8	
		F08F1.6	C50F4.5	C13C4.2	
		F53F4.15	K08H2.1	Y47H10A.5	
		F19H8.2	T24C4.4	F53C3.6b	
		W03D8.11	H09I01.2	C54C6.7	
		F14F3.4	Y53H1B.2	Y43F8B.2a	
		K01A2.11d	Y41D4B.17	D1005.3	
		T08G2.2	C37E2.2a	C06B3.7	
		F52E4.6	R07B1.7	C49A9.6	
		T26E4.4	K01F9.6	Y75B8A.28	
		Y57E12B.3	W03C9.9	C25H3.15	
		F16F9.2	C05D12.7	B0285.9	
		M03A1.7.2	T14D7.2	C49A9.8.1	
		W04G3.8	C42D4.6	F22B7.9	
		F41A4.1	M03D4.4a	T27F6.8	
		T14F9.4a	C16D9.10	F47E1.17	
		B0393.5	C35B8.4	F11G11.2	
		C09G5.3	Y43F8B.12	Y22D7AL.15	
		C48D5.3	H40L08.2a	C41C4.11	
		F27D9.6	VF15C11L.2	T14G8.4	
		F23H12.5	F53C3.5	Y97E10B.4	
		F13G3.1	F55H2.1b	T23F11.6	
		K09C4.5	F40F11.3a	R02E4.3	
		T17H7.1.1	C10F3.5a	F16B12.4	
		ZK1025.4a	F30H5.3	Y54F10BM.11	
		F09B12.1a	F45H7.11	C08E3.6	
		T05C12.10	Y75B12B.12	F17C11.11a	
		C34G6.6a	E01G4.6	K01F9.2	
		ZC373.7	C01G10.5	C33A12.19a	
		C31H2.2	F26D12.1a	C07A9.12	
		Y50D7A.12	B0496.7	Y51A2D.11.1	
		R07G3.6	M02A10.3a	T07C4.9a	

		ZK1025.6	R07E3.4	Y17G7B.14	
		ZC434.10	C02F5.7a.2	T12B5.8	
		R08B4.1a.1	K08B4.6	W01D2.7	
		Y41G9A.2	Y38H6C.5	F13B9.8a	
		ZK1025.7	ZK377.1	K02G10.15	
		F13B9.2	Y17G7B.23a	Y54F10BM.7	
		ZK1025.10	ZC443.4	F45B8.6	
		Y17D7B.10	K02D7.5	F46C3.1	
		Y47D3B.1	F59C6.18	C30F12.6	
		C35A5.11a	R13G10.1	W09D6.8	
		Y11D7A.5	T02G6.12	C34D10.1	
		R07B1.6	C06E1.8	Y58A7A.5	
		Y54F10AM.6	F22E12.13	R07B1.4	
		Y48G8AR.1a	CD4.14	T28D6.10	
		F19C7.7	B0303.7a	T23F2.4	
		F46F3.3a	F35B12.3	C02F5.8	
		F53B3.5	K06H6.5	Y82E9BL.18	
		Y37D8A.3	F56D1.5	ZK1037.5	
		R03H10.2	F11A6.4	F45D3.4a.1	
		C26F1.5	ZC334.10	C49G7.10	
		Y53C12B.5a	R12E2.16	F53B2.8	
		K08F8.2	T14G8.2	F19B2.5.1	
		Y47D7A.5	F47B8.2	C01F6.5	
		F13G3.3a	F08B1.1a.2	Y66A7A.6.2	
		D1086.3	K08E5.3a	C10H11.3	
		ZK1025.3.1	Y18D10A.7a	K08B4.7	
		ZK678.8	T03F7.8	ZC443.3	
		C34F6.1	W06B11.1	Y38E10A.14	
		K08E7.5a	Y39C12A.1	C08F8.7	
		T12E12.6	R03E9.7	Y6G8.5b	
		F53B3.6	M03D4.77	B0272.2	
		T09F5.1	C02B8.4	K02C4.8	
		C27C7.8	Y22F5A.6	C49A9.9a.1	
		Y65B4BR.2a	T05B11.1	C50F4.6	
		F59B10.5	T06A4.1a	Y38E10A.22a	
		C02F5.14	R01H10.4	T13C5.6	
		F58H1.2	ZK1055.6a	M04F3.4a	
		F56D6.2	ZK355.3	R10D12.9.2	
		ZC15.7	F58E10.4	Y48B6A.6a.2	
		F58A4.11	M163.13	K09D9.1	
		C17F4.2	Y80D3A.7a	T08A9.2	
		Y43F4A.1a	F36A2.3	C04F12.1	
		F25D1.3	F58D5.5	Y48E1B.10	
		F35G2.4	C34G6.11	Y71F9AM.7	

		Y39H10A.4	K12B6.3	F41B4.3	
		F26D11.2	C42D8.19	Y44A6C.1	
		B0395.2	W05H7.1	R11F4.1.2	
		F09C8.1	Y45F10A.3a	C34C6.7a	
		F53B1.6	F52E4.8	R05D11.1	
		F49C5.11a	F54D5.22	F55C12.7.1	
		H41C03.1	C09E8.3	F21C10.10.2	
		Y65B4BL.1a	ZK1067.6	F52H3.5	
		Y68A4A.13	F22H10.2	C01B7.4	
		D1005.2	C30E1.9a	F37C4.5a.1	
		C13C12.2	F45D3.3	Y15E3A.5.2	
		F59B10.1	T20D4.12	B0218.2	
		ZC13.3	F38E11.14	F28H1.1	
		T27A10.6.1	K07C5.11	ZC47.13a	
		F33H2.8a	C26E6.2	F48F7.2.2	
		C53B4.8	T01B6.1	T28F4.5.2	
		ZC449.2	B0304.3	W03F9.1	
		R166.1	H32C10.2a	Y38H6C.8	
		ZC250.3	C45G9.7	R03E9.9	
		ZK1025.2	Y55F3BR.2a	F53A9.7	
		ZK1025.2	K11D12.3a	ZC47.5	
		ZC123.1	C30F8.3	C06B3.6.1	
		C05G5.7	F57H12.6	E03E2.1.2	
		R07B1.13	W09C5.5	Y58A7A.3	
		C17B7.5	R09B5.11	K09A9.1	
		C26B9.2	M05D6.4	F33H12.5	
		F46G11.6	Y75B7AR.1	F01D5.6	
		K10D3.4	T01B7.13	F18H3.4	
		F13B6.1	F13D11.4.1	Y39A3CL.5a	
		C02G6.3	T08A9.12	C37H5.2	
		K02H11.4	R10D12.1	C10C6.8	
		Y71G12B.6a	Y38E10A.15	ZK1290.5	
		F18F11.4	B0457.6	F08G2.4	
		C34C12.6	C04G6.12	F09C6.1	
		T22B3.1	C42D8.5a	ZK637.14	
		F25E5.2	F16H6.10	Y69H2.8	
		B0348.5	ZK1290.3a	Y46H3A.5	
		D1014.5	F43D9.1	T09F5.12a	
		C35A11.2	F55C9.5	T23C6.3	
		T03D8.6a	ZC581.1	C04F12.3	
		Y55D5A.1a	F47H4.8	F25B3.5a	
		C06A6.5	F47B10.7	Y54G9A.12	
		C05C9.1	R07G3.8	W08F4.9	
		B0491.2.1	C33D9.13	F27E5.4	

		C52D10.3	T08B1.4a	C01A2.4	
		F01E11.1	CC8.2a	F44A6.5	
		C11H1.9a	T25G12.4	C16C10.10	
		JC8.12a	C33A11.2	H14N18.1a	
		C29E4.15	ZK381.2	K06H7.2	
		F56H1.1	Y55F3BR.11	Y45F10B.8	
		T23F4.3	F58E6.13a	R07B1.5	
		C28C12.4	F02D8.2	F44G3.6.2	
		F15E6.2a	R07E3.3a	T08A9.1	
		F11E6.4a	F47D12.6	F41E6.12	
		ZK154.1	C18B2.4	Y94H6A.6	
		F46B3.5	T21B6.5	F57B10.9	
		H42K12.3.1	Y38F2AR.14	ZC47.14	
		F19H6.1.1	F16B4.8	C34C12.9	
		R05G6.9	F17C11.5	Y54G2A.52	
		C45B2.7	C37F5.1a	F53A2.9	
		ZK669.2	T10B10.1	Y40B10A.2	
		Y81G3A.4a	ZC101.1	ZK355.8	
		H14E04.1	F31F6.5	T13C2.6a	
		C24H10.3	C05E11.7	F18C5.10.1	
		T10B5.10	W01A11.5	C33A12.3b	
		F33D4.6b	F44A2.13	F48C5.1	
		T13C5.7	F28D1.21	Y69A2AR.7a	
		F57F4.3	Y97E10B.3	F20D1.3	
		Y22D7AL.9	F37B12.7	Y73B6BL.27	
		F56D2.3	Y73B6BL.44	R107.5a	
		F54B11.10	C11G10.9	Y102A11A.9.1	
		Y11D7A.9	T09F3.1	F20B6.4	
		C02F4.4	F53C3.12	Y17G7B.13	
		ZC101.3	Y73B6BR.1a	Y58A7A.7	
		C40H1.4	F38B6.5a	Y58A7A.7	
		F49H12.5	F52G3.5	M60.4a	
		Y54G2A.45a	F13C5.1.1		
		F46F11.7	T24C2.5		
		T23F2.1.2	C10F3.2		
		T19B10.5	Y53F4B.45		
		Y110A2AL.8a	T04G9.2		
		Y57A10A.23	C06C6.4		
		T19H12.1a	K01A2.10		
		T02E9.2a	F58G1.5		
		F27C8.2	T19B10.9		
		F57F5.3	F11A6.2		
		C09G5.6	ZK856.7.2		
		F49E10.2a	F53H2.3b		

		T27C4.2	ZK1010.10		
		F12F6.9	ZC482.6		
		Y18H1A.13	Y38F1A.2		
		T22F7.3	Y71D11A.3a		
		W03D2.9	Y74E4A.1a		
		Y43F4A.1a	Y15E3A.1a.1		
		M79.2	F14H12.4a		
			F28H6.1a		
			K10H10.3a		
			C51F7.3		
			Y43F8C.22		
			Y43F8B.22		
			R06C1.6		
			T24C4.3		
			Y60A3A.23		
			R06B9.5		
			W02B8.3		
			F57B10.11		
			R148.5a		
			T04G9.4		
			F42G8.4a.1		
			F08G2.13		
			C03C11.2		
			Y116A8C.465		
			Y105C5A.12		
			C28G1.2		
			Y39A1B.2a		
			Y54E10BL.2		
			K07C5.10		
			C32H11.10		
			K01A2.5		
			F46G11.2		
			Y39B6A.6		
			C07A12.7a.1		
			C30G4.4a		
			F34H10.3.1		
			ZK813.4a		
			C31C9.2		
			C01B12.2		
			K07F5.16a		
			F17H10.3a		
			T20B5.3a		
			C27H5.2a		
			T10H10.2		

			F09E8.6		
			C34D10.4		
			Y17G7B.17.1		
			F55D10.3		
			C02C2.1		
			F31F6.8		
			C15H11.16		
			C14C10.3c		
			W02F12.8		
			K06A4.1		
			F29C6.1a		
			K07D4.8		
			T24H7.6		
			C35C5.4		
			Y54G2A.t2		
			Y75B12A.2		
			F23H12.12		
			C04G2.7		
			R03E9.1		
			F29D11.1		
			F07H5.13		
			Y110A7A.21		
			F41E6.6.1		
			C28C12.5		
			T28B4.4.1		
			F22D6.16		
			C48D5.1a		
			F42A10.4a		
			K06A1.3		
			C39E9.3		
			F55A12.9a		
			Y67A10A.14		
			F59B10.6		
			F31F7.1a		
			R09A8.5		
			T27E4.1		
			F21E9.2		
			F53B3.2		
			C53C11.5		
			Y41C4A.8		
			R31.1a		
			W02A11.5		
			K11D12.4		
			C44C8.2		

			Y71G12B.16		
			F13H10.6a		
			F59F5.7		
			ZK1055.7		
			C44F1.3		
			C43H6.4		
			W08A12.2		
			C01B12.1		
			F55G11.5a		
			E04F6.9		
			K07C5.12		
			F46H6.5		
			Y71G12B.18a		
			T05E11.9		
			Y48C3A.4		
			F32E10.10		
			E01G4.5		
			T28F2.2		
			C30C11.4.1		
			F53C3.4		
			Y54G2A.4		
			H21P03.1		
			F15B9.1		
			T05A7.2		
			Y38F1A.3		
			F10G2.9		
			T07F10.9		
			F26A10.2		
			W02A2.9		
			F11A10.9		
			Y23H5B.10		
			T07C12.9		
			T19B10.1		
			F29G9.14		
			Y53F4B.47		
			C36E8.3		
			T27D12.4a		
			D1069.2.2		
			Y47G6A.32		
			F16B4.2a.1		
			C24A11.2		
			C34D1.5b		
			M163.3		
			F54C9.12		

			T20D4.10		
			C44B7.4		
			W01D2.8		
			Y116A8C.465		
			T02E1.9		
			C24A1.2b.1		
			F01F1.6.2		
			C47D2.2		
			F20D1.2		
			Y22D7AR.6.1		
			F19H8.6		
			D1054.9a		
			Y59A8B.20		
			R151.5a		
			F35D2.3		
			F25H9.5a.2		
			F59F4.3		
			C25F6.2a		
			K09E9.4		
			C45B2.2		
			ZK418.7		
			F21G4.5		
			ZK836.3		
			F47G4.9		
			K10G6.2		
			F13H8.4		
			C33D9.6a		
			F25D7.3a		
			F22E5.6		
			T04A8.17		
			C04A11.4		
			R06B9.4		
			F17C11.15		
			T23H2.4		
			C15C8.2a		
			Y53F4B.27a		
			F14B8.2		
			F55A11.10		
			C50F4.13		
			K09E9.3		
			C34B2.1a		

Table A.9 Genes downregulated in wt and *pqm-1* (ko) ± HS

Downregulated genes

Adj. p value <0.05

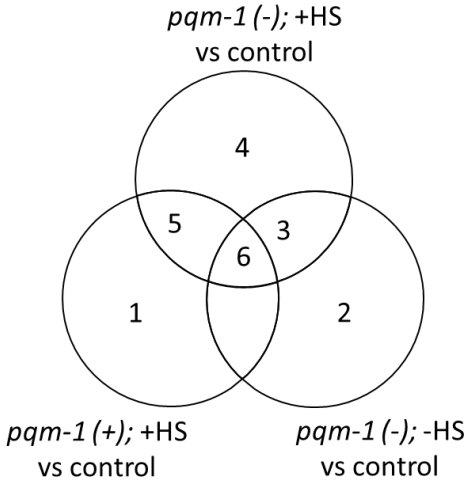

1	2	3	4	5	6
K12B6.11	C24F3.6.1	D1054.11	F54C9.8	R193.2	Y52E8A.4
F21C10.9.1	ZK354.5	C04F6.1	ZC513.6	F37B4.2	
T20D4.3	F42C5.7	F11G11.11	F28A12.4.1	T20D4.5	
T08E11.3	K08F9.3c	ZK813.7.1	C07G2.1a	T10B9.13	
F10G2.3	F35A5.3	Y37D8A.19	F22B3.4	F23B2.11.1	
C33D3.1	K10C2.7	ZC373.2	B0280.5	M01H9.1	
F49E12.9a	H01G02.1a	C45B2.1	B0410.3	Y71A12B.18	
C47G2.16	T13H10.5	ZK1193.1	C01G12.6	C15C8.3a	
T24E12.14	C27B7.9	F17E9.4	W05F2.3	T08B6.9	
MTCE.34	B0034.1	C08A9.10	F48G7.5	C08F11.8.1	
C06C6.2	K04C2.5	F41F3.4	Y45F10A.2	W07A12.7	
F01D5.2	C09G5.4	C34F6.3	C01G8.1a	F41H10.8	
F38A1.10	F39D8.1a	D1054.10	T18H9.1	T23F4.4	
F23F12.3	F56B6.6	K07A1.6	H31G24.4.2	F56H11.9	
C40H1.7		C34F6.2	ZK858.3	ZC116.3	
F49E12.9a		K10C2.8	R06C7.4.1	M88.1.1	
F35D2.1		F26F12.1a	W02D9.7	T11F9.4a	
R08E5.1.1		F59D8.2	F52E1.1	Y73B6BL.24	
T05B4.12		M18.1a	C05C10.5a	W07A12.6	
K04E7.2.1		F59D8.1	C28D4.3.1	F11C1.3	
Y102A11A.1		C54D10.10	C50B6.2	ZC416.6a	
F08A8.4.2		C09G5.5	T25E12.5	C37C3.10	
K06C4.10		F57A8.8	C17E4.3	F40F4.8	
Y45G5AM.1a.1		W03G11.1a	F26D10.10	K01D12.8	
W01A11.16		F07G6.10	Y46E12BL.3	C07H6.10	
D1025.2		Y77E11A.15	W06D11.3		
F41B5.4		Y51H4A.9	B0244.8		
		C15A11.6	Y51F10.2a		
		T11F9.3	C04B4.2		

		D1086.6	T01C3.3		
		F38A3.1	T05F1.2		
		F15A2.1a	F54C1.1		
		F55B11.2.1	Y116F11B.17		
		Y62H9A.5	C50E3.11		
		D1086.11a	T11F8.3a.1		
		T05A1.2	F44F4.2.1		
		C53B4.5	Y38H6C.21		
		F32A5.2a	R04B5.9		
		K07H8.6a	Y43E12A.1		
		F14B8.3	R01H2.3		
		F38A5.12	H02I12.1		
		F38A5.12	C01G6.3		
		H13N06.6a	Y75B12B.1a		
		C06E8.5	ZC53.7		
		C39D10.7.1	T21C9.13		
		C30G7.4.1	ZK430.8		
		K02B9.1	R12E2.10		
		H06A10.1	C42D4.2		
		C42D8.2a	W02F12.3		
		T06E4.6	W02D7.2		
		F11H8.3	C11E4.7a		
		Y57G11B.5	F47B8.6		
		Y45F10C.4	F32D1.7		
		K08E3.1	T24A11.3		
		ZC168.5	C43F9.5		
		F54F7.3	C30G12.2		
		F38A5.10	H02I12.5		
		F38A5.14	C05E7.2		
		C10C5.4	AH6.5		
		C44B7.5	F18A1.7		
		ZK512.7	ZC308.4a		
		ZK813.2	F02E8.4		
		F35B12.4	F32G8.5		
		T25B2.2a	C46H11.2		
		ZC262.10	F58G4.6		
		ZC262.10	C01G12.10.1		
		F58A4.20	T01D3.6a		
		F02D8.4	T06E4.10		
		R07G3.2	K10B2.3a		
		F16H11.3	C09B8.4		
		R09F10.2	F14H3.3		
		Y41C4A.19	T03F7.7a		
		Y62H9A.4.1	C17G1.2		

		C44B12.1	W03C9.7a.1		
		F14H3.6	F57B7.3		
		F07F6.5	C10C5.5		
		ZK813.3	F15E11.13		
		C01G12.11	ZC404.8.1		
		AC3.4	F36G9.3a		
		T12B5.15	F15E11.13		
		W01B11.5a	ZK637.11		
		F40H3.2	F09G8.6		
		K07E1.1	C26G2.2		
		H04M03.2	C15F1.1		
		K04C1.5	C10H11.10		
		F53H4.2.1	F02H6.3a.1		
		F54D1.2	C08F11.12.1		
		F23F1.6	F37A4.4		
		T12G3.6a	F59D8.3		
		Y25C1A.14	T06E4.8		
		B0513.4a	F47H4.1a		
		T03F6.4	F31D5.1		
		C08F11.11.1	T07C4.6		
		D1086.7	F35C5.10		
		F49E12.2	F56H11.1a		
		F48E3.4	F22E10.3		
		F55B11.3	F36H12.17		
		AC3.3	T10C6.7		
		C03A7.7	R17.3		
		R04D3.3	T03D3.1		
		T05A10.5	Y49G5B.5		
		Y47D7A.9	R13H4.3		
		F47E1.4	T01C8.3		
		C50F4.8	C41G11.1a		
		C01G12.2	Y11D7A.13		
		T15B7.3	F32D8.12a.1		
		AC7.1a	F21A3.3		
		B0334.13	C25A8.4		
		ZK39.6	Y69A2AR.19a		
		Y75D11A.3	W03F11.1a		
		F14H3.5	F19H6.4		
		W10G11.2	DY3.8		
		C53B7.7	K02D7.3a		
		W03F8.6a.1	W04A4.2		
		T07D3.1	C10A4.4		
		R03C1.1a	T21E3.1		
		F45G2.1	Y70D2A.1		

		E02H4.6	Y39E4B.5		
		Y62H9A.3	M01E11.6		
		R09F10.7	ZC434.9a		
		W03G11.2	T08B6.4		
		F15B9.11	F57C12.6		
		ZK829.5	T22D1.5		
		F49E12.1	C41G7.2		
		Y73B6BL.38	Y62H9A.6		
		F35B3.4	ZK1037.6		
		F52B11.4	Y45F10C.3		
		K09F5.2	F35B12.6		
		R03G8.6	F52D2.2		
		F45E4.5a	F52D2.2		
		F14B8.4	F22F7.8		
		W10G11.3	T07F10.1a		
		C03A7.4	C17E7.4		
		B0024.2	C41D7.2		
		F08F3.6	C30H6.5a		
		ZK177.1	F26C11.5		
		F14H3.4	C44B12.5		
		E02H9.7.1	E02C12.8a		
			T12B5.14		
			C50B6.4		
			K09B11.19		
			Y51A2D.4		
			K01C8.3a		
			T16G12.1		
			Y43D4A.4a		
			W02A2.7		
			C15B12.1		
			F09C6.15		
			Y106G6D.3		
			F38B7.1a		
			K10H10.4a		
			T10H9.1		
			Y43E12A.3a		
			C31B8.12		
			C01G5.2a		
			Y75D11A.2		
			C01F6.4a		
			ZK1127.1.1		
			T06A1.5		
			C31H1.5		
			Y47G6A.2.2		

			F36A4.5a		
			F18A11.1.1		
			Y4C6A.3		
			C04H5.7a		
			C44B9.3		
			F41B5.3		
			Y70D2A.2		
			C08B11.4		
			F38E1.7		
			ZK270.1		
			Y43D4A.3a		
			T01G5.7		
			T26F2.2		
			C17F3.3		
			F43C11.3		
			F27C8.6.1		
			Y11D7A.11		
			C09G9.6		
			K01D12.9		
			W09C3.7		
			T25G3.2.1		
			T28C12.6		
			Y43C5A.7		
			T10H4.11		
			C38D4.6a		
			Y59E9AL.4		
			K01C8.5		
			C45B11.8		
			F18E3.11		
			F57F4.4		
			C18B2.1		
			C25A1.8		
			C12C8.3a.1		
			C05E11.4		
			F22E5.17		
			C17E7.9a		
			T05G5.4		
			W06B4.1		
			F15E11.1		
			F15E11.1		
			F13H6.1b.1		
			T23G11.2		
			ZK1225.4		
			F56F3.2a		

			D1081.12		
			ZC449.8		
			W05B2.5		
			Y54G9A.5		
			F36H12.17		
			T01D1.6		
			T19D12.1		
			C07A4.3		
			F02G3.7		
			C10C5.3		
			W06F12.8		
			F59A6.12		
			M162.7		
			C01G6.9		
			T11F9.9		
			T04G9.7		
			C10A4.10		
			F14D7.2		
			F36G9.12		
			F02H6.4a		
			M28.9.1		
			C03E10.6		
			Y48G1A.2		
			T24D1.3		
			F57B1.3		
			ZK829.9		
			C03A7.8		
			C50H2.12		
			F22A3.5		
			B0244.9		
			ZC412.6		
			T05E12.10		
			F40G12.11		
			ZK507.4		
			T05A7.1		
			T19H5.7		
			F53E4.1a		
			C45E5.4		
			F08A8.3		
			C01G12.8		
			C46E10.8		
			M176.7.1		
			Y18D10A.23		
			ZK512.10		

			C28C12.2		
			C55B7.1		
			C28A5.2		
			F47C12.4		
			D1022.2		
			W05H7.2		
			C36C9.3		
			T20D4.4		
			C17C3.12a.1		
			Y75B8A.3		
			T04F3.1a		
			F08F3.3.2		
			F53G12.5b		
			Y39G10AR.27		
			ZK354.8		
			T02G6.5b		
			T24E12.1		
			F31B9.3		
			Y32F6B.1		
			C10H11.6a		
			F53H8.3		
			Y49E10.14a.1		
			T10E9.3		
			T08G3.2		
			ZK1055.1		
			T08B2.12		
			R13H9.6		
			C07A9.11		
			F54D5.5a		
			C38C10.4		
			C05G6.1		
			C38D4.4		
			R13.2		
			F15A2.5		
			F52F10.4		
			F30A10.14		
			AB023577		
			B0310.8		
			Y51H7C.16		
			Y51H7C.16		
			Y51H7C.16		
			Y51H7C.16		
			Y9C9A.6		
			H01M10.3		

			C05E11.2		
			C27D9.2		
			K10D11.1		
			T28F3.4a		
			F15H10.2		
			R09B5.5		
			B0495.11		
			R09F10.8		
			Y102E9.5		
			C12D8.17		
			T07F8.3a		
			Y116A8C.4.1		
			C18G1.9		
			T25B6.2		
			F46F11.2		
			R11.2		
			T11F9.6		
			C27C12.7		
			Y45G12C.1		
			Y43E12A.2		
			F27C1.1		
			H02I12.8		
			T01H3.4		
			F52C6.13		
			ZK550.2		
			E03H4.4		
			T02G5.11a		
			Y79H2A.2a		
			T15B7.16		
			F56D6.13		
			C18D11.7		
			Y38H6C.19		
			R05D8.9		
			Y46G5A.30		
			F26G5.1a		
			F07A5.3		
			Y54G2A.3a		
			ZK546.15		
			H06H21.36		
			T06E4.14		
			F18C5.4		
			T28H11.4a		
			K07C11.12		
			Y73B6BL.14		

			R04D3.4		
			Y37E11AR.1		
			F09A5.1		
			F26G1.3		
			C16E9.1		
			F47C10.8		
			Y2H9A.3		
			T06D4.1a		
			T22C8.2		
			R03D7.7		
			F25D7.4		
			C17E7.13		
			Y71F9B.15		
			ZK1127.7		
			C49G7.8		
			ZC266.1		
			Y71F9B.15		
			K08D9.3		
			Y11D7A.12a		
			ZK354.9		
			F18A12.7		
			F11E6.7		
			C31B8.16		
			T26E4.15.1		
			ZC455.4		
			K07A12.2		
			C49C3.1		
			Y49E10.29		
			C33F10.12		
			T01E8.9		
			C31G12.12		
			F17C11.10		

Table A.10 Genes differentially regulated by *pqm-1* following acute HS

Gene	transcript	log_2FC
fipr-26	F53B6.8	1.960146
F55B12.10	F55B12.10	1.91831
ZK970.7	ZK970.7	1.91212
C27B7.9	C27B7.9	1.867216
catp-3	C09H5.2a	1.802434
F23F1.2	F23F1.2	1.752565
T10E10.4	T10E10.4	1.727283
F48D6.4a	F48D6.4a	1.656268
K01A6.7	K01A6.7	1.535364
nlp-25	Y43F8C.1	1.499081
ZC168.2	ZC168.2	1.489996
F01F1.14	F01F1.14	1.46584
F12A10.1	F12A10.1	1.465147
fbxa-27	Y82E9BL.17	1.449368
ubc-23	C28G1.1	1.429083
fipr-22	C37A5.2	1.420667
C52A10.1	C52A10.1	1.41811
Y58A7A.4	Y58A7A.4	1.411757
F27D9.7	F27D9.7	1.401089
tyr-6	Y73B6BL.1	1.393677
T01B7.8	T01B7.8	1.393048
best-5	C07A9.8	1.387555
F47B10.9	F47B10.9	1.385807
F09F7.6	F09F7.6	1.385158
cutl-14	B0511.5	1.381481
Y37H2A.12a	Y37H2A.12a	1.37967
F25G6.1	F25G6.1	1.364559
nlp-34	B0213.17	1.361069
T27A1.2	T27A1.2	1.347643
K03A1.4a	K03A1.4a	1.347122
C29F3.3	C29F3.3	1.333988
C16D9.1	C16D9.1	1.333644
C55C3.1	C55C3.1	1.33234
lin-28	F02E9.2a	1.32699
T28F4.4	T28F4.4	1.299219
F28H7.8	F28H7.8	1.293839
ptr-8	F44F4.4	1.293683
T24B8.5	T24B8.5	1.285277
F21D9.8	F21D9.8	1.283018
E01G6.1	E01G6.1	1.278249
F56C3.9	F56C3.9	1.276628

Y38C1AA.6	Y38C1AA.6	1.273499
W06B11.9	W06B11.9	1.264398
F33D11.8	F33D11.8	1.262655
C44H9.5	C44H9.5	1.254891
F08C6.5	F08C6.5	1.239326
grl-4	F42C5.7	1.236526
Y55F3BR.13	Y55F3BR.13	1.234607
wht-1	C05D10.3	1.227517
C34D10.2a.1	C34D10.2a.1	1.227149
F19C6.2a	F19C6.2a	1.22634
tps-1	ZK54.2a	1.226044
F26G1.5	F26G1.5	1.225009
K12B6.11	K12B6.11	-1.89049
F21C10.9.1	F21C10.9.1	-1.55325
T20D4.3	T20D4.3	-1.522
math-40	T08E11.3	-1.505
clec-7	F10G2.3	-1.4917
elt-2	C33D3.1	-1.43725
drd-1	F49E12.9a	-1.41193
C47G2.16	C47G2.16	-1.38537
T24E12.14	T24E12.14	-1.35171
nduo-3	MTCE.34	-1.34876
str-233	C06C6.2	-1.33181
F01D5.2	F01D5.2	-1.32405
clec-165	F38A1.10	-1.32405
F23F12.3	F23F12.3	-1.31877
C40H1.7	C40H1.7	-1.28623
F35D2.1	F35D2.1	-1.28338
R08E5.1.1	R08E5.1.1	-1.27505
T05B4.12	T05B4.12	-1.27144
pept-1	K04E7.2.1	-1.26911
Y102A11A.1	Y102A11A.1	-1.26879
F08A8.4.2	F08A8.4.2	-1.25622
K06C4.10	K06C4.10	-1.24715
nhr-114	Y45G5AM.1a.1	-1.2364
W01A11.16	W01A11.16	-1.23534
gcsh-1	D1025.2	-1.23345
cyp-33C3	F41B5.4	-1.22145

Table A.11 Genes differentially regulated by *pqm-1* independent of heat stress

Gene	transcript	log_2FC
dpy-9	T21D12.2a	3.234617
Y102A11A.5	Y102A11A.5	2.915126
dpy-2	T14B4.6	2.900237
dpy-3	EGAP7.1	2.878003
spi-1	R10H1.4	2.862809
dpy-10	T14B4.7a	2.811727
B0365.9	B0365.9	2.744147
T06G6.6b	T06G6.6b	2.696066
nhr-74	C27C7.3	2.678798
Y38H6C.16	Y38H6C.16	2.653943
K08B12.1	K08B12.1	2.65178
C14A4.9	C14A4.9	2.650702
T26C5.2	T26C5.2	2.639168
lpr-6	W04G3.1a	2.611222
atf-8	F17A9.3	2.604511
dao-2	M03A1.7.2	2.583221
Y37A1B.7	Y37A1B.7	2.575891
wrt-1	U61235	2.57446
F30A10.2	F30A10.2	2.557228
lpr-5	W04G3.2	2.538063
H19M22.3a	H19M22.3a	2.535342
cuti-1	ZC328.1	2.51443
clec-180	F32E10.3a	2.512089
grl-15	Y75B8A.20	2.46912
C09F9.2	C09F9.2	2.461529
Y38H8A.1	Y38H8A.1	2.426001
T19C4.1	T19C4.1	2.41926
nhr-113	ZK1025.9	2.407374
T03G6.1	T03G6.1	2.387854
mlt-11	W01F3.3a	2.379302
wrt-2	F52E4.6	2.361221
let-4	C44H4.2	2.341665
C11H1.5	C11H1.5	2.324976
K02E10.4a	K02E10.4a	2.282952
mlt-9	F09B12.1a	2.280992
dpy-7	F46C8.6	2.270661
R57.2	R57.2	2.241676
ZK1025.10	ZK1025.10	2.188696
Y39A1A.9	Y39A1A.9	2.185
R07E3.6	R07E3.6	2.169699

ptr-10	F55F8.1.2	2.167552
Y65B4BL.1a	Y65B4BL.1a	2.162666
F13B9.2	F13B9.2	2.130062
C14F11.6.1	C14F11.6.1	2.126953
dpy-8	C31H2.2	2.122301
C01F1.5	C01F1.5	2.114278
F58H1.2	F58H1.2	2.107035
spp-13	F08F1.6	2.102712
C01F1.3a	C01F1.3a	2.096672
cbn-1	K01A2.11d	2.084398
noah-2	F52B11.3	2.080651
H42K12.3.1	H42K12.3.1	2.075343
H03E18.1	H03E18.1	2.069442
T20F5.4	T20F5.4	2.065127
T13F2.4	T13F2.4	2.047324
F22F4.1	F22F4.1	2.040586
Y73E7A.8	Y73E7A.8	2.034711
lipl-6	Y57E12B.3	2.033626
lpr-3	W04G3.8	2.030595
F20G2.3a	F20G2.3a	2.024884
let-653	C29E6.1a.2	2.01271
bli-2	F59E12.12	2.009906
qua-1	T05C12.10	2.007006
osm-8	R07G3.6	1.999343
F11E6.9	F11E6.9	1.996968
lpr-4	W04G3.3	1.996125
Y55F3AM.14	Y55F3AM.14	1.993585
sqt-1	B0491.2.1	1.991711
F56D2.3	F56D2.3	1.982735
M03B6.3	M03B6.3	1.972495
dhs-29	F27D9.6	1.960306
wrt-10	ZK1290.8	1.942389
Y46G5A.29	Y46G5A.29	1.939963
C15F1.2	C15F1.2	1.938184
F32D1.11	F32D1.11	1.926818
ZK1025.3	ZK1025.3	1.924946
ZC123.1	ZC123.1	1.917105
F23H12.5	F23H12.5	1.911847
atf-2	K08F8.2	1.909713
cdh-12	Y71D11A.1	1.900791
col-46	Y18H1A.13	1.896947
C26B9.7	C26B9.7	1.89575
cdh-7	R05H10.6	1.895165
Y41G9A.2	Y41G9A.2	1.891847

bah-1	ZK1025.7	1.879824
mltn-9	F19H8.4	1.878109
Y47D3B.1	Y47D3B.1	1.86387
noah-1	C34G6.6a	1.842659
col-176	ZC373.7	1.836881
R03H10.2	R03H10.2	1.827674
R07B1.6	R07B1.6	1.825508
bus-8	T23F2.1.2	1.819479
Y71G12B.6a	Y71G12B.6a	1.81635
grl-5	Y47D7A.5	1.815854
F33H2.8a	F33H2.8a	1.805242
W09C2.7	W09C2.7	1.802806
grh-1	Y48G8AR.1a	1.795907
F46F3.3a	F46F3.3a	1.780846
F31B9.4	F31B9.4	1.776598
col-79	C09G5.3	1.773858
C32D5.12	C32D5.12	1.771676
F59B10.5	F59B10.5	1.75044
ZC434.10	ZC434.10	1.724289
cnc-3	R09B5.8	1.722245
D1014.5	D1014.5	1.717762
T08G2.2	T08G2.2	1.714792
Y43D4A.5a	Y43D4A.5a	1.712239
Y105E8A.13a	Y105E8A.13a	1.710611
F09F9.2	F09F9.2	1.709915
nhr-244	ZK1025.6	1.705757
mltn-1	F32A11.7	1.695614
nstp-3	ZC250.3	1.686197
K10D3.4	K10D3.4	1.686031
col-110	F19C7.7	1.682081
F14F3.4	F14F3.4	1.678574
bus-12	JC8.12a	1.675655
fbn-1	ZK783.1	1.674499
ZK1025.4a	ZK1025.4a	1.667427
ZC449.2	ZC449.2	1.662525
T03D8.6a	T03D8.6a	1.646947
C30G12.4	C30G12.4	1.646417
F35G2.5a	F35G2.5a	1.640375
F26D11.2	F26D11.2	1.635019
C05G5.7	C05G5.7	1.634813
C44H4.10	C44H4.10	1.623075
F15H10.8	F15H10.8	1.620713
C48D5.3	C48D5.3	1.619993
nas-37	C17G1.6a	1.61548

C02F5.14	C02F5.14	1.612262
C02F4.4	C02F4.4	1.605118
F33D4.6b	F33D4.6b	1.602421
glf-1	H04M03.4	1.600735
mam-1	ZC13.3	1.600082
Y55D5A.1a	Y55D5A.1a	1.59766
C28C12.4	C28C12.4	1.596745
grl-7	T02E9.2a	1.591632
peb-1	T14F9.4a	1.591389
F53F4.15	F53F4.15	1.579309
T26E4.4	T26E4.4	1.556678
Y11D7A.5	Y11D7A.5	1.547352
gei-13	F58A4.11	1.545066
F18C5.5	F18C5.5	1.542948
B0348.5	B0348.5	1.541909
T27A10.6.1	T27A10.6.1	1.538806
ztf-2	F13G3.1	1.538748
dpy-6	F16F9.2	1.527977
T05C1.3	T05C1.3	1.524779
D1005.2	D1005.2	1.505556
K09C4.5	K09C4.5	1.503844
ugt-57	F01E11.1	1.503755
F01G10.9	F01G10.9	1.485064
F54B11.10	F54B11.10	1.481221
C06A6.5	C06A6.5	1.479021
C05C9.1	C05C9.1	1.474084
bli-1	C09G5.6	1.470654
C35A11.2	C35A11.2	1.466365
grl-10	C26F1.5	1.4608
lpr-1	Y65B4BR.2a	1.458307
K08E7.5a	K08E7.5a	1.457366
K02H11.4	K02H11.4	1.451646
clec-67	F56D6.2	1.448748
ugt-9	T19H12.1a	1.443621
F49C5.11a	F49C5.11a	1.44127
Y17D7B.10	Y17D7B.10	1.431679
Y11D7A.9	Y11D7A.9	1.431271
myrf-1	F59B10.1	1.42924
F53B3.6	F53B3.6	1.428326
T17H7.1.1	T17H7.1.1	1.422958
F49E10.2a	F49E10.2a	1.417252
B0205.4	B0205.4	1.41269
C29E4.15	C29E4.15	1.410353
Y50D7A.12	Y50D7A.12	1.409518

nhr-259	C27C7.8	1.383681
Y39H10A.4	Y39H10A.4	1.379429
F49H12.5	F49H12.5	1.373924
bus-17	ZK678.8	1.372843
F19H8.2	F19H8.2	1.372604
C34C12.6	C34C12.6	1.369216
Y54F10AM.6	Y54F10AM.6	1.366192
F46G11.6	F46G11.6	1.362402
C26B9.2	C26B9.2	1.359473
T13C5.7	T13C5.7	1.357729
sym-1	C44H4.3	1.356626
C35A5.11a	C35A5.11a	1.350859
Y22D7AL.9	Y22D7AL.9	1.349967
nekl-3	F19H6.1.1	1.348908
Y64H9A.2	Y64H9A.2	1.347427
cyp-42A1	Y80D3A.5	1.339434
F49D11.6	F49D11.6	1.33886
C45G7.5	C45G7.5	1.331761
phy-2	F35G2.4	1.330949
F57F5.3	F57F5.3	1.32683
col-128	F12F6.9	1.321125
T12E12.6	T12E12.6	1.319192
ptr-4	C45B2.7	1.31883
ZK1025.2	ZK1025.2	1.308614
ZK1025.2	ZK1025.2	1.308614
H14E04.1	H14E04.1	1.30808
F53B3.5	F53B3.5	1.297609
D1086.3	D1086.3	1.296379
lgc-22	F15E6.2a	1.291151
C13C12.2	C13C12.2	1.28476
Y43F4A.1a	Y43F4A.1a	1.284087
mab-3	Y53C12B.5a	1.279101
osr-1	C32E12.3	1.26301
Y81G3A.4a	Y81G3A.4a	1.260381
grd-2	F46B3.5	1.243008
grd-1	R08B4.1a.1	1.23818
swip-10	F53B1.6	1.237728
F18F11.4	F18F11.4	1.237326
mltn-12	C53B4.8	1.236395
mab-10	R166.1	1.234886
C17F4.2	C17F4.2	1.232483
B0393.5	B0393.5	1.229545
C02G6.3	C02G6.3	1.22524
F13B6.1	F13B6.1	1.223525

F11E6.4a	F11E6.4a	1.219199
T22F7.3	T22F7.3	1.199513
T19B10.5	T19B10.5	1.193302
C52D10.3	C52D10.3	1.188987
gfi-1	F57F4.3	1.187491
mboa-1	B0395.2	1.185314
F49C5.12	F49C5.12	1.180603
ZK154.1	ZK154.1	1.180507
dpy-20	T22B3.1	1.178931
ZK669.2	ZK669.2	1.17509
hhat-1	ZC101.3	1.174665
F46F11.7	F46F11.7	1.166114
M79.2	M79.2	1.16566
W03D2.9	W03D2.9	1.160831
F25D1.3	F25D1.3	1.157434
Y68A4A.13	Y68A4A.13	1.148608
mlt-4	ZC15.7	1.146882
T10B5.10	T10B5.10	1.140053
F09C8.1	F09C8.1	1.13856
ptc-3	Y110A2AL.8a	1.132319
hpo-36	T27C4.2	1.132234
T09F5.1	T09F5.1	1.126609
Y57A10A.23	Y57A10A.23	1.114212
elo-4	C40H1.4	1.10597
R07B1.13	R07B1.13	1.104952
acox-2	F08A8.2	1.101229
hsd-3	ZC449.6	1.083019
H41C03.1	H41C03.1	1.072394
W03D8.11	W03D8.11	1.07028
C11H1.9a	C11H1.9a	1.066021
C34F6.1	C34F6.1	1.065634
F25E5.2	F25E5.2	1.056841
R05G6.9	R05G6.9	1.042784
C24H10.3	C24H10.3	1.032879
F27C8.2	F27C8.2	1.020057
cutl-28	F41A4.1	1.001213
Y37D8A.3	Y37D8A.3	0.983396
che-14	F56H1.1	0.981384
C17B7.5	C17B7.5	0.962996
F13G3.3a	F13G3.3a	0.947359
Y54G2A.45a	Y54G2A.45a	0.943724
Y43F4A.1a	Y43F4A.1a	0.933439
dlhd-1	T23F4.3	0.932508
W03G11.2	W03G11.2	-0.94719

R09F10.7	R09F10.7	-0.98452
F58A4.20	F58A4.20	-1.03048
W10G11.2	W10G11.2	-1.06719
col-96	Y41C4A.19	-1.08878
W03F8.6a.1	W03F8.6a.1	-1.15499
fbxa-200	T07D3.1	-1.16652
F35B3.4	F35B3.4	-1.1815
nep-4	C53B7.7	-1.18254
col-146	T06E4.6	-1.18409
F23F1.6	F23F1.6	-1.18843
F45E4.5a	F45E4.5a	-1.19507
ZC262.10	ZC262.10	-1.20693
ZC262.10	ZC262.10	-1.20693
F15B9.11	F15B9.11	-1.21626
C08F11.11.1	C08F11.11.1	-1.23085
F47E1.4	F47E1.4	-1.24049
T03F6.4	T03F6.4	-1.25191
abu-6	C03A7.7	-1.28065
nas-1	F45G2.1	-1.3111
E02H9.7.1	E02H9.7.1	-1.31142
vit-1	K09F5.2	-1.34105
T25B2.2a	T25B2.2a	-1.34888
piit-1	F35B12.4	-1.35518
K07E1.1	K07E1.1	-1.38143
F14H3.5	F14H3.5	-1.38914
B0513.4a	B0513.4a	-1.41446
D1086.7	D1086.7	-1.41876
T12G3.6a	T12G3.6a	-1.43272
col-150	B0024.2	-1.44028
R03G8.6	R03G8.6	-1.46019
pqn-2	AC3.4	-1.4675
E02H4.6	E02H4.6	-1.47273
col-80	C09G5.5	-1.47575
col-122	T05A1.2	-1.48323
F55B11.3	F55B11.3	-1.50057
clec-97	ZK39.6	-1.5008
abu-15	C03A7.4	-1.50427
abu-1	AC3.3	-1.50966
F53H4.2.1	F53H4.2.1	-1.51586
F08F3.6	F08F3.6	-1.5167
nspb-9	C01G12.11	-1.54365
F14H3.4	F14H3.4	-1.54679
F54D1.2	F54D1.2	-1.55297
col-133	F52B11.4	-1.553

Y62H9A.3	Y62H9A.3	-1.56462
C50F4.8	C50F4.8	-1.57248
pqn-57	R09F10.2	-1.58231
R03C1.1a	R03C1.1a	-1.58854
pes-23	F14B8.3	-1.59548
lips-17	R07G3.2	-1.62871
perm-2	C44B12.1	-1.65358
grl-21	ZC168.5	-1.67052
F14B8.4	F14B8.4	-1.67134
C44B7.5	C44B7.5	-1.67903
Y25C1A.14	Y25C1A.14	-1.69815
W10G11.3	W10G11.3	-1.70593
col-129	M18.1a	-1.70911
tkr-3	AC7.1	-1.71537
F40H3.2	F40H3.2	-1.71754
skpo-1	F49E12.1	-1.73205
C30G7.4.1	C30G7.4.1	-1.74277
ZK177.1	ZK177.1	-1.75429
D1086.6	D1086.6	-1.75629
dod-23	F49E12.2	-1.75973
col-139	F41F3.4	-1.77301
F48E3.4	F48E3.4	-1.78639
Y57G11B.5	Y57G11B.5	-1.81861
tbx-36	ZK829.5	-1.81891
col-143	T15B7.3	-1.82548
tyr-2	K08E3.1	-1.84689
C45B2.1	C45B2.1	-1.84854
B0334.13	B0334.13	-1.85472
ZK813.3	ZK813.3	-1.87502
F54F7.3	F54F7.3	-1.89595
col-184	F15A2.1a	-1.89895
col-106	Y77E11A.15	-1.90258
puf-11	Y73B6BL.38	-1.91752
ent-5	F16H11.3	-1.91914
col-140	F26F12.1a	-1.92324
T12B5.15	T12B5.15	-1.92789
Y45F10C.4	Y45F10C.4	-1.92872
vap-2	T05A10.5	-1.93645
C54D10.10	C54D10.10	-1.95002
D1086.11a	D1086.11a	-1.97341
Y75D11A.3	Y75D11A.3	-1.98736
pqn-72	W01B11.5a	-1.99058
skpo-3	F32A5.2a	-1.99866
vit-2	C42D8.2a	-1.99942

F02D8.4	F02D8.4	-2.01171
C39D10.7.1	C39D10.7.1	-2.03814
F55B11.2.1	F55B11.2.1	-2.04794
F07G6.10	F07G6.10	-2.09143
Y62H9A.4.1	Y62H9A.4.1	-2.1052
Y47D7A.9	Y47D7A.9	-2.10543
C10C5.4	C10C5.4	-2.10726
ZK512.7	ZK512.7	-2.12574
R04D3.3	R04D3.3	-2.15439
dct-5	F07F6.5	-2.18476
col-119	C53B4.5	-2.18772
col-181	W03G11.1a	-2.18949
F17E9.4	F17E9.4	-2.25547
Y62H9A.5	Y62H9A.5	-2.25919
col-81	F38A3.1	-2.29282
nspb-6	H04M03.2	-2.30982
nspb-1	F38A5.14	-2.32876
nspb-4	F38A5.10	-2.37143
ZK813.2	ZK813.2	-2.38228
C08A9.10	C08A9.10	-2.38404
vit-6	K07H8.6a	-2.44642
ZK813.7	ZK813.7	-2.47139
col-8	F11H8.3	-2.48037
col-19	ZK1193.1	-2.50522
meg-1	K02B9.1	-2.5117
Y37D8A.19	Y37D8A.19	-2.52746
col-178	C34F6.2	-2.56235
K07A1.6	K07A1.6	-2.56953
nas-20	T11F9.3	-2.57296
nspb-2	F38A5.12	-2.61785
nspb-7	C01G12.2	-2.62224
H06A10.1	H06A10.1	-2.62592
nspb-2	F38A5.12	-2.63277
col-62	C15A11.6	-2.6364
tbh-1	H13N06.6a	-2.63883
ZC373.2	ZC373.2	-2.65071
C06E8.5	C06E8.5	-2.71331
col-179	C34F6.3	-2.72052
vit-4	F59D8.2	-2.8086
F14H3.6	F14H3.6	-2.82762
D1054.10	D1054.10	-2.84539
F59D8.1	F59D8.1	-2.92805
fipr-13	F57A8.8	-2.95768
col-137	Y51H4A.9	-3.03864

col-20	F11G11.11	-3.11625
K04C1.5	K04C1.5	-3.15398
ule-3	D1054.11	-3.18273
K10C2.8	K10C2.8	-3.59899
vit-5	C04F6.1	-4.15751

Table A.12 Genes with expression influenced by *pqm-1* post HS and identified by PQM-1 ChIP experiment (Niu et al.)

Transcript	Gene
F09F7.6	*F09F7.6*
C05D10.3	*wht-1*
C33D3.1	*elt-2*
F56C3.9	*F56C3.9*
T08E11.3	*math-40*
Y102A11A.1	*Y102A11A.1*
C44H9.5	*C44H9.5*
Y45G5AM.1a.1	*nhr-114*
C07A9.8	*best-5*
T28F4.4	*T28F4.4*
T01B7.8	*T01B7.8*

Table A.13 Genes with expression influenced by *pqm-1* presence independent of HS and identified by PQM-1 ChIP (Niu et al.)

Transcript	Gene
D1086.3	*D1086.3*
F56D6.2	*clec-67*
C52D10.3	*C52D10.3*
F58A4.11	*gei-13*
M79.2	*M79.2*
F09C8.1	*F09C8.1*
F57F4.3	*gfi-1*

Table A.14 Genes upregulated by both *pqm-1* and *hsf-1* following HS

Gene	transcript
fipr-26	*F53B6.8*
F55B12.10	*F55B12.10*
T10E10.4	*T10E10.4*
ZC168.2	*ZC168.2*
F01F1.14	*F01F1.14*
F12A10.1	*F12A10.1*
fbxa-27	*Y82E9BL.17*
ubc-23	*C28G1.1*
C52A10.1	*C52A10.1*
Y58A7A.4	*Y58A7A.4*
F27D9.7	*F27D9.7*
tyr-6	*Y73B6BL.1*
best-5	*C07A9.8*
F47B10.9	*F47B10.9*
F09F7.6	*F09F7.6*
cutl-14	*B0511.5*
Y37H2A.12a	*Y37H2A.12a*
F25G6.1	*F25G6.1*
K03A1.4a	*K03A1.4a*
C16D9.1	*C16D9.1*
C55C3.1	*C55C3.1*
lin-28	*F02E9.2a*
T28F4.4	*T28F4.4*
F28H7.8	*F28H7.8*
ptr-8	*F44F4.4*
F21D9.8	*F21D9.8*

E01G6.1	*E01G6.1*
Y38C1AA.6	*Y38C1AA.6*
W06B11.9	*W06B11.9*
F33D11.8	*F33D11.8*
C44H9.5	*C44H9.5*
F08C6.5	*F08C6.5*
grl-4	*F42C5.7*
Y55F3BR.13	*Y55F3BR.13*
wht-1	*C05D10.3*
C34D10.2a.1	*C34D10.2a.1*
F19C6.2a	*F19C6.2a*
tps-1	*ZK54.2a.1*

Table A.15 Genes differentially regulated in an *hsf-1 (sy441*) mutant at 20˚C compared to control

Gene	**transcript**	**log_2FC**
F15D4.5	F15D4.5	3.339142
F57F4.4	F57F4.4	2.915516
Y102A5C.36.1	Y102A5C.36.1	2.79214
Y37H2A.11	Y37H2A.11	2.414264
Y47H10A.5	Y47H10A.5	2.378126
hsp-16.48	T27E4.3	2.297951
T27E4.3	T27E4.3	2.297951
dsl-7	F15B9.9	2.178786
C30A5.16	C30A5.16	2.078961
C38D9.2.1	C38D9.2.1	2.057687
R08A2.9	R08A2.9	2.025536
F59C6.15	F59C6.15	1.744192
csp-3	Y47H9C.6	1.741473
hsp-16.1	T27E4.2	1.732766
R06C1.6	R06C1.6	1.714225
pqm-1	**F40F8.7.2**	**1.663714**
F17E9.10	F17E9.10	1.601882

rga-2	Y53C10A.4	1.582795
F58D5.2a	F58D5.2a	1.558746
C18H9.6	C18H9.6	1.514557
F44E5.5	F44E5.5	1.506728
T27E4.2	T27E4.2	1.469023
F08G2.5	F08G2.5	1.451873
C36C5.14	C36C5.14	1.436994
abt-5	Y53C10A.9	1.418854
M01G12.9	M01G12.9	1.417095
B0250.18a	B0250.18a	1.410296
srh-70	T21B4.9	1.368116
R07C12.2.1	R07C12.2.1	1.359492
rrf-2	M01G12.12	1.335563
D2062.6	D2062.6	-1.34286
Y17G7B.23a	Y17G7B.23a	-1.50542
Y71F9AL.8	Y71F9AL.8	-1.60615
M163.15	M163.15	-1.64497
F08G2.13	F08G2.13	-1.70071
F46F5.6	F46F5.6	-1.80621
NA	NA	-1.98282
E02C12.11	E02C12.11	-1.99792
rop-1	C12D8.11	-2.12811
F55G1.16	F55G1.16	-2.24046
Y57G11A.2	Y57G11A.2	-2.37156
M163.12	M163.12	-2.90049

Appendix B

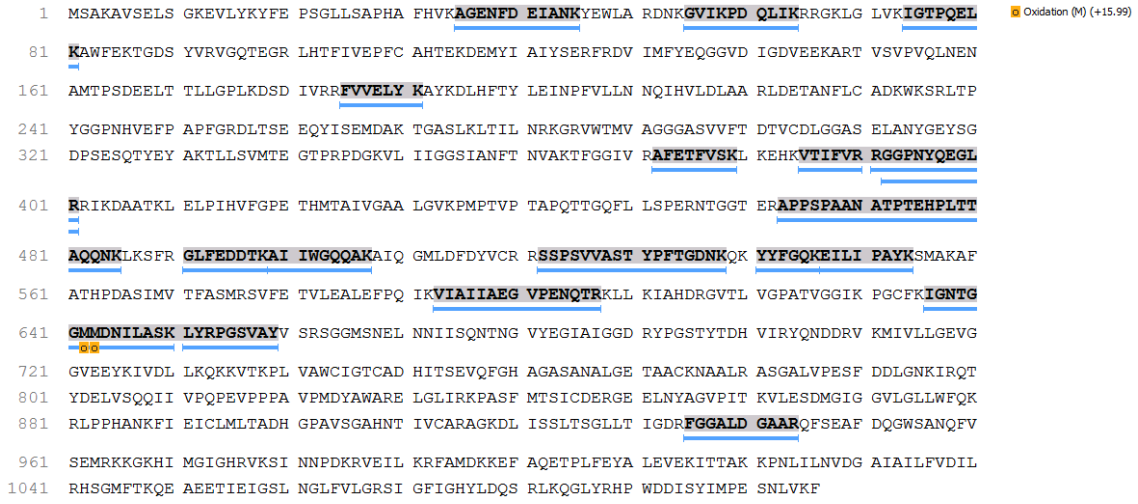

Figure B.1 ACLY-1 protein coverage

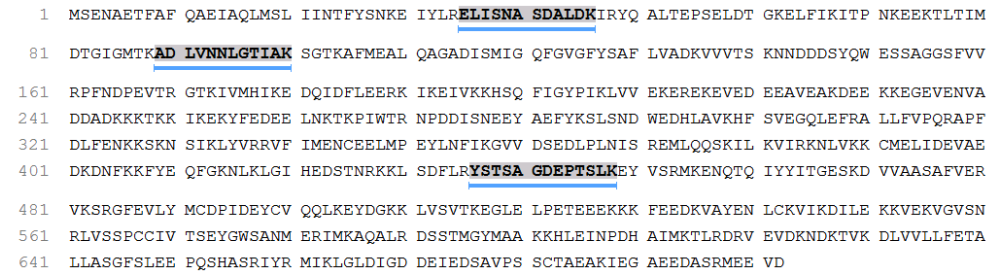

Figure B.2 HSP-90 protein coverage

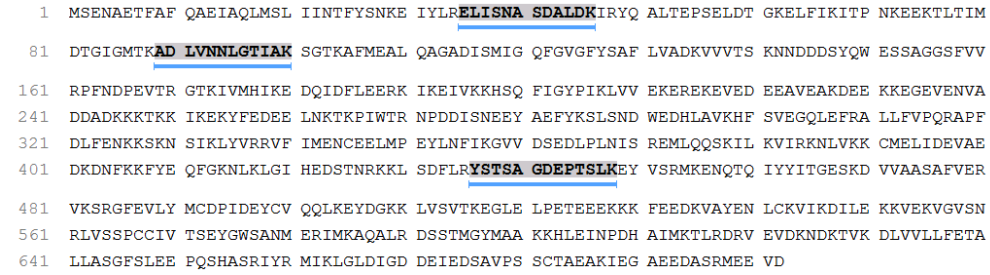

Figure B.3 Y37E3.17 protein coverage

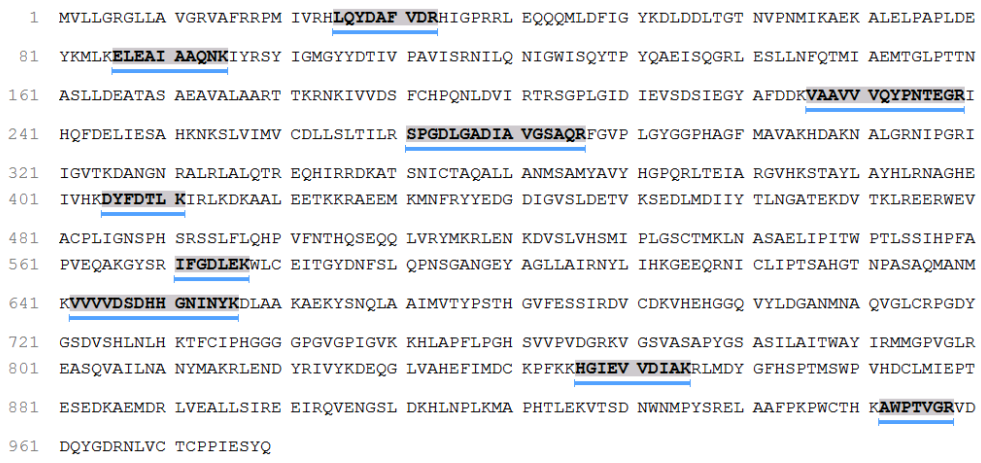

Figure B.4 GLDC-1 protein coverage

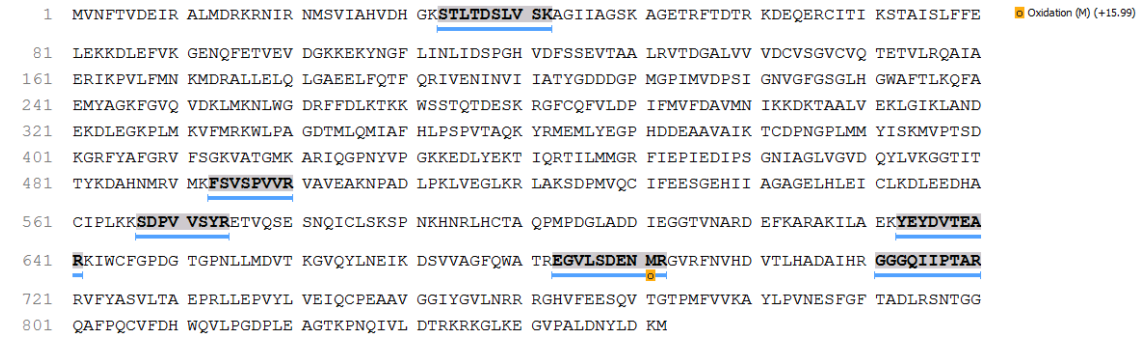

Figure B.5 EEF-2 protein coverage